Physics Area - PhD course in Theoretical Particle Physics

SISSA, Trieste

EXPLORING PHASES OF NON-ABELIAN GAUGE THEORIES WITH PERTURBATION THEORY

Supervisor:

Lorenzo Di Pietro
Marco Serone

Candidate:

Fabiana De Cesare

ACADEMIC YEAR 2023/2024

Forestiero che cerchi
La dimensione insondabile
La troverai
Alla fine della strada

Acknowledgments

Questo viaggio è stato lungo, sfidante ed emozionante. Certamente non sarebbe stato lo stesso se non avessi avuto la fortuna di percorrerlo insieme a una squadra di persone incredibili. Trovo giusto e necessario ringraziarle una per una, partendo dai luoghi che hanno contribuito a rendere questo cammino meraviglioso.

La scuola La SISSA è un posto incredibile e per me è stato un onore farne parte. Ringrazio Marco e Lorenzo, per avermi guidato in questo percorso, per tutto quello che mi hanno insegnato sulla fisica, e per aver sempre creduto in me. Ringrazio Bertmat, per il suo entusiasmo e la sua simpatia, e Riccardo, per il tempo e l'energia che ha dedicato al nostro lavoro.

Il bar Se vi trovate a Trieste e volete sapere quanti black russian si possono preparare con una bottiglia di kaluha dovete cercare un luogo che si chiama Barmacia. Non fidatevi delle insegne, sappiate solo che se vedete un'enorme cavallo nero siete nel posto giusto. Ringrazio tutti i compagni di serate, in particolare Andrea, Cri, Daniele, Diego 1, Diego 2, Giovanni, Giuà, Francesca e Martina. Ringrazio Max, per la sua follia e per aver organizzato la festa di compleanno più bella di sempre.

L'auto Da qualche parte in giro per l'Islanda corre una Dacia Duster grigia. Sicuramente chi la guida non conosce le avventure che ha vissuto quella macchina. Io, però, non posso dimenticarle. Ringrazio Vale, Vania e Mavi per avermi dimostrato ancora una volta che l'unione fa la forza e per avermi accompagnato nel viaggio più bello di questi ultimi anni.

La montagna Misurarsi con i propri limiti è l'unico modo per sopravvivere e non c'è nulla di meglio del dottorato per scoprirlo. Nulla, a parte la montagna. Ringrazio i compagni di salita, in particolare Jeki e Davide, per aver sempre rispettato il mio passo e le mie insicurezze.

Il mare Esiste a Trieste una spiaggia che non è una spiaggia ma che è il posto perfetto per lasciare che le preoccupazioni scivolino via. Non so contare le volte in cui mi sono incantata davanti a un tramonto a Barcola. Ringrazio chi si è incantato con me, in particolare Delpo per le birre, i bagni, le parole crociate e per essere il più sfrastico di tutti, persino di me.

L'ufficio In questi anni, ho avuto la fortuna di svegliarmi ogni mattina (rigorosamente presto) con la voglia sincera di andare a lavorare. Chiunque proverebbe lo stesso, se lavorasse nel 431. Ringrazio Niloo, Jack e Uriel. Ringrazio Fra, per la sua purezza, Giulio, per il suo entusiasmo, e Saman, per la sua splendida pazzia.

La casa Via della Pietà 37 è stata casa per tanti motivi. Ringrazio Emilia, per la sua capacità di emozionarsi, Nat, per la sua gentilezza, Gabri, per la sua compagnia, e Costi, per essere stata tutto quello di cui avevo bisogno.

Il bosco Nel cuore del parco della SISSA c'è uno spiazzo tra gli alberi con un tavolo di legno e due panche. Ringrazio Steph, per tutte le parole che ci siamo detti in quel luogo, di fisica e di vita. Alcune di queste le troverete nella tesi, sotto forma di commenti e equazioni. Altre, le più importanti, sono conservate dentro me come un ricordo prezioso. Lo ringrazio perché non è stato solo bosco, ma anche molo, castello, mare, montagna, lago e, soprattutto, casa.

La città Trieste è una città meravigliosa, con una natura splendida e un'anima ribelle. Condividerla con le persone di sempre è stato per me una gioia e un'onore. Ringrazio tutte le persone che mi sono venute a trovare in questi anni: la mitica Maria, le mie amiche dell'erasmus Kadija, Laura e Federica, i miei compagni di avventura Ale ed Emi, i miei cugini Kina e Luca, e i miei amici di sempre Claudia, Fede, Fra, Giogio, Giulia, Luke, Ric e Sandrino, Spin. Un grazie speciale ad Eli, per essermi sempre stata vicina anche quando ero più lontana, e a Chiara, per tutto quello che abbiamo condiviso in questa città.

Chi mi conosce sa quanto importante sia per me la mia famiglia. Ringrazio Angela e Andra, per il loro ruolo fondamentale, e Daniela, per avermi supportato costantemente durante questi anni. Ringrazio Mister e Simone, per essere i fratelli migliori che si possano desiderare, e mia madre, per la dolcezza con cui ogni giorno veglia su di me. Per finire, ringrazio mio padre, per me da sempre esempio di intelligenza, forza e amore. A lui questa tesi è dedicata.

Abstract

This thesis is devoted to the study of phases of non-abelian gauge theories by means of perturbation theory.

In the first part, we use the ϵ-expansion to investigate the fate of gauge theories in dimensions $d = 3$ and $d = 5$. Initially, we perform resummation of the five-loop $\beta-$function in $d = 4 + 2\epsilon$ to search for UV five-dimensional fixed points, focusing on the case of $SU(n_c)$ gauge theories with n_f Dirac fermions in the fundamental representation. We then compute the free energy F on the sphere as a perturbative series in ϵ to test RG trajectories in $d \neq 4$. To achieve that, we employ the generalized $\widetilde{F}$ theorem, which, given $\widetilde{F} = -\sin(\pi d/2)F$, imposes $\widetilde{F}_{\rm UV} > \widetilde{F}_{\rm IR}$. We extrapolate this result to $d = 3$ to test whether $\rm QCD_3$ with gauge group $SU(n_c)$ and n_f fundamental matter fields flows to a CFT or to a symmetry-breaking case. We then extrapolate to $d = 5$ to test whether the UV fixed points found with resummation can be reached via a susy-breaking deformation of the E_{n_f+1} SCFT.

In the second part, we consider $4d$ non-abelian gauge theories and we try to get insights about confinement by putting the theory in Anti-de Sitter space. In the small radius limit the theory is weakly coupled and admits both Dirichlet and Neumann boundary conditions, associated to a deconfined and a confined phase respectively. The Dirichlet boundary condition cannot exist at arbitrarily large radius because it would give rise to colored asymptotic states in flat space. This implies that a deconfinement/confinement transition must occur as the radius is increased. We investigate the nature of this transition using perturbation theory, by computing the anomalous dimensions of the lightest scalar operators in the boundary theory and the correction to the normalization of the current two-point function.

Declaration

The discussion of this PhD thesis is based on the following papers:

- F. De Cesare, L. Di Pietro, M.Serone, *Five-dimensional CFTs from the ϵ-expansion*, Phys.Rev.D **104** (2021) 10, 105015, [arXiv:2107.00342] [1]

- F. De Cesare, L. Di Pietro, M.Serone, *Free energy on the sphere for non-abelian gauge theories*, JHEP **04** (2023) 099, [arXiv:2212.11848] [2]

- R. Ciccone, F. De Cesare, L. Di Pietro, M.Serone, *Exploring Confinement in Anti-de Sitter Space*, [arXiv:2407.06268] [3]

Contents

1 Introduction **15**

2 General Background **19**

2.1 Quantum Field Theory and the Renormalization Group 19

2.1.1 Fixed points and conformal invariance 20

2.1.2 WF fixed points and the ϵ-expansion 29

2.1.3 Monotonicity theorems for the Renormalization Group 31

2.2 Non-Abelian Gauge theories: general properties 33

2.2.1 Gauge theories in $d = 4$: asymptotic freedom, confinement and the conformal window 36

2.2.2 Exploring gauge theories in $d \neq 4$ 43

2.3 Quantum Field Theory in Anti-de-Sitter space 45

2.3.1 Two-dimensional toy models at large N 46

2.3.2 Gauge theories in AdS: the confinement/deconfinement transition . . . 47

3 Five dimensional CFTs from the ϵ-expansion **49**

3.1 Introduction 49

3.2 Resummation techniques for perturbative series 50

3.3 Wilson-Fisher fixed point for Yang-Mills theories 52

3.4 Results 56

3.4.1 Existence of a fixed point in $d = 5$ for pure $SU(2)$ 56

3.4.2 Generalization to different values of n_f and n_c 58

3.5 Other approaches: a brief overview 61

4 Free Energy on the Sphere for Non-Abelian Gauge Theories **65**

4.1 Introduction 65

4.2 Free energy of gauge theories on the sphere: leading order 67

4.2.1 One-loop determinants 68

4.2.2 Computation in Landau gauge 69

4.3 Feynman rules on the sphere 73

4.3.1 Bitensors in maximally symmetric spaces 73

4.3.2 Propagators on S^d 75

4.3.3 Vertices on the sphere . . . 76
4.4 Next to leading contribution . . . 77
4.4.1 Computation of the diagrams . . . 77
4.4.2 Check with Jack [4] . . . 83
4.4.3 Renormalization . . . 86
4.4.4 Free energy at the fixed point . . . 86
4.5 Applications . . . 88
4.5.1 F-Theorem in $d = 3$ . . . 90
4.5.2 F-Theorem in $d = 5$ . . . 94

5 Exploring confinement with Anti-de Sitter space 97
5.1 Generalities of YM theory on AdS . . . 100
5.2 The gauge propagator in AdS . . . 103
5.2.1 Bulk-to-boundary gauge propagator . . . 107
5.2.2 Ghost propagator . . . 108
5.3 Anomalous dimensions of lightest scalar operators . . . 108
5.3.1 Anomalous dimension of the displacement operator . . . 109
5.3.2 Boundary RG flow from bulk dynamics . . . 113
5.3.3 Anomalous dimensions from $J^a J^b$ two-point function . . . 116
5.3.4 Projecting onto irreducible representations . . . 120
5.4 Current two-point function . . . 121
5.4.1 Computation of the diagrams: external points in the bulk . . . 122
5.4.2 Counterterm . . . 124
5.4.3 Final result . . . 125

6 Conclusions 129

A Sphere gauge propagator 133

B Subtleties on the computation of the free energy on the sphere 139
B.1 Contact terms and integration by parts on the sphere . . . 139
B.2 Alternative gauge-fixing procedure . . . 140
B.2.1 Gauge theories on S^d . . . 141
B.2.2 Computation of the ghost propagator . . . 144
B.2.3 Match with eq. (4.83) . . . 145

C Mean field theory of $SU(n_c)$ adjoint currents 147

D Bulk-to-bulk gauge propagator 151
D.1 Map to the notation of [5] . . . 151
D.2 Spectral representation . . . 152
D.3 General expression in any ξ-gauge . . . 154

E Tools for the computation of Witten diagrams **157**
E.1 Mass shift diagram 157
E.2 Integration by parts in AdS space 158
E.3 A useful integral 159

Chapter 1

Introduction

Quantum Field Theory (QFT) is the universal language of modern theoretical physics, serving as the basis for our current understanding of the fundamental laws of nature. It sits at the foundation of the Standard Model, describing the interactions of fundamental particles and forces, is crucial in early universe cosmology, and plays a key role in condensed matter physics, characterizing the behavior of various phases of matter.

Despite its major benefit, studying QFT is inherently complex [6]. One powerful tool to simplify this study is perturbation theory. The idea is to start from free, solvable theories and make approximate calculations by gradually introducing interactions. Despite being asymptotic and typically inadequate for providing an unambiguous definition of QFTs, perturbative expansions are particularly effective when the interactions are weak, enabling precise predictions and a deeper understanding of the underlying physics.

However, most of the space of theories is strongly coupled and therefore unreachable with perturbation theory. Non-perturbative methods are often needed to understand the fate of QFTs, e.g. by formulating theories on a discretized spacetime (lattice QFT [7–9]), by imposing consistency requirements to generic theories (bootstrap approach [10–13]), by studying the constraints imposed by global symmetries and their generalizations [14].

Still, giving up on perturbation theory would be a reckless choice. Several tricks can be used to improve the power of perturbation theory. There are specific situations where the set of perturbative data can be upgraded to non-perturbative results, thanks to the mathematical machinery of resurgence [15]. Even when this is not possible, Borel resummation and Padé approximation can be used to reorganize the perturbative series, improving the convergence of the series and providing more accurate results.

The possibility of finding approximate solutions can be enlarged if some parameters enter the theory, other than the coupling constants describing the interactions. This parameter may be for instance the number N of components of a field (large N expansion) or, analytically continuing the theory to a dimension d, the parameter $\epsilon = d - d_c$, quantifying the distance between d and a dimension d_c at which the theory is weakly coupled (ϵ-expansion).

Perturbation theory can help in the ambitious goal of understanding how theories evolve

when the length scale is increased. This evolution is described by the Renormalization Group (RG) flow. Central to this concept are the beta functions, which quantify the rate of change of coupling constants with respect to the energy scale, and anomalous dimensions, which measure the deviation of the operators' scaling behaviors from their classical expectations.

Notably, a special role in the space of theories is played by conformal field theories (CFTs), which are fixed points of the RG flow invariant under scale transformations. To any CFT, one can assign a positive quantity describing the number of degrees of freedom, which lowers as we flow in the space of theories. This makes the flow irreversible and provides a remarkable organizing principle for CFTs. In continuous dimension d this quantity is conjectured to be $\widetilde{F} = \sin(\pi d/2) \log Z_{S^d}$, where Z_{S^d} is the partition function of the theory on the d-dimensional sphere. Given two CFTs connected by an RG flow, one at high energy (UV fixed point) and one at low energy (IR fixed point), we then expect the inequality $\widetilde{F}_{\rm UV} > \widetilde{F}_{\rm IR}$ to be valid [16].

Among all QFTs, non-abelian gauge theories are undoubtedly one of the most challenging and interesting cases of study. Even in $4d$, where they are mostly studied, a deep understanding of their large-distance fate is far from being reached. The complexity of these theories derives from the fact that they are asymptotically free, meaning that they become strongly coupled at low energies, which prevents the possibility of using perturbation theory to study the RG flow. Asymptotically free theories possess a dynamically generated scale Λ, at which deep and interesting phenomena occur, which cannot be proved by starting from the weakly coupled theory. In particular, while at high energies massless and charged degrees of freedom are allowed, at low energies the observed states are massive and singlet under the gauge group. These phenomena are known as mass gap and confinement and represent one of the major open problems of modern theoretical physics.

A possible way out to study confinement relies on putting gauge theories in Anti-de-Sitter (AdS) space, which is a maximally symmetric space with negative curvature constant. Indeed, AdS posseses a dimensionless quantity - its radius L times the dynamically generated scale Λ - which can be tuned to interpolate between a weakly coupled regime ($L\Lambda \ll 1$) and a strongly coupled regime where the flat-space physics is recovered ($L\Lambda \gg 1$). AdS has a conformal boundary and then requires some boundary conditions to be imposed. In particular, the Dirichlet boundary condition gives rise to charged asymptotic states and therefore cannot survive up to flat-space. As observed in [17] this implies a deconfinement/confinement transition as the radius is increased.

Gauge theories and their phases are not interesting only in $4d$. In lower dimensions, they provide further examples of asymptotically free theories and have applications in condensed matter physics. In higher dimensions, they are IR free and are considered effective theories at high energy. Investigating their UV behavior may lead to the discovery of non-trivial fixed points, which are currently known to exist in five dimensions only in supersymmetric cases (SCFTs [18]).

The scope of this thesis is to study the phases of gauge theories by means of perturbation theory. In particular, to analyze gauge theories in $d = 3$ and $d = 5$ we use the ϵ-expansion,

while for $d = 4$ we put the theory in AdS and develop an expansion in $L\Lambda$. We summarize below the main results and outline the structure of the thesis.

Outlook

Chapter 1 We introduce the reader to some basic concepts that will be fundamental throughout the rest of the thesis. We start by presenting the Renormalization Group and its properties, focusing on the implications of conformal invariance and the definition of monotonic quantities along the flow. We also illustrate how to use the ϵ-expansion to find and study non-trivial fixed points. We then describe gauge theories and their phases, starting with the four-dimensional case and then providing a general description of their behavior in different dimensions. We end by presenting some general aspects of QFT in AdS space, directing our attention to how to exploit these properties for the study of asymptotically free theories.

Chapter 2 We look for UV fixed points of non-abelian $SU(n_c)$ gauge theories in $4 + 2\epsilon$ dimensions with n_f Dirac fermions in the fundamental representation, using the available five-loop $\overline{\text{MS}}$ beta function and employing Padé-Borel resummation techniques and Padé approximants to the series expansion in ϵ. We find evidence for a $5d$ UV fixed point for $SU(2)$ theories with $n_f \leq 4$. We also compute the anomalous dimensions γ and γ_g of respectively the fermion mass bilinear and the gauge kinetic term operator at the UV fixed point.

Chapter 3 We compute the S^d partition function of the fixed point of non-abelian gauge theories in continuous d, using the ϵ-expansion around $d = 4$. We illustrate in detail the technical aspects of the calculation, including all the factors arising from the gauge-fixing procedure, and the method to deal with the zero-modes of the ghosts. We obtain the result up to NLO, i.e. including two-loop vacuum diagrams. Depending on the sign of the one-loop beta function, there is a fixed point with real gauge coupling in $d > 4$ or $d < 4$. In the first case, we extrapolate to $d = 5$ to test a recently proposed construction of the UV fixed point of $5d$ $SU(2)$ Yang-Mills via a susy-breaking deformation of the E_1 SCFT [19]. We find that the generalized $\widetilde{F}$-theorem allows the proposed RG flow. In the second case, we extrapolate to $d = 3$ to test whether QCD_3 with gauge group $SU(n_c)$ and n_f fundamental matter fields flows to a CFT or to a symmetry-breaking case. We find that, within the regime with a real gauge coupling near $d = 4$, the CFT phase is always favored. For lower values of n_f, we compare the average of F between the two complex fixed points with its value at the symmetry-breaking phase to give an upper bound of the critical value n_f^* below which the symmetry-breaking phase takes over.

Chapter 4 We study Yang-Mills theory on four-dimensional Anti-de Sitter space. With Dirichlet boundary condition a deconfinement/confinement transition is expected to occur

as the radius is increased. We gather hints on the nature of this transition using perturbation theory. We compute the anomalous dimensions of the lightest scalar operators in the boundary theory, which are negative for the singlet and positive for non-trivial representations. We also compute the correction to the coefficient C_J, which gives the norm of the state associated with the current operator. We estimate that the singlet operator reaches a scaling dimension equal to 3 (marginality) before the coefficient C_J vanishes. These results favor the scenario of merger and annihilation of CFTs as the most promising candidate for the transition. For the Neumann boundary condition, the lightest scalar operator is found to have a positive anomalous dimension, in agreement with the idea that this boundary condition extrapolates smoothly to flat space. The perturbative calculations are made possible by a drastic simplification of the gauge field propagator in the Fried-Yennie gauge. We also derive a general result for the leading-order anomalous dimension of the displacement operator for a generic perturbation in Anti-de Sitter, showing that it is related to the beta function of bulk couplings.

Chapter 2

General Background

In this chapter we discuss the general theoretical background supporting our research. The main references are [20–24], along with those cited throughout the text.

2.1 Quantum Field Theory and the Renormalization Group

QFTs are a cornerstone of theoretical physics, with a huge variety of applications both in high energy and condensed matter physics. Global symmetries provide a powerful tool to analyze and organize quantum field theories efficiently. These symmetries may act on the spacetime on which the theory is defined, or on internal degrees of freedom. All conventional QFTs at least have a spacetime Poincaré symmetry, which consists of translations and rotations of spacetime.

Thanks to the pioneering work of Wilson [25], we now understand that all the parameters of a QFT are defined as scale-dependent objects. This scale may be the lattice spacing in condensed matter systems or the momentum cutoff in particle physics applications. The Renormalization Group (RG) relates how theories are modified when this scale is changed. This is described by simple differential equations known as renormalization group equations. Solving these equations leads to the trajectory of a given theory in the space of all possible theories: different reference scales correspond to different values of the coupling constant and so to different points in the space of theories.

A special role in the vast landscape of QFTs is played by CFTs, which are fixed points invariant under the RG flow and hence scale invariant. In addition to Poincaré and scaling symmetry, they are also invariant under special conformal transformations.[1] These symmetries combine to form a group $SO(d+1,1)$, where d is the dimension of spacetime, and provide powerful constraints on correlation functions. CFTs have a number of practical applications,

[1] A scale invariant theory is typically also conformally invariant, hence a CFT. There exist however known examples of theories which are scale but not conformally invariant, e.g. Maxwell theory in $d \neq 4$ or more in general free p-forms theories in $d \neq 2p+2$.

from providing a description of critical systems near continuous phase transitions to playing an important role in gravity by means of the renowned AdS/CFT correspondence [26–28].

The simplest example of fixed points is given by free massless theories, also known as Gaussian fixed points. These theories lack interactions, thus preventing any quantum corrections from altering them. In some special cases, it is possible to find other non-trivial fixed points. Interacting fixed points are generally strongly coupled, but some exceptions may occur, as in the Caswell-Banks-Zaks (CBZ) fixed points and the Wilson-Fisher (WF) fixed points, which will be presented in the following sections.

2.1.1 Fixed points and conformal invariance

CFTs and RG flows

Being fixed points of the RG flow, CFTs may be seen as endpoints of RG trajectories. A QFT can be instead seen as a deformation of a CFT obtained by turning on some interaction

$$S = S_{\text{CFT}} + \int d^d x \lambda O \,. \tag{2.1}$$

Depending on the scaling dimension Δ_O of the operator at the fixed point ($\lambda = 0$), different scenarios occur. Among all possible deformations, only operators with $\Delta_O < d$ and $\Delta_O = d$, called respectively relevant and marginal, trigger interesting RG flows. When $\Delta_O > d$ instead, i.e. for irrelevant operators, the RG flow is trivial and drives back to the fixed point. In the special case $\Delta_O(\lambda) = d$ even for $\lambda \neq 0$, operators are said to be exactly marginal and the corresponding deformations move along a continuous space of CFTs, referred to as the conformal manifold. Given a set of fields, the number of relevant (and marginal) operators is finite and small, while most operators are instead irrelevant. This simplifies dramatically the description of physical systems and sits at the basis of universality, which is the fact that many different high-energy theories are described by the same physics at low energy.[2]

The crucial object describing the RG flow at a scale μ triggered by the interaction in eq.(2.1) is the beta function, defined as

$$\beta(\lambda) = \mu \frac{d\lambda}{d\mu} \,. \tag{2.2}$$

Solving this equation is in general too complicated, but it can be made easier by considering a weakly coupled deformation around a free CFT. In this situation perturbation theory is reliable and $\beta(\lambda)$ admits an expansion as follows:

$$\beta(\lambda) = (\Delta_O^{(0)} - d)\lambda + \beta_0 \lambda^2 + \beta_1 \lambda^3 + \mathcal{O}(\lambda^4) \,, \tag{2.3}$$

[2]Note that irrelevant operators cannot always be discarded. It can happen that, when multiple deformations are turned on, including a relevant one, irrelevant operators become relevant along the RG flow. These operators are said to be dangerously irrelevant. See appendix A of ref. [29] for a more detailed description and chapter 4 for an example.

where we denoted by $\Delta_O^{(0)}$ the dimension of the operator in the free theory. In the case of $\Delta_O^{(0)} = d$, i.e. for classically marginal deformations, the leading term cancels and the asymptotic behavior of the theory depends only on the sign of β_0. If $\beta_0 > 0$ the coupling is marginally irrelevant and goes to zero at long distances; the theory is said to be infrared (IR) free and cease to be perturbative at some high energy scale. If instead $\beta_0 < 0$ the coupling is marginally relevant and decreases in the ultraviolet (UV). These theories are perturbative at high energies and are said to be asymptotically free.

Solving eq.(2.3) at leading order for marginal deformations, we get

$$\lambda(\mu) = \frac{\lambda(\mu_0)}{1 - \lambda(\mu_0)\beta_0 \log(\mu/\mu_0)} \,. \tag{2.4}$$

Note that in asymptotically free theories this expression formally diverges at a scale

$$\Lambda = \mu e^{\frac{1}{\lambda(\mu)\beta_0}} \,. \tag{2.5}$$

This energy scale, which is RG invariant, is said to be dynamically generated and is purely a quantum effect of the theory.

The beta function vanishes at the fixed points, which satisfy

$$\beta(\lambda^*) = 0 \,. \tag{2.6}$$

This is clearly true at zero coupling, i.e. for free theories, but may also occur in interacting cases. Unfortunately, most of non-trivial fixed points are strongly coupled and cannot be accessed with perturbation theory. There are however two remarkable exceptions. Let us first consider a scenario where the coefficients β_0 and β_1 in eq.(2.3) have different signs and accidentally satisfy $|\beta_0/\beta_1| \ll 1$. In such a case, there exists a non-trivial perturbative solution of eq.(2.3), which is

$$\lambda^* = -\frac{\beta_0}{\beta_1} \,. \tag{2.7}$$

This fixed point is said to be of the CBZ type [30, 31].

Another possibility to find perturbative non-trivial fixed points is by analytic continuation of the spacetime dimension. The technique used to investigate the existence and properties of such fixed points is known as the ϵ-expansion and will be described in detail in sec.2.1.2.

Fixed points can be classified depending on the direction of the incoming RG flow: they are said to be IR fixed points if they are reached at low energies and UV fixed points otherwise. The value of the coupling at the fixed point is a scheme-dependent quantity, but there exist physical quantities associated with the fixed point which are unambiguous. The most important example is given by the anomalous dimension γ_O of operators, which are defined

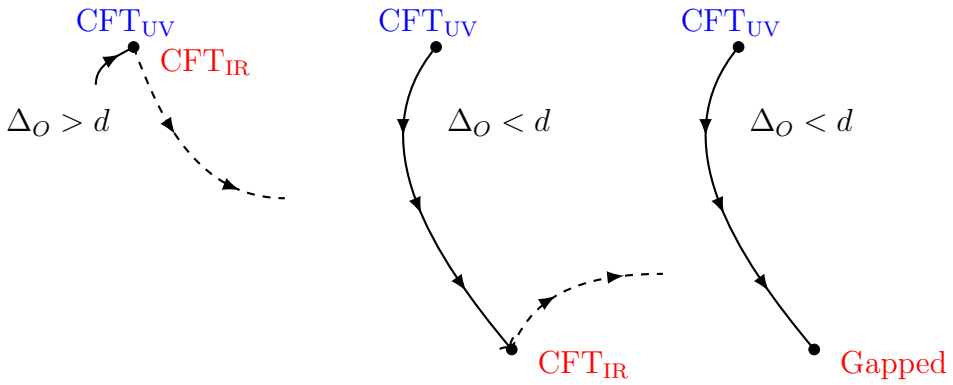

Figure 2.1: Pictorial representation of the RG flow triggered by an operator with dimension Δ_O. If $\Delta_O > d$ the deformation is irrelevant and the theory flows back to the original CFT. If $\Delta_O < d$, the trajectory may end up in a gapless theory (free or interacting CFT) or in a gapped theory (trivial or TQFT). The first two cases can be the starting point of new RG flows (dashed lines).

as the difference between the quantum dimensions of operators and their classical values:

$$\gamma_O = \Delta_O(\lambda) - \Delta_O^{(0)} \,. \tag{2.8}$$

Let us now describe different scenarios for the RG flow triggered by the deformation in eq.(2.1) (see fig.2.1). Typically, the starting point of the RG flow is a free CFT. The deformed action is then weakly coupled and can be studied with perturbation theory. If the theory remains weakly coupled throughout the RG flow, this description remains valid even in the IR. However, in most cases, the theory becomes strongly coupled along the RG trajectory, requiring a different description.

RG trajectories often end up in theories where all excitations are massive. These are said to be gapped, meaning that there is a gap in the energy spectrum between the ground state ($E = 0$) and the first excited state ($E > 0$). Below the mass scale of the lightest particle, all degrees of freedom become heavy and can be integrated out, leaving only the vacuum state. Gapped phases may be trivial, but may also develop topological aspects: in this case, theories are described by Topological QFTs (TQFTs), a special class of quantum field theories that are insensitive to local details of the system.

Sometimes, suitable RG trajectories can lead to another CFT in the IR, which can either be free or interacting, rendering the QFT gapless. Note that these endpoints of the RG flow, being CFTs themselves, can serve as the starting point for new RG flows induced by new deformations. It is important to note that aside from the free case and some notable exceptions, CFTs do not admit a Lagrangian description and require alternative methods for study.

To be more concrete, let us consider a few examples:

- Massive free particles can be seen as CFTs deformed by relevant operators, providing the simplest example of gapped theories.

- A scalar theory with quartic interactions $\lambda\phi^4$ in $d = 4$ can be viewed as a deformation of a free CFT, leading to either gapped or gapless theories depending on the presence of mass deformations. In smaller dimensions and with a fine-tuned value for the mass, the theory develops a WF fixed point which persists down to $d = 2$.

- Quantum Electrodynamics (QED) in $d = 4$ gives a trivial example of a theory with massless particles in the IR: for energies much smaller than the mass of the electron, only free photons survive. If the electron were massless, the theory would still be gapless, but the IR phase would be reached very slowly (logarithmically).[3]

- Quantum Chromodynamics (QCD) in $d = 4$ with a small number of massive quarks is asymptotically free: it has a weakly coupled description in the UV, but becomes strongly coupled in the IR, undergoing confinement and chiral symmetry breaking. This results in gapped states, where massive excitations are bound states of gluons and quarks: mesons, baryons, and glueballs.

- Massless QCD in $d = 4$ has different behaviors depending on the number of quarks: if it is small spontaneous breaking of the chiral symmetry occurs, leading to a theory of massless Goldstone bosons (free CFT). For some larger number of quarks, the theory flows to a CBZ fixed point, resulting in a gapless interacting IR theory.

We will discuss in detail the last two points in sec.2.2.1, while describing the properties of four-dimensional non-abelian gauge theories.

Conformal symmetry and constraints on correlation functions

The conformal group of symmetries is the set of spacetime transformations that rescale lengths but locally preserve angles. It is an extension of the Poincaré group: besides space-time translations and rotations, it includes scale transformations and the so-called special conformal transformation (SCT). For scalar fields, the generators are[4]

$$\begin{aligned} &P_\mu = \partial_\mu && \text{(translation)} \\ &M_{\mu\nu} = (x_\nu\partial_\mu - x_\mu\partial_\nu) && \text{(rotation)} \\ &D = x_\mu\partial_\mu && \text{(dilation)} \\ &K_\mu = -x^2\partial_\mu + 2x_\mu x_\nu\partial_\nu && \text{(SCT)} \end{aligned} \tag{2.9}$$

[3] In this case and in the previous one the strict UV limit is not defined: the couplings get larger and larger as the energy scale increases and become infinite at a scale $\Lambda_L = \mu e^{\frac{1}{\lambda(\mu)\beta_0}}$ (Landau pole), resulting in a breakdown of perturbation theory.

[4] We use the conventions for the generators of [32].

Taking commutators of these generators, one can show that the conformal algebra is in fact isomorphic to $SO(d+1,1)$. A generic conformal transformation $x^\mu \to x'^\mu$ satisfies

$$\delta_{\mu\nu}\frac{\partial x'^\mu}{\partial x^\alpha}\frac{\partial x'^\nu}{\partial x^\beta} = \Omega(x)^2\delta_{\alpha\beta} \tag{2.10}$$

with $\Omega(x)$ arbitrary function of the coordinates. At the infinitesimal level $x'^\mu = x^\mu + \epsilon^\mu$ and $\Omega(x) = 1 + \omega(x)/2$, implying

$$\partial_\mu\epsilon_\nu + \partial_\nu\epsilon_\mu = \omega(x)\delta_{\mu\nu}\,. \tag{2.11}$$

This equation has a finite number of solutions for $d > 2$, which read

$$\begin{aligned}
&\epsilon^\mu = \text{constant} && \text{(translation)}\\
&\epsilon^\mu = x^\nu\omega_{[\nu\mu]} && \text{(rotation)}\\
&\epsilon^\mu = \lambda x^\mu && \text{(dilation)}\\
&\epsilon^\mu = 2(a\cdot x)x^\mu - x^2a^\mu && \text{(SCT)}\,,
\end{aligned} \tag{2.12}$$

where a^μ is an arbitrary vector. The case $d = 2$ has infinite solutions and requires indeed special attention: the conformal transformations correspond in this case to holomorphic transformations from the complex plane onto itself and the algebra of generators is infinite-dimensional.[5] To find the finite form of the transformations we only need to integrate eq.(2.12). The only nontrivial case is that of SCT, which gives

$$x'^\mu = \frac{x^\mu - a^\mu x^2}{1 - 2(a\cdot x) + a^2x^2}\,. \tag{2.13}$$

It is convenient to think about SCT as the composition of an inversion

$$x'^\mu = \frac{x^\mu}{x^2}\,. \tag{2.14}$$

followed by a translation followed by another inversion.

Let us now focus on how conformal symmetry constrains correlation functions of local operators in a CFT. Consider first scalar operators. Operators transforming as

$$O(x) = \left|\frac{dx'}{dx}\right|^{\frac{\Delta}{d}} O'(x') \tag{2.15}$$

under a conformal transformation are called primaries. Specifying to a dilation $x'^\mu = \lambda x^\mu$, primary operators satisfy

$$O(x) = \lambda^\Delta O'(x')\,. \tag{2.16}$$

Operators that are not primaries are said to be descendants and can be obtained by differentiating primary operators.

[5] See e.g. chapter 5 of ref. [33] for a complete introduction on the topic.

Conformal symmetry gives constraints on correlation functions of primary operators. In particular, the one-point functions $\langle O(x)\rangle$ vanish for any primary except for the identity operator (which is the unique operator with $\Delta = 0$). The two-point functions are different from zero only if the dimensions of the operators are the same

$$\langle O_i(x)O_j(y)\rangle = C_{O_i}\frac{\delta_{ij}}{|x-y|^{2\Delta_i}}\,, \tag{2.17}$$

while three-point functions are constrained to be

$$\langle O_i\left(x_i\right)O_j\left(x_j\right)O_k\left(x_k\right)\rangle = \frac{C_{O_iO_jO_k}}{|x_i-x_j|^{\Delta_i+\Delta_j-\Delta_k}\,|x_j-x_k|^{\Delta_j+\Delta_k-\Delta_i}\,|x_k-x_i|^{\Delta_k+\Delta_i-\Delta_j}}. \tag{2.18}$$

Note that after normalizing the two-point function to have unit coefficient $C_{O_i} = 1$, the normalization of the three-point function is physically meaningful. This choice is commonly taken, but for our purposes, it is more convenient to keep C_{O_i} to be a general real number.

Let us now consider operators with spin $J \neq 0$. If operators have spin, the transformation rule of primaries changes into

$$O_a(x) = \Omega\left(x'\right)^{\Delta} D\left(R\left(x'\right)\right)^{a}{}_{b}\, O'^{b}\left(x'\right)\,, \tag{2.19}$$

where

$$\frac{\partial x'^{\mu}}{\partial x^{\nu}} = \Omega(x')R^{\mu}{}_{\nu}(x'), \quad R^{\mu}{}_{\nu}(x') \in SO(d). \tag{2.20}$$

and $D(R)^a{}_b$ implements the action of the $SO(d)$ rotation R in the representation of O. In particular, tensor primary fields of scaling dimension Δ and integer spin J transform as follows

$$T_{\mu_1\ldots\mu_J}(x) = \left|\frac{\partial x'}{\partial x}\right|^{\frac{\Delta-J}{d}} \frac{\partial x'^{\nu_1}}{\partial x^{\mu_1}}\cdots\frac{\partial x'^{\nu_J}}{\partial x^{\mu_J}} T'_{\nu_1\ldots\nu_J}\left(x'\right). \tag{2.21}$$

Imposing this transformation on correlation function we find again that one-point functions need to vanish. Given

$$I_{\mu\nu}(x) = \eta_{\mu\nu} - 2\frac{x_\mu x_\nu}{x^2}, \tag{2.22}$$

the two-point functions for vector and spin 2 symmetric traceless operators satisfy

$$\langle J_\mu(x)J_\nu(y)\rangle = \frac{C_J}{|x-y|^{2\Delta}} I_{\mu\nu}(x-y) \tag{2.23}$$

$$\langle T_{\mu\nu}(x)T_{\alpha\beta}(y)\rangle = \frac{C_T}{|x-y|^{2\Delta}}\left(\frac{(I_{\mu\alpha}(x-y)I_{\nu\beta}(x-y)+I_{\mu\beta}(x-y)I_{\nu\alpha}(x-y))}{2} - \frac{\eta_{\mu\nu}\eta_{\alpha\beta}}{d}\right) \tag{2.24}$$

respectively. One can also compute the most general three-point function of three spin-J operators. The number of tensor structures consistent with conformal symmetry is more

than one in general, but it is always finite.

Among local operators, a special role is played by the currents J_μ associated with global symmetries and the stress tensor $T_{\mu\nu}$. These objects are conserved

$$\partial_\mu J^\mu = 0 \quad , \partial_\mu T^{\mu\nu} = 0\,, \tag{2.25}$$

which fixes their dimension to be $\Delta_J = d-1$ and $\Delta_T = d$ respectively. To obtain this, it is sufficient to impose the conservation laws to eq.(2.23) and eq.(2.24), knowing that the stress-tensor is traceless at the fixed points, as we prove in the following section.

Unitary CFT cannot have primary operators with any dimension. Indeed, there exist bounds restricting the possible dimensions of primary fields. We have inequalities that depend on the Lorentz quantum number:

$$\begin{aligned} &\Delta > \frac{d}{2} - 1 && \text{(scalars)} \\ &\Delta > \frac{d-1}{2} && \text{(fermions)} \\ &\Delta > d + J - 2 && \text{(spin } J \text{ tensors)}\,. \end{aligned} \tag{2.26}$$

State/operator correspondence and OPEs

A powerful concept of CFTs is the state-operator correspondence, which establishes a direct connection between local operators on $\mathbb{R}^d$ and quantum states on S^{d-1}. The correspondence is obtained by using radial quantization on $\mathbb{R}^d$. Writing the radial coordinate as $r = e^\tau$ and acting with a Weyl transformation

$$ds^2 = dr^2 + r^2 d\Omega_{d-1}^2, \qquad \to \quad ds^2 = d\tau^2 + d\Omega_{d-1}^2\,, \tag{2.27}$$

flat space $\mathbb{R}^d$ can be mapped into a cylinder $\mathbb{R} \times S^{d-1}$. The distance from the origin is then identified with the time τ. A rescaling $r \to \lambda r$ then corresponds to a shift in time $\tau \to \tau + \log\lambda$. Since the generator of time translations is the Hamiltonian, the scaling dimension of an operator in $\mathbb{R}^d$ corresponds to the energy of the state on S^{d-1}. If no local operator is inserted, then the state created on S^{d-1} is the vacuum state. If an operator O_Δ is inserted at the origin, the corresponding state $|O_\Delta\rangle$ is the one created on S^{d-1} at $\tau \to -\infty$ with energy $E = \Delta$. On the other hand, a state on a constant time slice of the cylinder corresponds to a boundary condition on a sphere around the origin, which can be made arbitrarily small thanks to conformal invariance (if no other operator is inserted), boiling down to a local operator. Note that the state/operator correspondence can be used to prove the unitarity bounds of eq.(2.26), simply by imposing that all descendants correspond to states with positive norms.

Consider now the insertion of two local operators O_i and O_j in $\mathbb{R}^d$, respectively at a point x inside a sphere and at the origin. By the state/operator map, they correspond to a state

$|\Psi\rangle = O_i(x)O_j(0)|0\rangle$ on the surface of the sphere. This state can be decomposed in energy eigenstates

$$|\Psi\rangle = \sum_n c_n \, |E_n\rangle \, , \quad c_n = c_n(x) \, . \tag{2.28}$$

which are in one-to-one correspondence with eigenstates of the dilation generator, either primaries or descendants. We can thus write

$$O_i(x)O_j(0)|0\rangle = \sum_k C_O^k \, (x, \partial_y) \, O_k(y)\big|_{y=0} \, |0\rangle, \tag{2.29}$$

where k runs over all the primaries of the theory and $C_O^k \, (x, \partial_y)$ denotes implicitly a power series in ∂_y. The product of two operators at nearby points can be then rewritten as a series of operators at one point only. The existence of this series, known as operator product expansion (OPE), is a general fact of local QFTs, but gives rise to particularly powerful properties in CFTs. Conformal symmetry, indeed, ensures convergence of the series as far as the sphere around the two operators hits another operator. Moreover, it relates the coefficients of the series to the coefficients of two-point and three-point functions of primaries. Restricting O_i and O_j to be scalar primaries, we get

$$O_i(x)O_j(0) = \sum_k C^{O_k}_{O_iO_j} |x|^{\Delta_k - \Delta_i - \Delta_j} (O_k(0) + \text{descendants } \ldots) \, , \tag{2.30}$$

where $C^{O_k}_{O_iO_j} = C_{O_iO_jO_k}/C_{O_k}$ and $C_{O_iO_jO_k}, C_{O_k}$ are defined in (2.17) and (2.18) respectively. Note that the series in eq.(2.30) includes also spinning operators (traceless symmetric). The set of coefficients $C^{O_k}_{O_iO_j}$, the dimensions Δ_i, and the spin of the operators appearing in the OPE expansion is referred to as the CFT data and allows to compute all correlation functions, i.e. to solve the theory.

The OPE lowers the number of operators in correlation functions and can be then used as a tool to reduce them. Notably, different procedures of reduction must give the same result. This concept is known as OPE associativity and provides conditions to define consistent CFT data. Imposing this constraint together with unitarity and, if needed, the existence of a primary operator with $\Delta = d$ (playing the role of the stress energy tensor) allows to restrict remarkably the allowed set of CFTs. This idea is at the foundation of an active and challenging research field, known as the conformal bootstrap (see e.g. [32] for an introduction and [34, 35] for extensive reviews).

Stress-energy tensor and anomalous breaking of scale-invariance

Given a QFT, the stress-energy tensor is the conserved tensor associated with the translational symmetries.[6] It can be directly computed by coupling the QFT to gravity and deriving

[6]The minimal set of QFT axioms (Wightman axioms [36]), does not require the existence of the stress tensor as the energy and momentum density. However, assuming the existence of this operator is natural and implies locality of the theory.

$$T_{\mu\nu} = -\frac{2}{\sqrt{g}}\frac{\delta S}{\delta g^{\mu\nu}}\bigg|_{g_{\mu\nu}=\delta_{\mu\nu}}, \tag{2.31}$$

where $g_{\mu\nu}$ is the metric and $g = \det(g_{\mu\nu})$. If the QFT is classically scale invariant, i.e. if it contains only marginal operators in its action, the stress-tensor is classically traceless. Indeed, the current associated with scaling transformations, known as the dilation current D_μ, satisfies

$$D_\mu = x^\nu T_{\mu\nu}\,. \tag{2.32}$$

Conservation of D_μ then implies that $T_{\mu\nu}$ is traceless.[7]

At the quantum level, scale invariance is instead typically broken. Invariance of the quantum action under scaling transformations $x^\mu \to e^{-\sigma}x^\mu$ implies that

$$\begin{aligned}&\int d^dx\,\mathcal{L}(\phi(x),\partial_\mu\phi(x),\lambda(x)) = \int d^dx\,\mathcal{L}(e^{-\sigma\Delta}\phi(e^{-\sigma}x),e^{-\sigma(\Delta+1)}\partial_\mu\phi(e^{-\sigma}x),\lambda(x))\\ &= \int d^dx\,e^{d\sigma}\mathcal{L}(e^{-\sigma\Delta}\phi(x),e^{-\sigma(\Delta+1)}\partial_\mu\phi(x),\lambda(e^{\sigma}x)),\end{aligned} \tag{2.33}$$

For a classically scale-invariant theory,

$$\mathcal{L}(e^{-\sigma\Delta}\phi(x),e^{-\sigma(\Delta+1)}\partial_\mu\phi(x),\lambda) = e^{-d\sigma}\mathcal{L}(\phi(x),\partial_\mu\phi(x),\lambda). \tag{2.34}$$

Under an infinitesimal transformation $\sigma \ll 1$,

$$\lambda(x+\sigma x) = \lambda(x) - \sigma\beta(\lambda), \tag{2.35}$$

and so the violation of the scaling symmetry is given by

$$\delta S = \int d^dx\,(\mathcal{L}(\phi(x),\partial_\mu\phi(x),\lambda(x+\sigma x)) - \mathcal{L}(\phi(x),\partial_\mu\phi(x),\lambda(x))) = -\sigma\int d^dx\frac{\partial\mathcal{L}}{\partial\lambda}\beta(\lambda)\,. \tag{2.36}$$

Correspondingly, the divergence of the dilatation current is anomalous and the trace of the stress tensor is non-vanishing, with the anomaly given by the β-function:

$$\partial_\mu D^\mu = T^\mu_\mu = \beta(\lambda)\frac{\partial\mathcal{L}}{\partial\lambda}\,. \tag{2.37}$$

Note that, as the beta function vanishes at the fixed points, CFTs have traceless stress-tensor also at the quantum level.

Adding a boundary: an introduction to BCFTs

Let us now consider a CFT in a space with a boundary, known as boundary conformal field theory (BCFT). Here we consider the simplest case of a CFT in half-flat space, but the

[7] Usually the stress-energy tensor defined in eq.(2.31) is not traceless on its own, but can be made traceless by adding a manifestly conserved tensor.

formulas below can be generalized to other spaces with boundaries and, more generally, to theories with conformal defects (DCFTs). To be consistent with the notation of the rest of this thesis, we take here d, $d+1$ to be the dimension of the boundary and the bulk respectively.

The fusion of primary operators in the bulk is clearly unaffected by the presence of the boundary and controlled by the usual bulk OPE of eq.(2.30). However, when a bulk operator is brought close to the boundary, it becomes indistinguishable from a boundary excitation, which we denote by adding hats on operators. Therefore, a new bulk-to-boundary OPE (bOPE) has to be introduced, which is

$$O(x,z) = \sum_{\hat{O}_k} z^{\hat{\Delta}_k - \Delta} B_O^{\ \hat{O}_k} \hat{O}_k(x) + \dots \,, \tag{2.38}$$

where x is the coordinate on the boundary and $z \geq 0$ is the coordinate perpendicular to it. Like its bulk counterpart, conformal symmetry ensures convergence of the bOPE and relates the bOPE coefficients to coefficients of primary correlation functions. The coefficients $B_O^{\hat{O}_k}$, indeed, are related to the two-point function of a bulk and a boundary operator. In the scalar case, we have

$$\langle O(x,z)\hat{O}(0)\rangle = B_{O\hat{O}} z^{\hat{\Delta}-\Delta} x^{-2\hat{\Delta}}, \tag{2.39}$$

where $B_{O\hat{O}} = B_O^{\ \hat{O}}/C_{\hat{O}}$ if we consider non unit-renormalized primaries. Among the bulk-to-boundary OPE coefficients, the one of the identity $B_O^{\hat{\mathbf{1}}}$ plays a special role, as it allows bulk operators to acquire an expectation value. This is typical of BCFTs and cannot occur in CFTs without a boundary.

Finally, boundary operators can be fused as well, so that one last boundary-to-boundary OPE exists, which is equivalent to the bulk OPE in one dimension less.

In every BCFT a boundary operator with protected dimension $\Delta = d+1$ appears in the spectrum. This is known as the displacement operator, and is related to the breaking of translational invariance at the boundary. The stress tensor is indeed not fully conserved and its divergence has a delta-function contribution located at the boundary, proportional to the displacement operator itself. In half-flat space, for instance, the displacement operator $\mathcal{D}$ can be defined as

$$\partial^\mu T_{\mu z}(x,z) = \mathcal{D}(x)\delta(z)\,, \tag{2.40}$$

where again x and z are the parallel and perpendicular directions with respect to the boundary.

2.1.2 WF fixed points and the ϵ-expansion

Studying RG flows in strongly coupled regimes is a hard task. Several techniques were developed to overcome this problem. The most successful certainly are the large N expansion [37] (see also [38] for a more general review) and the ϵ-expansion [25, 39]. The first is based

on the fact that when the number of degrees of freedom N in the theory is very large, only a few diagrams contribute to correlation functions, which can be resummed and computed exactly. The second instead relies on the analytic continuation of the spacetime dimension d and on the expansion of d around a critical dimension d_c at which the theory is perturbative. Let us present more in detail this technique, known as ϵ-expansion.

It is sometimes possible to continue RG flows to non-integer dimensions, at least formally. When a flow to an interacting fixed point can be continued to the vicinity of its upper or lower critical dimension, it becomes short and controllable in perturbation theory. This strategy can lead to a useful approximation of strongly coupled fixed points. The idea is to introduce a parameter $\epsilon = d_c - d$ and to compute the RG functions as perturbative expansions in ϵ. The resulting expansions are obviously reliable for $\epsilon \ll 1$, but may provide surprisingly good results even for larger value of ϵ. This technique was first applied to $\lambda\phi^4$ theories in $d < 4$, in the breakthrough work of Wilson and Fisher [39]. Consider the action for a scalar field in $d = 4 - \epsilon$:

$$S = \int d^d x \left(\frac{1}{2}(\partial\phi)^2 + \frac{1}{2} t \mu^2 \phi^2 + \frac{1}{4!} \lambda \mu^{d-4} \phi^4 \right). \tag{2.41}$$

One can compute the beta functions at small coupling:

$$\begin{aligned} \beta(\lambda) &= -(4-d)\lambda + c_1 \lambda^2 + \dots \\ \beta(t) &= -2t + c_2 t\lambda + \dots, \end{aligned} \tag{2.42}$$

where c_1 and c_2 are constants that depend on the renormalization scheme. These beta functions have two zeros: $t = 0,\ \lambda = 0$ and $t = 0,\ \lambda = \lambda^* \equiv (4-d)/c_1$. The first zero corresponds to the Gaussian fixed point, while the other is the WF fixed point, weakly coupled at $\epsilon \ll 1$.[8] Thanks to the good behavior of the asymptotic expansion, one can extract the value of the anomalous dimensions up to $\epsilon = 1, 2$, corresponding to $d = 3, 2$. These results reproduce quite accurately the experimental results of critical exponents for the Ising model.[9]

Since its first appearance, the ϵ-expansion has been widely used. Let us list the most famous applications (see fig.2.2):[10]

- Critical $O(N)$ universality class in $2 < d < 4$ can be studied as the IR fixed point of $\lambda(\phi_i\phi_i)^2$ theory in $d = 4 - \epsilon$ or equivalently as the UV fixed point of the non-linear sigma model (NLσM) in $d = 2 + \epsilon$.

- Critical Gross-Neveu universality class can be instead reached from $d = 2 + \epsilon$ Gross-Neveu (UV fixed point) or from Gross-Neveu-Yukawa theory in $d = 4 - \epsilon$ (IR fixed

[8] In order to reach this fixed point we need to fine-tune the mass coupling to be precisely zero. If the initial value of t is slightly different, then we end up with a theory of massive particles, either $t \to \infty$ ($\mathbb{Z}_2$ preserving), or $t \to -\infty$ ($\mathbb{Z}_2$ breaking).

[9] The ϵ-expansion, when properly resumed, is a competitive technique, but an even better estimate can be obtained with the conformal bootstrap [40].

[10] Note that in most cases the ϵ-expansion results where matched with large-N results, which can be obtained for a generic value of the spacetime dimension.

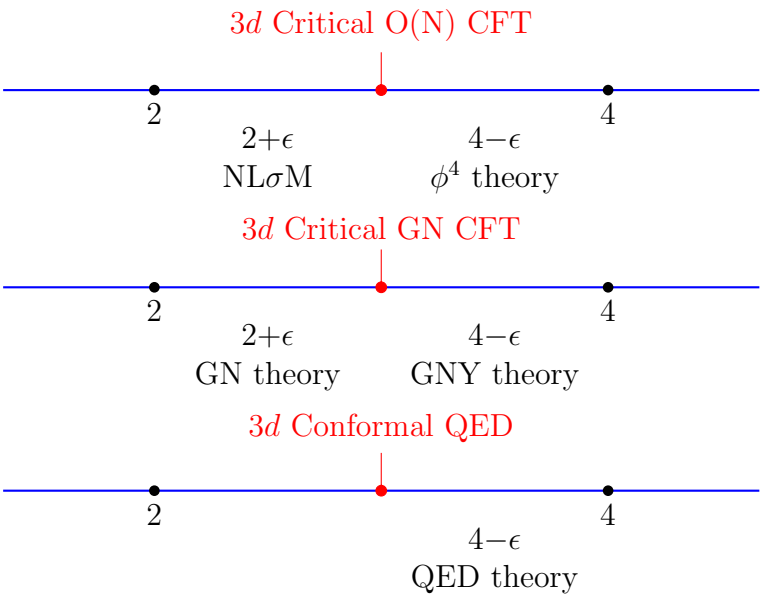

Figure 2.2: Interacting CFTs exist for $O(N)$ models, GN models and QED with a sufficently large number of fermions in $2 < d < 4$.

point).

- In three dimensions, QED with a sufficiently large number of fermion flavors can exhibit a fixed point, which can be understood as the IR WF fixed point of QED in $d = 4 - \epsilon$.

- Non-abelian gauge theories may develop a non-trivial fixed point in $d < 4$ when the number of flavors is large (IR fixed point) and in $d > 4$, when the number of flavors is small (UV fixed point). We refer to chapter 3 for a more complete analysis of the latter fixed point.

2.1.3 Monotonicity theorems for the Renormalization Group

A relevant topic in the study of d-dimensional QFTs concerns the search for constraints on the RG trajectories. It was indeed proven that certain quantities can only decrease when flowing from a short-distance fixed point (UV) to a long-distance one (IR), expressing the reduction of degrees of freedom as the energy scale is lowered. Such quantities were first found in even dimensions [41–44] and identified with the universal Weyl anomaly a, defined as

$$\langle T^{\mu}_{\mu} \rangle \sim (-1)^{d/2} a E_d + \sum_i c_i I_i \tag{2.43}$$

where E_d is the Euler density term, which is present in all even $d \geq 2$, and c_i are the coefficients of other Weyl invariant curvature terms. We have indeed

$$a_{\text{UV}} > a_{\text{IR}} \,. \tag{2.44}$$

This is still a conjecture in $d = 6$, while it was rigorously proven in lower even dimension. In $d = 2$ this is well-known as the c-theorem [41], as in this case the unique Weyl anomaly coefficient can be expressed in terms of the Virasoro central charge c through the relation $a = c/3$.

As there are no Weyl anomalies in odd dimensions, some different quantity should be found in this case. The free energy on the sphere, defined as

$$F = -\log Z_{S^d}, \tag{2.45}$$

plays such role in $d = 3$, satisfying

$$F_{\rm UV} > F_{\rm IR}. \tag{2.46}$$

This inequality, known as the F-theorem, was proven rigorously by exploiting the equivalence among the free energy and the entanglement entropy across a circle in $d = 3$ [45, 46]. Notice that the free energy in even dimensions diverges and cannot be used to this purpose. For other odd dimensions it is conjectured that the decreasing quantity becomes $(-1)^{(d+1)/2}F$. This has not been rigorously proven yet but is supported by several examples.

The Generalized $\widetilde{F}$-theorem

Motivated by the ϵ-expansion results, ref. [47] proposed to unify all the previously mentioned inequalities in a single relation valid in continuous dimensions. The authors defined

$$\widetilde{F} = -\sin\left(\frac{\pi d}{2}\right) F, \tag{2.47}$$

which in odd d exactly reproduces the $(-1)^{(d+1)/2}F$ term, while in even d provides a smooth limit proportional to the a-anomaly: the factor $\sin(\frac{\pi d}{2})$ cancels the pole in the free energy leading to the finite limit $\widetilde{F} = \pi a/2$. Therefore, the inequality

$$\widetilde{F}_{\rm UV} > \widetilde{F}_{\rm IR} \tag{2.48}$$

automatically encodes all the previous relations, and extends them to non-integer values of d.

A first check of this inequality, known as the Generalized $\widetilde{F}$-theorem, is provided by conformally coupled scalars and fermions. Their free energies were computed in ref. [48] and read

$$\widetilde{F}_{\text{free-S}}(d) = \frac{1}{\Gamma(d+1)} \int_0^1 du\ u\ \sin(\pi u)\, \Gamma\left(\frac{d}{2}+u\right) \Gamma\left(\frac{d}{2}-u\right)\ . \tag{2.49}$$

$$\widetilde{F}_{\text{free-F}}(d) = \frac{\text{tr}\mathbb{1}}{\Gamma(1+d)} \int_0^1 du\ \cos\left(\frac{\pi u}{2}\right) \Gamma\left(\frac{1+d+u}{2}\right) \Gamma\left(\frac{1+d-u}{2}\right)\ , \tag{2.50}$$

where $\text{tr}\mathbb{1}$ is the trace of the identity in the Dirac matrices space. These functions are positive

for all d. If we add a mass term these theories flow to trivial ones, where $\widetilde{F} = 0$, consistently with the inequality in eq.(2.48).

Anther interesting application involves RG flows produced by double-trace operators in large N theories. Consider a CFT perturbed by the square of a primary scalar operator O_Δ of dimension $\Delta < d/2$. In the large N limit, this is a relevant perturbation that triggers a flow to another CFT where the corresponding operator has dimension $d - \Delta + \mathcal{O}(1/N)$ [49, 50]. This produces the following change in $\tilde{F}$ [47, 51]:

$$\tilde{F}_{\rm IR} - \tilde{F}_{\rm UV} = \frac{1}{\Gamma(1+d)} \int_0^{\Delta - \frac{d}{2}} du\, u \sin \pi u\, \Gamma\left(\frac{d}{2} + u\right) \Gamma\left(\frac{d}{2} - u\right) + \mathcal{O}(1/N)\,. \tag{2.51}$$

This result is negative throughout the range $(d-2)/2 < \Delta < d/2$, confirming consistency with the Generalized F-Theorem. Nevertheless, when Δ falls significantly below the unitarity bound, the condition (2.48) fails to hold. Indeed, the theorem may not apply in non-unitary theories.

The generalized $\widetilde{F}$-theorem can also be applied to RG trajectories which end up into WF fixed points. Let us consider for example critical $O(N)$ in $d < 4$, which we presented in the previous section. Ref. [48] computed $\widetilde{F}_{O(N)}$ as a perturbative expansion in ϵ and verified that it is smaller than the value of $\widetilde{F}$ at the free point: $\widetilde{F}_{O(N)} < N \widetilde{F}_{\text{free-S}}$, consistently with the Generalized $\widetilde{F}$-theorem. The authors also verified the possibility to reach the same interacting fixed point starting from N copies of Ising theory and acting with an S_N-invariant relevant deformation. They found that in $d = 3$ the flow is allowed only for $N \leq N^*$, with $N^* \simeq 4$.[11] Performing a relevant deformation to critical $O(N)$, one may flow to a theory in which $O(N)$ is spontaneously broken to $O(N-1)$. In this phase there are $N-1$ Goldstone bosons and the sphere free energy is $\widetilde{F}_{\rm SB} = (N-1)\widetilde{F}_{\text{free-S}}$. The inequality $\widetilde{F}_{\rm SB} < \widetilde{F}_{O(N)}$ is verified for all values of N and so the flow is allowed. We refer to fig.2.3 for a pictorial representation of this expected RG flow.

2.2 Non-Abelian Gauge theories: general properties

Gauge theories are a cornerstone of modern theoretical physics, playing a central role in understanding the fundamental forces that govern the universe. They have been crucial in the development of the Standard Model of particle physics and have also found applications in other areas of physics, such as condensed matter physics. They are redundant theories, meaning that they make sense only by identifying states related by some local (gauge) transformations. This redundancy means that only gauge invariant quantities should be considered physical.

Non-abelian gauge theories are gauge theories in which gauge transformations do not necessarily commute with each other. This introduces a rich structure, including phenomena like

[11] For higher values of N, the same relevant deformation leads to another fixed point, known as the cubic fixed point, which is S_N-symmetric instead.

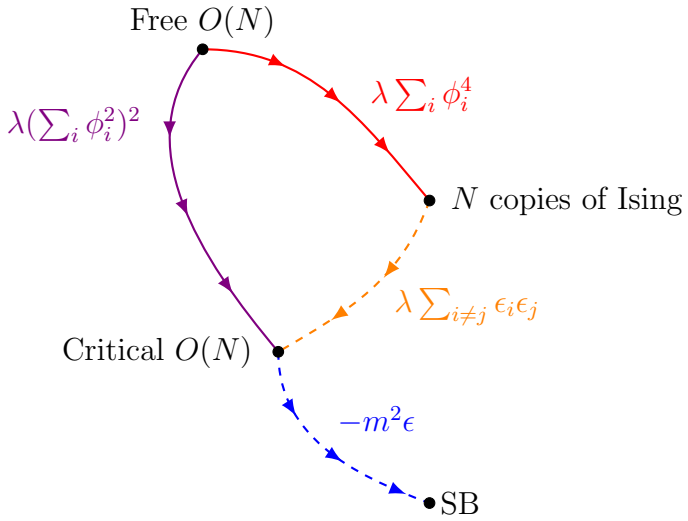

Figure 2.3: Expected RG flow from and towards $3d$ critical $O(N)$. This may be reached in two different ways: by perturbing the free theory (purple line) or, for $N \lesssim 4$, by deforming N copies of the Ising theory (dashed orange line). The N copies of Ising are themselves obtained from a deformation of the free theory (red line). With a relevant deformation, one may flow from critical $O(N)$ to a spontaneously broken phase (dashed blue line). All these flows are allowed by the Generalized $\widetilde{F}$-theorem.

confinement and asymptotic freedom, which are absent in abelian theories. The prototypical example is QCD, the theory of the strong interaction, which describes the interactions between quarks and gluons via the $SU(3)$ gauge group. Another significant application is the electroweak theory, part of the Standard Model of particle physics, which unifies the weak and electromagnetic interactions under an $SU(2) \times U(1)$ gauge group.

Non-abelian gauge theories are constructed starting from a compact Lie group G and the corresponding Lie algebra g, whose generators t^a satisfy

$$[t^a, t^b] = i f^{abc} t^c \tag{2.52}$$

where $a, b, c = 1 \dots \dim(g)$ and f^{abc} are fully anti-symmetric structure constants. We mainly focus on the case $G = SU(n_c)$, even if other options are possible and interesting. We take the generators in the fundamental representation to be normalized as

$$\mathrm{tr}\,[t_f^a t_f^b] = T_f \delta^{ab}\,, \quad T_f = \frac{1}{2}\,, \tag{2.53}$$

while other representations R satisfy

$$\mathrm{tr}\,[t_R^a t_R^b] = T_R \delta^{ab}\,, \tag{2.54}$$

where T_R is called the Dynkin index. The generators in a given representation R also satisfy

$$t_R^a t_R^a = C_R \mathbb{1}\,, \tag{2.55}$$

where C_R is the quadratic Casimir of the representation. Among all representations, a special role is played by the adjoint, whose generators are related to the structure constants themselves ($(t^{ab}_{\text{adj}})^c = if^{abc}$). The corresponding Dynkin index $T_{(\text{adj})}$ equals C_A, which is n_c for $SU(n_c)$ group.

For each element of the Lie algebra, we associate a gauge field A^a_μ and the field strength

$$F^a_{\mu\nu} = \partial_\mu A^a_\nu - \partial_\nu A^a_\mu + f^{abc} A^b_\mu A^c_\nu \,, \tag{2.56}$$

which will be used to construct the action. The set of maps $U(x)$ from spacetime to G is known as the gauge group. Under such transformations, the gauge field and the field strength transform respectively as

$$A_\mu \to U(x) A_\mu U(x)^{-1} + iU(x)\partial_\mu U(x)^{-1} \tag{2.57}$$

and

$$F^{\mu\nu} \to U(x) F^{\mu\nu} U(x)^{-1} \,, \tag{2.58}$$

where we used the compact notation $A^\mu = A^\mu_a t^a_f$ and $F^{\mu\nu} = F^{\mu\nu}_a t^a_f$. Pure gauge theories (i.e. without matter) are called Yang-Mills theories and have the action

$$S_{\text{YM}} = \frac{1}{2g^2} \int d^d x \ \text{tr}\, F^{\mu\nu} F_{\mu\nu} = \frac{1}{4g^2} \int d^d x F^{\mu\nu}_a F^a_{\mu\nu} \,, \tag{2.59}$$

where g^2 is the gauge coupling. The corresponding equations of motion read

$$D_\mu F^{\mu\nu} = 0 \,, \tag{2.60}$$

where D_μ is the covariant derivative which will be defined in a moment.

To add matter fields ψ, we need to specify some representation R of the gauge group G and couple to gauge field through covariant derivatives, defined by

$$D^\mu \psi^i = \partial^\mu \psi^i - iA^\mu_a (t^a_R)^i_j \psi^j \,, \tag{2.61}$$

with $i, j = 1 \ldots \dim R$. In our discussion, we will mainly focus on the case of fermionic matter fields in the fundamental representation.

The quantization of gauge theories is a non-trivial task. The problem arises becaus the redundancy introduced by the gauge symmetry leads to an overcounting in the path integral formulation. All pure gauge configurations are not damped by the action and lead to a divergence in the gauge propagator. This can be cured by adding a gauge-fixing term in the action and introducing in the theory anticommuting scalar fields (ghosts) [52]. The final action is then

$$S_{\text{gauge}} = S_{\text{YM}} + S_{\text{matter}} + S_{\text{GF}} + S_{\text{ghost}} \,, \tag{2.62}$$

with

$$S_{\rm GF} = \frac{1}{2\xi}(\partial_\mu A_a^\mu)^2 \tag{2.63}$$

and

$$S_{\rm ghost} = \bar{c}^a \partial_\mu D^\mu c_a \,, \tag{2.64}$$

where ξ is the gauge-fixing parameter and c and $\bar{c}$ are the ghost and anti-ghost respectively.

2.2.1 Gauge theories in $d = 4$: asymptotic freedom, confinement and the conformal window

Gauge theories present different phases at low energies, with incredibly rich properties and physical phenomena. Understanding the full phase diagram of gauge theories, in particular of $4d$ non-abelian gauge theories, is an extremely hard task. We present here the basic classification of non-abelian gauge theories, pure and with the addition of fermionic matter (QCD-like).

The fundamental quantity to describe the RG flow of non-abelian gauge theories is the beta function of the gauge coupling, which is the only coupling appearing in the action. It is convenient to introduce the loopwise expansion parameter

$$a = \frac{g^2}{16\pi^2}, \tag{2.65}$$

with related beta function

$$\beta^{\rm 4d}(a) = \mu \frac{da}{d\mu} = \sum_{n=0}^{\infty} \beta_n \, a^{n+2} \,. \tag{2.66}$$

Note that, from now on, unless explicitly specified, the notation β_n will refer to the coefficient defined above.

The IR fate of Yang-Mills theories

At leading order in $d = 4$, Yang-Mills theories have

$$\beta_0 = -\frac{22}{3} C_A, \tag{2.67}$$

which is crucially negative, making the theory asymptotically free. As we explained previously, this means that the theory is well-described by perturbation theory at high energy. In this regime, it is a theory of massless interacting vector fields (gluons). As we decrease the energy and reach the dynamically generated scale

$$\Lambda_{\rm YM} = \mu e^{\frac{1}{\beta_0 a}} \tag{2.68}$$

the physics of the theory gets much more complicated. At this scale, the gluons bind together to form particles of mass $m \sim \Lambda_{\rm YM}$ (glueballs), making the theory gapped in the IR. The theory also undergoes confinement, meaning that the only observed physical states are singlet under the gauge group. The electric flux is confined in a region of radius $\sim (\Lambda_{\rm YM})^{-1}$ and, if we insert heavy probe particles, the energy between them grows linearly with the distance.[12] The reason is the following. In Coulomb-like (unconfined) theories, the electric flux is uniformly distributed over a sphere surrounding a charge and falls off as $1/r^2$, making the potential between two probe particles decrease as $V(r) \sim 1/r$. In confining theories, instead, the electric flux is confined in a region of radius $\sim (\Lambda_{\rm YM})^{-1}$ independently of r. This implies that the potential grows linearly with the distance $V(r) \sim r$, makes charged particles bind together into gauge singlets, and prevents them from escaping.

The existence of the mass gap and confinement are supported by numerical and experimental evidence, but have never been analytically proved: this is one of the most difficult open problems in theoretical physics [53].

Introducing massless fermionic matter: QCD-like theories

Let us now add massless Dirac fermions in the fundamental representation (quarks) and specify to $SU(n_c)$ gauge group. The action is that in eq.(2.62), with

$$S_{\rm matter} = -\sum_{i=1}^{n_f} \bar{\psi}^i \not{D} \psi^i \,, \tag{2.69}$$

where $\not{D} = \gamma^\mu(\partial_\mu - iA_\mu)\psi$. The number n_f of matter fields is known as the flavor number, while the number n_c entering in the gauge group is referred to as the color number. This action is classically invariant under

$$G_F = U\left(n_f\right)_L \times U\left(n_f\right)_R \tag{2.70}$$

which acts as

$$U\left(n_f\right)_L : \psi_{-i} \mapsto L_{ij}\psi_{-j} \,, \quad U\left(n_f\right)_R : \psi_{+i} \mapsto R_{ij}\psi_{+j} \,, \tag{2.71}$$

with L, R are $n_f \times n_f$ unitary matrices and ψ_-, ψ_+ are the left-handed and the right-handed components of the fermionic field respectively. At the quantum level, the axial symmetry $U(1)_A$, under which left-handed and right-handed fermions transform with an opposite phase, is anomalous.[13] The global symmetry group at the quantum level is then

$$G_F = U(1)_V \times SU\left(n_f\right)_L \times SU\left(n_f\right)_R \,, \tag{2.72}$$

[12] We refer to the next sections for the case of insertion of light (or massless) particles.

[13] In the abelian case, this anomalous symmetry can be promoted to an exact discrete non-invertible symmetry. However, a similar upgrading cannot be done when we consider the $SU(n_c)$ gauge group case [54, 55].

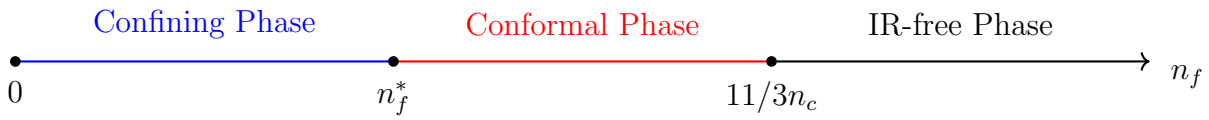

Figure 2.4: IR phases of QCD-like theories: for $0 \leq n_f \leq n_f^*$ the theory confines and spontaneously breaks the chiral symmetry, for $n_f^* \leq n_f \leq 11/2n_c$ the theory flows to an interacting CFT, and for $n_f > 11/3n_c$ the theory is free in the IR. The value of n_f^* is not known exactly.

where $U(1)_V$ is the vector symmetry, under which left-handed and right-handed fermions transform with the same phase. The beta function coefficients of this theory, defined as in eq.(2.66), read

$$\beta_0 = -\Big(\frac{22}{3}n_c - \frac{4}{3}n_f\Big)\,, \tag{2.73}$$

and

$$\beta_1 = -\Big(\frac{68}{3}n_c^2 + \frac{2n_f(n_c^2-1)}{n_c} + \frac{20n_f n_c}{3}\Big)\,. \tag{2.74}$$

The theory exhibits drastically different behaviors depending on the ratio n_f/n_c. Let us present them (see fig.2.4 for a summary).

IR-free phase

For $n_f > 11n_c/2$, the sign of β_0 gets positive, making the theory no longer asymptotic free. The degrees of freedom at low energy are massless gauge bosons and fermions which become free in the deep IR. This is the same behavior of massless QED. When $n_f = 11n_c/2$, β_0 vanishes and one should consider the two-loop contribution β_1 instead. Now, since $\beta_1 > 0$ at this value, the theory remains IR free also in this case.

The potential of a pair of probe particles is Coulombesque in this case, meaning that it takes the form $V(r) \sim 1/(r\log(\Lambda r))$, with the logarithmic term being a consequence of the running of the gauge coupling.

Conformal phase

Next, we consider the case of n_f slightly smaller than $11n_c/2$. In this case β_0 and β_1 have different signs, allowing for the existence of a CBZ fixed point

$$a^* = -\frac{\beta_0}{\beta_1}\,, \tag{2.75}$$

which is weakly coupled as long as we do not take n_f to be too small. In this case the theory is an interacting CFT, which persists in the interval $n_f^* \leq n_f \leq 11n_c/2$, known as the QCD conformal window. Ref. [56] proposed an explanation for the loss of conformality at $n_f = n_f^*$, based on the merger and annihilation of fixed points. The idea is that when n_f is reduced to n_f^*, a four-fermion operator approaches marginality. This operator is responsible for the flow from another UV fixed point, close to QCD, known as QCD*. At $n_f = n_f^*$, the four-fermion

operator gets marginal and QCD, QCD* merge, becoming complex at lower values of n_f. After merging, conformality is lost, and chiral symmetry breaking occurs.

Determining the value n_f^* is a non-trivial task because as we lower n_f the theory gets strongly coupled and not accessible with perturbation theory. Several techniques were used to propose an estimate:

- Approximation of Schwinger-Dyson gap equations ($n_f^* \approx 11.9$ for $n_c = 3$ [57]).
- Truncations of exact RG equations ($n_f^* \approx 10$ for $n_c = 3$ [58] or $n_f^* \approx 12$ for $n_c = 3$ [59]).
- Analysis based on the perturbative series in the gauge-coupling ($n_f^* \approx 9$ for $n_c = 3$ [60, 61]), and on the Banks-Zaks conformal expansion around the parameter $\epsilon = 11n_c/2 - n_f$ ($n_f^* \approx 10$ [62] or $n_f^* \approx 9$ [63] for $n_c = 3$). More refined analysis were done thanks to the employment of Borel resummation techniques[14] ($n_f^* \leq 11$ for $n_c = 3$ [64]).

Scale invariance of the theory implies that external electric probes experience a Coulomb-like potential $V(r) \sim 1/r$.

Confining phase

When $n_f < n_f^*$, quarks, which are well-defined fundamental objects at high energy, confine at low energy in massive particles with $m \sim \Lambda_{\rm QCD}$ (baryons). On the other hand, some massless degrees of freedom exist, due to the spontaneous breaking of the chiral symmetry G_F.[15] This occurs because of the formation of a vacuum condensate $\langle \bar{\psi}^i \psi^j \rangle \sim \delta^{ij}$, with $i, j = 1 \dots n_f$, which breaks

$$G_F \to U(1)_V \times SU(n_f)_V \,, \tag{2.76}$$

where $SU(n_f)_V$ is the diagonal subgroup of $SU(n_f)_L \times SU(n_f)_R$. The spontaneous breaking of a continuous symmetry introduces as many massless spinless particles as many broken generators exist. This is known as the Goldstone theorem [65]. Consequently, the gauge theory is again gapless, but now with the massless fields arising as Goldstone bosons (mesons).

Note that, as for pure Yang-Mills, all physical excitations are gauge singlets in this case. However, even if we call this confining phase, the theory does not strictly confine, in the sense that quarks can escape from bound states. Consider the situation in which a highly energetic electron hits a bound state of quarks, e.g. a proton, kicking one of the quark far from the others. A large amount of energy, in the form of chromoelectric field, emerges in the region between the escaping quark and the rest of the bound state. When the field becomes strong enough, it becomes energetically favorable to break the flux line and create out of the vacuum a particle-antiparticle pair. Therefore, the original quark does escape, even if not

[14] We refer to sec.3.2 for an introduction on Borel resummation and more generally to the whole chapter 3 for an application of this technique.

[15] We are assuming a scenario in which chiral symmetry breaking and quark confinement occur at the same value n_f^*, but we might also have an intermediate phase $n_f^{**} \leq n_f \leq n_f^*$, in which the theory is confining and the chiral symmetry is unbroken.

alone, and the force between it and the remaining bound state drops to zero. This is why confinement in the presence of fundamental matter is sometimes denoted quark confinement or charge screening, to distinguish it from the strict confinement of pure theories, where flux lines cannot break.

Adding masses to the fermions

Let us add a mass term to the matter action:

$$S_{\text{matter}} = \sum_{i=1}^{n_f} (-\bar{\psi}^i \not{D} \psi^i + m_q \bar{\psi}^i \psi^i) \,. \tag{2.77}$$

Chiral symmetry is explicitly broken by this deformation, but in the limit $m_q \ll \Lambda_{\text{QCD}}$ it still is an approximate symmetry.[16] Spontaneous breaking of approximate symmetries is associated with the appearance of pseudo-Goldstone bosons, which are spinless particles with a mass m_π that is linearly proportional to the explicit breaking term [66] ($m_\pi^2 \sim m_q$). The consequence is that the mesons introduced in the previous section get a mass.

Wilson loops as order parameters for confinement

Usually, we can identify the phase of a QFT by computing the expectation value of some order parameter. In the case of non-abelian gauge theories, this role is played by the vacuum expectation value (VEV) of the Wilson loop, defined as

$$W(C) = \text{tr}_R \mathcal{P} \exp\left(\int_C A_\mu dx^\mu \right) , \tag{2.78}$$

where R is the representation of the field along the path C and $\mathcal{P}$ is the path-ordering operator, which orders the A_μ's obtained expanding the exponential so that those at earlier times are placed to the left. The Wilson loop is a gauge invariant non-local operator. Specifying to the fundamental representation and to the path in fig.2.5, it measures the potential of a quark-antiquark pair at a distance r created in the past and then annihilated after a time T. In the presence of the probe particles and in the large-time limit, the system increases its energy by a quantity $V(r)$. This means that we expect the path integral to give

$$\lim_{T\to\infty} \langle W(C) \rangle \sim e^{-V(r)T}. \tag{2.79}$$

In the limit of large distance r, this then provides a way to detect confinement:

- If the theory strictly confines $V(r) \sim r$ and the Wilson loop scale with the area of the path (area law).

[16] Note that if $m_q > \Lambda_{\text{QCD}}$ the quarks can be integrated out and the IR theory is governed by the pure gauge theory.

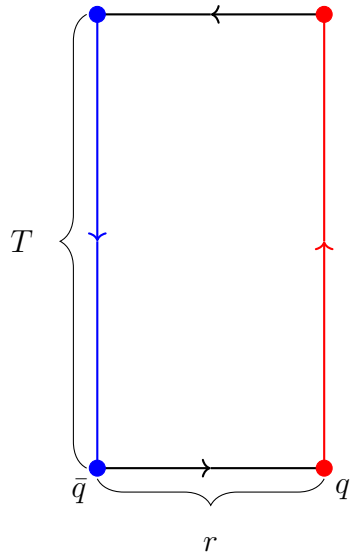

Figure 2.5: Rectangular Wilson loop in the fundamental representation corresponding to the production of a quark-antiquark pair, its evolution in time at a distance r, and its annihilation after a time T.

- In the presence of light (or massless) quarks the theory develops charge screening, $V(r)$ is approximately constant, and the Wilson loop scales with the time T (perimeter law).

- If the phase is IR-free or conformal $V(r)$ the potential is Coulomb-like and the VEV of the Wilson loop is non-vanishing.

In the limit of infinitely large paths $r \to \infty$, both the area and the perimeter become infinite. Therefore one may believe that the VEV of the Wilson loop vanishes in both these cases. This is not true, because the perimeter infinities can be reabsorbed by local counterterms on the line, while the area infinities cannot. Showing that $\langle W(C) \rangle = 0$ corresponds then to proving strict confinement. Unfortunately, unless we put the theory on a lattice, this cannot be done, leaving this fundamental problem open.

Non-perturbative contributions: instantons and renormalons

In eq.(2.59) we presented the action for Yang-Mills theories in a generic d. In $4d$, an additional quadratic term is admitted by gauge invariance. This is the theta term

$$S_\theta = \frac{\theta}{16\pi^2} \int d^4x \ \mathrm{tr} \, {}^\star F^{\mu\nu} F_{\mu\nu} \,, \tag{2.80}$$

with ${}^\star F^{\mu\nu} = \frac{1}{2} \epsilon^{\mu\nu\rho\sigma} F_{\rho\sigma}$ and $\theta = [0, 2\pi)$. Note that this is a total derivative, meaning that it can be rewritten as

$$S_\theta = \frac{\theta}{8\pi^2} \int d^4x \ \partial_\mu K^\mu \tag{2.81}$$

with

$$K^\mu = \epsilon^{\mu\nu\rho\sigma}\text{tr}\left(A_\nu\partial_\rho A_\sigma - \frac{2i}{3}A_\nu A_\rho A_\sigma\right). \tag{2.82}$$

Total derivatives do not affect the equations of motion and have a non-vanishing contribution only for non-trivial behaviors at infinity. Namely, eq.(2.81) can be rewritten as an integral over the sphere S^3 at infinity. Now, configurations with finite YM action asymptote to pure gauge at infinity, implying

$$A_\mu = iU\partial_\mu U^{-1}\,, \quad |x| \to \infty\,. \tag{2.83}$$

Substituting in eq.(2.81), we get that

$$S_\theta = k\theta\,, \quad k \in \mathbb{Z}\,, \tag{2.84}$$

where k is the number of times that $U(x)$ winds around the asymptotic S^3 at infinity, also known as the winding number. Knowing this, one can write the following bound for YM action (Bogomolnyi bound):

$$S_{\text{YM}} = \frac{1}{4g^2}\int d^4x\ \text{tr}\,[F_{\mu\nu} \pm^\star F_{\mu\nu}]^2 \pm \frac{1}{2g^2}\int d^4x\ \text{tr}\,[F^\star_{\mu\nu}F^{\mu\nu}] \geq \frac{8\pi^2}{g^2}|k|\,. \tag{2.85}$$

A special class of configurations with a non-trivial winding number is given by the instantons/anti instantons, which satisfy the self-dual/anti self-dual YM equations

$$F_{\mu\nu} = \pm^\star F_{\mu\nu} \tag{2.86}$$

and then minimize the Bogomolnyi bound. They are solutions of the classical equation of motions and have an action which reads

$$S_{\text{inst}} = \frac{8\pi^2}{g^2}|k| + ik\theta\,. \tag{2.87}$$

The action of an instanton/anti instanton pair is then given by

$$S_{\text{pair}} = \frac{16\pi^2}{g^2}|k| = \frac{|k|}{a}\,. \tag{2.88}$$

In the path integral, this can be rewritten in terms of the dynamically generated scale Λ, as in[17]

$$e^{-S_{\text{pair}}} = \left(\frac{\Lambda}{\mu}\right)^{-k\beta_0}. \tag{2.89}$$

This shows that instantons are non-perturbative effects, which vanish for $\Lambda/\mu \to 0$, and are exponentially suppressed in the perturbative regime.

Instantons are not the only non-perturbative effect that arises in $4d$ non-abelian gauge the-

[17]This is true for both pure gauge theories and QCD-like theories, so we write generically Λ, meaning Λ_{YM} and Λ_{QCD} respectively.

ories. There is indeed another contribution given by renormalons. While instanton singularities are associated with the factorial proliferation of Feynman diagrams in QFT, renormalons are related to a specific set of Feynman diagrams that give a factorially growing contribution to the perturbative series. Contrary to instantons, renormalons are not known to be associated with semi-classical configurations of the theory and we still lack their complete understanding.

In non-abelian gauge theories, renormalons may manifest as non-perturbative corrections associated with irrelevant operators in the UV. Consider an operator with classical dimension $4+k$, with associated coupling h of dimension $-k$. By dimensional analysis this can only appear in the RG function in the combination $h\Lambda^k$, which in terms of the dimensionless coupling $\hat{h} = h\mu^k$ can be rewritten as

$$\hat{h}\left(\frac{\Lambda}{\mu}\right)^k = \hat{h}\, e^{\frac{k}{\beta_0 a}} \ . \tag{2.90}$$

Ref. [64] proposed that the leading non-perturbative correction is associated with the four-fermion operator which gets marginal at the edge of the conformal window in the merger and annihilation scenario. This operator has dimension 6, corresponding to an $k = 2$ IR renormalon singularity.

The presence of such non-perturbative contributions suggests that we should rewrite RG functions as trans-series, which are formal linear combinations of power series with exponential prefactors

$$\beta^{\rm 4d}(a) \sim \sum_{n=0}^{\infty} \beta_n a^{n+2} - \sum_{k=2}^{\infty} e^{\frac{k}{\beta_0 a}} \sum_{n=0}^{\infty} \beta^R_{k,n} a^{n+2} + \sum_{k=1}^{\infty} e^{-\frac{k}{a}} \sum_{n=0}^{\infty} \beta^I_{k,n} a^{n+2} + \dots \ , \tag{2.91}$$

where $\beta^R_{k,n}$ are the coefficients of the renormalon expansion, while $\beta^I_{k,n}$ are those related to instantons corrections. A similar expression can be written for the expansions of anomalous dimensions.

2.2.2 Exploring gauge theories in $d \neq 4$

Four-dimensional gauge theories have been extensively studied due to their outstanding implications in the Standard Model. However, there exist several reasons to explore gauge theories in dimensions other than four. As we go down in dimension, indeed, we find an increased richness in the interactions that a field theory admits: the number of relevant and marginally relevant interactions is higher, providing an interesting playground for the study of asymptotically free theories. On the other side, gauge theories in higher dimensions are IR free and should be thought as effective theories at high energy. Studying their UV fate may give rise to the discovery of non-trivial fixed points, currently known to exist in $d = 5$ only in supersymmetric cases.

Gauge theories in $d = 3$: the symmetry breaking scenario

Non-abelian $3d$ gauge theories have received particular attention in the last years due to their possible emergence in quantum phase transitions with deconfined criticality [67] and as theories governing domain walls among different vacua in non-abelian $4d$ gauge theories [68]. Theoretically, they are of course also interesting theories by themselves. Note that $3d$ gauge theories may also contain Chern-Simons terms with parameter k, but we consider the case $k = 0$ in this thesis.

In $d < 4$, the gauge coupling g^2 has a positive dimension, which makes gauge theories asymptotically free for purely dimensional reasons, independently of the number of fermions and the gauge group (either abelian or not). Weakly coupled at short distances, these theories get strongly coupled as we approach the IR, opening the possibility for many interesting physical phenomena. When the number of flavors is sufficiently high, the screening properties of fermionic fluctuations generate an IR fixed point. It is indeed known since the early work [69, 70] that at large n_f QED_3 and QCD_3 flow in the IR to a CFT. Here we consider non-abelian theories with n_f 4-component Dirac fermions. For $n_f \leq n_f^*$, with n_f^* an unknown parameter, a phase with spontaneous symmetry breaking of the $U(2n_f)$ global symmetry is expected. The only pattern of spontaneous breaking of the global symmetry $U(2n_f)$ compatible with the results of [71, 72] is

$$U(2n_f) \to U(n_f) \times U(n_f)\,, \tag{2.92}$$

occurring through the appearance of a parity-conserving dynamical mass for each 4-component fermion.

Similarly to what happens with QCD in $4d$, merger and annihilation of fixed points is believed to occur at $n_f = n_f^*$, separating the conformal and the spontaneously broken phase. Ref. [73] used the generalized $\widetilde{F}$-theorem to estimate the value of n_f^* in the abelian case. We explain the logic of this estimate in sec.4.5.1 and repeat the same analysis in the non-abelian case.

Gauge theories in $d = 5$: the possibility of a continuum limit

In $d > 4$, gauge theories are perturbatively non-renormalizable and should be considered effective field theories which become free theories in the IR. Therefore in $d > 4$ the natural question is whether there exists a UV fixed point, i.e. an interacting CFT that when deformed by a relevant operator admits an effective description as a non-abelian gauge theory. The existence of such a fixed point for Yang-Mills theories in $d > 4$ would be analogous to well-known lower-dimensional examples of perturbatively non-renormalizable theories with a non-trivial continuum limit, such as the non-linear σ-model.

A parametrically weakly coupled UV fixed point in non-abelian gauge theories can in fact be established in $4 + 2\epsilon$ dimensions with $\epsilon \ll 1$ [74]. It is of course crucial to understand

if this UV fixed point persists up to $d = 5$. Note that no example of non-supersymmetric interacting unitary CFTs is currently known in $d = 5$. A conjectural example was the UV fixed point of the $O(N)$ model, whose $1/N$ expansion was shown in [75] to be compatible with unitarity for N larger than a certain critical value N_c. However it was later realized that this fixed point is rendered non-unitary even for $N > N_c$ by certain instantonic contributions to the imaginary part of observables, that are exponentially small at large N [76]. Evidence that the UV fixed point of non-abelian theories survives at $d = 5$ has been provided by [77], where fixed points of this kind have been studied up to $\mathcal{O}(\epsilon^4)$. The analysis in [77] used the then-available four loop beta function for non-abelian gauge theories and was based on the optimal truncation of the series in ϵ. We refer to chapter 3 for a more refined study, based on Padé-Borel resummation of the now-available five loop beta function, and to section 4.5.2 for an application of the generalized $\widetilde{F}$-theorem to this expected fixed point.

2.3 Quantum Field Theory in Anti-de-Sitter space

Anti-de-Sitter (AdS) space is a maximally symmetric space with constant negative curvature. Studying quantum field theories in this background has several advantages [78]. First, it provides a dimensionful parameter, the AdS radius L, which acts as a regulator for the IR physics halting the RG flow at the scale $1/L$. This is more sophisticated than imposing a hard cutoff in flat space, as the latter would sacrifice some spacetime symmetries. Instead, AdS has the same number of generators as flat space, with the isometry group being $SO(d+1,1)$ in this case.

Thanks to the existence of a conformal boundary (∂AdS), AdS admits a notion analogous to that of asymptotic states in flat space, namely the states associated with the insertions of local operators at the boundary. Connecting these states to scattering states in the flat-space limit is a well-studied problem [79–92]. The isometries of the background ensure that the correlators of the boundary operators encompass a CFT, whose operator content and data depend on the choice of boundary conditions for the bulk fields. Note that we take AdS to be a rigid background and we do not include dynamical gravity. As a result the CFT on the boundary does not have a stress tensor operator.

Another advantage of AdS space is that it has infinite volume even at finite L, allowing the possibility of spontaneous symmetry breaking and phase transitions, phenomena which are forbidden on compact spaces.

Thanks to these nice properties, quantum field theory in rigid AdS has been the object of a revived interest. Recent works focused on strongly coupled theories of self-interacting scalars and fermions, namely the $O(N)$ and Gross-Neveu models, respectively, in the limit of large N and finite coupling [93, 94]. Other recent works on QFT in AdS described how to encode the bulk RG in the boundary correlation functions [89, 95–99], studied thermal properties [100, 101], or considered the special case in which the bulk theory is conformal, as an efficient tool to study conformal defects [102–107] or boundary conditions [108–110].

2.3.1 Two-dimensional toy models at large N

The presence of a dimensionful parameter makes AdS an ideal background to study asymptotically free theories. The reason is that the finite radius L can be combined with the strong coupling scale Λ to give a dimensionless, RG-invariant parameter $L\Lambda$ that can be tuned at will. The standard situation is that some boundary conditions (bc's) corresponding to gapless bulk theories are allowed for $L\Lambda \ll 1$ but cease to exist at some critical value of $L\Lambda$. The only allowed bc persisting at larger values of $L\Lambda$ corresponds instead to gapped theories in the bulk, that smoothly connect to the flat space limit.

Motivated by these ideas, one can investigate confinement in four-dimensional non-abelian gauge theories. Before moving to this ambitious subject, let us consider the case of $O(N)$ non-linear σ models and $O(N)$ Gross-Neveu models in $d = 2$ [94]. These two-dimensional theories have a dynamically generated scale and are solvable in the large N limit, providing excellent toy models for gauge theories in $d = 4$.

Both $O(N)$ non-linear σ models and $O(N)$ Gross-Neveu models admit a bc that breaks the global symmetry of the bulk G to a subgroup $G_\perp$ at $L\Lambda \ll 1$. One can show that the pullback of bulk conserved currents associated to the broken generators gives rise to exactly marginal operators, known as boundary tilt operators. This implies the existence of a conformal manifold $\mathcal{M}_{G/G_\perp}$, encoding the spontaneous symmetry-breaking in the bulk. Analogously to what happens in flat space due to the Goldstone's theorem, this corresponds to a gapless phase. As the symmetry is unbroken in the flat space limit, these bc's must disappear at some critical value of $L\Lambda$. In both cases, this happens because a singlet boundary operator, irrelevant at weak coupling, gets marginal at larger radius, triggering an RG flow to the symmetry-preserving bc and consequently to a gapped phase. This boundary transition occurs in two different ways:

- **Continuous transition**: $\mathcal{M}_{G/G_\perp}$ shrinks to zero and the symmetry-breaking (SB) bc merges into the symmetry-preserving (SP) one. CFT data at the boundary change continuously across the critical point.

- **Discontinuous transition**: $\mathcal{M}_{G/G_\perp}$ becomes unstable and cease to exist abruptly. CFT data at the boundary jump discontinuously across the critical point.

The two-dimensional models examined in [94] exhibit different kinds of transition. Let us review them:

- $O(N)$ **sigma model**: in flat space the vacuum preserves $O(N)$ symmetry and the scalar fields ϕ^i, $i = 1, \dots, N$ acquire a dynamically generated mass; in AdS, at small $L\Lambda$, there exists a bc $\phi^i|_{\partial AdS} = \Phi^i$ breaking $O(N)$ to $O(N-1)$. The associated conformal manifold $\mathcal{M}_{O(N)/O(N-1)}$ shrinks to zero at $L\Lambda$=1, when this bc merges with the SP bc $\phi^i|_{\partial AdS} = 0$. At the merging, the lightest scalar operator $\hat{\sigma}^{\mathrm{SB}}$ of the SB bc, irrelevant at smaller radius, hits marginality. The second lightest $\hat{\sigma}_2^{\mathrm{SB}}$ reaches the value of the lightest one of the SP bc ($\hat{\sigma}^{\mathrm{SP}}$), leading to a continuous interpolation from one

phase to the other. At larger values of $L\Lambda$, $\hat{\sigma}^{\rm SP}$ remains irrelevant, keeping the SP bc stable all the way to flat space.

- $O(N)$ **Gross Neveu model**: the model has a symmetry $G = O(2N)_V \times \mathbb{Z}_2^{F_L}$, which contains a $\mathbb{Z}_4^A$ axial symmetry. In flat space the $\mathbb{Z}_4^A$ is broken to $\mathbb{Z}_2^F$, generating a condensate which gives rise to a mass for the fermions. In AdS, at small radius, there exists a $\mathbb{Z}_4^A$-preserving (vector-breaking) bc which prevents this condensation and therefore gives rise to a gapless phase. Deforming this Gross Neveu bc with an irrelevant double trace operator, leads to a shadow $\mathbb{Z}_4^A$-preserving bc. At some critical value of $L\Lambda$, the double-trace operator becomes marginal and the Gross Neveu bc and its shadow merge together. The conjecture is that this triggers an instability which leads to another bc, vector-preserving and $\mathbb{Z}_4^A$-breaking, which interpolates smoothly to flat space. The CFT data jump at the critical value, leading to a discontinuous transition from one phase to the other.

2.3.2 Gauge theories in AdS: the confinement/deconfinement transition

The study of four-dimensional non-abelian gauge theories on the background of Euclidean AdS space, i.e. hyperbolic space, was advocated long ago in [78] as a way to have better control on the non-perturbative effects. The meaning of confinement in AdS space was later explored in [17], which pointed out the existence of a deconfinement/confinement transition as the radius L is increased. When L is small in units of the dynamically-generated scale $\Lambda_{\rm YM}$ the theory can be placed in AdS by imposing the standard Dirichlet boundary condition (D bc) for the gauge fields,

$$A_i^a(x,z) \underset{z\to 0}{\sim} z\, g^2\, J_i^a(x)\,, \tag{2.93}$$

and the bulk gauge symmetry G becomes a global symmetry on the boundary. We are now restricting to (Euclidean) AdS_4, with metric

$$ds^2 = L^2 \frac{dz^2 + dx_i^2}{z^2}\,, \quad i = 1,2,3\,, \tag{2.94}$$

and g^2 is the YM coupling. The spectrum of operators in the boundary CFT contains conserved currents J_i^a of the non-abelian symmetry G, and more generally operators in non-trivial representations of G. Moreover, the conserved currents cannot continuously recombine at $g^2 = 0$ and therefore they keep the protected dimension $\Delta_J = 2$ for a finite range of L around $L = 0$. If these operators would still exist for arbitrarily large L, they would give rise to asymptotic states of massless gluons in the limit $L \to \infty$. Therefore [17] argued that a necessary condition for the existence of the mass gap in flat space is that there is a transition at some finite value of L to a different boundary condition, one in which the currents and the associated symmetry are not present on the boundary. This has to be contrasted with

the case of the Neumann boundary condition (N bc)

$$A_i^a(x,z) \underset{z\to 0}{\sim} a_i^a(x)\,, \tag{2.95}$$

where the boundary mode is a $3d$ gauge field, and the group G remains a gauge symmetry of the boundary. As a result in this case all the physical operators of the boundary CFT are color singlets, and it is possible for this boundary condition to smoothly approach the flat-space limit $L \to \infty$.

Mechanisms for the transition

The deconfinement/confinement transition happens at strong coupling, a natural estimate for the critical radius being $L_{\text{crit}} \sim \Lambda_{\text{YM}}^{-1}$, and therefore it is hard to make precise statements about it. Various alternative mechanisms for the transition can be envisioned, as explained in [17] and recently revisited in [94]:

- **Higgsing:** A scalar operator O^a in the adjoint representation of G becomes marginal at L_{crit} and recombines with the current $\partial^i J_i^a = O^a$, allowing the latter to get an anomalous dimension and breaking the G global symmetry;
- **Decoupling:** The positive coefficient C_J of the current two-point function, which gives the norm of the state associated with the current operator, goes to 0 at L_{crit}, forcing the current operator to decouple from the theory;
- **Marginality:** A singlet scalar operator O becomes marginal at L_{crit}, causing the D bc to merge and annihilate [56, 111] with a second one, and to stop existing as a unitary boundary condition.

The third mechanism was advocated as the most likely in [94], based on the analogy with 2d asymptotically-free models which can be studied in the $1/N$ expansion.

Signals of the transition can be then found by investigating the spectrum of the gauge theory in the bulk as a function of $L\Lambda$, or equivalently by computing OPE coefficients and scaling dimensions of the dual boundary theory. In chapter 5, we will compute the leading-order perturbative corrections to the CFT data. This is clearly not sufficient to extract information about the transition, but can be used as a guide for the numerical conformal bootstrap.

Chapter 3

Five dimensional CFTs from the ϵ-expansion

3.1 Introduction

CFTs play a major role in theoretical physics. They are the starting and ending points of RG flows in quantum field theories, they describe second-order phase transitions in critical phenomena and they possibly allow us to have a non-perturbative definition of quantum gravity theories by means of the AdS/CFT correspondence. In the absence of extra symmetries, most notably supersymmetry, finding interacting CFTs becomes increasingly difficult as the dimension of space-time d increases. The only analytical evidence of the existence of $4d$ non-supersymmetric CFTs comes from the Veneziano limit (large number of colors and flavors) of non-abelian gauge theories, where we can tune the one-loop coefficient of the beta function to be parametrically small and negative, while having a positive two-loop coefficient (CBZ [112, 113] fixed points). To what extent the IR fixed point persists at finite n_c is a non-trivial question which still has to be settled.

As explained in sec.2.2.2, non-abelian gauge theories may have non-trivial continuum limit in $d > 4$, which can be studied as a WF fixed point in $d = 4 + 2\epsilon$. This was performed in [77], with optimal truncation of the series in ϵ for the fixed point. The aim of this chapter is to extend the analysis of [77] by adding one more term, thanks to the by-now known five loop beta function [114–117], and to use Borel resummation techniques, which allow us to have better control on the (plausibly) asymptotic series in ϵ.

We consider $SU(n_c)$ gauge theories with n_f Dirac fermions in the fundamental representation of the gauge group. We find evidence for the existence of UV fixed points when both n_c and n_f are small enough. The evidence gets weaker and weaker as either n_c or n_f increases, so the most reliable result applies for pure $SU(2)$ non-abelian gauge theories. Very similar results are obtained using ordinary Padé approximants, without using Borel resummation techniques.

This chapter is structured as follows. In section 3.2 we provide a brief review about

asymptotic expansion, Borel resummation and Padé approximation. In section 3.3 we briefly set the stage of our computation, which follows the same logic used in [64] to study the conformal window in $4d$ QCD. We present our results in section 3.4, which include also the computation of the anomalous dimensions γ_g and γ, of the gauge kinetic term operator $\mathrm{tr}\,[F_{\mu\nu}F^{\mu\nu}]$ and of the fermion mass operator $\bar{\psi}\psi$ (when present) respectively . The existence of a $5d$ UV fixed point in non-abelian gauge theories is debated in the literature. We briefly review in section 3.5 previous studies by means of different techniques aimed at looking for $5d$ non-supersymmetric CFTs.

Conventions We stress that the beta function $\beta(a)$ introduced in this chapter differs by a factor 2 from eq.(2.2) of ref. [1], to be consistent with the general definition in eq.(2.66). All following equations are modified accordingly.

3.2 Resummation techniques for perturbative series

Computing observables in QFT is a hard task. An important tool that comes to our help is perturbation theory, which consists of deforming free theories with small perturbations parametrized by a coupling $\lambda \ll 1$ and expanding equations in powers of this coupling. The results are then asymptotic expansions satisfying

$$f(\lambda) - \sum_{n=0}^{N} \alpha_n \lambda^n = O(\lambda^{N+1})\,, \quad \lambda \to 0\,. \tag{3.1}$$

Asymptotic expansions in QFT are often divergent. The motivation, first pointed out by Dyson [118] in the context of QED, is that negative deformations of free theories, unlike the positive ones, lead to unstable ill-defined theories. This prevents the possibility to have a finite radius of convergence at $\lambda = 0$.

Contrary to convergent series, asymptotic expansions do not fix uniquely the estimated function. This is simply revealed by the fact that exponentially suppressed terms like $e^{-1/\lambda}$ are not captured by asymptotic expansions and therefore functions differing by such terms end up being asymptotically equal. In convergent series, the more terms are added in the series, the more accurate is the result. This is not the case for asymptotic series, where there is an optimal number of terms that one should keep, after which adding more terms results in worse and worse accuracy. The coefficients α_n of the QFT asymptotic expansion are often factorially growing at large n, satisfying

$$\alpha_n \sim n!\alpha^n n^c\,, \quad n \gg 1\,, \tag{3.2}$$

for some real parameters c and α. Using Stirling's formula

$$n! \sim n^{n+\frac{1}{2}}\sqrt{2\pi}e^{-n}\,, \tag{3.3}$$

we can compute the ratio of two successive terms of the expansion and find the optimal truncation at the largest term which keeps this ratio smaller than 1, which is $N_{\text{opt}} \sim 1/|\lambda\alpha|$. Resumming beyond this term would only worsen the approximation of the series. The error generated by the truncation is generally given by $\Delta_N \sim \alpha_n \lambda^N$. In the optimal case this leads to an exponentially suppressed error

$$\Delta_{\text{opt}} \sim e^{-\frac{1}{|\lambda\alpha|}}\,, \tag{3.4}$$

independently of c at leading order.

Divergent asymptotic series may be manipulated in order to be resummed. Let us consider the asymptotic series in eq.(3.1). We define the Le Roy-Borel transform as

$$\mathcal{B}_b f(\lambda) = \sum_{n=0}^{\infty} \frac{\alpha_n}{\Gamma(n+1+b)} \lambda^n\,, \tag{3.5}$$

with $b > -1$.[1] Suppose that the integral

$$f_B(\lambda) = \int_0^{\infty} dz\ z^b e^{-z} \mathcal{B}_b f(z\lambda) \tag{3.6}$$

has no singularities on the real positive axis. Then, if we expand using (3.5) and integrate term by term, we get that (3.6) has the same asymptotic expansion of the original function. In this case, the series is said to be Borel resummable. In general, the Borel resummed function $f_B(\lambda)$ is not guaranteed to coincide with the original function $f(\lambda)$, as it can differ by exponentially suppressed terms. Only imposing certain analyticity properties of $f(\lambda)$ near the origin ensures that (3.6) resums to the exact result. However, it turns out that these conditions are too strong for renormalizable theories.

When instead singularities are in the domain of integration of eq.(3.6), the perturbative series is said to be non-Borel summable. We can still perform the resummation, by analytically continuing the integrand in the complex plane and properly deforming the contour of integration to avoid singularities. This will lead to an ambiguity, which has the same order of magnitude of the leading non-perturbative terms which is however missed. The total error after Borel resummation is therefore given by

$$\Delta_B(\lambda) \sim e^{-\frac{\lambda_1}{\lambda}}\,, \tag{3.7}$$

where $\lambda_1 > 0$ is the location of the positive singularity closest to origin. Independently of Borel summability, the singularity of $\mathcal{B}_b f(\lambda)$ closest to the origin in the whole complex plane is at $|\lambda_0| = 1/\alpha$. So, by definition, we have $\lambda_1 \geq \lambda_0$ and therefore $\Delta_B(\lambda) < \Delta_{\text{opt}}(\lambda)$, suggesting that it is convenient to Borel resum functions even if they are non-Borel resummable.

Anyway, the inherent problem with Borel summation is that all terms of the divergent

[1] The standard Borel transform corresponds to setting $b = 0$.

series must be known exactly to improve accuracy: any finite truncation of the series would yield, after applying (3.5) and (3.6), the same asymptotic expansion we started with. This occurs because integrating over the entire positive axis extends beyond the radius of convergence of the Borel transform. This implies that the entire series does not commute with the integral and therefore does not reproduce the initial result, whereas the truncated sum does.

This issue can be addressed by adding an intermediate step to the resummation procedure, known as Padé approximation. The idea is to replace a truncated power series by a rational function with the same expansion around $\lambda = 0$. In simple Padé approximation, the first $N+1$ terms of the expansion in eq.(3.1) are replaced by

$$P^{[m/n]}(\lambda) = \frac{\sum_{p=0}^{m} c_p \lambda^p}{1 + \sum_{q=1}^{n} d_q \lambda^q}\,, \tag{3.8}$$

with $m+n=N$. The $m+n+1$ coefficients c_p and d_q are determined by expanding eq.(3.8) around $\lambda = 0$ and matching the result up to the λ^N term in the asymptotic expansion. When combined with Borel transform, this yelds the Padé-Borel approximation. Given the first $N+1$ terms of the series expansion of the Borel function (3.5), its $[m/n]$ Padé approximation reads

$$\mathcal{B}_b^{[m/n]}(\lambda) = \frac{\sum_{p=0}^{m} c_p(b) \lambda^p}{1 + \sum_{q=1}^{n} d_q(b) \lambda^q}\,, \tag{3.9}$$

with again $m+n=N$. Plugging eq. (3.9) in eq. (3.6) leads to an approximation of the function $f_B(\lambda)$ given by

$$f_B^{[m/n]}(\lambda) = \int_0^\infty dz\; z^b e^{-z} \mathcal{B}_b^{[m/n]}(z\lambda)\,, \tag{3.10}$$

which is now different from the initial truncated series.

3.3 Wilson-Fisher fixed point for Yang-Mills theories

The existence of a Wilson-Fisher fixed point for Yang-Mills theories in $d = 4+2\epsilon$ with $\epsilon \ll 1$ is easily established. In $d = 4+2\epsilon$ dimensions, we have

$$\beta^\epsilon(a) = \frac{da}{d\log\mu} = 2\epsilon a + \beta^{4\mathrm{d}}(a)\,, \tag{3.11}$$

where $\beta^{4\mathrm{d}}$ denotes the ordinary $4d$ beta function defined in eq.(2.91). For $n_f < \frac{11}{2} n_c$ the leading contribution to $\beta^{4\mathrm{d}}(a)$ is famously negative and hence the existence of a parametrically weakly coupled UV stable fixed point can be established for $\epsilon \ll 1$, as pointed out long ago by Peskin [74]. The question of whether or not this result can be extended to a physical number of dimensions, in particular $d = 5$ ($\epsilon = 0.5$), requires an analysis of higher order terms in $\beta^{4\mathrm{d}}$. This beta function, as well as the fermion mass anomalous dimension γ, for generic gauge

groups with n_f fundamental fermions is known up to five-loop orders [114–117, 119–121] in $\overline{\rm MS}$.[2] As is well-known, in quantum field theory the loopwise expansion of physical observables is generally divergent asymptotic. In non-abelian gauge theories the asymptotic expansion is also non-Borel resummable because of instantons and renormalon singularities. On the other hand, the nature of the coupling expansion of non-physical quantities, like the beta function, depends on the renormalization scheme. It is still unclear whether β in $\overline{\rm MS}$ is convergent or divergent asymptotic and, in the latter case, if the associated series is Borel resummable or not.

Theoretical and numerical arguments supporting a non-Borel resummable nature of the series for β and γ have been given in [64]. This is revealed by the presence of non-perturbative terms in $\beta^{\rm 4d}(a)$, corresponding to instantons and renormalons contributions (see eq.(2.66)). If the series expansion of $\beta^{\rm 4d}(a)$ is divergent, so is also the series of the function $\epsilon(a^*)$ obtained by solving $\beta^\epsilon(a^*) = 0$, and its inverse $a^*(\epsilon)$:

$$a^*(\epsilon) = \epsilon \sum_{n=0}^{\infty} b_n \epsilon^n \,, \quad \beta^\epsilon(a^*) = 0 \,. \tag{3.12}$$

We will assume in the following the most conservative and worst-case scenario, namely that the coupling expansion of $\beta(a)$ is divergent asymptotic and non-Borel resummable. As explained in the previous section, depending on the location of the leading singularity in the Borel plane, the numerical reconstruction of a formally non-Borel resummable function might lead to a better accuracy in the ending result compared to perturbation theory or optimal truncation. We use Padé-Borel approximants to estimate $a^*(\epsilon)$ as well as $\gamma^* = \gamma(a^*)$ and $\gamma_g^* = \gamma_g(a^*)$.[3] The numerical implementation of our procedure essentially follows that used in [64] to study the QCD conformal window, but we exclude in this case approximants with poles.

The existence of the fixed point a^* will be considered reliable only if the error band does not reach negative values, which would correspond to a possibly unphysical fixed point.

Since we do not know whether the series in ϵ are convergent or divergent asymptotic, we are not guaranteed to do better with Padé-Borel rather than simple Padé approximants. Theoretically, namely by knowing a parametrically large number of perturbative coefficients, we would expect to better reconstruct a quantity using simple Padé approximants if that is analytic at $\epsilon = 0$, or Padé-Borel approximants if that is non-analytic at $\epsilon = 0$. In practice, having only a few perturbative coefficients at our disposal, such considerations cannot be tested. For this reason, we have also considered ordinary Padé approximants for a^*, γ^* and γ_g^*, defining an error band to each approximant. This error is identical to that used in the Padé-Borel method but does not contain the contribution (3.19). The results obtained by taking ordinary Padé approximants and by Padé-Borel resummations are nicely in remarkable

[2] General expressions for $\beta^{\rm 4d}(a)$ and $\gamma(a)$ can be found in, e.g., [115] and [121], respectively.

[3] Our knowledge of the analyticities properties of the Borel function associated to these observables is unfortunately too limited to implement more efficient resummation techniques based on conformal mappings.

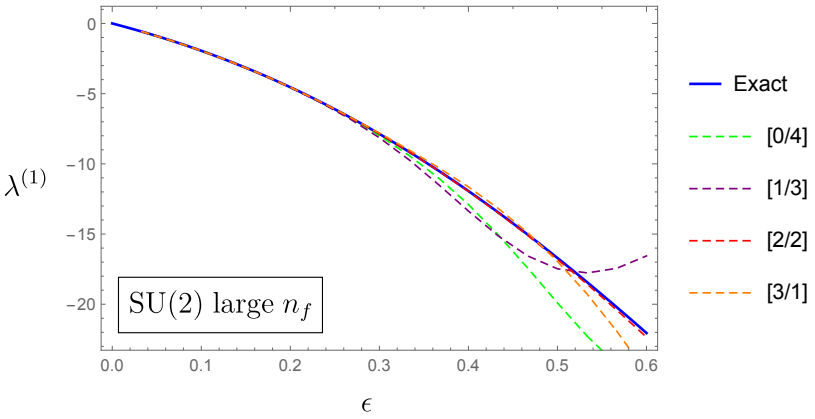

Figure 3.1: Comparison of $\lambda^{(1)}$ as a function of ϵ for $SU(2)$ gauge theory. The continuous blue line denotes the exact result obtained using large-n_f methods, the dashed lines denote the Borel resummation using Padé-Borel approximants as indicated in the legend.

agreement. The central values are essentially identical and often the error bands are very close. Only in a few cases Padé-Borel resummations give more accurate results. For this reason we will report in section 3.4 only the results obtained using the Padé-Borel method.

Large n_f and Selection of Padé-Borel Approximants

The choice of the Padé-Borel (and ordinary Padé) approximant for a given truncated sum is not univocal. We show here, following [64], how one can use exact results in the large-n_f limit to test the accuracy of different approximants and possibly select optimal ones. To this aim we can compare the results obtained with the known exact functions $\beta^{(1)}$ and $\gamma^{(1)}$ at large n_f with the approximations found with Padé-Borel resummation.

The large-n_f limit is defined as $n_f \to \infty$, $a \to 0$, with n_c and the 't Hooft-like coupling $\lambda = n_f a$ held fixed. In this limit (3.11) becomes

$$\beta(\lambda) = 2\epsilon\lambda + \frac{4}{3}\lambda^2 + \frac{1}{n_f}\beta^{(1)}(\lambda) + \mathcal{O}\left(\frac{1}{n_f^2}\right), \tag{3.13}$$

with $\beta^{(1)}$ a known function [122], analytic at $\lambda = 0$ (see e.g. [123] for a particularly nice explicit form). Correspondingly, (3.12) turns into

$$\lambda^*(\epsilon) = -\frac{3}{2}\epsilon + \frac{1}{n_f}\lambda^{(1)}(\epsilon) + \mathcal{O}\left(\frac{1}{n_f^2}\right), \quad \lambda^{(1)}(\epsilon) = -\frac{1}{2\epsilon}\beta^{(1)}\left(-\frac{3}{2}\epsilon\right). \tag{3.14}$$

As expected, the fixed point turns negative for large n_f and is unphysical. In this regime, we choose the Padé-Borel approximant that better reproduces the exact result and assume that this remains valid at finite n_f, when the fixed point is possibly physical. It is clear from fig.3.1 that the [2/2] approximant is the one that better matches the exact function, at least in the interval of interest. We have reported the result for $SU(2)$, but the same applies for $n_c = 3, 4$.

We can use a similar procedure for γ^* and γ_g^*. In the large-n_f limit the expression for γ can be expanded as

$$\gamma^*(\epsilon) = \frac{1}{n_f}\gamma^{(1)}\left(-\frac{3}{2}\epsilon\right) + \mathcal{O}\left(\frac{1}{n_f^2}\right), \tag{3.15}$$

with $\gamma^{(1)}$, like $\beta^{(1)}$, a known function analytic at $\lambda = 0$ [124, 125]. For γ_g we have

$$\gamma_g^*(\epsilon) = \left.\frac{\partial\beta(\lambda)}{\partial\lambda}\right|_{\lambda=\lambda^*(\epsilon)} = -2\epsilon + \frac{1}{n_f}\gamma_g^{(1)}\left(-\frac{3}{2}\epsilon\right) + \mathcal{O}\left(\frac{1}{n_f^2}\right), \tag{3.16}$$

with $\gamma_g^{(1)}$ obtained deriving eq.(3.13) and replacing the fixed point of eq.(3.14). In the case of $\gamma^{(1)}$ the comparison to the exact function does not lead to a clear choice of an approximant with respect to the others: a good matching is obtained with [3/1], [2/2] and [1/3] Padé-Borel approximants. None of them has poles in the real positive axis. The comparison for $\gamma_g^{(1)}$ leads us to select the [3/1] approximant, the others having poles at finite n_f or being too far from the exact result at large n_f.

Estimate of the Error

We now review the procedure used for the estimate of the error. Let us consider the function f with Padé-Borel approximation defined as in eq.(3.10). We define the total error $\Delta^{[m/n]}$ as the sum of three contributions:

$$\Delta^{[m/n]} = \Delta_{\rm conv}^{[m/n]} + \Delta_b^{[m/n]} + \Delta_{\rm np}\,. \tag{3.17}$$

As only Padé-Borel approximants without poles in the real positive axis are selected, no contributions from the residues, denoted by $\Delta_r^{[m/n]}$ in [64], enter in the error. In order to be reasonably conservative we have included a new term in the error, not present in [64], which estimates the convergence of the approximants and is relevant in the present analysis. Such uncertainty, denoted by $\Delta_{\rm conv}^{[m/n]}$, can be estimated by computing the distance among the Padé-Borel approximant and the subsequent one belonging to the same family:[4]

$$\Delta_{\rm conv}^{[m/n]} = \left| f_B^{[m/n]} - f_B^{[m-1/n-1]} \right|. \tag{3.18}$$

If the $[m-1/n-1]$ approximant is not avalaible, the $[m-1/n]$ is selected instead.

The term $\Delta_b^{[m/n]}$ measures the error caused by the arbitrariness on the choice of the LeRoy parameter b. It is indeed convenient to select a whole grid of values $\mathcal{B} = [b_0 - \Delta b,\ b_0 + \Delta b]$ and repeat the approximation for each of them; in our computation we choose $b_0 = 10$, $\Delta b = 10$

[4] In order to avoid misleading results, we have checked that the approximants used for such comparisons have small residues in the real positive axis or, even better, no poles at all.

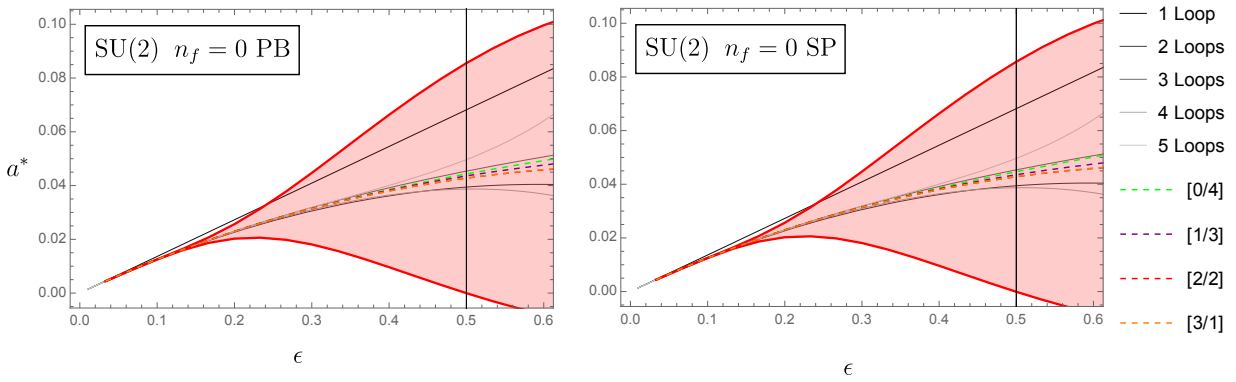

Figure 3.2: The value of the coupling at the fixed point a^* as a function of ϵ for pure $SU(2)$ gauge theory in $d = 4 + 2\epsilon$. (Left) Results of perturbation theory (grey lines) and of Padé-Borel (PB) approximation (dashed lines). (Right) Results of perturbation theory (grey lines) and of Simple Padé (SP) approximants (dashed lines). The shaded area in both panels corresponds to the error band associated to the optimal approximant [2/2], whose central value is given by the red dashed line.

and the spacing of the grid equal to 2 for a^*, γ_g^* and γ^*. The error can be then defined as

$$\Delta_b^{[m/n]} = \frac{1}{2}\left|\max_{b\in\mathcal{B}} f_B^{[m/n]}(b) - \min_{b\in\mathcal{B}} f_B^{[m/n]}(b)\right|. \tag{3.19}$$

The last contribution to the error is not due to the resummation technique but corresponds instead to non-perturbative corrections, which we write as

$$\Delta_{\rm np} = c_{\rm np} e^{-\frac{1}{\beta_0 a^*}}, \tag{3.20}$$

where $c_{\rm np}$ is an arbitrary coefficient that we take equal to 1, a^* is the value of the fixed point and $1/\beta_0$ is the leading renormalon term in eq.(2.91). In all the cases analyzed here the first instanton/anti-instanton singularities provide indeed subleading non-perturbative corrections.

3.4 Results

We report in this section our results starting from the case of pure $SU(2)$ gauge theory, our best example, and then we generalise to different values of n_c and n_f. We will consider fermion matter in the fundamental representation, but clearly other choices could be investigated too.

3.4.1 Existence of a fixed point in $d = 5$ for pure $SU(2)$

We report in the left panel of fig.3.2 the value of the fixed point coupling a^* as a function of ϵ obtained with both simple perturbation theory and Padé-Borel approximation. In order not to clutter the picture, the error band is shown only for the optimal approximant [2/2],

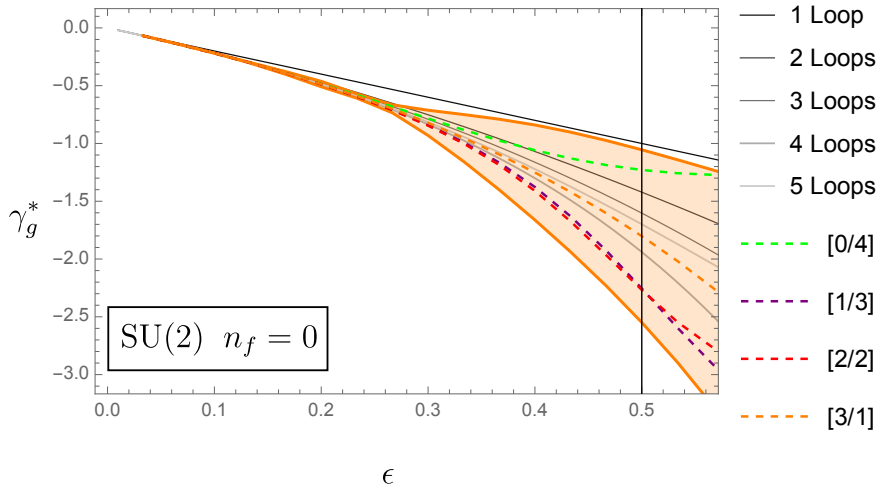

Figure 3.3: The value of the anomalous dimension γ_g^* in $d = 4+2\epsilon$ at the fixed point for pure $SU(2)$ gauge theories. Grey lines correspond to perturbative results, while dashed lines refer to Padé-Borel approximations. The orange shaded area represents the error band for the [3/1] approximant, whose central value is the orange dashed line.

which has been determined by using exact $\mathcal{O}(1/n_f)$ results for β in the large-n_f limit, as explained in the end of section 3.3. We see that up to five-loops every order in perturbation theory would predict a fixed point at $\epsilon = 1/2$, i.e. $d = 5$ dimensions. On the other hand the values of a^* differ substantially from order to order, an indication that the ϵ-expansion is not convergent there. Note how Padé-Borel techniques give more consistent results than the loop expansions. As the error band goes barely below zero, we expect the fixed point to exist, even if we cannot draw a strong conclusion. For illustration of the nice agreement between Padé-Borel and Padé methods mentioned in section 3.3, we report in the right panel of fig.3.2 the results obtained using simple Padé approximation, together again with those coming from perturbation theory. The good agreement among the two results is evident, being the two panels almost indistinguishable.

In fig.3.3 we report the anomalous dimension γ_g^* of the gauge kinetic operator $\mathrm{tr}[F_{\mu\nu}F^{\mu\nu}]$ defined as

$$\Delta_{F^2} = d + \gamma_g^* \,, \tag{3.21}$$

as a function of ϵ. As for a^*, the error band is shown only for the optimal approximant [3/1], determined again by using exact $\mathcal{O}(1/n_f)$ results for γ_g in the large-n_f limit and excluding Padé-Borel approximants with poles on the positive real axis. For $\epsilon = 1/2$, γ_g^* is quite large and negative, but above the unitarity bound for scalar operators $\Delta \geq (d-2)/2$, which corresponds to

$$\gamma_g^* > -3 - \epsilon \tag{3.22}$$

in $d = 4+2\epsilon$ dimensions. The value of $a^*(\epsilon = 1/2) \sim 4 \times 10^{-2}$ could naively led us to believe that the putative UV fixed point is relatively weakly coupled. This number is however renormalization scheme dependent and per se not that relevant, in contrast to γ_g^* which is

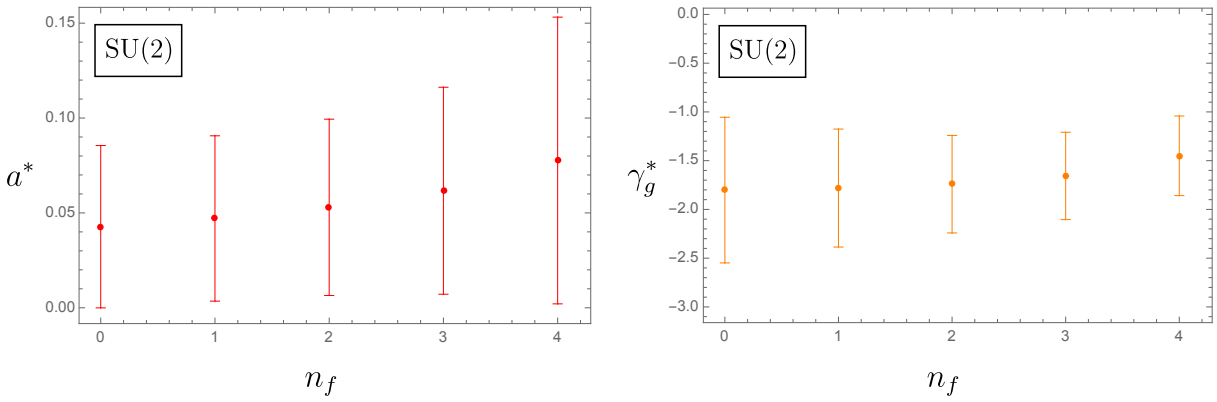

Figure 3.4: The value of the coupling at the fixed point a^* (left) and of the anomalous dimension γ_g^* (right) as a function of n_f for $SU(2)$ gauge theories at $\epsilon = 1/2$ ($d = 5$). The central values and the corresponding error bands are obtained using the best Padé-Borel approximants, respectively [2/2] and [3/1].

a scheme-independent observable. The large value of $\gamma_g^* \sim -2$ points instead towards a putative strongly coupled fixed point. As a comparison, we note that a IR fixed point with a similar value of a^* was found in ordinary $4d$ QCD with $n_f = 12$ fundamental fermion flavors using the same resummation techniques (and the same scheme $\overline{\text{MS}}$) used here, but resulted in values of γ_g^* roughly one order of magnitude smaller [64]. While the main source of error in the study of the QCD conformal window was given from the numerical reconstruction of the Borel function, in the $5d$ case analyzed here this is the case only for γ_g, as the dominant error for a^* comes from the non-perturbative term, eq.(3.20).[5]

As can be seen from fig.3.3, the operator $\text{tr}\,[F_{\mu\nu}F^{\mu\nu}]$ is strongly relevant in the UV and is in fact the relevant deformation driving the UV CFT to the $SU(2)$ pure Yang-Mills theory. Whether this is the only possible relevant singlet deformation of the UV theory remains an open question.

3.4.2 Generalization to different values of n_f and n_c

The results reported in the previous section are easily generalized in presence of fermion matter and for other simple gauge groups. Again, the Padé-Borel technique provides particularly similar results to those obtained with simple Padé approximation, which we will not report in this case.

Let us first consider the addition of n_f Dirac fermion fields in the fundamental representation coupled to $SU(2)$ gauge bosons. In the left panel of fig.3.4 we report the value of the fixed point coupling a^* as a function of n_f. By increasing the number of fermionic fields the value of a^* increases. This is simple to understand by noting that the one-loop fixed point is given by

$$a^*_{1-\text{loop}} = \frac{2\epsilon}{\beta_0}\,. \tag{3.23}$$

[5]Note that removing the non-perturbative contribution to the error of a^* would make the error bands much smaller, providing stronger evidence for the existence of the fixed point.

n_f	0	1	2	3	4
γ_g^*	-1.80(75)	-1.78(61)	-1.74(50)	-1.66(45)	-1.45(41)
γ^*	—	-0.47(12)	-0.52(17)	-0.59(27)	-0.69(46)

Table 3.1: Values of the anomalous dimensions γ_g^* and γ^* for $SU(2)$ gauge theory with n_f Dirac fermion fields in the fundamental representation at $\epsilon = 1/2$ ($d = 5$). The central values are obtained averaging over the Padé-Borel approximants without poles in the real positive axis and well behaved in the large-n_f limit. The error band is obtained combining in quadrature the errors related to each approximant.

Since, at fixed n_c, β_0 decreases as n_f increases, we expect a^* to increase, at least for sufficiently small ϵ.

The dominant source of error comes from the non-perturbative contribution, which is proportional to $\exp(-1/(\beta_0 a^*))$. This is independent of n_f and proportional to $\exp(-1/\epsilon)$ if we use the leading 1-loop order result (3.23) for a^*. The non-perturbative source of error is actually smaller, because the resummed value of a^* is typically smaller than $a^*_{1-\text{loop}}$. However, the value of a^* gets closer and closer to $a^*_{1-\text{loop}}$ as n_f increases and becomes even larger at some point. This explains why the error bands increases with n_f. With our choice of the error the largest value of n_f for which we can confirm the existence of a UV fixed point is $n_f = 4$. This result depends on the choice of the non-perturbative error; as we believe to have been quite conservative, we conclude that the maximum value n_f^* for which the theory admits a UV fixed point is expected to be in the range

$$4 \leq n_f^* \leq 10 \,, \tag{3.24}$$

where the upper bound comes from the requirement of asymptotic freedom in $d = 4$.

In the right panel of fig.3.4 we show γ_g^* as a function of n_f. In fig.3.5 we report the anomalous dimension γ^* for the fermion mass operator defined as

$$\Delta(\bar{\psi}\psi) = d - 1 + \gamma^* \,, \tag{3.25}$$

as a function of n_f, obtained using the optimal Padé-Borel approximant. By increasing the number of fermions, a larger value of $|\gamma^*|$ is found, as expected since the fixed point is more and more strongly coupled. The unitarity bound requires in this case

$$\gamma^* > -2 - \epsilon \,, \tag{3.26}$$

and is always well satisfied, taking also into account the error. Perturbation theory is more stable in this case, not deviating much from the Padé-Borel approximations, at least in the range of interest. Again, the values are compatible with the unitarity bound.

In tab.3.1 we report the results for γ^* and γ_g^* at $n_f = 1, 2, 3, 4$ obtained averaging all

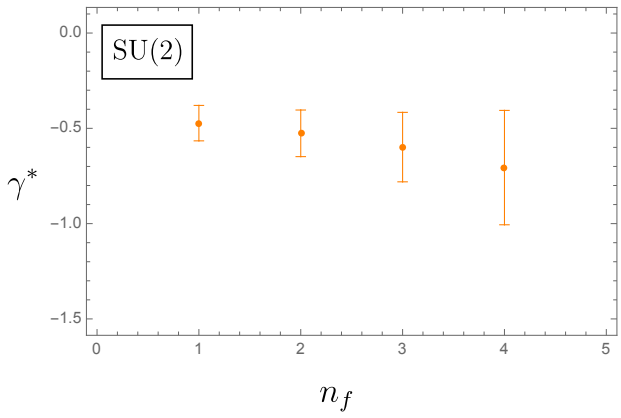

Figure 3.5: Value of the anomalous dimension γ^* for $SU(2)$ as a function of n_f at $\epsilon = 1/2$ ($d = 5$). The central values and the error bands are obtained using the best Padé-Borel approximant [3/1].

well-behaved Padé-Borel approximants weighted with the individual errors σ_i:

$$\gamma^* = \sqrt{\frac{\sum_i (\gamma_i^* \sigma_i^{-2})}{\sum_i \sigma_i^{-2}}}, \qquad \sigma = \sqrt{\sum_i \sigma_i^2}\ , \tag{3.27}$$

and the same for γ_g^*.

Let us now consider pure Yang-Mills theories with $n_c > 2$. We report in the left panel of fig.3.6 the value of the fixed point a^* as a function of n_c. The value of the fixed point decreases as the number of colors increases, while the error band, which is mostly composed by the non-perturbative contribution, keeps almost the same size. This is again simple to understand using (3.23). Given that β_0 increases linearly with the rank of the gauge group, we expect a^* to decrease, at least for sufficiently small ϵ.

The dominant source of error comes again from the non-perturbative contribution. In contrast to the case where we vary n_f at fixed n_c, this error is approximately constant as n_c varies, since so is $|a^* - a^*_{1-\text{loop}}|$. For $n_c \geq 3$, even though the central value remains positive, the error bars in our estimate cross distinctly zero, so we cannot draw a definite conclusion. As in the $SU(2)$ case, adding fermion matter makes the fixed point more strongly coupled. In the right panel of fig.3.6 and in tab.3.2 we report γ_g^* as a function of n_c using the optimal Padé-Borel approximant. The stability of γ_g^* as n_c varies is to some extent expected, since the first three terms of the perturbative series are independent of n_c. It is nevertheless curious that the central values are almost identical for $n_c = 2, 3, 4$. This is most likely a numerical coincidence, but more speculatively one could conjecture that these CFTs are all indistinguishable at the level of local operators.[6]

The existence of a UV fixed point can also be analyzed in the Veneziano limit, $n_f, n_c \to \infty$, $a \to 0$, with $x = n_f/n_c$ and $\lambda_V = a n_c$ held fixed. We omit the details of this analysis and report only the main conclusion, which is the evidence of a fixed point in the range

[6]These theories are anyhow expected to be different at the level of line operators, since they have different discrete one-form global symmetries, independently of the global structure of the gauge group.

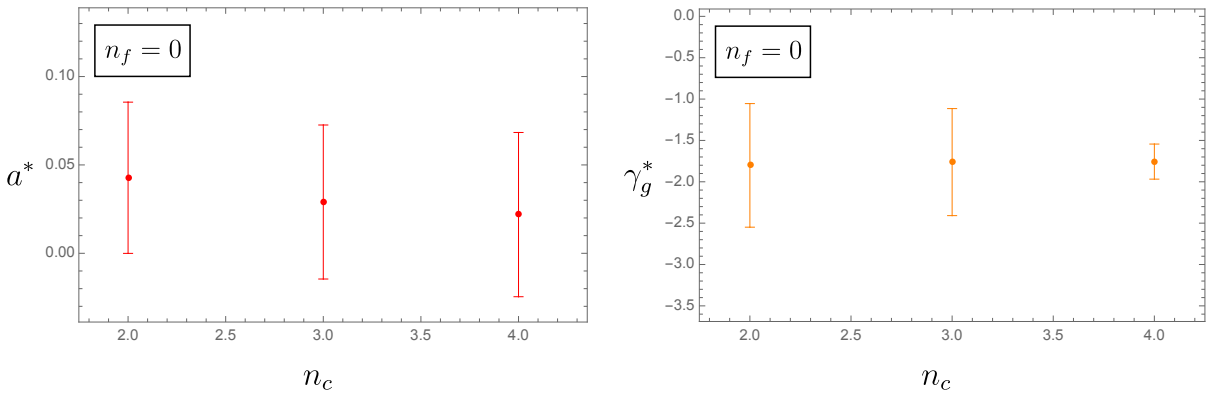

Figure 3.6: The value of the coupling at the fixed point a^* (left) and of the anomalous dimension γ_g^* (right) as a function of n_c for pure SU(n_c) gauge theories at $\epsilon = 1/2$ ($d = 5$). The central values and the error bands are obtained using the best Padé-Borel approximants, respectively [2/2] and [3/1].

$0 \leq x \leq 2.6$. Large values for γ^* and γ_g^* are also found in this case, suggesting the presence of strongly coupled CFTs. The unitarity bound is well satisfied in the whole interval.

3.5 Other approaches: a brief overview

We briefly review in this subsection the main studies developed up to now on the existence of a UV stable fixed point in $5d$ non-abelian gauge theories.

As mentioned, our study is an extension of the previous work [77]. This reference applied optimal truncation to the series in ϵ obtained from the then-available four-loops beta function and suggested evidence for the existence of a $5d$ fixed point for pure gauge theories with $n_c \geq 2$. Optimal truncation is however reliable only when the smallest term in the series is not the last available one and it is not conclusive if the terms are too few for this to happen. This is why numerical results were reported in [77] only for $n_c = 2$, in the case of a^*, and $n_c = 2, 3$, in the case of ν^*, which is an index related to the gauge anomalous dimension by the expression $\nu^* = -2/\gamma_g^*$. Such results are in agreement with ours, taken into account that we were more conservative in the estimate of the error.[7]

Let us now present other methods used to address the problem. Ref. [126] applied the exact RG equations to a certain truncated set of higher dimensional operators in $SU(n_c)$ YM, and found that the critical dimension above which the fixed point disappears is $d_{\rm cr} > 5$ for $n_c = 2, 3, 5$. The result seems to indicate the existence of a continuum limit in five dimensions, however the conclusion is based on the truncation of the flow equations whose reliability is hard to assess.

This problem was also approached using the lattice. Given a lattice Lagrangian that reduces to the continuum $5d$ Lagrangian at large distances, one looks for a second-order

[7] Note that in ref. [77] a different notation was chosen: in order to properly compare the results one should rescale our value of a^* by a factor 4.

n_c	2	3	4
γ_g^*	-1.80(75)	-1.76(65)	-1.76(21)

Table 3.2: Values of the anomalous dimensions γ_g^* for Yang-Mills theory with different numbers of colors n_c at $\epsilon = 1/2$ ($d = 5$). The central values are obtained averaging over the Padé-Borel approximants without poles in the real positive axis and well behaved in the large-n_f limit. The error band is obtained combining in quadrature the errors related to each approximant.

phase transition by varying the lattice couplings. If such a transition is not found, then this could be a consequence of the fact that the starting Lagrangian was not general enough, and no definite conclusion can be reached about the existence of the UV fixed point in the continuum. The simplest choice for the initial action is the Wilson plaquette in the fundamental representation. With this choice and $n_c = 2$, $n_f = 0$, both [127] and [128] found a confinement-deconfinement phase-transition of first rather than second order. Ref. [128] went further and analyzed also a modified action with the inclusion of the Wilson plaquette in the adjoint representation. Again, in the region of the coupling space that they managed to explore they only found a first order transition, though a weaker one as the fundamental coupling was increased. The problem was revisited almost 30 years later in the recent paper [129]. This reference extended the analysis of [128] to a larger region of the coupling space and larger lattice size, and still found only first order transitions for the fundamental+adjoint action. They went on to consider a different lattice action with the fundamental Wilson plaquette of doubled size and observed the disappearance of a first order transition. Their preliminary extrapolations indicate that the disappearance is robust in the infinite volume limit. This suggests the existence of a second order transition.

A different non-perturbative approach is the numerical conformal bootstrap [34]. Finding interacting non-supersymmetric CFTs in $d \geq 4$ with the conformal bootstrap is generally hard (see e.g. [130] for a recent attempt in $d = 4$). Moreover one cannot easily input that the CFT to be looked for should be related to a non-abelian gauge theory. A method to try to target conformal gauge theories in $4d$ and $5d$ has been put forward in [131]: the idea is to consider the bootstrap bounds for the four-point function of $SO(N)$ vectors and look for families of kinks that are conjecturally associated to the four-point function of flavor-adjoint fermionic bilinears in the conformal gauge theory with fermionic matter. In the specific application to $5d$, [34] found such a family of kinks only for relatively large values of N. At the moment there is neither enough evidence that such kinks are associated to CFTs nor a definite prediction from the conformal bootstrap for the would-be scaling dimension of the leading irrelevant operator at this kink. The approach proposed in [34] is based on the flavor symmetry and therefore it is not suited to the pure YM case. For the latter, a naive possibility is to consider simply the four-point function of identical scalar operators $\mathcal{O}$, bounding the dimension of the operators appearing in their OPE coefficients, with the hope of finding features corresponding to the UV completion of YM, in which $\mathcal{O}$ can be identified with $\mathrm{tr}\,[F_{\mu\nu}F^{\mu\nu}]$. In absence of a selection rule (such as a $\mathbb{Z}_2$ symmetry) forbidding to $\mathcal{O}$ itself to

appear in the OPE, this vanilla bootstrap bound cannot succeed without further assumptions on the spectrum, because the interesting CFT, if it exists, would sit well within the allowed region, below the generalized free theory line. Further predictions from ϵ-expansion or other methods might help in narrowing down the appropriate gap assumptions to be made.

Ref.s [19, 132] provide concrete attempts to realize the UV completion of $5d$ $SU(2)$ YM as a second-order transition in continuum QFT. The starting point is the UV completion of the $SU(2)$ supersymmetric YM theory (SYM), the interacting super-conformal field theory known as E_1 theory [133]. These references consider deforming E_1 by both the supersymmetric deformation that leads to SYM, and by a particular supersymmetry-breaking relevant deformation. For small values of the supersymmetry breaking deformation the theory is calculable and it can be shown to flow to YM in the deep IR. It was shown in [19] that certain contact terms in the correlation functions of global symmetry currents depend on the sign of the supersymmetric deformation. This signals that a transition of some kind must happen in the un-calculable region in which the supersymmetric deformation is smaller than the non-supersymmetric one. However at the moment there is no conclusive argument that this phase transition is of second order. Ref. [132] further showed an instability at infinite (bare) gauge coupling when the supersymmetry-breaking deformation is turned on, implying the existence of an intermediate phase between the two YM phases with different contact terms.

Ref. [134] proposes a realization of the UV fixed point of non-abelian gauge theories in $4 < d < 6$ as the IR fixed point of an RG starting from a non-unitary free theory with a higher-derivative kinetic term. This RG becomes weakly coupled in $6-\epsilon$ expansion. However this alternative description is only known to be valid in the limit of a large number of flavors, in which the fixed point in $4 < d < 6$ only exists for negative g^2.

Outlook In this chapter we studied the extrapolation of UV fixed points of non-abelian gauge-theories from $d = 4+2\epsilon$ to $d = 5$ using Padé-Borel resummation techniques. Our main result is illustrated in fig.s 3.2 and 3.4, where we found evidence for a $5d$ fixed point for the $SU(2)$ gauge theory with $n_f \leq 4$. We also used the method to provide a prediction for the dimension of the leading relevant operator at those fixed points, see fig.3.4.

Chapter 4

Free Energy on the Sphere for Non-Abelian Gauge Theories

4.1 Introduction

In this chapter, we apply the generalized $\widetilde{F}$ theorem to non-abelian gauge theories. We compute the quantity $\widetilde{F}$ for the WF fixed points in an expansion around $d = 4$. The existence of such fixed points was discussed extensively in the previous chapter for the case of $d > 4$ and a small number of matter fields. Alternatively, it can be investigated in the case of $d < 4$ with a large number of matter fields (so that $\beta_0 > 0$). The quantity $\widetilde{F}$ was computed in [138] for d-dimensional QED with n_f four-component fermionic matter fields, for which β_0 is always positive. It was then extrapolated to $d = 3$ to study the existence of an interacting IR CFT for QED in 3 spacetime dimensions, by comparing with the quantity F for the spontaneously broken phase of $2n_f^2 + 1$ massless Goldstone bosons.

The calculation in non-abelian gauge theories presents several new challenges compared to the abelian case. Firstly, the gauge fixing requires a more careful analysis, because it becomes unavoidable to include the interaction with the ghost fields. On the sphere massless scalar fields like the ghosts have zero modes. Due to the fermionic nature of ghosts, this naively leads to a zero in the partition function, which manifests as an IR divergence in $\widetilde{F}$. This divergence needs to be cured by an appropriate regulator (or alternatively by appropriately modifying the gauge-fixing procedure, as we describe in an appendix). Note that, in order to obtain $\widetilde{F}$, it is crucial to carefully keep track of the normalization of the path integral on S^d when implementing the gauge-fixing through the Faddeev-Popov procedure [52]. Secondly, the derivative self-interaction of the gluon leads to diagrams with two derivatives acting on the propagator, and it is important to include also the contact-term contributions in order to evaluate correctly the integrals over the positions of the vertices. Thirdly, unlike QED the renormalization in the gauge sector is not simply encoded in the definition of a renormalized gauge coupling, instead one needs to consider also wave-function counterterms for the gluons and the ghosts. We perform the calculation, taking care of all these issues, up to the next-

to-leading (NLO) order, i.e. including up to two-loop vacuum diagrams. The result is in eq. (4.140). Note that, while we compute the two-loop diagrams in generic ξ-gauge, which allows us to compare with heat-kernel results for generic background [4], we keep track of the normalization of the path integral only in the special case of the Landau gauge, i.e. $\xi = 0$.

We then apply this result to the fixed points of $SU(n_c)$ non-abelian gauge theories in $d = 3$ and in $d = 5$. In $d = 3$, just like in the QED case mentioned above, the theory is known to flow to a CFT in the IR for a sufficiently large number of matter flavors n_f [70], and it is conjectured to change its behavior for n_f smaller than an unknown critical value n_f^*, flowing instead to a phase with spontaneous breaking of the global symmetry [70–72, 139]. We adopt the same logic as in [138], and compare F of the fixed point to that of the putative Goldstone bosons phase. We find that when $\beta_0 > 0$, so that $a^*_{\text{1-loop}} > 0$, the conformal phase is always favored compared to the symmetry-breaking phase. For $\beta_0 < 0$ the fixed point is complex in the ϵ-expansion, but a unitary fixed point in $d = 3$ can still exist.[1] We propose a more speculative approach to estimate F of the $3d$ CFT in this case, by taking an average value of $\widetilde{F}$ among the two complex fixed points. With this method we find that the Goldstone boson phase becomes favored for small n_f, allowing us to put an upper bound on n_f^*. The values found for $2 \leq n_c \leq 5$ are reported in eq. (4.156). The result for $n_c = 2$ favorably compares with previous bounds found using again the F-theorem combined with supersymmetry [140], or lattice methods [141]. We also give an estimate for the upper bound on x^* in the Veneziano limit in eq. (4.157), where $x = n_f/n_c$.

In $d = 5$ we use our calculation to investigate the existence of interacting CFTs that UV complete $5d$ non-abelian gauge theories. If such CFTs exist they would be an example of a non-supersymmetric interacting CFT in $d > 4$. An interesting construction in the case of $SU(2)$ Yang-Mills theory was recently proposed in [19], and further refined in [132], using the E_1 superconformal field theory that UV completes $SU(2)$ Super Yang-Mills. The putative non-supersymmetric CFT is obtained as the IR endpoint of the RG flow triggered by a certain non-supersymmetric deformation of E_1, and by construction it is endowed with a relevant deformation that flows to ordinary $SU(2)$ Yang-Mills theory. Using our extrapolation to $5d$ we can compare the quantity F of the non-supersymmetric CFT with that of the E_1 SCFT, known from supersymmetric localization [142], and test if the RG flow is allowed. We can also easily repeat this check in the case with fundamental flavors n_f and compare with the F quantity of the E_{n_f+1} SCFT that UV completes the supersymmetric gauge theory with flavors. In all cases in which we have evidence for a fixed point in $d = 5$, namely $n_f \leq 4$, we obtain that the $\widetilde{F}$-theorem allows the proposed RG flow.

The rest of the chapter is organized as follows: in section 2 we explain some generalities about the calculation of the sphere partition function, we perform the gauge-fixing and compute the one-loop determinants for non-abelian gauge theories. In section 3 we derive the Feynman rules on the sphere, including the gauge field propagator in an arbitrary ξ-gauge.

[1] The opposite situation can also occur, a fixed point for $\epsilon \ll 1$ which disappears in physical integer dimensions.

In section 4 we compute the two-loop vacuum-vacuum diagrams and obtain our main result. We also show a sanity check of our results, by comparing in detail the UV divergences obtained for pure Yang-Mills theory in ref. [4] in the Feynman gauge $\xi = 1$ with our results. In section 5 we apply the result to the $d = 3$ and $d = 5$ models described above. Most of the technical points of the calculation are relegated in the first two appendices of this thesis. In appendix A we compute the gauge propagator on the sphere for a generic ξ. In appendix B.1 we discuss subtleties about integration by parts and contact terms on the sphere. In appendix B.2 we explain a possible alternative gauge-fixing procedure (used already in [143]) where ghost zero modes are treated more carefully by introducing ghosts for ghosts, which we also use to partially check the results in the main body.

Conventions In this chapter n_f always refers to the number of $4d$ Dirac fermions. Given the way we analytically continue fermions, n_f $4d$ Dirac fermions give rise to $2n_f$ Dirac fermions in $3d$ and n_f Dirac fermions in $5d$.

4.2 Free energy of gauge theories on the sphere: leading order

Let us consider a non-abelian gauge theory with n_f massless Dirac fermions in the fundamental representation. We want to compute the sphere free energy in $d = 4 + 2\epsilon$, defined as

$$F = -\log Z_{S^d} \ , \qquad Z_{S^d} = \frac{1}{\mathrm{vol}(\mathcal{G})} \int \mathcal{D}A\mathcal{D}\psi\mathcal{D}\bar{\psi} \, \exp\left(-S[A, \psi, \bar{\psi}, g]\right) \ . \tag{4.1}$$

Here g denotes the round metric $g_{\mu\nu}$ on S^d with radius R and coordinate x, while $\mathrm{vol}(\mathcal{G})$ is the volume of the space of all gauge transformations, which in our choice of normalization does not depend on the gauge coupling g. We can split the action on the sphere in

$$S = S_{\mathrm{YM}} + S_{\mathrm{matter}} + S_{\mathrm{curv}} \ , \tag{4.2}$$

with

$$S_{\mathrm{YM}} = \int d^d x \sqrt{g} \left(\frac{1}{2g_0^2} \mathrm{tr}[F_{\mu\nu}(x) F^{\mu\nu}(x)] \right) \ , \tag{4.3}$$

$$S_{\mathrm{matter}} = \int d^d x \sqrt{g} \left(-\sum_{i=1}^{n_f} \bar{\psi}_i \gamma^\mu \left(\nabla_\mu - i A_\mu \right) \psi^i \right) \ , \tag{4.4}$$

$$S_{\mathrm{curv}} = \int d^d x \sqrt{g} \left(b_0 E + c_0 \mathcal{R}^2/(d-1)^2 \right) , \tag{4.5}$$

where $g = \det g_{\mu\nu}$, g_0 is the bare gauge coupling constant, ψ^i are n_f four-component Dirac fermions and ∇_μ is the curved space covariant derivative which includes the spin connection term when acting on fermions. As the action should contain all operators that are marginal

in $d = 4$, we have added the curvature terms together with their bare coupling parameters b_0 and c_0.[2] For future purposes, we recall the expression for the Ricci scalar $\mathcal{R}$ and the Euler density E on S^d:

$$\mathcal{R} = \frac{d(d-1)}{R^2} \ , \quad E = \mathcal{R}_{\mu\nu\lambda\rho}\mathcal{R}^{\mu\nu\lambda\rho} - 4\mathcal{R}_{\mu\nu}\mathcal{R}^{\mu\nu} + \mathcal{R}^2 = \frac{d(d-1)(d-2)(d-3)}{R^4} \ . \tag{4.6}$$

4.2.1 One-loop determinants

At leading order in a loopwise expansion the free energy is determined by one loop determinants. As a consequence of the splitting in eq. (4.2), we can divide the leading term of the sphere free energy F_{Free} in three parts:

$$F_{\text{Free}} = F_{\text{free-YM}} + F_{\text{free-F}} + F_{\text{curv}} \ , \tag{4.7}$$

with

$$F_{\text{free-YM}} = -\log\left(\frac{1}{\text{vol}(\mathcal{G})}\int \mathcal{D}A e^{-S_{\text{free-YM}}[A,g]}\right), \tag{4.8}$$

$$F_{\text{free-F}} = -\log\left(\int \mathcal{D}\psi\mathcal{D}\bar{\psi}\, e^{-S_{\text{free-F}}[\psi,g]}\right), \tag{4.9}$$

$$F_{\text{curv}} = \Omega_d R^{d-4}(d(d-1)(d-2)(d-3))b_0 + d^2 c_0), \tag{4.10}$$

where $S_{\text{free-YM}}$ is the quadratic part of the Yang-Mills action, $S_{\text{free-F}}$ the free fermion action and $\Omega_d = 2\pi^{\frac{d+1}{2}}/\Gamma(\frac{d+1}{2})$ is the volume of the d-dimensional sphere with unit radius.

For the expression of $F_{\text{free-F}}$ we use eq.(2.50). Let us now focus on the computation of $F_{\text{free-YM}}$. The gauge field A^μ on the sphere can be written as the sum of a longitudinal part $A^\mu_{(0)}$ and a transverse part $A^\mu_{(1)}$, which can be separately decomposed in orthonormal eigenvectors of the sphere Laplacian $-\nabla^2$:

$$\begin{aligned} A^\mu &= A^\mu_{(0)} + A^\mu_{(1)} \ , \quad \text{such that} \quad \nabla_\mu A^\mu_{(1)} = 0 \ , \\ A^\mu_{(0)} &= \sum_{l>0} a^\ell_{(0)} A^{\mu\ \ell}_{(0)} \ , \quad A^\mu_{(1)} = \sum_{l>0} a^\ell_{(1)} A^{\mu\ \ell}_{(1)} \ , \end{aligned} \tag{4.11}$$

with corresponding eigenvalues $\lambda^{(1)}_\ell$, $\lambda^{(0)}_\ell$ and degeneracies $g^{(1)}_\ell$, $g^{(0)}_\ell$ given by [144]

$$\lambda^{(1)}_\ell = \tfrac{(\ell(\ell+d-1)-1)}{R^2} \ , \qquad g^{(1)}_\ell = \frac{\ell(\ell+d-1)(2\ell+d-1)\Gamma(\ell+d-2)}{\Gamma(\ell+2)\Gamma(d-1)} \ , \quad \ell > 0 \ , \tag{4.12}$$

$$\lambda^{(0)}_\ell = \tfrac{\ell(\ell+d-1)-(d-1)}{R^2} \ , \qquad g^{(0)}_\ell = \frac{(2\ell+d-1)\Gamma(\ell+d-1)}{\Gamma(\ell+1)\Gamma(d)} \ , \quad \ell > 0 \ . \tag{4.13}$$

Note that the eigenfunctions of the longitudinal part can be rewritten in terms of the covariant

[2] In a generic Euclidean manifold we should also include a term with the square of the Weyl tensor, omitted here as it vanishes on the sphere.

derivative of the spherical harmonics $Y_\ell(x)$

$$A^{\mu\ \ell}_{(0)} = \frac{1}{\sqrt{\lambda^{(S)}_\ell}} \nabla^\mu Y_\ell(x) \ , \quad \text{for } \ell \geq 1 \ . \tag{4.14}$$

We take the spherical harmonics to be normalized as

$$\int d^d x \sqrt{g}\ Y_\ell(x) Y_{\ell'}(x) = \delta_{\ell\ell'} \ . \tag{4.15}$$

In order to make the basis $A^{\mu\ \ell}_{(0)}$ orthonormal, we have fixed the normalization factor in terms of the eigenvalue of the laplacian operator associated to $Y_\ell(x)$

$$\lambda^{(S)}_\ell = \frac{\ell(\ell+d-1)}{R^2} \ , \tag{4.16}$$

which has degeneracy $g^{(0)}_\ell$. Note a crucial difference between the spectrum for a scalar and for the longitudinal modes of a vector: the former includes a constant mode with eigenvalue $\lambda^{(S)}_0 = 0$ and degeneracy $g^{(0)}_0 = 1$, while for the latter the modes are restricted to $\ell > 0$ and as a result the constant is excluded.

In dimensional regularization the following identities are valid, which will be useful later in the computation:

$$\sum_{\ell=1}^{\infty} g^{(1)}_\ell = 1 \quad \text{and} \quad \sum_{\ell=1}^{\infty} g^{(0)}_\ell = -1 \ . \tag{4.17}$$

With this decomposition in longitudinal and transverse mode the path integral measure can be rewritten as

$$\int \mathcal{D}A = \int \prod_{\ell=1}^{\infty} da^\ell_{(0)} \ \int \prod_{\ell=1}^{\infty} da^\ell_{(1)} \ . \tag{4.18}$$

4.2.2 Computation in Landau gauge

We want to compute

$$F_{\text{free-YM}} = -\log\left(\frac{1}{\text{vol}(\mathcal{G})}\int \mathcal{D}A\, e^{-S_{\text{free-YM}}[A,g]}\right), \tag{4.19}$$

with

$$S_{\text{free-YM}} = \int d^d x \sqrt{g}\, \frac{1}{g_0^2} \text{tr}\left[A_\nu(-\delta^\nu_\mu \nabla^2 + R^\nu_\mu + \nabla^\nu \nabla_\mu) A^\mu\right] \tag{4.20}$$

and $R^\nu_\mu = \frac{d-1}{R^2}\delta^\nu_\mu$ on S^d. In order to perform the explicit computation it is convenient to add a gauge-fixing term to the action. We work in Landau gauge and set to zero the longitudinal component of the gauge field. In order to do that we insert in the path integral of eq. (4.1)

the following functional identity, valid for any fixed $A_\mu(x)$:

$$1 = \int_{\mathcal{G}'} \mathcal{D}\mu_g(U)\delta(\nabla^\mu A^U_\mu) \left|\det \frac{\delta \nabla^\mu A^U_\mu}{\delta\epsilon}\right| \ , \tag{4.21}$$

where $A^U_\mu(x)$ is the gauge-transformed field under $U(x)$

$$A_\mu(x) \to A^U_\mu(x) = U(x)i(\nabla_\mu - iA_\mu(x))U^{-1}(x) \equiv U(x)iD^A_\mu U^{-1}(x) \ . \tag{4.22}$$

Taking the components in the Lie Algebra, denoted with indices $a, b, c, \ldots$, and also writing $U = \exp(i\epsilon^a t^a)$ in terms of the parameter ϵ^a and the generators t^a, we get the infinitesimal transformation

$$\delta A^a_\mu(x) = (D^A_\mu \epsilon)^a(x) = \nabla_\mu \epsilon^a(x) + f^{abc}A^b_\mu(x)\epsilon^c(x) \ . \tag{4.23}$$

The integration in eq. (4.21) is performed over the functional Haar measure μ_g and is restricted to the set of gauge transformations $\mathcal{G}'$ that act non-trivially on $A_\mu(x)$, i.e. those that give a non-zero functional determinant. In the functional derivative the variation $\delta\epsilon$ is an infinitesimal variation away from U (the integration variable) and tangential to $\mathcal{G}'$, hence $\delta\epsilon$ is any fluctuation not annihilated by the covariant derivative with connection A^U_μ. So we have

$$\left|\det \frac{\delta \nabla^\mu A^U_\mu}{\delta\epsilon}\right| = \det{}' \left(-\nabla^\mu D^{A^U}_\mu\right) \ , \tag{4.24}$$

where the prime denotes that we need to exclude the zero eigenvalue and the minus sign is taken to ensure positivity of the determinant, at least perturbatively. At this point in order to proceed we restrict ourselves to the case of Landau gauge, and use that in Landau gauge the operator is self-adjoint as ∇^μ and $D^{A^U}_\mu$ commute. Therefore, we can implement the prime by excluding constant modes instead of covariantly constant ones. We will always assume this meaning of the prime from now on, as this will lead to a great simplification in the following manipulations.

Inserting the identity in the path integral and exchanging the order of the integrals we obtain

$$F = -\log\left(\frac{1}{\mathrm{vol}(\mathcal{G})}\int_{\mathcal{G}'}\mathcal{D}\mu_g(U)\int \mathcal{D}A\, \exp\left(-S[A,\psi,\bar\psi,g]\right)\, \delta(\nabla^\mu A^U_\mu)\det{}'\left(-\nabla^\mu D^{A^U}_\mu\right)\right) . \tag{4.25}$$

Using gauge invariance of the integration measure and of the action, the integral in A can be rewritten in terms of the variable A^U, renamed A. As a result the integral over μ_g yields just the volume of $\mathcal{G}'$ and we get

$$F = -\log\left(\frac{\mathrm{vol}(\mathcal{G}')}{\mathrm{vol}(\mathcal{G})}\int \mathcal{D}A\, \exp\left(-S[A,\psi,\bar\psi,g]\right)\, \delta(-\nabla^\mu A_\mu)\det{}'\left(-\nabla^\mu D^A_\mu\right)\right) . \tag{4.26}$$

The ratio of the two infinite-dimensional volumes gives the volume of the constant gauge transformations, i.e. the volume of the group G, multiplied by an additional factor that arises by requiring an orthonormal mode decomposition in the path integral.[3] In order to explain this factor, consider separating a generic gauge transformation $f : S^d \to G$ in a constant and a non-constant part $f(x) = f_0 + f'(x)$. This can be done via the decomposition in spherical harmonics: $f(x) = \sum_{\ell=0}^{\infty} F_\ell Y_\ell(x)$. In terms of this decomposition the measure of the path integral is

$$\int \mathcal{D}f = \int \prod_{\ell=0}^{\infty} dF_\ell \ . \tag{4.27}$$

Because of the normalization in (4.15) we have $Y_0 = 1/\sqrt{\text{vol}(S^d)}$, which implies $f_0 = F_0/\sqrt{\text{vol}(S^d)}$ and

$$\text{vol}(\mathcal{G}) = \int dF_0 \, \text{vol}(\mathcal{G}') = \text{vol}(S^d)^{\frac{\dim(G)}{2}} \, \text{vol}(G) \, \text{vol}(\mathcal{G}') \ . \tag{4.28}$$

This leads to

$$F = -\log\left(\frac{\text{vol}(S^d)^{\frac{-\dim(G)}{2}}}{\text{vol}(G)} \int \mathcal{D}A \, \exp\left(-S[A,\psi,\bar{\psi},g]\right) \, \delta(\nabla^\mu A_\mu) \text{det}'\left(-\nabla^\mu D^A_\mu\right) \right) . \tag{4.29}$$

We then introduce non-constant c' and $\bar{c}'$ ghost modes to rewrite the det$'$ as

$$\text{det}'\left(-\nabla^\mu D^A_\mu\right) = \int \mathcal{D}c' \, \mathcal{D}\bar{c}' \exp\left(- \int d^d x \sqrt{g(x)} \, \bar{c}'_a(x) \nabla^\mu D^A_\mu c'^a(x)] \right) . \tag{4.30}$$

The final step is to use the decomposition (4.11) to rewrite the δ-functional in eq. (4.29) in terms of the coefficients of the decomposition

$$\delta(\nabla^\mu A_\mu) = \delta\left(\sum_{\ell=1}^{\infty} \frac{a^\ell_{(0)}}{\sqrt{\lambda^{(S)}_\ell}} \nabla^2 Y_\ell(x) \right) = \prod_{\ell=1}^{\infty} \left(\frac{\ell(\ell+d-1)}{R^2} \right)^{-\frac{g^{(0)}_\ell}{2}\dim(G)} \delta\left(a^\ell_{(0)}\right) \ . \tag{4.31}$$

This sets to zero the longitudinal modes and provides a crucial factor in the path integral. Plugging eq. (4.31) in eq. (4.29) and focusing on the Yang-Mills leading contribution gives

$$\begin{aligned} F_{\text{free-YM}} = -\log\Bigg(& \frac{1}{\text{vol}(G)\sqrt{\text{vol}(S^d)^{\dim(G)}}} \prod_{\ell=1}^{\infty} \left(\frac{\ell(\ell+d-1)}{R^2} \right)^{-\frac{g^{(0)}_\ell}{2}\dim(G)} \\ & \int \mathcal{D}A_{(1)} \, \mathcal{D}c' \, \mathcal{D}\bar{c}' \, \exp\left(-S_{\text{YM-Free}}[A_{(1)},g] - 2\int d^d x \sqrt{g(x)} \, \text{tr}[\bar{c}'(x) \nabla^2 c'(x)] \right) \Bigg) . \end{aligned} \tag{4.32}$$

[3]The normalization of the path integral is chosen following ref. [143]. There is however a difference in the computation of the volume of the gauge group as in our notation the coupling does not appear in the volume expression.

We are finally ready to compute the integral. We start from the integration over $A_{(1)}$. Using the decomposition in eqs.(4.11-4.13) and the normalization in eq. (4.27) we get

$$\begin{aligned}\int \mathcal{D}A_{(1)}\, \exp\left(-\int d^dx\sqrt{g}\frac{1}{2g_0^2}\left(A^a_{(1)\mu}(-\nabla^2+(d-1))A^\mu_{(1)a}\right)\right)\\ =\prod_{\ell=1}^{\infty}\left(\frac{2\pi g_0^2R^2}{(\ell+1)(\ell+d-2)}\right)^{\frac{g_\ell^{(1)}}{2}\dim(G)}\,.\end{aligned} \tag{4.33}$$

For the computation of the ghost path integral we again decompose in spherical harmonics:

$$c'(x)=\sum_{\ell=1}^{\infty}C_\ell Y_\ell(x),\quad \int\mathcal{D}c'=\int\prod_{\ell=1}^{\infty}dC_\ell\,. \tag{4.34}$$

As we are dealing with Grassmann variables, we have

$$\int \mathcal{D}C_\ell\mathcal{D}\bar{C}_\ell\exp\left(\bar{C}_\ell C_\ell\right)=1\,, \tag{4.35}$$

implying

$$\int\mathcal{D}c'\,\mathcal{D}\bar{c}'\,\exp\left(-\int d^dx\sqrt{g(x)}\,\bar{c}'_a(x)\nabla^2c'^a(x)]\right)=\prod_{\ell=1}^{\infty}\left(\frac{\ell(\ell+d-1)}{R^2}\right)^{g_\ell^{(0)}\dim(G)}\,. \tag{4.36}$$

Replacing in eq. (4.32), we get

$$\begin{aligned}F_{\text{free-YM}}=\log\text{vol}(G)+\frac{\dim(G)}{2}\left(\log\text{vol}(S^d)+\sum_{\ell=1}^{\infty}g_\ell^{(1)}\log\left(\frac{(\ell+1)(\ell+d-2)}{2\pi g_0^2R^2}\right)\right.\\ \left.-\sum_{\ell=1}^{\infty}g_\ell^{(0)}\log\left(\frac{\ell(\ell+d-1)}{R^2}\right)\right)\,.\end{aligned} \tag{4.37}$$

In order to find an explicit expression for these series one can follow [138], who performed the same computation in the abelian case. Their procedure is based on the rewriting of the logarithms appearing in eq. (4.37) with the identities

$$\log(y)=\int_0^\infty\frac{dt}{t}\left(e^{-t}-e^{-yt}\right)\,,\quad \frac{1}{t}=\frac{1}{1-e^{-t}}\int_0^1du\,e^{-ut}\,. \tag{4.38}$$

Then, using gamma function identities, eq. (4.17), and performing the t-integrals, one can find an analytical expression for $F_{\text{free-YM}}$. The only subtle point concerns the ghost determinant. It is necessary to add and remove the zero mode, regulating with a mass parameter δ which

is set to zero in the end. This provides

$$\sum_{\ell=1}^{\infty} g_\ell^{(0)} \log\left(\ell(\ell+d-1)\right) = \lim_{\delta\to 0}\left[\sum_{\ell=0}^{\infty} g_\ell^{(0)} \log\left((\ell+\delta)(\ell+d-1)\right) - \log\left(\delta(d-1)\right)\right] , \quad (4.39)$$

For the sum over ℓ we use again eq. (4.38), while for the $\log\left(\delta(d-1)\right)$ we use [138]

$$\log(\delta) = -\int_0^1 \frac{1}{u+\delta} + \log(1+\delta)\,. \quad (4.40)$$

Putting everything together we find a smooth limit $\delta \to 0$, which reads

$$F_{\text{free-YM}}(d) = \dim(G) F_{\text{Max}}(d) - \frac{\dim(G)}{2}\log\left(g_0^2 R^{4-d}\right) + \log\frac{\text{vol}(G)}{(2\pi)^{\dim(G)}}\,. \quad (4.41)$$

where $F_{\text{Max}}(d)$ reads

$$\begin{aligned} F_{\text{Max}}(d) = \; & \frac{1}{2}\log(2\pi(d-1)^2\Omega_d) - \frac{1}{\sin\left(\frac{\pi d}{2}\right)}\int_0^1 du\,\left(\frac{\sin\left(\frac{\pi d}{2}\right)(d-2)}{(d-2)^2-u^2} + \frac{\sin\left(\frac{\pi d}{2}\right)}{u}\right. \\ & + \left(d^2+1-3d(1+u)+2u(u+2)\right)\frac{\sin\left(\frac{\pi}{2}(2u-d)\right)\Gamma(d-2-u)\Gamma(1+u)}{2\Gamma(d)} \\ & \left. + (2u-d)\sin\left(\frac{\pi}{2}(d-2u)\right)\frac{\Gamma(d-u)\Gamma(u)}{\Gamma(d+1)}\right)\,. \end{aligned} \quad (4.42)$$

4.3 Feynman rules on the sphere

In this section we discuss the Feynman rules on S^d for non-abelian gauge theories. We start by reviewing some preliminary notion on maximally symmetric spaces. We then generalize the computation of the vector propagator presented in [5] in the Feynman gauge to an arbitrary ξ-gauge. The ghost propagator requires some care in order to remove the zero mode, while the propagator of the Dirac fermion is computed by a Weyl transformation from flat space. We then derive the Feynman rules for the vertices.

4.3.1 Bitensors in maximally symmetric spaces

The two-point function of a spinning operator in a curved space M defines a bitensor, namely a bilocal function that is a tensor with respect to both of its arguments. In maximally symmetric spaces bitensors can be expressed as sums and products of a few building blocks. Let us briefly review these building blocks following ref. [5]. Starting with the geodesic distance $\mu(x,x')$, which is a biscalar, other basic geometric objects are the parallel propagator $g^{\nu}{}_{b'}(x,x')$ transporting vectors along geodesics from x to x', and the unit vectors $n_\nu(x,x')$ and $n_{\nu'}(x,x')$ tangent to the geodesic at x and x' respectively:

$$n_\nu(x,x') = \nabla_\nu \mu(x,x) \quad \text{and} \quad n_{\nu'}(x,x') = \nabla_{\nu'}\mu(x,x')\,. \quad (4.43)$$

$g^{\nu}{}_{b'}(x,x'), n_\nu(x,x')$ and $n_{\nu'}(x,x')$ are examples of bitensors. We use the following notation: a bitensor (n,m) is a rank n tensor at x and a rank m tensor at x'. So for instance $g^{\nu}{}_{b'}(x,x'), n_\nu(x,x')$ and $n_{\nu'}(x,x')$ are respectively $(1,1)$, $(1,0)$ and $(0,1)$ bitensors. In general objects written as the contraction of two bitensors depend on both x and x', even if they contain only primed or unprimed indices. An exception is the following identity relating the metric $g_{\nu\lambda}$ to the parallel propagator

$$g_{\nu\lambda}(x) = g_\nu{}^{\rho'}(x,x') g_{\rho'\lambda}(x',x) \,, \tag{4.44}$$

and similarly for $g_{\nu'\lambda'}(x')$. Covariant derivatives of bitensors can be taken with respect to either x or x' and are denoted by ∇_ν and $\nabla_{\nu'}$ respectively.

It is possible to prove that any bitensor in a maximally symmetric space can be expressed as sums and products of the building blocks $g_{\nu\lambda}$, $g_{\nu'\lambda'}$, n_ν, $n_{\nu'}$ and $g_{\nu\lambda'}$, with coefficients that are only functions of μ. This provides a remarkable simplification in finding the structure of propagators and their explicit expressions.

Let us list some properties, useful for the derivation of propagators:

$$\begin{aligned} \nabla_\nu n_\lambda &= A\,(g_{\nu\lambda} - n_\nu n_\lambda) \,, \\ \nabla_\nu n_{\lambda'} &= C\,(g_{\nu\lambda'} + n_\nu n_{\lambda'}) \,, \\ \nabla_\nu g_{\lambda\rho'} &= -(A+C)\,(g_{\nu\lambda} n_{\rho'} + g_{\nu\rho'} n_\lambda) \,, \end{aligned} \tag{4.45}$$

where

$$\begin{aligned} A(\mu) &= \frac{1}{R}\cot(\mu/R) \,, \\ C(\mu) &= -\frac{1}{R}\frac{1}{\sin(\mu/R)} \,, \end{aligned} \tag{4.46}$$

where R is the radius, defined in terms the constant value of the Ricci curvature scalar in eq. (4.6). For future convenience it is useful to introduce the variable

$$z(x,x') \equiv \cos^2\left(\frac{\mu(x,x')}{2R}\right) . \tag{4.47}$$

which is the chordal distance between the points.

Let us now specify to a sphere S^d_R of radius R. Using stereographic coordinates x^μ we write the metric as

$$ds^2 = g_{\mu\nu} dx^\mu dx^\nu \,, \qquad g_{\mu\nu} = \frac{4R^4}{(R^2+|x|^2)^2}\delta_{\mu\nu} \,. \tag{4.48}$$

The geodesic distance is given by the following identity

$$\cos\left(\frac{\mu(x,x')}{R}\right) = 1 - \frac{2R^2|x-x'|^2}{(R^2+|x|^2)\,(R^2+|x'|^2)} = 2z(x,x') - 1 \,. \tag{4.49}$$

When $x' = 0$, we denote for simplicity

$$z \equiv z(x,0) = \frac{R^2}{R^2 + x^2}\,. \tag{4.50}$$

The variable z will be useful to write propagator expressions and, in particular, their expansion around coincident points.

4.3.2 Propagators on S^d

Vector propagator on S^d

Vector propagators for maximally d-dimensional symmetric spaces have been computed in [5]. For our purpose we need the expression of the massless vector field on the sphere. It follows from the quadratic part of the gauge action

$$S_{\text{free-YM}} = \int d^dx\sqrt{g}\frac{1}{g_0^2}\text{tr}\left[A_\nu(-\delta^\nu_\mu\nabla^2 + R^\nu_\mu + \left(1-\frac{1}{\xi}\right)\nabla^\nu\nabla_\mu)A^\mu\right], \tag{4.51}$$

that the vector propagator $Q^{ab}_{\nu\lambda'}(x,x') = \langle A^a_\nu(x)A^b_{\lambda'}(x')\rangle = g_0^2\delta^{ab}Q_{\nu\lambda'}(x,x')$ satisfies the equation

$$\left(-g^{\mu\nu}\nabla^2 + R^{\mu\nu} + \left(1-\frac{1}{\xi}\right)\nabla^\mu\nabla^\nu\right)Q_{\nu\lambda'}(x,x') = \delta(x-x')g^\mu_{\lambda'}\ . \tag{4.52}$$

The propagator $Q_{\nu\lambda'}(x,x')$ is a maximally symmetric (1,1) bitensor and can be decomposed as

$$Q_{\nu\lambda'}(x,x') = \alpha(\mu)g_{\nu\lambda'} + \beta(\mu)n_\nu n_{\lambda'}, \tag{4.53}$$

where α and β are generic functions of the geodesic distance. Their expression is found in eqs. (A.14), (A.19) and (A.21) in appendix A, where the interested reader can also find their detailed derivation.

Ghost propagator on S^d

The ghost propagator $G^{ab}(x,x') = \langle c'^{\,a}(x)\bar{c}'^{\,b}(x')\rangle$ satisfies

$$\nabla^2 G^{ab}(x,x') = \delta(x-x')\delta^{ab}\ . \tag{4.54}$$

As explained in section 4.2.2, c' has the zero mode removed, so we need to subtract the constant part from this propagator. This is also clear from the expansion of the propagator in terms of the spherical harmonics (4.16):

$$G^{ab}(x,x') = \sum_{\ell>0}\frac{R^2}{-\ell(\ell+d-1)}Y_\ell(x)Y_\ell(x')\delta^{ab}\ , \tag{4.55}$$

where the constant mode $\ell = 0$ is excluded from the sum, otherwise giving a divergence.

In order to resum this expression we need to introduce a small regulator, as we did for the one-loop computation of the free energy:

$$G^{ab}(x,x') = \lim_{\delta\to 0}\left[\sum_{\ell\geq 0}\frac{R^2 Y_\ell(x)Y_\ell(x')}{-\ell(\ell+d-1)+\delta(d-1+\delta)} - \frac{R^2 Y_0^2}{\delta(d-1+\delta)}\right]\delta^{ab}\,. \tag{4.56}$$

The first term corresponds to the propagator $G_{\rm reg}(x,x')$ associated to a scalar field with mass $m^2=\delta(d-1+\delta)/R^2$, whose expression as a function of z is

$$G_{\rm reg}(z;\delta) = -\frac{\Gamma(d-1+\delta)}{4(4\pi)^{\frac{d}{2}-1}R^{d-2}\Gamma(1+\delta)\sin(\pi\delta)\Gamma(\frac{d}{2})}{}_2F_1\Big(-\delta,-1+d-\delta,\frac{d}{2},z\Big). \tag{4.57}$$

Plugging in eq. (4.56) and taking the limit $\delta\to 0$, we find a well-defined expression for the ghost propagator:

$$G^{ab}(z) = \delta^{ab}G(z) = \frac{\delta^{ab}\left(dH(d-2)-2(d-1)z_3F_2\big(1,1,d;2,1+\frac{d}{2};z\big)\right)}{4d(4\pi)^{\frac{d}{2}-1}R^d\sin(\pi d)\Gamma(2-d)\Gamma(\frac{d}{2})}\,, \tag{4.58}$$

where H denotes the harmonic number, which can be written in terms of the digamma function ψ and the Euler constant γ_E as $H(x)=\gamma_E+\psi(x+1)$.

Fermion propagator on S^d

The fermion propagator on S^d is easily computed from its known expression in flat space by performing a Weyl rescaling, see eq. (4.48). We have

$$S^i_j(x,0) = \langle\psi^i(x)\bar\psi_j(0)\rangle_{\rm sphere} = \frac{\langle\psi^i(x)\bar\psi_j(0)\rangle_{\rm flat}}{\Omega(x)^{\frac{d}{2}}\Omega(0)^{\frac{d}{2}}} = \delta^i_j\frac{\Gamma\left(\frac{d}{2}\right)(R^2+x^2)^{\frac{d}{2}}\gamma^\mu x_\mu}{2^{(d+1)}\pi^{\frac{d}{2}}(x^2)^{\frac{d}{2}}R^d}\,, \tag{4.59}$$

where in the last equality we used

$$\langle\psi^i(x)\bar\psi_j(0)\rangle_{\rm flat} = \delta^i_j\frac{\Gamma\left(\frac{d}{2}\right)\gamma^\mu x_\mu}{2\pi^{\frac{d}{2}}(x^2)^{\frac{d}{2}}}\,,\qquad \Omega(x)=\frac{2R^2}{R^2+x^2}\,. \tag{4.60}$$

4.3.3 Vertices on the sphere

The Feynman rules for the vertices can be read from the gauge-fixed action giving

$$g_0\Gamma^{\rm TR}(x) = -\frac{1}{g_0^2}f^{abc}\nabla_\nu A^a_\lambda A^b_\nu A^c_\lambda(x)\,, \tag{4.61}$$

$$g_0^2\Gamma^{\rm QU}(x) = -\frac{1}{4g_0^2}f^{abc}f^{ade}g_0A^b_\nu A^c_\lambda A^d_\nu A^e_\lambda(x)\,, \tag{4.62}$$

$$g_0\Gamma^{\rm GH}(x) = f^{abc}\nabla_\nu\bar c'^a A^b_\nu c'^c(x)\,, \tag{4.63}$$

$$g_0\Gamma^{\rm FE}(x) = -i(t^a_f)_{\alpha\beta}\bar\psi^\alpha_i\gamma^\mu\psi^\beta_i A^a_\mu(x)\,, \tag{4.64}$$

respectively the triple gluon, the quartic gluon, the ghost-gluon and the fermion-gluon interactions.

4.4 Next to leading contribution

In the previous section we have obtained the Feynman rules for gauge theories on the sphere. We now have all the ingredients to compute the free energy at the next-to-leading order. For n_f Dirac fermions in the fundamental representation of the gauge group $G = SU(n_c)$ we have

$$\begin{aligned} F =&(n_c^2-1)F_{\text{Max}}(d) - \frac{1}{2}(n_c^2-1)\log\left(g_0^2 R^{4-d}\right) + \log\left(\frac{\text{vol}(SU(n_c))}{(2\pi)^{n_c^2-1}}\right) \\ &+ n_f n_c F_{\text{free-F}} + F_{\text{curv}} - \frac{1}{2}g_0^2 G_2 + \dots , \end{aligned} \tag{4.65}$$

where G_2 includes all the two-loop vacuum diagrams. Note that we have kept all the couplings bare. In section 4.4.1 we compute the various diagrams contributing to G_2 in eq. (4.65): the divergent terms in a generic ξ-gauge and the finite pieces in the Landau gauge $\xi = 0$. As a check of the validity of our results we verify in section 4.4.2 that the divergences that we obtain match with those computed with heath-kernel methods in ref. [4] in the Feynman gauge $\xi = 1$. Renormalization is discussed in section 4.4.3.

4.4.1 Computation of the diagrams

The leading interacting part of the free energy is given by connected vacuum diagrams up to order g_0^2. The corresponding contribution, which we will call G_2, is composed by the following two-loop diagrams:

$$G_2 = G_2^{\text{triple}} + G_2^{\text{ghost}} + G_2^{\text{ferm}} + G_2^{\text{quart}} + G_2^{\text{CT-vec}} + G_2^{\text{CT-gh}} . \tag{4.66}$$

The first four terms in (4.66) are genuine two-loop graphs:

$$\begin{aligned} G_2^{\text{triple}} &= \quad = \int d^d x d^d x' \sqrt{g}\sqrt{g'}\langle \Gamma^{\text{triple}}(x)\Gamma^{\text{triple}}(x')\rangle , \\ G_2^{\text{ghost}} &= \quad = \int d^d x d^d x' \sqrt{g}\sqrt{g'}\langle \Gamma^{\text{ghost}}(x)\Gamma^{\text{ghost}}(x')\rangle , \\ G_2^{\text{ferm}} &= \quad = \int d^d x d^d x' \sqrt{g}\sqrt{g'}\langle \Gamma^{\text{fermion}}(x)\Gamma^{\text{fermion}}(x')\rangle , \\ G_2^{\text{quart}} &= \quad = 2\int d^d x \sqrt{g}\langle \Gamma^{\text{quart}}(x)\rangle . \end{aligned} \tag{4.67}$$

The last two ones are instead one-loop graphs with (one-loop) counterterm insertions:

$$G_2^{\text{CT-vec}} = \quad = -2\delta_L \int d^dx \langle \frac{1}{2\xi} \left(\nabla_\mu A^{\mu a}(x)\right)^2 \rangle - 2\delta_T \int d^dx \langle \frac{1}{4} \left(\nabla_\mu A^a_\nu(x) - \nabla_\nu A^a_\mu(x)\right)^2 \rangle \,,$$

$$G_2^{\text{CT-gh}} = \quad = -2\delta_c \int d^dx \langle \left(\bar{c}_a(x) \nabla^2 c^a(x)\right) \rangle \,. \tag{4.68}$$

These counterterms are defined from the renormalized Lagrangian

$$\frac{Z_T}{Z_{g^2} g^2} \frac{1}{4} \left(\nabla_\mu A^a_\nu(x) - \nabla_\nu A^a_\mu(x)\right)^2 + \frac{Z_L}{2g^2\xi} \left(\nabla_\mu A^{\mu a}(x)\right)^2 - \frac{Z_T^{3/2}}{Z_{g^2} g^2} f^{abc} \nabla_\mu A^a_\nu A^{\mu b} A^{\nu^c} + \dots \,, \tag{4.69}$$

where $g_0^2 = Z_g^2 g^2$ is the relation between the bare and the renormalized coupling and $Z_\bullet = 1 + \delta_\bullet g^2$. Thanks to the vector equations of motion, we have

$$\int d^dx \langle \frac{1}{4} \left(\nabla_\mu A^a_\nu(x) - \nabla_\nu A^a_\mu(x)\right)^2 \rangle = - \int d^dx \langle \frac{1}{2\xi} \left(\nabla_\mu A^\mu_a(x)\right)^2 \rangle + \mathcal{O}(g) \,, \tag{4.70}$$

modulo a $\delta^{(d)}(0)$ factor, which vanishes in dimensional regularization. The counterterms δ_T and δ_L entering the vector propagator can be computed in flat space and they read (see e.g. [145][4])

$$\delta_L = 0 \,, \qquad \delta_T = C_A \frac{3+\xi}{32\pi^2\epsilon} \left(1 + \mathcal{O}(g_0^2)\right) \,, \tag{4.71}$$

with $C_A = n_c$ for the $SU(n_c)$ group. The presence of the ghost counterterm is instead a peculiarity of S^d, consequence of the removal of zero modes from the propagator. We refer to next section for its computation. The final result is

$$\delta_c = -C_A \frac{3-\xi}{64\pi^2\epsilon} \left(1 + \mathcal{O}(g_0^2)\right) . \tag{4.72}$$

Computation of the ghost counterterm

The ghost wave function renormalization can be computed by imposing finiteness of the ghost propagator at one loop. We compute the divergence in configuration space:

$$\quad \Big|_{\text{div.}} = \delta_{ab} g_0^2 \, C_A \int d^dx_1 \, d^dx_2 \sqrt{h}\sqrt{h'} \, G(x, x_1) \, \nabla_{\mu_1} G(x_1, x_2) \, Q^{\mu_1\mu_2}(x_1, x_2) \nabla_{\mu_2} G(x_2, 0) \,. \tag{4.73}$$

[4]Comparing our Lagrangian (4.69) with the definitions in section 26.5 of [145], we see that the relation between our counterterms and the counterterms δ_3 and δ_{A^3} defined there are: $g^2\delta_T = \delta_{A^3} - \delta_3$, and $g^2\delta_{g^2} = \delta_{A^3} - \frac{3}{2}\delta_3$. Moreover since there is no correction proportional to the longitudinal part of the propagator, $\delta_L = 0$. Note also that $\epsilon_{\text{there}} = -2\epsilon_{\text{here}}$.

Since we are dealing with UV divergences, we can take the limit of coincident points $x_1 \sim x_2$. Taylor expanding the propagator $G(x_2, 0)$ around x_1, we get

$$G(x_2,0) = G(x_1,0) + (x_2^\mu - x_1^\mu)\nabla_\mu G(x_1,0) + \frac{1}{2}(x_2^\mu - x_1^\mu)(x_2^\nu - x_1^\nu)\nabla_\nu\nabla_\mu G(x_1,0) + \dots \quad (4.74)$$

Replacing this expression in eq. (4.73) we find that the only non-vanishing contribution comes from the third term: the first vanishes when derived with respect to x_2, while the second is zero because of Lorentz invariance. All other terms in the expansion provide convergent result and are therefore not relevant for the computation of counterterms. We have then

$$\delta_{ab}\ \frac{g_0^2}{2}\ C_A \int d^dx_1\sqrt{h}\ G(x,x_1) I^{\mu\nu}\ \nabla_\nu\nabla_\mu G(x_1,0), \quad (4.75)$$

with

$$I^{\mu\nu} = \int d^dx_2\sqrt{h'}\,(\nabla_{\mu_1}G(x_1,x_2)\ Q^{\mu_1\mu_2}(x_1,x_2)\nabla_{\mu_2}(x_2^\mu - x_1^\mu)(x_2^\nu - x_1^\nu))\ . \quad (4.76)$$

By spherical invariance this integral does not depend on the position of x_1, which can be set to zero. We can use Lorentz invariance to rewrite the integral as

$$I^{\mu\nu} = \frac{g^{\mu\nu}}{d}(I^{\lambda\sigma}g_{\lambda\sigma})\,. \quad (4.77)$$

The divergence can be computed by using stereographic coordinates and expanding around coincident points, as done in sec.4.4.1: we get

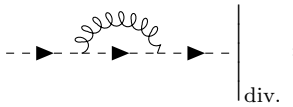

$$\Big|_{\text{div.}} = \delta_{ab}\frac{3-\xi}{64\pi^2\epsilon}\ g_0^2 C_A \int d^dx_1\sqrt{h}\ G(x,x_1)\,\nabla^2 G(x_1,0)\,. \quad (4.78)$$

This divergence can be removed by taking the following wave function renormalization:

$$c = Z_c^{\frac{1}{2}}c_R\ , \qquad \bar{c} = Z_c^{\frac{1}{2}}\bar{c}_R\,, \quad (4.79)$$

with

$$Z_c = 1 + \delta_c = 1 - g_0^2\frac{3-\xi}{64\pi^2\epsilon}C_A + \mathcal{O}(g^4)\,, \quad (4.80)$$

which reproduces eq. (4.72). Note that since there is no divergence proportional to

$$\int d^dx_1\sqrt{h}\ G(x,x_1)G(x_1,0), \quad (4.81)$$

there is no mass renormalization, as expected.

Results

Applying Wick's contraction and the previously listed Feynman rules to eq. (4.67), we get

$$G_2^{\text{triple}} = \kappa \int d^dx\ d^dx' \sqrt{g}\sqrt{g'}\ \Big(\nabla^\mu\nabla^{\mu'}Q^{\nu\nu'}(Q_{\mu\mu'}Q_{\nu\nu'} - Q_{\mu\nu'}Q_{\nu\mu'}) \tag{4.82}$$
$$+ \nabla^\nu Q^{\mu\mu'}(\nabla^{\nu'}Q_{\nu\mu'}Q_{\mu\nu'} - Q_{\nu\nu'}\nabla^{\nu'}Q_{\mu\mu'}) + \nabla_\nu Q^{\mu\nu'}(\nabla_{\nu'}Q^{\nu\mu'}Q_{\mu\mu'} - Q^{\nu\mu'}\nabla_{\nu'}Q_{\mu\nu'})\Big)\,,$$

$$G_2^{\text{ghost}} = \kappa \int d^dx\ d^dx' \sqrt{g}\sqrt{g'}\ (\nabla_\mu G\ \nabla_{\mu'}G\ Q^{\mu\mu'})\,, \tag{4.83}$$

$$G_2^{\text{ferm}} = n_f T_f \left(n_c^2 - 1\right) \int d^dx\ d^dx' \sqrt{g}\sqrt{g'}\ (\text{tr}\,[\gamma_\mu S \gamma_{\mu'} S]\ Q^{\mu\mu'})\,, \tag{4.84}$$

$$G_2^{\text{quart}} = -\frac{\kappa}{2}\int d^dx\sqrt{g}\ (Q^\mu{}_\mu Q^\nu{}_\nu - Q_{\mu\nu}Q^{\mu\nu})\,, \tag{4.85}$$

$$G_2^{\text{CT-vec}} = \kappa\frac{3+\xi}{16\pi^2\epsilon}\int d^dx\sqrt{g}\ \left(\frac{1}{2\xi}\nabla^\mu\nabla^\nu Q^\mu{}_\nu\right)\,, \tag{4.86}$$

$$G_2^{\text{CT-gh}} = \kappa\frac{3-\xi}{32\pi^2\epsilon}\int d^dx\sqrt{g}\ (\nabla^2 G)\,. \tag{4.87}$$

where $T_f = 1/2$ for the fundamental representation and we have defined

$$\kappa = C_A\left(n_c^2 - 1\right)\,. \tag{4.88}$$

Note that the first term in the triple diagram (4.82) includes a double derivative of the vector propagator, which should be treated with care, because it contains a term proportional to a δ-function at coincident points, which contributes to the integral. A simple way to circumvent this problem consists in integrating by parts the first term of eq. (4.82) getting

$$G_2^{\text{triple}} = \kappa \int d^dx\ d^dx' \sqrt{g}\sqrt{g'}\ \Big(\nabla^{\mu'}Q^{\nu\nu'}\nabla^\mu(-Q_{\mu\mu'}Q_{\nu\nu'} + Q_{\mu\nu'}Q_{\nu\mu'}) \tag{4.89}$$
$$+ \nabla^\nu Q^{\mu\mu'}(\nabla^{\nu'}Q_{\nu\mu'}Q_{\mu\nu'} - Q_{\nu\nu'}\nabla^{\nu'}Q_{\mu\mu'}) + \nabla_\nu Q^{\mu\nu'}(\nabla_{\nu'}Q^{\nu\mu'}Q_{\mu\mu'} - Q^{\nu\mu'}\nabla_{\nu'}Q_{\mu\nu'})\Big)\,.$$

We refer to appendix B for more details on how to treat contact terms and integration by parts on S^d in presence of delta function singularities.

For the first three integrals (t = triple, g = ghost, f = fermion) we proceed as follows. As the integrals only depend on the geodesic distance, or equivalently on z, we can use spherical invariance to put x' to zero and reduce the integration over x' to a volume factor:

$$G_2^i = \int d^dx d^dx' \sqrt{g}\sqrt{g'}\ g^i(z) = \Omega_d R^d \int d^dx\sqrt{g}\ g^i(z)\,, \quad i = t, g, f\,. \tag{4.90}$$

Then we use stereographic coordinates to convert the remaining integral in x to a one-dimensional integral in the variable z defined in eq. (4.50):

$$\int d^dx\sqrt{g} = \Omega_{d-1}R^{2d}\int_0^\infty dx \frac{2^d x^{d-1}}{(R^2+x^2)^d}\,. \tag{4.91}$$

In this way we write

$$G_2^i = \int_0^1 dz\ f^i(z)\,, \quad i = t, g, f\,, \tag{4.92}$$

for some functions $f^i(z)$. The integral (4.92) cannot be computed directly as it contains UV divergences in $d = 4$. We isolate them by expanding $f^i(z)$ around coincident points, i.e. $z = 1$:

$$f^i(z) = \sum_{k=n_i}^{N_i} \left(f_{1k}^i(d)(1-z)^{k-1} + f_{2k}^i(d)(1-z)^{k-d/2+1} + f_{3k}^i(d)(1-z)^{k-d+3} \right) + \tilde{f}^i(z)\,, \tag{4.93}$$

where $f_{jk}^i(d)$ are analytic functions of d and $\widetilde{F}^i$ remainder terms. The lower bound n_i in the sum appearing in eq. (4.93) is the leading UV divergence of the integrand, and the upper bound N_i is chosen in such a way that the integral of $\tilde{f}^i(z)$ over z between 0 and 1 is finite. We write

$$G_2^i = (G_2^i)_{N_i} + \widetilde{G_2^i}, \tag{4.94}$$

with

$$(G_2^i)_{N_i} = \int_0^1 dz\ \sum_{k=n_i}^{N_i} \left(f_{1k}^i(d)(1-z)^{k-1} + f_{2k}^i(d)(1-z)^{k-d/2+1} + f_{3k}^i(d)(1-z)^{k-d+3} \right) \tag{4.95}$$

and

$$\widetilde{G_2^i} = \int_0^1 dz\ \tilde{f}^i(z)\,, \tag{4.96}$$

with $\widetilde{G_2^i}$ finite. The integral $(G_2^i)_{N_i}$ can be computed analytically using

$$\int_0^1 (1-z)^{a-1} = \frac{1}{a}\,, \tag{4.97}$$

which is valid for $a > 0$, but is extendable to any d-dependent a by analytic continuation in d.[5] We then set $d = 4 + 2\epsilon$ and extract the divergent part of eq. (4.95) by expanding the result in powers of ϵ and isolating the negative powers of ϵ. Note that the divergence of the integral has a double source: it comes from both integration over z when $k = 0$ and from the expansion of the functions $f_{jk}^i(d)$ around $d = 4$.[6] This explains the presence of double poles in the final result.

For the quartic and the counterterm diagrams the situation is simpler, as we have an integration over a single variable. Spherical invariance then means that we need to compute the integrand at coincident points and multiply it by a volume factor. We work out the

[5] Luckily, $f_{1k}^i(d)$ is zero for $k \leq 0$ in all the integrals that we have computed. Otherwise, analytic continuation of the dimension would not be sufficient to regulate the integral of eq. (4.97).

[6] The functions $f_{jk}^i(d)$ remain separately divergent $k > 0$, but for $k > N_i$ these divergences cancel when the $j = 1, 2, 3$ contributions are summed up.

procedure for the quartic case (4.85) as example. We have

$$G_2^{\text{quart}} = 2\kappa R^d \Omega_d \left. \frac{\alpha(z)(d-1)(2\beta(z) - d\alpha(z))}{4z^2} \right|_{z\to 1} , \tag{4.98}$$

where α and β are the coefficients of the two components of the vector propagator defined in eq. (4.53). For physical values of d, eq. (4.98) is UV divergent. We expand it around coincident points for generic d, obtaining

$$G_2^{\text{quart}} = \left. \sum_{k=0}^{N} \left(g_{1k}^{\text{q}}(d)(1-z)^k + g_{2k}^{\text{q}}(d)(1-z)^{-d/2+1+k} + g_{3k}^{\text{q}}(d)(1-z)^{-d+2+k} \right) \right|_{z\to 1} , \tag{4.99}$$

where $N \geq 1$ and g_{jk}^{q} are analytic functions of d. For sufficiently small d all terms in the expansion vanish, except g_{1k}^{q}, with $k = 0$. We then get

$$\begin{aligned} G_2^{\text{quart}} = g_{10}^{\text{q}}(d) = & -\frac{\kappa R^{d-4}\Gamma(d-1)}{2^{d+2}\pi^{\frac{d}{2}}(d-3)^2\Gamma\left(\frac{d}{2}+1\right)} \left(\gamma_E(d-3)\xi + \pi((d-3)\xi - d + 1)\cot\left(\frac{\pi d}{2}\right) \right. \\ & \left. + \big(d(\xi-1) - 3\xi + 1\big)\psi(d) - \gamma_E d + d + \gamma_E \big)^2 \right) . \end{aligned} \tag{4.100}$$

The analytic continuation of eq. (4.100) for any d gives us the final result. A similar computation of the integrals in eqs. (4.86) and (4.87) gives just -1 and $-1/2$, respectively, for any d.

We finally expand eqs. (4.82)-(4.87) around $\epsilon = 0$ with $d = 4 + 2\epsilon$, keeping terms up to constant order, and we get:

$$G_2^{\text{triple}}\Big|_{\text{div.}} = \kappa \left(\frac{(\xi-3)(3\xi-7)}{192\pi^2\epsilon^2} + \frac{\xi(31\xi-64) - 71 - 2(\xi-3)(3\xi-7)(\gamma_E + \log(4\pi R^2))}{384\pi^2\epsilon} \right) , \tag{4.101}$$

$$G_2^{\text{ghost}}\Big|_{\text{div.}} = \kappa \left(\frac{3-\xi}{96\pi^2\epsilon^2} + \frac{-\xi - 13 + 2(\xi-3)(\gamma_E + \log(4\pi R^2))}{192\pi^2\epsilon} \right) , \tag{4.102}$$

$$G_2^{\text{ferm}}\Big|_{\text{div.}} = (n_c^2 - 1)\frac{n_f T_f}{12\pi^2\epsilon} , \tag{4.103}$$

$$G_2^{\text{quart}}\Big|_{\text{div.}} = \kappa \left(-\frac{(\xi-3)^2}{64\pi^2\epsilon^2} + \frac{(3-\xi)(3+31\xi) + 6(\xi-3)^2(\gamma_E + \log(4\pi R^2))}{384\pi^2\epsilon} \right) , \tag{4.104}$$

$$G_2^{\text{CT-vec}}\Big|_{\text{div.}} = -\kappa\frac{3+\xi}{32\pi^2\epsilon} , \tag{4.105}$$

$$G_2^{\text{CT-gh}}\Big|_{\text{div.}} = \kappa\frac{3-\xi}{32\pi^2\epsilon} . \tag{4.106}$$

Summing all the contributions gives

$$G_2|_{\text{div.}} = -(n_c^2 - 1)\frac{11C_A - 4n_f T_f}{48\pi^2\epsilon} . \tag{4.107}$$

Note that the results in eq. (4.101)-(4.104) have double poles, which cancel in the sum.

Moreover, after summation the ξ-dependence of G_2 cancels, as required from gauge invariance of the total free energy.

As explained before, we compute finite terms only in the Landau gauge $\xi \to 0$. These are computed numerically. However, thanks to the integer-relation finding algorithm PSLQ [146], we can obtain the exact result from the approximated one:

$$G_2^{\text{triple}}\Big|_{\text{fin.}} = \kappa \frac{-562 + 63\pi^2 + 6(\gamma_E + \log(4\pi R^2))(71 + 21(\gamma_E + \log(4\pi R^2)))}{2304\pi^2}\,, \tag{4.108}$$

$$G_2^{\text{ghost}}\Big|_{\text{fin.}} = \kappa \frac{97 + 9\pi^2 + 6(\gamma_E + \log(4\pi R^2))(13 + 3(\gamma_E + \log(4\pi R^2)))}{1152\pi^2}\,, \tag{4.109}$$

$$G_2^{\text{ferm}}\Big|_{\text{fin.}} = -(n_c^2 - 1) n_f T_f \frac{5 + 3(\gamma_E + \log(4\pi R^2))}{36\pi^2}, \tag{4.110}$$

$$G_2^{\text{quart}}\Big|_{\text{fin.}} = \kappa \frac{128 - 9\pi^2 - 6(\gamma_E + \log(4\pi R^2))(1 + 3(\gamma_E + \log(4\pi R^2)))}{256\pi^2}\,, \tag{4.111}$$

and zero for the counterterms, leading to

$$G_2|_{\text{fin.}} = (n_c^2 - 1)\left(C_A \frac{49 + 33(\gamma_E + \log(4\pi R^2))}{144\pi^2} - n_f T_f \frac{5 + 3(\gamma_E + \log(4\pi R^2))}{36\pi^2}\right). \tag{4.112}$$

4.4.2 Check with Jack [4]

The poles of the diagrams (4.101), (4.102), (4.104), and (4.105) can also be computed with a different procedure. This procedure, which is based on the heat-kernel expansion of the propagators, is more general because it works on any curved background. We show in this section how the divergences which were obtained in this way for pure Yang-Mills theory in ref. [4] in the Feynman gauge $\xi = 1$ agree with our previous results. Matching with the results of [4] requires a bit of manipulations. It is then useful to briefly recall the key results found in [4, 147] using heat kernel methods. Let us consider an elliptic differential operator of the form

$$M(x) = -\nabla^2 + Y(x) \tag{4.113}$$

and the corresponding propagator satisfying

$$M(x) G_M(x, x') = \delta(x - x')\,. \tag{4.114}$$

Around coincident points $x \sim x'$ the following expansion holds [147]:

$$G_M \sim -\frac{1}{16\pi^2\epsilon} a_{1\,\text{diag}}^M + H_{\text{diag}}^M\,, \tag{4.115}$$

where H_{diag}^M is in general a complicated non-local expression satisfying

$$M(x) H_{\text{diag}}^M = \frac{1}{16\pi^2} a_{2\,\text{diag}}^M\,. \tag{4.116}$$

The coefficients $a_{1\,\mathrm{diag}}^{M}$ and $a_{2\,\mathrm{diag}}^{M}$ admit instead a local expression in terms of the curvature tensors and they can be computed for any elliptic operator M. From the propagator equations in sec. 4.3, we see that the ghost differential operator is indeed of the form (4.113), while the vector one is not for a generic choice of the gauge. This is why ref. [147] provides results only in the Feynman gauge $\xi = 1$, for which also the vector operator is of the form (4.113). The coefficients then read

$$\begin{aligned} a_{1\mathrm{diag}}^{\mathrm{gh}} &= \frac{1}{6}\mathcal{R}\,, \\ a_{2\mathrm{diag}}^{\mathrm{gh}} &= \frac{1}{180}(\mathcal{R}_{\mu\nu\rho\sigma}\mathcal{R}^{\mu\nu\rho\sigma} - \mathcal{R}_{\mu\nu}\mathcal{R}^{\mu\nu}) + \frac{1}{72}\mathcal{R}^2\,, \end{aligned} \tag{4.117}$$

for the ghost and

$$\begin{aligned} a_{1\mathrm{diag}\ \mu\nu}^{\mathrm{vec}} &= \frac{1}{6}\mathcal{R}g_{\mu\nu} - \mathcal{R}_{\mu\nu}\,, \\ a_{2\mathrm{diag}}^{\mathrm{vec}} &= \frac{1}{360}(2(d-15)\mathcal{R}_{\mu\nu\rho\sigma}\mathcal{R}^{\mu\nu\rho\sigma} - 2(d-90)\mathcal{R}_{\mu\nu}\mathcal{R}^{\mu\nu} + 5(d-12)\mathcal{R}^2)\,, \end{aligned} \tag{4.118}$$

for the vector. Ref. [4] provides the expressions for the poles of diagrams as a function of the curvature tensors and of the derivatives of H_{diag}, more specifically, $\nabla^2 H_{\mathrm{diag}}^{\mathrm{gh}}$, $H_{\mathrm{diag}}^{\mathrm{vec}\ \mu\nu}$, $g_{\mu\nu}\nabla^2 H_{\mathrm{diag}}^{\mathrm{vec}\ \mu\nu}$ and $\nabla_\mu\nabla_\nu H_{\mathrm{diag}}^{\mathrm{vec}\ \mu\nu}$.[7] Now, from eq. (4.116) we have

$$-\nabla^2 H_{\mathrm{diag}}^{\mathrm{gh}} = \frac{1}{16\pi^2} a_{2\ \mathrm{diag}}^{\mathrm{gh}}\,, \tag{4.119}$$

$$-\nabla^2 H_{\mathrm{diag}}^{\mathrm{vec}\ \mu\nu} g_{\mu\nu} = \frac{1}{16\pi^2} a_{2\ \mathrm{diag}}^{\mathrm{vec}} - H_{\mathrm{diag}}^{\mathrm{vec}\ \mu\nu}\mathcal{R}_{\mu\nu}\,. \tag{4.120}$$

The first equation allows us to find a simple expression for $\nabla^2 H_{\mathrm{diag}}^{\mathrm{gh}}$ in terms of the curvature tensors. However we cannot solve the second equation to obtain a similar simple expression for $H_{\mathrm{diag}}^{\mathrm{vec}\ \mu\nu}$. A way to compute $\nabla_\mu\nabla_\nu H_{\mathrm{diag}}^{\mathrm{vec}\ \mu\nu}$ is by imposing the cancellation of poles in the total free-energy inserting the expression for the diagrams obtained in ref. [4] (detailed in footnote 8 below) in eq. (4.65). Note that only $\nabla_\mu\nabla_\nu H_{\mathrm{diag}}^{\mathrm{vec}\ \mu\nu}$ and $\nabla^2 H_{\mathrm{diag}}^{\mathrm{gh}}$ enter the expression for these diagrams, not $H_{\mathrm{diag}}^{\mathrm{vec}\ \mu\nu}$. In order to obtain a result valid on a generic manifold, we use the one-loop free energies computed in refs. [4, 147] and the renormalization of the curvature coefficient a. We get

$$\nabla_\mu\nabla_\nu H_{\mathrm{diag}}^{\mathrm{vec}\ \mu\nu} = \frac{1}{8\pi^2}\left(\frac{109}{3960}\mathcal{R}_{\mu\nu\rho\sigma}\mathcal{R}^{\mu\nu\rho\sigma} - \frac{229}{3960}\mathcal{R}_{\mu\nu}\mathcal{R}^{\mu\nu} + \frac{5}{1584}\mathcal{R}^2 + 3\right)\,. \tag{4.121}$$

The above relations apply to any manifold. We can now focus on S^d to get explicit results. The term $H_{\mathrm{diag}}^{\mathrm{vec}\ \mu\nu}$ can be computed by expanding the propagator around coincident points and using eq. (4.115). Taking the expression for the gauge propagator of eq. (4.53) for $\xi = 1$

[7] In ref. [4] $H_{\mathrm{diag}}^{\mathrm{gh}}$ is denoted H_{diag}^{0}, while $H_{\mathrm{diag}}^{\mathrm{vec}\ \mu\nu}$ is denoted $H_{\mathrm{diag}}^{1\ \mu\nu}$.

we get

$$Q^{\mu}{}_{\nu}(z) = R^{2-d}\left(\frac{\Gamma\left(\frac{d}{2}-1\right)}{2^d\pi^{\frac{d}{2}}}(1-z)^{1-\frac{d}{2}} + \frac{\Gamma\left(\frac{d}{2}-2\right)(d^2-6d+4)}{2^{d+2}\pi^{\frac{d}{2}}}(1-z)^{2-\frac{d}{2}} + \frac{\Gamma\left(\frac{d-3}{2}\right)\left(-d+2\pi\cot\left(\frac{\pi d}{2}\right)+2\left(\psi(d)+\gamma_E\right)\right)}{8\pi^{\frac{d+1}{2}}d}\right)\delta^{\mu}{}_{\nu} + \dots . \tag{4.122}$$

Using analytic continuation in d, we can set to zero the powers $(1-z)^{1-\frac{d}{2}}$ and $(1-z)^{2-\frac{d}{2}}$ of the expansion. The remaining part can be computed at $d = 4+2\epsilon$ and expanded around $\epsilon = 0$. Plugging the result in eq. (4.115) gives

$$H^{\text{vec}\ \mu\nu}_{\text{diag}}(S^4) = -\frac{1+3\gamma_E+3\log(4\pi\mu^2R^2)}{48\pi^2R^2}\delta^{\mu\nu}\,. \tag{4.123}$$

From eq. (4.121) we have

$$\nabla_\mu\nabla_\nu H^{\text{vec}\ \mu\nu}_{\text{diag}}(S^4) = \frac{61}{240\pi^2R^4}\,. \tag{4.124}$$

Using eq. (4.120) we can similarly get the expressions for $\nabla^2 H^{\text{gh}}_{\text{diag}}$ and $\nabla_\mu\nabla_\nu H^{\text{vec}\ \mu\nu}_{\text{diag}}$:

$$g_{\mu\nu}\nabla^2 H^{\text{vec}\ \mu\nu}_{\text{diag}}(S^4) = -\frac{232+120\big(-1+3\gamma+\log(4\pi\mu^2R^2)\big)}{480\pi^2R^4}\,, \tag{4.125}$$

$$\nabla^2 H^{\text{gh}}_{\text{diag}}(S^4) = -\frac{29}{240\pi^2R^4}\,. \tag{4.126}$$

Substituting in the results of ref. [4], we find[8]

$$G^{\text{triple}}_{2J}\Big|_{\text{div.}} = \kappa\left(\frac{1}{24\pi^2\epsilon^2} - \frac{13+2(\gamma_E+\log(4\pi\mu^2R^2))}{48\pi^2\epsilon}\right), \tag{4.127}$$

$$G^{\text{ghost}}_{2J}\Big|_{\text{div.}} = \kappa\left(\frac{1}{48\pi^2\epsilon^2} - \frac{1+2(\gamma+\log(4\pi\mu^2R^2))}{96\pi^2\epsilon}\right), \tag{4.128}$$

$$G^{\text{quart}}_{2J}\Big|_{\text{div.}} = \kappa\left(-\frac{1}{16\pi^2\epsilon^2} + \frac{17+6(\gamma+\log(4\pi\mu^2R^2))}{96\pi^2\epsilon}\right), \tag{4.129}$$

$$G^{\text{CT}-\text{vect}}_{2J}\Big|_{\text{div.}} = \kappa\left(-\frac{1}{8\pi^2\epsilon}\right). \tag{4.130}$$

Eqs. (4.127), (4.129) and (4.130) match respectively eqs. (4.101), (4.104) and (4.105) evaluated at $\xi = 1$. As explained, the ghost counterterm (4.102) arises because of ghost zero modes, specific for S^d. Heat kernel methods apply to generic manifolds and therefore there is no ghost counterterm in ref. [4]. The ghost contribution (4.128) should then match the sum of eq. (4.102) and the counterterm (4.106) for $\xi = 1$, and this is indeed the case. We then have a check diagram by diagram of our computation.

[8] See eq. (2.55) of ref. [4] for G^{triple}_{2J}, eq. (2.52) for G^{ghost}_{2J}, eq. (2.33) for G^{quart}_{2J} and eqs. (2.31),(2.59) for $G^{\text{CT}-\text{vect}}_{2J}$. Note that in our convention $d = 4+2\epsilon$, while in ref. [4] the authors used $d = 4-\epsilon$. Moreover, all diagrams in ref. [4] are multiplied by a factor 1/2, which we factorized instead outside G_2.

4.4.3 Renormalization

Let us now check that the free-energy (4.65) is UV finite up to order g^2, when expressed in terms of renormalized couplings. The bare curvature couplings in eq. (4.5) renormalize as follows [148]:

$$b_0 = \mu^{2\epsilon}\left(b + \frac{62(n_c^2-1)+11n_f n_c}{720(4\pi)^2\epsilon} + \mathcal{O}(g^4)\right), \tag{4.131}$$

$$c_0 = \mu^{2\epsilon}\left(c + \mathcal{O}(g^6)\right), \tag{4.132}$$

while for the gauge coupling we have the well-known relation

$$g_0^2 = \mu^{-2\epsilon}\Big(g^2 + \frac{11C_A - 4n_f T_f}{3\epsilon}\frac{g^4}{(4\pi)^2} + \mathcal{O}(g^6)\Big), \tag{4.133}$$

where μ is the RG sliding scale. Expanding in ϵ for $d = 4+2\epsilon$, we get the following divergent contribution from eq. (4.65) at $\mathcal{O}(g^0)$:

$$\begin{aligned} F_{\text{free-YM}}|_{\text{div.}} &= -\frac{31(n_c^2-1)}{90\epsilon}, \\ n_f n_c F_{\text{free-F}}|_{\text{div.}} &= -\frac{11 n_f n_c}{180\epsilon}, \\ F_{\text{curv}}|_{\text{div.}} &= \frac{31(n_c^2-1)}{90\epsilon} + \frac{11 n_f n_c}{180\epsilon}, \end{aligned} \tag{4.134}$$

which cancel in the sum. At $\mathcal{O}(g^2)$ we have

$$\begin{aligned} -\frac{1}{2}(n_c^2-1)\log(g_0^2)|_{\text{div.}} &= -g^2(n_c^2-1)\frac{11C_A - 4n_f T_f}{96\pi^2\epsilon} + \mathcal{O}(g^4), \\ -\frac{1}{2}g_0^2 G_2|_{\text{div.}} &= g^2(n_c^2-1)\frac{11C_A - 4n_f T_f}{96\pi^2\epsilon} + \mathcal{O}(g^4), \end{aligned} \tag{4.135}$$

which also cancel in the sum. Therefore we obtained, as expected, a finite result for the total free-energy at order $\mathcal{O}(g^2)$, and in any ξ-gauge.

4.4.4 Free energy at the fixed point

We determine here the final form of the free-energy at the fixed point obtained in the ϵ-expansion up to $\mathcal{O}(\epsilon)$. The fixed point is obtained by setting to zero the gauge and the curvature beta-functions β_g, β_b and β_c. β_b and β_c, computed in [148]. At the fixed point g^*, b^*, c^* we have

$$F_{\text{conf}}(\epsilon) = F(g^*, b^*, c^*, \mu R), \tag{4.136}$$

of order ϵ up to two loops. Note that F_{conf} has to be conformal invariant and therefore the dependence on R has to cancel in the final result. The expressions for β_g, β_b and β_c –up to

the order required to get $F_{\text{conf}}(\epsilon)$ to order $\epsilon-$ are[9]

$$\begin{aligned}
\beta_g &= \epsilon g - \Big(\frac{11}{3}C_A - \frac{4}{3}T_f n_f\Big)\frac{g^3}{(4\pi)^2} - \Big(\frac{34}{3}{C_A}^2 - \frac{20}{3}C_A T_f n_f - 4C_f T_f n_f\Big)\frac{g^5}{(4\pi)^4} + \mathcal{O}(g^7)\,,\\
\beta_b &= -2\epsilon b - \frac{62(n_c^2-1)+11 n_f n_c}{360(4\pi)^2} - \frac{(n_c^2-1)}{8}\left(\frac{34}{3}{C_A}^2 - \frac{20}{3}C_A T_f n_f - 4C_f T_f n_f\right)\frac{g^4}{(4\pi)^6} + \mathcal{O}(g^6)\,,\\
\beta_c &= -2\epsilon c + \mathcal{O}(g^6)\,,
\end{aligned} \tag{4.137}$$

from which we get

$$\begin{aligned}
g_* &= 4\pi\sqrt{\frac{3\epsilon}{11C_A - 4n_f T_f}}\left(1 - \frac{3(17C_A^2 - 10C_A n_f T_f - 6C_f n_f T_f)}{(11C_A - 4n_f T_f)^2}\epsilon + \mathcal{O}(\epsilon^2)\right)\,,\\
b_* &= -\left(\frac{62(n_c^2-1)+11 n_f n_c}{720(4\pi)^2\epsilon} + \frac{(n_c^2-1)(17C_A^2 - 10C_A n_f T_f - 6C_f n_f T_f)}{24\epsilon}\frac{g_*^4}{(4\pi)^6}\right) + \mathcal{O}(\epsilon^2)\,,\\
c_* &= \mathcal{O}(\epsilon^2)\,,
\end{aligned} \tag{4.138}$$

where

$$C_f = \frac{n_c^2-1}{2n_c}\,. \tag{4.139}$$

Note that, since β_b contains a constant term, b^* starts at order $1/\epsilon$.

Plugging eq. (4.138) in the free energy (4.65) and using the results for G_2 obtained in section 4.4.1, including the finite pieces computed in the $\xi = 0$ gauge, we obtain

$$\begin{aligned}
F_{\text{conf}} = (n_c^2-1)&\left(F_{\text{Max}}(d) - \frac{1}{2}\log\left(\frac{48\pi^2\epsilon}{11C_A - 4n_f T_f}\right)\right) + n_f n_c F_{\text{free-F}}(d)\\
&+ \log\left(\frac{\text{vol}(SU(n_c))}{(2\pi)^{n_c^2-1}}\right) + (n_c^2-1)\left(\frac{-n_f T_f(1089C_f - 913C_A + 584 n_f T_f)}{121(11C_A - 4n_f T_f)^2}\right.\\
&\left. - \frac{386 + 363\big(\gamma + \log(4\pi)\big)}{726}\right)\epsilon + \mathcal{O}(\epsilon^2)\,,
\end{aligned} \tag{4.140}$$

where F_{Max} and $F_{\text{free-F}}$ are given in eqs. (4.42) and (2.50), respectively. The volume of the $SU(n_c)$ group reads (see e.g. [149])

$$\text{vol}(SU(n_c)) = \frac{(2\pi)^{\frac{n_c(n_c+1)-2}{2}}}{\prod_{k=1}^{n_c-1} k!}\,. \tag{4.141}$$

The cancellation of the $\log(\mu R)$ term[10] present in the two loop correction (4.112) with those arising from the replacement of the bare coupling b_0 in eq. (4.10) and g_0 in the log term in

[9] Note that β_g can be obtained by changing variable $a = g^2/(16\pi^2)$ in $\beta(a)$ of eq.(2.66).

[10] All the $\log R$ terms appearing in the loop computations of section 4.4.1 arise from the expansion of an overall R^{d-4} factor present in all the contributions. When moving from g_0 to g via eq. (4.133) we effectively have $R \to \mu R$.

eq. (4.65) is a check of the result. Equation (4.140) is the main result of this chapter.

As discussed in the introduction, the conjectured generalized F-theorem (2.48) involves the modified free energy (2.47). Using the expression for F_{conf} we get

$$\begin{aligned}\widetilde{F}_{\text{conf}} =&(n_c^2-1)\left(\widetilde{F}_{\text{Max}}(d)+\frac{1}{2}\sin\left(\frac{\pi d}{2}\right)\log\left(\frac{48\pi^2\epsilon}{11C_A-4n_fT_f}\right)\right)+n_fn_c\widetilde{F}_{\text{free-F}}(d)\\&-\frac{1}{2}\sin\left(\frac{\pi d}{2}\right)\log\left(\frac{\text{vol}(SU(n_c))}{(2\pi)^{n_c^2-1}}\right)\\&+(n_c^2-1)\left(\frac{n_fT_f(1089C_f-913C_A+584n_fT_f)}{121(11C_A-4n_fT_f)^2}+\frac{386+363(\gamma+\log(4\pi)}{726}\right)\pi\epsilon^2+\mathcal{O}(\epsilon^3),\end{aligned}\tag{4.142}$$

where

$$\widetilde{F}_{\text{Max}}=-\sin\left(\frac{\pi d}{2}\right)F_{\text{Max}}\,,\qquad \widetilde{F}_{\text{free-F}}=-\sin\left(\frac{\pi d}{2}\right)F_{\text{free-F}}\,.\tag{4.143}$$

For completeness we report its expression in the Veneziano limit, where $n_c, n_f\to\infty$ with $x=n_f/n_c$ fixed. We get

$$\begin{aligned}F_{\text{conf}}=n_c^2\Bigg(&F_{\text{Max}}(d)-\frac{1}{2}\log\left(\frac{48\pi^2\epsilon}{11-2x}\right)+xF_{\text{free-F}}(d)+\frac{3}{4}-\frac{1}{2}\log(2\pi)\\&-\left(\frac{193}{363}-\frac{737x-584x^2}{484(11-2x)^2}+\frac{1}{2}(\gamma+\log(4\pi))\right)\epsilon\Bigg)+\mathcal{O}(n_c)\,.\end{aligned}\tag{4.144}$$

Note that $n_c^2\log(n_c)$ terms are induced from both log terms appearing in eq. (4.140) and they precisely cancel. The same cancellation occurs in the t' Hooft limit. This cancellation is expected from large n_c considerations and the fact that a log term is not expected in the genus expansion.

4.5 Applications

In this section we are going to use the conjectured monotonicity of $\widetilde{F}$ along RG flows [47] to test some proposed RG flows in $d=3$ and $d=5$, using our result (4.140). The perturbative expression in eq. (4.140) is not adequate to extrapolate to physical dimensions with $|\epsilon|=1/2$. The number of available terms (three) is too limited to attempt a Borel resummation. In the same spirit of ref. [138], we will instead look for Padé approximants for $\widetilde{F}$. We also use the knowledge of $\widetilde{F}$ for special values of d to effectively increase by one order the expansion in ϵ.

Note that $\widetilde{F}$ contains a $\log(\epsilon)$ term, which, being non-analytic, prevents the application of standard Padé approximants. Moreover, the free-fermion one-loop determinant is known exactly as a function of d and it is convenient to keep it not expanded in ϵ. For these reasons, we split the total $\widetilde{F}$ in two parts, one that we keep in d dimensions and contains the non-analytic term, and one that is a series in ϵ. Following ref. [138], we split $\widetilde{F}_{\text{conf}}$ as

$$\widetilde{F}_{\text{conf}}=n_fn_c\widetilde{F}_{\text{free-F}}+\frac{1}{2}\sin\left(\frac{\pi d}{2}\right)(n_c^2-1)\log\left(\frac{2\epsilon}{11C_A-4n_fT_f}\right)+\delta\widetilde{F}(\epsilon),\tag{4.145}$$

and we use Padé approximants only on the $\delta\widetilde{F}(\epsilon)$ term. The latter includes the free photon contribution, which is evaluated numerically, and reads

$$\delta\widetilde{F}(\epsilon) = (n_c^2-1)\frac{31\pi}{90} + \left((n_c^2-1)4.696 - \pi\log\left(\frac{\mathrm{vol}(SU(n_c))}{(2\pi)^{n_c^2-1}}\right)\right)\epsilon \tag{4.146}$$
$$+ (n_c^2-1)\left(\frac{n_f\pi(584 n_f n_c - 1089 - 737 n_c^2)}{484 n_c(11n_c-2n_f)^2} + \frac{386\pi + 363\pi(\gamma+\log(4\pi)}{726} - 10.098\right)\epsilon^2 + \mathcal{O}(\epsilon^3)\,.$$

For presentation purposes we rounded to the first 4 digits the $\mathcal{O}(\epsilon)$ and $\mathcal{O}(\epsilon^2)$ contribution coming from the photon free energy, but the result is available to higher precision. Let us stress the fact that the above splitting is arbitrary and that the corresponding choice significantly affects the final results. This is a signal of the poor knowledge that we have on the series. For the same reason we have not attempted to estimate an error bar in our results.

The fixed points we get in $d = 4+2\epsilon$ of QCD_d with gauge group $SU(n_c)$ and n_f massless Dirac fermions in the fundamental representation are expected to match two known CFTs:

- For $\epsilon = -1$ ($d = 2$) the IR fixed point of QCD_d with gauge group $SU(n_c)$ and $2n_f$ massless Dirac fermions in the fundamental representation is an $SU(2n_f)_{n_c}$ Wess-Zumino-Witten model with an additional decoupled free boson [150,151]. This CFT has central charge

$$c = \frac{n_c(4n_f^2-1)}{2n_f+n_c} + 1\,, \tag{4.147}$$

and

$$\widetilde{F}_{\mathrm{WZW}}(d=2) = \frac{\pi}{6}c\,. \tag{4.148}$$

Plugging $d = 2$ in eq. (4.145) and identifying $\widetilde{F}_{\mathrm{conf}}$ with $\widetilde{F}_{\mathrm{WZW}}$ gives

$$\delta\widetilde{F}(\epsilon=-1) = \widetilde{F}_{\mathrm{WZW}} - n_c n_f \widetilde{F}_{\text{free-F}} = -\frac{\pi}{3}\frac{n_f(n_c^2-1)}{2n_f+n_c}\,. \tag{4.149}$$

- For $\epsilon = 1$ ($d = 6$) the theory is conjectured to have a non-unitary UV fixed point described by a Lagrangian with a higher-derivative kinetic term $F^a_{\mu\nu}\nabla^2 F_a^{\mu\nu}$ [134, 152], whose anomaly coefficient is $a = -(n_c^2-1)\frac{55}{84}$ [138]. This leads to

$$\delta\widetilde{F}_{d=6} = \frac{\pi}{2}a = -\frac{55\pi}{168}(n_c^2-1)\,. \tag{4.150}$$

To improve the numerical estimate of our result we constrain the Padé approximants of $\delta\widetilde{F}$ to these known points. In order to avoid misleading results, we exclude approximants with poles in the range between the constraint and $d = 4$.

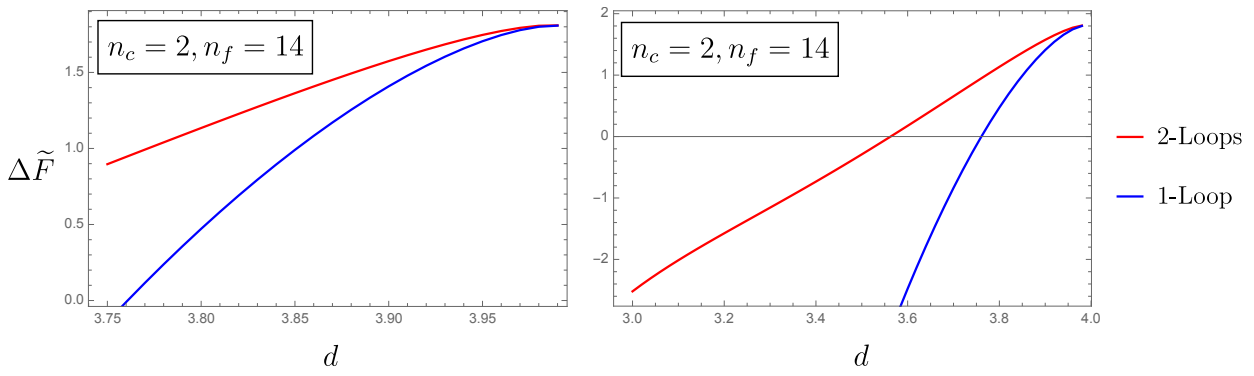

Figure 4.1: Left panel: Comparison between $\Delta\widetilde{F}$ as a function of the dimension d for small ϵ computed by using the result for $\widetilde{F}$ in eq. (4.142) (red) or only its free part given by the first two rows of eq. (4.142) (blue). Right panel: Same comparison extended up to $d = 3$.

4.5.1 F-Theorem in $d = 3$

In sec.2.2.2 we have described the possible phases of gauge theories in $d = 3$. At large n_f, QCD_3 flows to a non-trivial CFT in the IR. As n_f is reduced, an irrelevant operator in the CFT spectrum, responsible for the flow between the QCD_3 fixed point and an additional putative fixed point QCD_3^* , may reach marginality at $n_f = n_f^*$ [56]. In this scenario, merging and annihilation of fixed point occurs and the theory flows directly to a broken symmetry phase at $n_f < n_f^*$.

A qualitative phase diagram of the theory as a function of the number of flavors n_f, a fermion mass term, and the level k of a possible Chern-Simons term has been suggested [139]. We will focus on $k = 0$ in the following and use the F-theorem to put an upper bound on n_f^*. A naive way to check if the spontaneous symmetry breaking phase (2.92) can be realized would be to compare $F_{\text{IR}} = F_{\text{SB}}$ as given by $2n_f^2$ Goldstone bosons (free in the deep IR), with F_{UV} given in the deep UV by n_c^2-1 free photons and $n_f n_c$ free fermions. Unfortunately, due to the log term in (4.41), F_{UV} diverges and no useful information can be extracted. We overcome this problem by assuming that conformality is lost at $n_f = n_f^*$ by annihilation between the critical QCD_3 fixed point with another one, known as QCD_3^*. A similar analysis for QED_3 has been performed in [138]. Treating n_f as a continuous parameter, for $n_f = n_f^* + \eta$ and $0 < \eta \ll 1$, the theory flows to the IR fixed point QCD_3. On the other hand, for $n_f = n_f^* - \eta$ the theory is expected to undergo a weak first-order phase transition [111] (i.e. a walking regime, see [153] for an explicit realization in $4d$ gauge theories) with a slow RG passing close to the (now complex) fixed points, reaching eventually the spontaneously broken phase (2.92). By continuity and the generalized F-theorem, we then expect that

$$\Delta\widetilde{F}(n_f^*) = \widetilde{F}_{\text{conf}}(n_f^*) - \widetilde{F}_{\text{SB}}(n_f^*) > 0\,. \tag{4.151}$$

Note that values of n_f such that $\Delta\widetilde{F}(n_f) < 0$ are incompatible with a symmetry breaking phase. On the other hand, values of n_f with $\Delta\widetilde{F}(n_f) > 0$ are compatible with either a

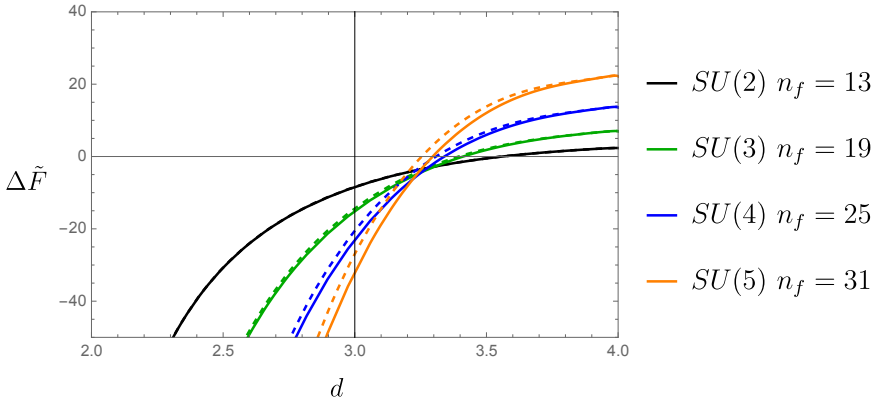

Figure 4.2: Values of $\Delta\widetilde{F}$ for $SU(n_c)$ as a function of the dimension d computed with Padé-approximants [2/1] (continuous line) and [1/2] (dashed line) at $n_c = 2, 3, 4, 5$. The value of n_f is set to the smallest integer without poles in both approximants in $2 < d < 4$ satisfying $g^{*2} > 0$.

n_f	12	13	14	15	16
SB	18.38	21.57	25.01	28.71	32.67
[2/1]	12.1	13.1	13.6	13.9	14.16
[1/2]	–	13.2	13.9	15.01	16.10

Table 4.1: Comparison between the $3d$ values of $\widetilde{F}$ in the broken phase $\widetilde{F}_{\rm SB}$ (red) with those obtained from Padé-approximants [2/1] and [1/2] of $\widetilde{F}_{\rm conf}$ for QCD_3 with $n_c = 2$. In all cases $\Delta\widetilde{F} < 0$.

CFT or a symmetry breaking phase. For this reason we can only determine an upper bound $n_f^* \leq n_f^0$, where $\Delta\widetilde{F}(n_f^0) = 0$.

An early previous estimate of n_f^* was based on Schwinger-Dyson gap equations [70] and resulted in $n_f^* \approx 128(n_c^2-1)/(3\pi^2 n_c)$. More recently, a lattice analysis [141] found $n_f^* \leq 4$ for $n_c = 2$. An estimate based on the F-theorem already appeared in [140], where as UV theory it was used a SUSY version of QCD_3, a genuine CFT with finite F which can flow to QCD_3 by appropriate deformations. By comparing $F_{\rm SUSY}$ computed by means of supersymmetric localization with $F_{\rm SB}$ (and assuming that we can flow from the IR SCQD_3 fixed point to the IR QCD_3 fixed point), it was found $n_f^* < 13/2$ for $n_c = 2$.

The value of $\widetilde{F}_{\rm SB}(n_f)$ is easily computed by noting that the $2n_f^2$ Goldstone bosons associated to the breaking pattern (2.92) become free in the deep IR. The contribution to the free energy for a single real scalar is reported in eq.(2.49). We then have

$$\widetilde{F}_{\rm SB}(n_f) = 2n_f^2 \widetilde{F}_{\rm free-S}\,. \tag{4.152}$$

For $d = 3$ it reads

$$\widetilde{F}_{\rm SB} = 2n_f^2 \left(\frac{\log 2}{8} - \frac{3\zeta(3)}{16\pi^2}\right)\,. \tag{4.153}$$

Before presenting the results of our extrapolations to $d = 3$, it is useful to see the effect of the 2-loop correction to the free energy with respect to the one-loop free theory contribution in the controlled regime with $|\epsilon| \ll 1$. This is shown in fig. 4.1 where we plot $\Delta\widetilde{F}$ (for $n_c = 2$

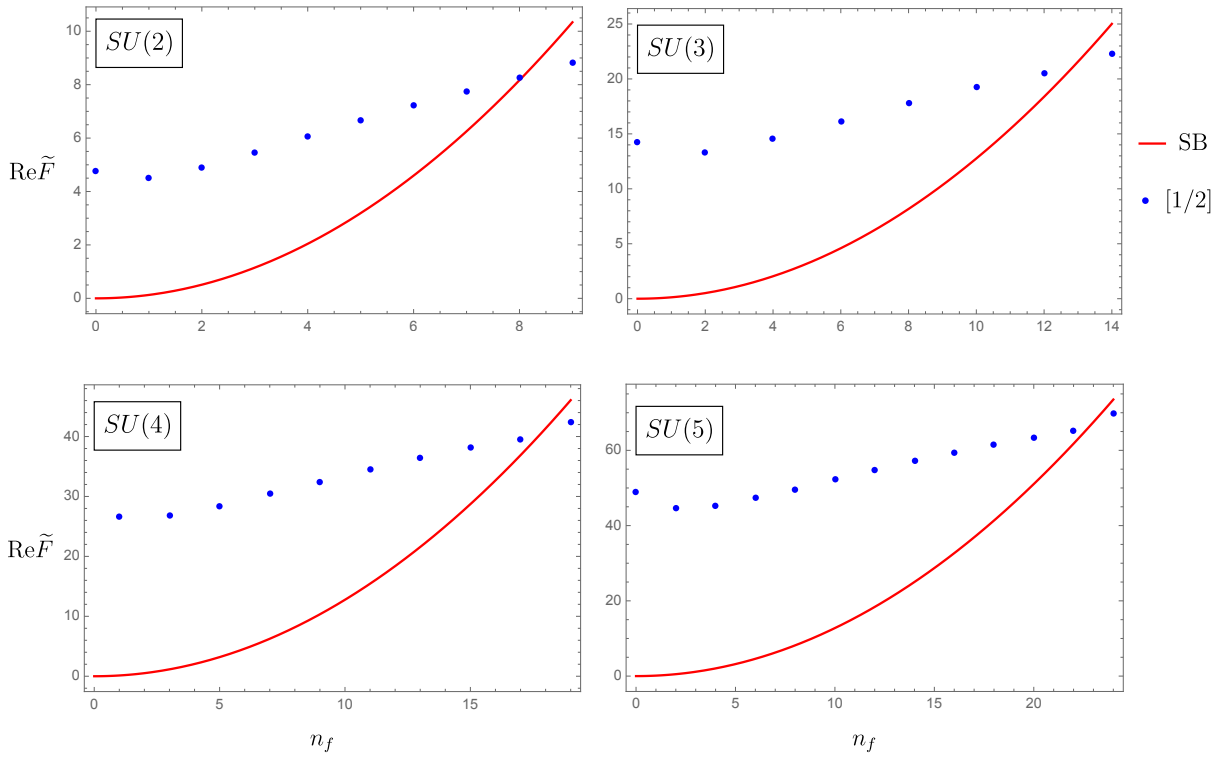

Figure 4.3: Comparison between the $3d$ value of $\widetilde{F}_{\rm SB}$ (red line) and of the real part of $\widetilde{F}_{\rm conf}$ (blue points) as a function of n_f for $n_c = 2, 3, 4, 5$. The [1/2] approximants provide $\mathrm{Re}[\widetilde{F}_{\rm conf}] > \widetilde{F}_{\rm SB}$ for $n_f \leq 8, 12, 17, 22$ suggesting that a chiral symmetry breaking may occur in these ranges of values.

and $n_f = 14$) defined as in eq. (4.151) as a function of the dimension d. We compare the result for $\widetilde{F}_{\rm conf}$ obtained using eq. (4.142) (red line) with the one obtained using only the first two rows of the same equation (blue line), i.e. only its free part. We note that the effect of the interactions is to favor the SB phase with respect to the conformal one and that the latter is more favored as we lower the space-time dimensions. More importantly, we see from the left panel in the figure that when $|\epsilon| \approx 0.1$ the one and two-loop results differ significantly and that there is no hope to get reliable results from perturbation theory in $d = 3$ (for illustration purposes we report in the right panel of fig. 4.1 the same plot extended up to $d = 3$). As anticipated at the beginning of the section, we then consider Padé approximants of (4.146). For $d < 4$ we augment the approximant by one more term by imposing the constraint (4.149).

In fig. 4.2 we show the value of $\Delta\widetilde{F}$ as a function of the dimension d for $n_c = 2, 3, 4, 5$ and n_f equal to the smallest integer without poles in approximants [1/2] and [2/1] satisfying $a^* > 0$, i.e. $n_f = 13, 19, 25, 31$ respectively.[11]

We see that at $d = 3$ $\Delta\widetilde{F} < 0$ in all these cases, indicating the presence of the conformal phase. As expected, this behavior persists for higher values of n_f: we report in tab. 4.1 the comparison between the free energy $\widetilde{F}_{\rm conf}$ and that of the broken phase for $n_c = 2$, $12 \leq n_f \leq 16$. Not only the value of $\widetilde{F}_{\rm SB}$ remains above $\widetilde{F}_{\rm conf}$, but also the gap between the

[11]Note that regions in n_f close to $11n_c/2$ are more subject to instabilities as g^{*2} blows up there, producing a pole of order two in the free energy. This is another reason to avoid smaller values of n_f which still satisfy $a^* > 0$ (i.e. $n_f = 12$ for $n_c = 2$).

two values gets larger and larger.

Small n_f

The one-loop beta-function of the gauge coupling vanishes at $n_f = 11n_c/2$ and changes sign below that, making $a^*_{\text{1-loop}} < 0$. Of course, a unitary fixed point in $d = 3$ does not necessarily appear as a real *one-loop* fixed point when $\epsilon \ll 1$.[12] As mentioned, lattice results for $SU(2)$ find that $n_f^* \leq 4$, suggesting that even if $a^*_{\text{1-loop}} < 0$, there exists a range in n_f where the $3d$ theory is conformal in the IR. For $n_f < 11n_c/2$ we could still use the free energy to extract information on the RG flow. For $a^* < 0$, or equivalently $g^{*2} < 0$, the free energy becomes complex, due to the log term in eq. (4.145), with an opposite phase depending on which of the two imaginary fixed points is chosen:

$$\log(g^{*2}) = \log(|g^{*2}|) \pm i \log(\pi)\,. \tag{4.154}$$

We propose to estimate the value of F at the strongly coupled real fixed point by an extrapolation of the half-sum of the two complex values obtained with the ϵ-expansion, i.e. of their real part. The stability of the conformal phase then requires this value to be smaller than $\widetilde{F}_{\text{SB}}$. As a result, our more speculative criterion in the range $n_f < 11n_c/2$ is

$$\text{Re}\,\Delta\widetilde{F}(n_f^*) = \widetilde{F}_{\text{conf}}(n_f^*) - \text{Re}\,\widetilde{F}_{\text{SB}}(n_f^*) > 0\,. \tag{4.155}$$

We report in fig. 4.3 the real part of $\widetilde{F}_{\text{conf}}$ compared to $\widetilde{F}_{\text{SB}}$ for $n_c = 2, 3, 4, 5$ computed with the Padé approximant [1/2]. We see that in all cases there is a wide range of n_f for which the conformal phase appears to be unstable. We have

$$\begin{aligned} n_f^* &\lesssim 8\,, && SU(2)\,, \\ n_f^* &\lesssim 12\,, && SU(3)\,, \\ n_f^* &\lesssim 17\,, && SU(4)\,, \\ n_f^* &\lesssim 22\,, && SU(5)\,. \end{aligned} \tag{4.156}$$

The upper bound for $SU(2)$ is consistent with the bound $n_f^* < 13/2$ of [140], and $n_f^* \leq 4$ of [141]. A similar analysis can be done in the Veneziano limit, by taking the large n_c, n_f limit of eq. (4.155). The resulting bound is

$$x^* \lesssim 4.5\,. \tag{4.157}$$

[12] A notable example of this sort is provided by the abelian Higgs model of n complex scalar fields. It is known that in this theory a real one-loop Wilson-Fisher fixed-point appears for $n > 183$ [154] and this number greatly varies with the order, see e.g. [155]. It is in fact likely that the $3d$ abelian Higgs theory has an IR conformal phase for values of n well below 183.

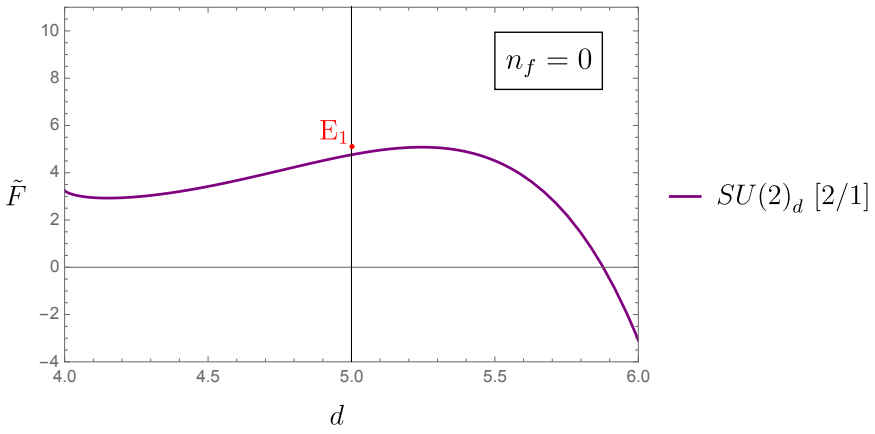

Figure 4.4: Values of $\widetilde{F}_{\text{conf}}$ for pure $SU(2)$ YM as a function of the dimension d computed with the Padé-approximant [2/1] (purple line), compared to the value of the $5d$ supersymmetric fixed point E_1, the UV completion of $SU(2)$ SYM gauge theory (red point).

4.5.2 F-Theorem in $d = 5$

In this section we extrapolate $\widetilde{F}$ to $5d$ to test a proposed construction of an interacting CFT that provides a UV completion of $5d$ $SU(2)$ YM theory. Ref. [19] proposed to construct this CFT as the IR fixed point of a supersymmetry-breaking deformation of the interacting superconformal field theory known as E_1 theory [133]. The latter is known to provide the UV completion of $SU(2)$ supersymmetric YM theory (SYM). Ref. [19] studied the various phases in the two-dimensional space of relevant deformations of the E_1 theory, which includes both the supersymmetric deformation to SYM and the non-supersymmetric one, and suggested the existence of a second-order transition between two phases that are described by $SU(2)$ YM theory and a different symmetry-protected topological order. The CFT capturing this phase transition would therefore be a UV completion of YM, and provide an example of a non-supersymmetric interacting CFT in $d > 4$. This scenario was further explored in [132], that showed that actually the phase transition should be viewed as separating the YM phase from a phase with spontaneous breaking of the instantonic $U(1)$, and in [156] where a certain generalization of the theory admitting a large N limit was argued to have a second order transition in that limit.

A possible test for the proposal of ref. [19, 132] relies on the F-theorem: the sphere free energy $\widetilde{F}_{E_1}$ of the SCFT and that of the non-supersymmetric CFT $\widetilde{F}_{\text{CFT}}$ should satisfy $\widetilde{F}_{E_1} > \widetilde{F}_{\text{CFT}}$. The quantity $\widetilde{F}_{E_1}$ has been computed using localization in [142]. It is natural to conjecture that the non-supersymmetric fixed point is the continuation to $d = 5$ of the UV fixed point visible in the ϵ-expansion in $d = 4 + 2\epsilon$, and therefore to estimate $\widetilde{F}_{\text{CFT}}$ by an extrapolation of our result (4.140). In chapter 2 we found evidence for the persistence of the $d = 4+2\epsilon$ fixed point up to $d = 5$, both for the pure $SU(2)$ YM theory and for the theory with n_f fundamental Dirac fermions, with $n_f \leq 4$. Note that the continuation from $d = 4 + 2\epsilon$ suggests that the critical point should separate a free YM phase from a confined phase (the only phase realized in $d = 4$) rather than a second YM phase, similarly to the refined

n_f	0	1	2	3	4
E_{n_f+1}	5.097	6.140	7.395	8.959	11.007
[2,1]	4.8	5.1	5.4	5.7	6.2

Table 4.2: Comparison between the value of $\widetilde{F}_{E_{n_f+1}}$ (red) and the $[2,1]$ Padé approximant of $\widetilde{F}_{\text{conf}}$ in $d = 5$ (black) as a function of n_f for $0 \leq n_f \leq 4$.

proposal of [132] and in agreement with a recent lattice study that sees hints of a second order confinement/deconfinement transition [129]. We therefore proceed to extrapolate $\widetilde{F}_{\text{conf}}$ using the only available Padé approximant that is constrained also by the $d = 6$ boundary condition (4.150) and without poles in the interval $4 \leq d \leq 6$. In fig. 4.4 we plot the resulting extrapolation of $\widetilde{F}_{\text{conf}}$ as a function of the dimension. The value ranges between a local minimum of ~ 2.9 and a maximum of ~ 5.0, before turning negative in the vicinity of $d = 6$. The value in $d = 5$ is ~ 4.8, remarkably close to the known value ~ 5.1 of $\widetilde{F}$ in the E_1 theory, and below it consistently with the proposals of [19, 132].

The UV completion of the supersymmetric theory is also known in the case with $0 < n_f \leq 7$ flavors and is given by the E_{n_f+1} SCFT [133]. The value of $\widetilde{F}$ can be obtained from localization similarly to the E_1 case [142]. It is possible that also these theories flow to a non-supersymmetric fixed point when perturbed by a susy-breaking deformation. This fixed point would then provide a UV completion of the non-supersymmetric $SU(2)$ gauge theory with n_f flavors. We test this possibility by comparing our extrapolation of $\widetilde{F}_{\text{conf}}$ to $\widetilde{F}_{E_{n_f+1}}$. We limit ourselves to the range $n_f \leq 4$ in which the fixed point in $d = 4 + 2\epsilon$ was seen to persist up to $d = 5$. We collect the values of the two $\widetilde{F}$'s in tab. 4.2. We always find $\widetilde{F}_{E_{n_f+1}} > \widetilde{F}_{\text{conf}}$, consistently with the existence of the RG flow.

Outlook In this chapter, we obtained the NLO result for the free energy on S^d in non-abelian gauge theories in Euclidean d dimensions evaluated at their perturbative fixed point. Our main result is reported in eq.(4.140). We extrapolated the result to compute the quantity F for the corresponding CFTs in $d = 3$ or $d = 5$ and used our best estimates together with the monotonicity property of F to test the existence and/or proposed constructions of these CFTs, see fig.s 4.3 and 4.4 and tab.4.2.

Chapter 5

Exploring confinement with Anti-de Sitter space

In the previous chapters, we have explored the fate of non-abelian gauge theories in $d \neq 4$ by means of the ϵ-expansion. Despite being a very interesting topic, it is clear that this subject does not measure up to the greatest of the problems of gauge theories: understanding confinement in the four-dimensional case. Obviously, the ϵ-expansion cannot help to this purpose. As outlined in sec.2.2.1, standard perturbation theory has also limited application because of the strong coupling nature of this phenomenon. Another possible approach to address this problem is to consider non-abelian gauge theories in Anti-de Sitter (AdS) space. Indeed, as explained in sec.2.3, asymptotically free theories in AdS possess a dimensionless parameter $L\Lambda$, that allows to interpolate between different regimes and to reproduce flat-space when this is taken to infinity.

In this chapter, we study gauge theories in AdS starting from the small radius limit, at which the theory is weakly coupled. In this regime, Yang-Mills theories admit both a deconfined and a confined bc, D and N bc respectively. Since the D bc cannot persist up to flat space, a deconfinement/eeconfinement transition must occur. Proving the existence of this transition is a very interesting problem. Understanding the nature of the transition and having quantitative control over it could potentially offer new perspectives on the mass gap and confinement problem. In this chapter, we investigate this problem using perturbation theory, testing the different transition scenarios that were described in detail in sec.2.3. We will argue that perturbation theory can play a valuable role in discerning between the various proposed scenarios, besides providing data that can be later used as inputs for the numerical conformal bootstrap. Working in an expansion around small radius, or equivalently in the Yang-Mills coupling g^2 at the scale L^{-1}, we compute the following quantities at next-to-leading order (NLO):

- the scaling dimension of the lightest singlet scalar operator, both for D and N bc's;
- the scaling dimensions of the lightest scalar operators in non-trivial representations of the G global symmetry for the D bc;

- the coefficient C_J of the current two-point function for the D bc.

These are the quantities that are more directly related to the possible scenarios for the transition. Moreover, the quantity C_J is the CFT proxy for the bulk gauge coupling, and our result allows to map any bulk calculation in an expansion in the gauge coupling in dimensional regularization to an expansion in $1/C_J$, up to NLO.

Let us provide a description of our main results. Considering for definiteness $G = SU(n_c)$, we find that the lightest singlet scalar operator in the D bc, namely $\mathrm{tr}[J_i J^i]$, has negative anomalous dimension:

$$D: \quad \Delta_{\mathrm{tr}[JJ]} = 4 - \frac{11 n_c}{24\pi^2}\, g^2 + \mathcal{O}(g^4)\,, \tag{5.1}$$

while the lightest scalars in non-trivial representations of the gauge group, which are also bilinear in the currents at weak coupling and therefore also start from dimension 4, all get a positive anomalous dimension at the leading order, see (5.114). We find this to be a rather strong indication that the Marginality scenario is more likely than the Higgsing one, in agreement with [94]. Truncating at NLO we can roughly estimate the transition to happen at

$$\Delta_{\mathrm{tr}[JJ]} = 3 \quad \Rightarrow \quad a_{\mathrm{crit}}|_{\mathrm{NLO}} = \frac{3\pi^2}{22 n_c} \approx \frac{0.14}{n_c}\,, \quad \text{or equivalently } (L\Lambda_{\mathrm{YM}})_{\mathrm{crit}}|_{\mathrm{NLO}} = \frac{1}{e} \approx 0.37\,. \tag{5.2}$$

Note that the estimated value of $a_{\mathrm{crit}} = g^2_{\mathrm{crit}}/(16\pi)^2$ is quite small, suggesting that perturbation theory is still sufficiently reliable. The indication towards Marginality is further confirmed by the fact that for the N bc instead the lightest scalar singlet operator, namely $\mathrm{tr}[f_{ij} f^{ij}]$, has positive anomalous dimension

$$N: \quad \Delta_{\mathrm{tr}[ff]} = 4 + \frac{11 n_c}{24\pi^2}\, g^2 + \mathcal{O}(g^4)\,. \tag{5.3}$$

This agrees with the idea that the N bc smoothly interpolates to the flat space limit, and therefore no singlet operator is expected to cross marginality. The first correction to C_J also happens to be negative

$$C_J = \frac{2}{\pi^2 g^2}\left(1 - \frac{10 + 3\gamma_E}{324\pi^2}\; n_c\, g^2 + \mathcal{O}(g^4)\right)\,, \tag{5.4}$$

but the NLO estimate of the critical coupling in the Decoupling scenario gives

$$C_J = 0 \quad \Rightarrow \quad a_{\mathrm{crit}}|_{\mathrm{NLO}} = \frac{17}{\pi^2 n_c} \approx \frac{1.72}{n_c}\,, \quad \text{or equivalently } (L\Lambda_{\mathrm{YM}})_{\mathrm{crit}}|_{\mathrm{NLO}} \approx 0.92\,. \tag{5.5}$$

Compared to (5.2), this estimate suggests that the transition in the Marginality scenario happens before.

The conjectural picture that is suggested by these results is illustrated in figure 5.1. The

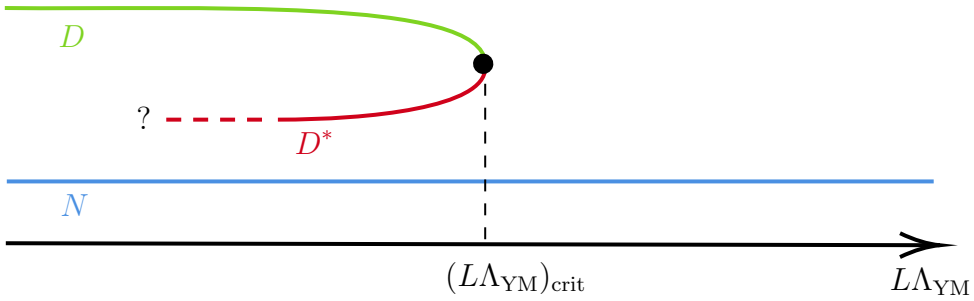

Figure 5.1: Schematic representation of the conjectured evolution of the D and N bc's as a function of the bulk coupling $L\Lambda_{\rm YM}$. The D bc merges and annihilates with D^*, a second boundary condition with G global symmetry, which must exist for $L\Lambda_{\rm YM} \lesssim (L\Lambda_{\rm YM})_{\rm crit}$, but is not guaranteed to exist at weak coupling.

D bc exists for a finite range of $L\Lambda_{\rm YM}$, but at the critical value $(L\Lambda_{\rm YM})_{\rm crit}$ the operator $\mathrm{tr}[JJ]$ becomes marginal and the associated boundary coupling η has a beta function [161]

$$\beta_\eta = c_1\eta^2 + c_2\left(\frac{1}{g^2} - \frac{1}{g^2_{\rm crit}}\right) + \text{subleading}\,. \tag{5.6}$$

As we review, the coefficients $c_{1,2}$ can be expressed in terms of data of the boundary CFT for $g^2 = g^2_{\rm crit}$, whose value is not calculable. Even without knowing their values, the existence of the D bc for $g^2 < g^2_{\rm crit}$ ensures that the condition $\beta_\eta = 0$ must have two real solutions for $g^2 \lesssim g^2_{\rm crit}$, one of them being the D bc, and the second being an additional boundary condition with G global symmetry, which we call D^*. The theories D and D^* merge and annihilate at $g^2_{\rm crit}$, and become complex at larger values of the coupling. In this way, the D bc stops being a viable boundary condition for $g^2 > g^2_{\rm crit}$. This picture raises the question of better understanding the nature of the D^* bc, which we will not study in this thesis. On the other hand, the N bc is suggested to exist for all values of $L\Lambda_{\rm YM}$, as envisioned in [17].

Besides the standard perturbative computation, we discuss a different approach for the calculation of the anomalous dimensions of $\mathrm{tr}[JJ]$ in the D bc and $\mathrm{tr}[ff]$ in the N bc. This approach is based on the fact that in the limit $g^2 \to 0$ the bulk theory is the free UV CFT of YM theory. As a result, the whole setup can be mapped via a Weyl rescaling to flat-space boundary CFT (BCFT), and the two operators can be identified with the displacement operator of the respective boundary condition. We provide a general argument based on multiplet recombination that fixes the anomalous dimension of the displacement operator for a generic perturbation of a CFT in AdS, see (5.54). In particular, we find that for a classically marginal deformation this anomalous dimension is determined by the one-loop beta function in the bulk, see (5.56). This is the reason why the coefficient of the one-loop beta function of YM theory appears in (5.1) and (5.3). The result in the case of the D bc is then matched with the explicit diagrammatic calculation.

In preparation for the perturbative calculation, we also discuss in detail the propagators for gauge fields in AdS_{d+1} (generic d is needed for dimensional regularization) with R_ξ gauge

fixing, both in D and N bc's. We find that choosing the gauge fixing parameter as $\xi = \frac{d}{d-2}$, i.e. the Fried-Yennie (FY) gauge [162,163], leads to drastic simplifications in the propagators, e.g. from derivatives of hypergeometric functions to rational functions. For instance, for the D bc the expression (D.17) for the bulk-to-bulk propagators in generic ξ collapses to (5.32) in FY gauge. It is only thanks to these remarkable simplifications that we are able to carry through the brute-force calculation of the diagrams in position space.

The rest of the chapter is organized as follows: in section 5.1 we discuss the generalities of YM in AdS space and the D and N bc's at weak coupling, in particular the spectrum of boundary operators in the free limit; in section 5.2 we derive the propagators for gauge fields in AdS in R_ξ gauge, and the special properties of the FY gauge; in section 5.3 we first present the general multiplet recombination argument for the anomalous dimension of the displacement operator induced by AdS deformations, then we apply it to compute the anomalous dimensions of the lightest singlet operators for the D and N bc's, and finally we perform the diagrammatic calculation of the anomalous dimensions of all current bilinear operators in the D bc, both singlet and non-singlet; in section 5.4 we perform the pertubative calculation of C_J. Several appendices contain technical details.

Conventions Throughout the chapter, we denote by d the dimension of the boundary, the dimension of the bulk being $d+1$. We use late lowercase Greek letters $\mu, \nu, \ldots$ for indices on Euclidean AdS_{d+1} space, early lowercase Latin letters $a, b, \ldots$ for gauge group indices, late lowercase Latin letters $i, j, \ldots$ for indices on $\mathbb{R}^d$, and early uppercase Latin letters $A, B, \ldots$ for embedding space indices. We use the following notation for integration over bulk points,

$$\int dx\, f(x) \equiv \int_{\mathrm{AdS}} d^{d+1}x \sqrt{g(x)}\; f(x)\,. \tag{5.7}$$

In embedding coordinates, the integral (5.7) is expressed as

$$\int dX\, f(X) \equiv \int d^{d+2}X\; \delta(X^2 + L^2)\Theta(X^0) f(X)\,. \tag{5.8}$$

Note that some conventions used in ref. [3] were changed here for consistency with the rest of the thesis. The normalization for the generators in the fundamental representation is that of eq.(2.53), which differs by a factor 2 from that of ref. [3]. A different notation for the counterterms is also used.

5.1 Generalities of YM theory on AdS

The action of Yang-Mills theory on Euclidean AdS_{d+1} in ξ-gauge reads (ghost terms omitted)

$$S_{\mathrm{YM}} = \frac{1}{g^2}\int dx\; \mathrm{tr}\left[\frac{1}{2}F_{\mu\nu}F^{\mu\nu} + \frac{1}{\xi}(\nabla_\mu A^\mu)^2\right], \tag{5.9}$$

where $F^{\mu\nu} = F_a^{\mu\nu} t_f^a$, with

$$F^a_{\mu\nu} = \nabla_\mu A^a_\nu - \nabla_\mu A^a_\nu + f^a{}_{bc} A^b_\mu A^c_\nu \,. \tag{5.10}$$

We are interested in the physics for $d = 3$, but keeping d generic is needed for dimensional regularization. We will mostly use Poincaré coordinates $x^\mu = (x^i, z)$ with $z > 0$ and $i = 1, \ldots, d$, in which the metric $g_{\mu\nu}$ reads

$$ds^2 = g_{\mu\nu} dx^\mu dx^\nu = L^2 \frac{dz^2 + dx_i^2}{z^2} \,. \tag{5.11}$$

L is the radius of AdS, which we set to 1 unless explicitly specified. The boundary is at $z = 0$.

The allowed boundary conditions of A_μ can be worked out by looking at the behavior of the equations of motion close to $z = 0$. One has [164, 165]

$$\begin{aligned} D: &\quad A^a_i(x,z) \underset{z\to 0}{\sim} z^{d-2} g^2 J^a_i(x) \,, \\ N: &\quad A^a_i(x,z) \underset{z\to 0}{\sim} a^a_i(x) \,. \end{aligned} \tag{5.12}$$

In the first case, for $d > 2$ the bulk gauge field vanishes at the boundary and we have D bc, with $J^a_i(x)$ a conserved non-abelian vector current with scaling dimension $\Delta_J = d - 1$. In the second case, the bulk gauge field does not vanish at the boundary and we have N bc, with $a^a_i(x)$ a non-abelian gauge connection with scaling dimension $\Delta_a = 1$. This value is below the unitarity bound for spin 1 operators but this is not an issue because a^a_i is not a gauge-invariant primary operator.

We will mostly focus on D bc. When the gauge interactions are switched off, the bulk gauge field A gives rise to a boundary CFT which is the mean-field theory [166] of the non-abelian conserved currents J^a_i. Its two-point function reads

$$\langle J^a_i(x_1) J^b_j(x_2) \rangle = \frac{C^0_J}{g^2} \delta^{ab} \frac{I_{ij}}{x_{12}^{2(d-1)}} \,, \tag{5.13}$$

where $x_{12} = x_1 - x_2$, and

$$I_{ij} = \delta_{ij} - \frac{2(x_{12})_i (x_{12})_j}{x_{12}^2} \,, \quad C^0_J = \frac{\Gamma(d)}{2(d-2)\pi^{\frac{d}{2}} \Gamma(\frac{d}{2})} \,. \tag{5.14}$$

Let us now focus on the case of $d = 3$. At $g^2 = 0$ the D boundary theory is given by all the primary operators of the schematic form $J^{n_1} \Box^p \partial^m J^{n_2}$ with correlation functions entirely determined by (5.13) and Wick's contractions. In table 5.1 we report the first "double trace" JJ primary operators up to $\Delta \leq 7$, including their representation under the global symmetry, taken to be $G = SU(n_c)$ for definiteness. This is obtained using the standard technique based on characters and the partition function of single particle states [167, 168].

$\mathcal{O}$	$(\Delta,\ell)_\pi$	$R(SU(n_c))$
$[J_i^a J_i^b]$	$(4,0)_+$	R_+
$[J_i^a J_j^b]$	$(4,2)_+$	R_+
$[J_i^a \partial_i J_j^b]$	$(5,1)_+$	R_-
$[J_i^a \partial_j J_k^b]$	$(5,3)_+$	R_-
$[J_i^a \Box J_i^b]$	$(6,0)_+$	R_+
$[J_i^a \Box J_j^b]$	$(6,2)_+$	R_+
$[\widetilde{J}_i^a \widetilde{J}_j^b]$	$(6,2)_+$	R_+
$[J_i^a \partial_j \partial_k J_l^b]$	$(6,4)_+$	R_+
$[J_i^a \Box \partial_i J_j^b]$	$(7,1)_+$	R_-
$[\widetilde{J}_i^a \partial_j \widetilde{J}_k^b]$	$(7,3)_+$	R_-
$[J_i^a \Box \partial_j J_k^b]$	$(7,3)_+$	R_-
$[J_i^a \partial_j \partial_k \partial_l J_m^b]$	$(7,5)_+$	R_-

$\mathcal{O}$	$(\Delta,\ell)_\pi$	$R(SU(n_c))$
$[\epsilon_{ijk} J_i^a J_j^b]$	$(4,1)_-$	R_-
$[J_i^a \widetilde{J}_i^b]$	$(5,0)_-$	R_+
$[J_i^a \widetilde{J}_j^b]$	$(5,2)_-$	$R_+ \oplus R_-$
$[J_i^a \partial_j \widetilde{J}_i^b]$	$(6,1)_-$	R_-
$[J_i^a \partial_j \widetilde{J}_k^b]$	$(6,3)_-$	$R_+ \oplus R_-$
$[J_i^a \Box \widetilde{J}_i^b]$	$(7,0)_-$	R_+
$[J_i^a \Box \widetilde{J}_j^b]$	$(7,2)_-$	$R_+ \oplus R_-$
$[J_i^a \partial_j \partial_k \widetilde{J}_l^b]$	$(7,4)_-$	$R_+ \oplus R_-$

Table 5.1: Double trace JJ primary operators up to $\Delta \leq 7$ in the mean field theory of $SU(n_c)$ adjoint currents, $\mathcal{O}$ being their schematic form. We have distinguished between parity-even $\pi = +1$ primaries (left) and parity-odd $\pi = -1$ primaries (right). Here $\widetilde{J}_i^a \equiv \epsilon_{ijk}\partial_j J_k^a$. R_+ (resp. R_-) labels the $SU(n_c)$ representations corresponding to the symmetric (resp. antisymmetric) product of two adjoint representations, see appendix C for details. In particular, R_+ always contains the singlet $\mathbf{1}$ and the adjoint representation R_A.

The non-abelian structure allows for more primaries than those appearing in the mean-field theory of an abelian $U(1)$ current, as Bose symmetrization of J_i^a, J_j^b can be achieved either by symmetrizing or anti-symmetrizing both their spacetime and adjoint flavor indices. When restricted to the singlet flavor representation, the spectrum of double trace primary operators in table 5.1 reduces to that obtained from an abelian current J_i, see e.g. [169]. We refer the reader to appendix C for details and for the complete list of operators up to $\Delta \leq 7$ which includes "triple trace" operators. When $g^2 \neq 0$, the interactions mix operators with the same quantum numbers, which also get anomalous dimensions.

At $g^2 = 0$ the N boundary theory is the direct sum of $n_c^2 - 1$ mean field theories of abelian antisymmetric tensor fields, f_{ij}^a, at the unitarity bound. These fields are dual to the currents: $J_i^a = \epsilon_{ijk} f_{jk}^a$, which are conserved due to the Bianchi identity satisfied by f_{ij}^a. The table 5.1 can then be used also to extract the spectrum of local operators of the N CFT at $g^2 = 0$. However, these results have to be interpreted with care when interactions are turned on. At $g^2 \neq 0$, all non-singlet operators become unphysical and we are left only with the singlet ones, which mix among each other and would in general acquire anomalous dimensions.[1]

[1]The presence of many more local operators in the $g^2 = 0$ theory can be seen to arise from endpoints of line operators, which in the limit $g^2 \to 0$ become local operators.

5.2 The gauge propagator in AdS

In spaces with boundaries, we can distinguish between bulk-to-bulk, bulk-to-boundary, and boundary-to-boundary propagators. The knowledge of the former clearly allows to derive the other two by sending the bulk points to the boundaries. Bulk-to-boundary gauge propagators in AdS (with D bc) are entirely fixed by conformal symmetry, are ξ-independent, and have been determined since the first years of the AdS/CFT correspondence [27, 170]. In contrast, bulk-to-bulk gauge propagators are significantly more involved. Bulk-to-bulk propagators for massive spin 1 fields have been determined in ambient space in [171, 172] and rederived more elegantly using embedding space techniques in [173]. As far as we know the only computation of the bulk-to-bulk gauge propagator for massless gauge fields in configuration space dates back to [5], where it has been computed in the Feynman gauge $\xi = 1$ using ambient space techniques. The resulting expression is quite complicated and consists of a sum of hypergeometric functions and their derivatives with respect to the parameters a, b, c.[2]

In this section, we compute the bulk-to-bulk gauge propagator in AdS_{d+1} space by using techniques of harmonic analysis, for any ξ-gauge. Quite remarkably, we find that the propagator dramatically simplifies for an appropriate gauge choice.

It is useful to adopt embedding coordinates to write the propagators. Embedding space techniques for AdS_{d+1} have been worked out in [173], building on previous work where they have been developed for CFTs in d dimensions [177]. We report below a quick overview on few basic aspects of the use of embedding techniques in AdS, referring the reader to [173] for further details.

As well-known, AdS_{d+1} is the hyperbolic space $\mathbb{H}^{d+1}$ which can be embedded into a $(d+2)-$dimensional flat Minkowski space $\mathbb{R}^{d+1,1}$ with coordinates X^A as

$$X^2 = \eta_{AB} X^A X^B = -1\,, \tag{5.15}$$

where $\eta_{AB} = \text{diag}\,(-+\cdots+)$. Tensor fields in AdS can be uplifted to tensors in the embedding space by demanding tangentiality to the hyperboloid. Given a generic tensor $t_{\mu_1\ldots\mu_J}$ in AdS_{d+1}, its extension to $\mathbb{R}^{d+1,1}$ is a tensor $T(X)$ with components $T_{A_1\ldots A_J}(X)$:

$$t_{\mu_1\ldots\mu_J}(x) = \frac{\partial X^{A_1}}{\partial x^{\mu_1}} \cdots \frac{\partial X^{A_J}}{\partial x^{\mu_J}} T_{A_1\ldots A_J}(X)\,, \tag{5.16}$$

subject to the transversality condition

$$X^{A_1} T_{A_1\ldots A_J}(X) = 0\,. \tag{5.17}$$

[2] An expression for the bulk-to-bulk gauge propagator, that however neglects matters related to gauge-fixing, was given in [174,175]. Moreover, very recently the bulk-to-bulk gauge propagator has been determined in a mixed momentum-configuration space in the $A_z = 0$ and the Landau $\xi = 0$ gauges [176].

We can use the induced AdS metric

$$G_{AB} = \eta_{AB} + X_A X_B \,, \tag{5.18}$$

to define embedding derivatives tangent to AdS:

$$\nabla_A = G_A^{\ B} \frac{\partial}{\partial X^B} \,, \tag{5.19}$$

where $G_A^{\ B} = G_{AC}\eta^{CB}$ acts as a projector.

We wish to have a more economical way of encoding AdS_{d+1} tensors, without having to deal with all the indices and constraints arising from the linear realization of the $SO(d+1,1)$ symmetry. Let us first recall how this can be achieved in the case of $\mathbb{R}^d$ tensors, extensively discussed in [11]. In this case a symmetric traceless tensor with components $F_{A_1\cdots A_J}(P)$ is defined on the light-cone $P^2 = 0$ of the embedding space with the requirement that $F(\lambda P) = \lambda^{-\Delta} F(P)$, for $\lambda > 0$, where Δ is the conformal dimension. This tensor can be encoded in the polynomial

$$F(P,Z) = Z^{A_1} \dots Z^{A_J} F_{A_1\cdots A_J}(P),$$

where $Z^2 = 0$ encodes the traceless condition. To be tangent to the light-cone $P^2 = 0$ the embedding tensor must satisfy $P^{A_1} F_{A_1\cdots A_J} = 0$, which can be implemented by requiring $F(P, Z + \alpha P) = F(P,Z)$ for any α. In addition, we can impose the orthogonality condition $P \cdot Z = 0$ because $F_{A_1\cdots A_J} = P_{(A_1} \Psi_{A_2\cdots A_J)}$ has vanishing projection into physical $\mathbb{R}^d$ tensors. Moving to the case of AdS, an index-free notation for symmetric traceless tensors can be obtained by introducing polarization vectors W^A and writing

$$H(X,W) = W^{A_1} \dots W^{A_J} H_{A_1\dots A_J}(X) \,, \tag{5.20}$$

where $W^2 = 0$ and $X \cdot W = 0$ to ensure respectively the traceless and the tangentiality condition. Acting on $H(X,W)$ with suitable projector operators multiple times allows us to recover the index-full tensor [173].

Expressions in the AdS_{d+1} ambient space are given in the Poincaré coordinates $x^\mu \equiv (x^i, z)$, which are related as follows with the embedding coordinates X^A:

$$X = (X^+, X^-, X^i) = \frac{1}{z}(1, x^2 + z^2, x^i) \,, \tag{5.21}$$

where $x^2 = x_i x^i$, and $X^\pm = X^0 \pm X^{d+1}$ are light-cone coordinates on $\mathbb{R}^{d+1,1}$. We parametrize the distance between points $x^\mu = (x^i, z)$ and $y^\mu = (y^i, w)$ by

$$u(x,y) = \frac{(x_i - y_i)^2 + (z-w)^2}{2zw} = \frac{(X-Y)^2}{2} = -(1 + X \cdot Y) \,. \tag{5.22}$$

At the AdS boundary $z = 0$ we have a correspondence between points and light rays, which is

$$P^A = \lim_{z\to 0} zX^A = (1, x^2, x^i)\,, \tag{5.23}$$

where

$$P^2 = 0\,, \quad P \sim \lambda P\,, \quad \lambda \neq 0\,. \tag{5.24}$$

The embedding space formalism at the boundary of AdS boils down to the one used in CFT_d, which dates back to [178]. We will not review how the embedding space techniques works in this case. We use the notation and conventions of [177] and refer the reader to this reference for explanations.

The gluon propagator $\langle A_\mu(x)A_\nu(y)\rangle := g^2\Pi_{\mu\nu}$ satisfies the following equation in ambient space,

$$\left(-\delta^\rho_\mu\nabla^2 + R^\rho_\mu + \left(1 - \tfrac{1}{\xi}\right)\nabla^\rho\nabla_\mu\right)\Pi_{\rho\nu}(x,y) = g_{\mu\nu}\delta(x-y)\,, \tag{5.25}$$

where $R_{\mu\nu} = -dg_{\mu\nu}$. The uplift in embedding space of (5.25), in index-free notation, reads

$$\left(-\nabla_1^2 - d + (1-\tfrac{1}{\xi})\tfrac{2}{d-1}(W_1\cdot\nabla_1)(K_1\cdot\nabla_1)\right)\Pi(X_1,X_2;W_1,W_2) = (W_1\cdot W_2)\delta(X_1,X_2)\,, \tag{5.26}$$

where

$$\Pi\left(X_1,X_2,W_1,W_2\right) = (W_1\cdot W_2)g_0(u) + (W_1\cdot X_2)\left(W_2\cdot X_1\right)g_1(u)\,, \tag{5.27}$$

and $g_{0,1}$ are the two scalar functions to be determined. In ambient space, we have

$$\Pi_{\mu\nu}(x,y) = -g_0(u)\nabla_\mu\nabla_\nu u + g_1(u)\nabla_\mu u\nabla_\nu u\,. \tag{5.28}$$

The propagator (5.28) can also be expressed in terms of the bi-tensors $g_{\mu\nu'}(x,y)$ and $n_\mu(x,y)$ introduced in [5], see appendix D.1 for the explicit map.

We determine Π using the spectral representation, see appendix D.2 for an overview and [173] for further details. The first point to note is that the transverse part of the gauge field does not depend on ξ and is given by the massless limit of the first row of the spin 1 bulk propagator in (D.15), with $\Delta = d-1$. We then have

$$\begin{aligned}\Pi(X_1,X_2;W_1,W_2) = &\int d\nu\,\gamma_1(\nu)\Omega^{(1)}_\nu(X_1,X_2;W_1,W_2)\\ &+ (W_1\cdot\nabla_1)(W_2\cdot\nabla_2)\int d\nu\,\gamma_0(\nu)\Omega^{(0)}_\nu(X_1,X_2)\,,\end{aligned} \tag{5.29}$$

where the functions $\Omega^{(\ell)}_\nu$ are defined in (D.8), and

$$\gamma_1(\nu) = \frac{1}{\nu^2 + \left(\frac{d}{2}-1\right)^2}\,. \tag{5.30}$$

Plugging (5.29) into (5.26) we then obtain [179]

$$\gamma_0(\nu) = \frac{\xi}{\left(\nu^2 + \frac{d^2}{4}\right)^2} \,. \tag{5.31}$$

An explicit expression of the propagator is obtained by evaluating the residues of the spectral integrals. As reviewed in appendix D.2, we can get both D and N bulk gauge propagators by an appropriate choice of contour for ν. The D propagator is found by taking $\nu \in (-\infty, \infty)$ and closing the contour at infinity in such a way that the contributions at infinity vanish. This selects the appropriate poles for γ_0 and γ_1; the choice of contour that leads to the opposite choice of poles determines the N bulk propagator. The explicit form of the N and D bulk propagators in a general ξ-gauge is rather involved and is reported in appendix D.3. Interestingly enough, the D gauge propagator remarkably simplifies for $\xi = d/(d-2)$. In this case, we have

$$\begin{aligned} g_0^{(D)}(u) &= \frac{\Gamma\left(\frac{d+1}{2}\right)}{2\pi^{\frac{d+1}{2}}(u(u+2))^{\frac{d-1}{2}}(d-2)} \,, \\ g_1^{(D)}(u) &= \frac{u+1}{u(u+2)} g_0^{(D)}(u) \,, \end{aligned} \qquad \xi = \frac{d}{d-2} \,, \tag{5.32}$$

where $g_0^{(D)}$ and $g_1^{(D)}$ are the scalar functions entering (5.27) and (5.28) for the D bc. For the N bc we were not able to find a similar simplification in general d, however both D and N propagators have very simple expressions in this gauge in $d = 3$, namely

$$\begin{aligned} g_0^{(D,N)}(u) &= \frac{1}{4\pi^2}\left(\frac{1}{u} \mp \frac{1}{u+2}\right) \,, \\ g_1^{(D,N)}(u) &= \frac{1}{8\pi^2}\left(\frac{1}{u^2} \mp \frac{1}{(u+2)^2}\right) \,, \end{aligned} \qquad d = 3 \,, \quad \xi = 3 \,, \tag{5.33}$$

where the sign $-$ refers to D and $+$ to N.

There are two reasons why this gauge choice is special. First, the gauge propagator enjoys the peculiar transversality condition

$$X^B \Pi_{AB}(X,Y) = Y^A \Pi_{AB}(X,Y) = 0 \,, \qquad \xi = \frac{d}{d-2} \,. \tag{5.34}$$

In ambient space, in the basis (D.3) of [5], the propagator is proportional to $g_{\mu\nu'} + n_\mu n_{\nu'}$ and the condition (5.34) turns into the transversality[3]

$$n^\mu \Pi_{\mu\nu'} = n^{\nu'} \Pi_{\mu\nu'} = 0 \,. \tag{5.35}$$

[3]Recall that while $n^\mu g_{\mu\nu} = n_\nu$, we have $n^\mu g_{\mu\nu'} = -n_{\nu'}, n^{\nu'} g_{\mu\nu'} = -n_\mu$. Here $g_{\mu\nu}$ is the usual metric tensor, while $g_{\mu\nu'}$ is a bi-tensor. See appendix D.1 and [5] for details.

Second, in flat $d+1$-dimensional space the gauge $\xi = d/(d-2)$ is known as the Fried-Yennie gauge [162] and is known to lead to a remarkable reduction of IR divergences in QED, to all orders in perturbation theory [163]. Given that AdS can be seen as an IR regulator of flat space, it is perhaps not so surprising that such a gauge leads to remarkable simplifications. We will refer, in what follows, to this gauge as the Fried-Yennie (FY) gauge.

5.2.1 Bulk-to-boundary gauge propagator

The bulk-to-boundary gauge propagator $K_{AB}(X,P)$ can be obtained from the bulk-to-bulk propagator by sending one of the two bulk points to the boundary. Note that, for the D bc we also need to divide by a factor g^2 to recover the current at the boundary, as expressed in eq.(5.12),

$$\langle J_A(P)\dots\rangle = \lim_{z\to 0}\frac{1}{g^2}z^{d-2}\langle A_A(X)\dots\rangle\,. \tag{5.36}$$

Here and in the rest of the section we suppress color indices. This gives, in embedding space,

$$K^{(D)}_{AB}(X,P) = \frac{\Gamma(d)}{2(d-2)\pi^{\frac{d}{2}}\Gamma\left(\frac{d}{2}\right)}\frac{(-2P\cdot X)\eta_{AB}+2P_AX_B}{(-2P\cdot X)^d}\,. \tag{5.37}$$

Note that this propagator does not depend on ξ. The bulk-to-boundary D propagator (5.37) can also be fixed using exclusively d-dimensional conformal invariance at the boundary.

For the N bc, the bulk-to-boundary propagator reads instead

$$\begin{aligned}K^{(N)}_{AB}(X,P) = &-g^2\frac{2\Gamma(1+\frac{d}{2})\sin(\frac{\pi d}{2})}{\pi^{\frac{d+2}{2}}(d-2)^2 d}\left(\frac{(d-1)(-2P\cdot X)\eta_{AB}+2P_AX_B}{(-2P\cdot X)^2}\right)\\ &-g^2\zeta\frac{2\Gamma(1+\frac{d}{2})\sin(\frac{\pi d}{2})}{\pi^{\frac{d+2}{2}}d^2}\left[C(d)+\log\left(-2P\cdot X\right)\right]\left(\frac{(-2P\cdot X)\eta_{AB}+2P_AX_B}{(-2P\cdot X)^2}\right)\\ &+g^2\zeta\frac{4\Gamma(1+\frac{d}{2})\sin(\frac{\pi d}{2})}{\pi^{\frac{d+2}{2}}d^2}\frac{P_AX_B}{(-2X\cdot P)^2}\,,\end{aligned} \tag{5.38}$$

where we have introduced the shifted gauge-fixing parameter

$$\zeta = \xi - \frac{d}{d-2}\,, \tag{5.39}$$

which vanishes in FY gauge, and

$$C(d) = \pi\cot\left(\tfrac{\pi d}{2}\right) + 2\psi(d) - \psi\left(\tfrac{d+1}{2}\right) + \gamma_E - \log 4\,, \tag{5.40}$$

ψ being the digamma function and γ_E being the Euler-Mascheroni constant. Note the appearance of log terms in a generic gauge and how also the bulk-to-boundary N propagator simplifies considerably in the FY gauge. The presence of ζ-dependent terms is due to the fact that the corresponding boundary operator, the gauge connection a, is not gauge invariant.

On the other hand, the bulk-to-boundary propagator for the field strength,

$$\langle F_{AB}(X) f_{CD}(P)\rangle = \frac{4g^2\Gamma(\frac{d}{2})\sin(\frac{\pi d}{2})(\mathcal{P}_{AC}(X,P)\mathcal{P}_{BD}(X,P) - \mathcal{P}_{AD}(X,P)\mathcal{P}_{BC}(X,P))}{(d-2)(-2P\cdot X)^2}\,, \tag{5.41}$$

where we have introduced the projector

$$\mathcal{P}_{AB}(X,P) = \eta_{AB} + \frac{2P_A X_B}{(-2P\cdot X)}\,, \tag{5.42}$$

is ζ-independent and has the appropriate structure for the bulk-to-boundary correlator of an antisymmetric rank-2 tensor. Contrary to the D case, (5.38) has a factor g^2, because the boundary limit in (5.12) does not require to divide by g^2 in this case.

5.2.2 Ghost propagator

The two possible boundary conditions for the ghost fields c are $c(x,z) \underset{z\to 0}{\sim} z^\Delta \hat{c}_\Delta(x)$, with either $\Delta = 0$ or $\Delta = d$. They are constrained by the choice of boundary condition on the gauge fields: with N bc, the presence of dynamical gauge fields at the boundary requires the gauge transformation (and equivalently the ghost field) to persist at the boundary, i.e. $\Delta = 0$; with D bc, the gauge transformations should instead decay faster than the gauge fields at the boundary, as the bulk gauge fields are dual to global currents in this case, therefore the correct bc is $\Delta = d$. The ghost propagator with D bc $G^{(D)}_{\rm GH}$ is simply the propagator of a massless scalar field

$$G^{(D)}_{\rm GH}(X_1,X_2) = \frac{\Gamma\left(\frac{d+1}{2}\right)}{2d\pi^{\frac{d+1}{2}}u^d}\,{}_2F_1\left(d,\frac{d+1}{2},d+1,-\frac{2}{u}\right)\,. \tag{5.43}$$

Contrary to the ghost propagator on the sphere in (4.56), here zero modes are not allowed and therefore the propagator does not need to be regularized. The N ghost propagator can similarly be derived, but it will not be needed in this chapter.

5.3 Anomalous dimensions of lightest scalar operators

In this section, we compute the anomalous dimension of the lightest scalar singlet boundary operator, in both the D and the N bc's. The operator is $\mathrm{tr}[J_i J^i]$ for D bc, and $\mathrm{tr}[f_{ij}f^{ij}]$ for N bc, where $f_{ij} = \partial_i a_j - \partial_j a_i - i[a_i,a_j]$. As already mentioned in the introduction, for both cases in the limit $g^2 \to 0$ this operator has dimension 4 and it coincides with the displacement operator of the theory at the free UV fixed point. The latter statement can be proved either by using the expression for the bulk stress tensor and taking the boundary OPE (bOPE) limit, or by noticing that it is the only singlet dimension 4 operator in the boundary spectrum (see table 5.1), and therefore the only candidate to be the displacement

operator, which must exist in the spectrum when the bulk is a CFT.

To do the computation we will first exploit a multiplet-recombination argument, that fixes the leading-order anomalous dimension of the displacement operator for any perturbation of a CFT in AdS background. We present the argument in this general setting in subsection 5.3.1. We then discuss what this result teaches us regarding the disappearance/persistence of the D/N bc as we increase the AdS radius. For the case of D bc, we then check the result with an explicit diagrammatic calculation in subsection 5.3.3.

5.3.1 Anomalous dimension of the displacement operator

A CFT in AdS_{d+1} is equivalent up to a Weyl rescaling to a BCFT. A general BCFT result then implies that any CFT in AdS_{d+1} must have a boundary operator $\mathcal{D}$ of dimension $\Delta_{\mathcal{D}} = d+1$, which appears in the bOPE of the bulk stress tensor [180]. This operator is the so-called displacement operator. The two-point function between the traceless bulk stress tensor and the boundary displacement operator is fixed by the isometries. In embedding space, it reads

$$\text{CFT:} \quad \langle T_{AB}(X)\mathcal{D}(P)\rangle = \frac{C_{T\mathcal{D}}}{(-2P\cdot X)^{d+1}}\left(\frac{G_{AC}(X)G_{BD}(X)P^C P^D}{(-2P\cdot X)^2} - \frac{G_{AB}(X)}{4(d+1)}\right), \tag{5.44}$$

where $G_{AB}(X) = \eta_{AB} + X_A X_B$ is the projector to the tangent space at X. The two-point function (5.44) is fixed up to normalization by the two requirements

$$\nabla_X^A \langle T_{AB}(X)\mathcal{D}(P)\rangle = 0\,, \tag{5.45}$$

$$G^{AB}(X)\langle T_{AB}(X)\mathcal{D}(P)\rangle = 0\,, \tag{5.46}$$

where the first is the conservation, and the second is the traceless condition appropriate to a CFT. Assuming the bulk stress tensor is normalized via the Ward identities for the isometries, the coefficient $C_{T\mathcal{D}}$ depends on the normalization of the operator $\mathcal{D}$. For the sake of our argument, we can leave the precise choice of normalization unspecified.

Next, we turn on a deformation in the bulk, i.e.

$$S_{\text{bulk}} = S_{\text{CFT}} + \lambda \int dx\, O(x)\,, \tag{5.47}$$

where O is an operator of scaling dimension Δ_O of the bulk CFT. As a consequence of the deformation the stress tensor acquires a non-zero trace. In embedding space we have

$$\Delta_O \neq d+1: \quad G^{AB}(X)T_{AB}(X) = (\Delta_O - d - 1)\lambda\, O(X) + \alpha(\lambda)\mathbf{1}\,. \tag{5.48}$$

Besides the operator violation of scale-invariance proportional to the deformation O, we also allow a c-number contribution proportional to the identity operator, which is generally present due to the curvature of the background, with a coefficient $\alpha(\lambda)$ that depends on the

deformation λ.[4] In the special case $\Delta_O = d+1$ the coupling λ is classically marginal and we have instead (assuming for simplicity that there is a single marginal operator in the CFT)

$$\Delta_O = d+1: \quad G^{AB}(X)T_{AB}(X) = \beta_\lambda(\lambda)\, O(X) + \alpha(\lambda)\mathbf{1}\,. \tag{5.49}$$

Here β_λ is the beta function, which for small λ behaves as

$$\beta_\lambda(\lambda) = \beta_0\, \lambda^n + \mathcal{O}(\lambda^{n+1})\,, \tag{5.50}$$

for some integer $n > 1$ and some real coefficient β_0.[5]

As a consequence of the trace being non-zero, there is an additional structure in the two-point function, and the dimension $\Delta_\mathcal{D}(\lambda)$ of the operator $\mathcal{D}$ will depend on λ and no longer be protected, so the two-point function is

$$\begin{aligned}\lambda > 0: \quad \langle T_{AB}(X)\mathcal{D}(P)\rangle = \frac{C_{T\mathcal{D}}(\lambda)}{(-2P\cdot X)^{\Delta_\mathcal{D}(\lambda)}}\Bigg(&\frac{G_{AC}(X)G_{BD}(X)P^C P^D}{(-2P\cdot X)^2} - \frac{G_{AB}(X)}{4(d+1)} \\ &-\frac{(\Delta_\mathcal{D}(\lambda)-d-1)d}{4(d+1)\Delta_\mathcal{D}(\lambda)}G_{AB}(X)\Bigg)\,.\end{aligned} \tag{5.51}$$

The coefficient of the additional structure in the second line is fixed in terms of $\Delta_\mathcal{D}$ and $C_{T\mathcal{D}}$ once we impose the conservation of the stress tensor. Note that besides $\Delta_\mathcal{D}$ also the normalization $C_{T\mathcal{D}}$ acquires a dependence on λ as we have indicated. The two-point correlator between the deformation O and the displacement is fixed by bulk isometries to have the form

$$\langle O(X)\mathcal{D}(P)\rangle = \frac{C_{O\mathcal{D}}(\lambda)}{(-2P\cdot X)^{\Delta_\mathcal{D}(\lambda)}}\,. \tag{5.52}$$

Taking the trace of equation (5.51), using the operator equation (5.48) and substituting (5.52) we obtain the relation

$$\Delta_O \neq d+1: \quad \Delta_\mathcal{D}(\lambda) - d - 1 = -\frac{4(\Delta_O - d - 1)\lambda}{d}\frac{C_{O\mathcal{D}}(\lambda)}{C_{T\mathcal{D}}(\lambda)}\Delta_\mathcal{D}(\lambda)\,. \tag{5.53}$$

Note that the c-number contribution given by $\alpha(\lambda)$ in (5.48) drops from the two-point function because it gives rise to a one-point function for the boundary operator $\mathcal{D}$, which vanishes. Expanding this expression at small λ and denoting $\Delta_\mathcal{D}(\lambda) - d - 1 = \gamma_\mathcal{D}(\lambda)$ we obtain that the leading order anomalous dimension of the displacement operator is

$$\Delta_O \neq d+1: \quad \gamma_\mathcal{D}(\lambda) = -\frac{4(d+1)(\Delta_O - d - 1)}{d}\frac{C_{O\mathcal{D}}}{C_{T\mathcal{D}}}\lambda + \mathcal{O}(\lambda^2)\,. \tag{5.54}$$

[4] In the special case of $d+1 = 4$, this coefficient is a linear combination of beta functions for curvature terms [181–184], with couplings denoted by a, b and c. There is no need to specify their form since, as we will see, they will not play any role in our analysis.

[5] As pointed out in [147, 185], in $d+1 = 4$ and in presence of continuous global symmetries, the beta functions β_i are subject to a possible ambiguity and are replaced by well-defined functions B_i. This issue will not appear in the YM application as there are no continuous global symmetries.

When the λ dependence is not explicitly indicated in the normalization coefficients $C_{T\mathcal{D}}$ and $C_{O\mathcal{D}}$, we mean their values at $\lambda = 0$, i.e. in the CFT. Note that the normalization choice for $\mathcal{D}$ does not matter in this formula because it cancels in the ratio between normalization coefficients. The relative normalization between T and λO on the other hand is fixed by the operator equation (5.48). In the special case of a classically marginal deformation with $\Delta_O = d + 1$, following the same steps and using the operator equation (5.49) instead, we obtain the relation

$$\Delta_O = d+1: \quad \Delta_{\mathcal{D}}(\lambda) - d - 1 = -\frac{4\beta_\lambda(\lambda)}{d}\frac{C_{O\mathcal{D}}(\lambda)}{C_{T\mathcal{D}}(\lambda)}\Delta_{\mathcal{D}}(\lambda)\,, \tag{5.55}$$

which is valid to all orders in perturbation theory. The same remark applies as well to (5.53). Expanding (5.55) at small λ gives the following result for the leading order anomalous dimension

$$\Delta_O = d+1: \quad \gamma_{\mathcal{D}}(\lambda) = -\frac{4(d+1)}{d}\frac{C_{O\mathcal{D}}}{C_{T\mathcal{D}}}\,\beta_0\,\lambda^n + \mathcal{O}(\lambda^{n+1})\,. \tag{5.56}$$

Therefore, in the presence of a classically marginal running coupling in the bulk, the leading anomalous dimension of the displacement is fixed by the leading coefficient in the beta function of the bulk coupling.

Application to YM

YM theory does not fall straightforwardly in the setup described above of a CFT with a small deformation. For definiteness, we discuss $SU(n_c)$ YM, the generalization to other gauge groups is straightforward. At the level of local operators, the UV CFT is the abelian theory of $n_c^2 - 1$ free gluons (see e.g. [186] for a discussion of the global structure of the theory in this limit). The deforming operator is the Lagrangian itself, with a large coefficient $\frac{1}{g^2}$. Nevertheless, this can be treated perturbatively because of the factors of g^2 in each gluon propagator.

The stress tensor of YM theory is

$$T_{\mu\nu} = \frac{1}{g^2}\mathrm{tr}\left[2F_\mu{}^\rho F_{\nu\rho} - \frac{g_{\mu\nu}}{2}F^{\rho\sigma}F_{\rho\sigma}\right]\,. \tag{5.57}$$

Its trace is given by

$$T^\mu{}_\mu = \beta_{\frac{1}{g^2}}\mathrm{tr}\left[\frac{1}{2}F^{\rho\sigma}F_{\rho\sigma}\right] + \alpha(g^2)\mathbb{1} = -\frac{1}{g^4}\beta_{g^2}\mathrm{tr}\left[\frac{1}{2}F^{\rho\sigma}F_{\rho\sigma}\right] + \alpha(g^2)\mathbb{1}\,. \tag{5.58}$$

Like in the previous section, we allowed a c-number contribution with a g^2-dependent coefficient, whose form has been first determined in [184]. This contribution drops from the

anomalous dimension. The one-loop beta function is

$$\beta_{g^2}(g^2) = -\frac{22n_c}{3}\frac{g^4}{(4\pi)^2} + \mathcal{O}(g^6)\,. \tag{5.59}$$

In the notation of the previous section, calling

$$O = -\frac{1}{g^2}\mathrm{tr}\left[\frac{1}{2}F^{\rho\sigma}F_{\rho\sigma}\right]\,, \tag{5.60}$$

eq. (5.56) gives

$$\gamma_{\mathcal{D}}(g^2) = \frac{16}{3}\frac{C_{O\mathcal{D}}}{C_{T\mathcal{D}}}\frac{22n_c}{3}\frac{g^2}{(4\pi)^2} + \mathcal{O}(g^4)\,. \tag{5.61}$$

We now specify the boundary conditions and compute the coefficients that enter the anomalous dimension, which are given by the diagrams in figure 5.2. For the D bc, we have $\mathcal{D} = \mathrm{tr}[J_i J^i]$ and using the propagator (5.37) we get

$$D: \quad \begin{aligned} C_{T\mathcal{D}} &= (n_c^2-1)\frac{256}{\pi^4 g^2}\,, \\ C_{O\mathcal{D}} &= -(n_c^2-1)\frac{48}{\pi^4 g^2}\,. \end{aligned} \tag{5.62}$$

Substituting in (5.61) we obtain

$$D: \quad \gamma_{\mathrm{tr}[JJ]}(g^2) = -\frac{11n_c}{24\pi^2}g^2 + \mathcal{O}(g^4)\,. \tag{5.63}$$

For the N bc, on the other hand, $\mathcal{D} = \mathrm{tr}[f_{ij}f^{ij}]$. Using the propagator (5.38) we get

$$N: \quad \begin{aligned} C_{T\mathcal{D}} &= -(n_c^2-1)\frac{512g^2}{\pi^4}\,, \\ C_{O\mathcal{D}} &= -(n_c^2-1)\frac{96g^2}{\pi^4}\,. \end{aligned} \tag{5.64}$$

Substituting in (5.61) we obtain

$$N: \quad \gamma_{\mathrm{tr}[ff]}(g^2) = \frac{11n_c}{24\pi^2}g^2 + \mathcal{O}(g^4)\,. \tag{5.65}$$

Interestingly enough, the leading corrections (5.63) and (5.65) are equal and opposite. We do not know if this is a mere coincidence of the leading contribution or if there is some mechanism explaining this relation. It would be interesting to better understand this point.

As we mentioned in the introduction, if a boundary singlet scalar operator is marginal for some value of g^2, or equivalently for some value of Λ_{YM} in units of the AdS radius, then the corresponding boundary condition goes through merger and annihilation [56, 111] and it stops existing as a unitary boundary condition. This phenomenon, first envisioned in [95],

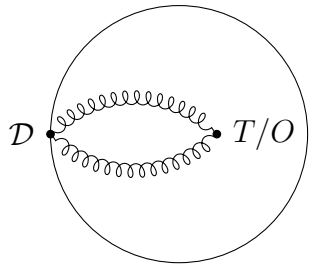

Figure 5.2: Diagrams that compute the coefficients $C_{O\mathcal{D}}$ and $C_{T\mathcal{D}}$ in the free UV limit $g \to 0$.

was explained in detail in [161] and it was applied to two-dimensional theories in [94]. The leading order anomalous dimensions obtained above are suggestive that the displacement operator indeed becomes marginal for the D bc and not for the N bc. This matches the expectation that the D bc should not exist for arbitrary large AdS because it would give rise to massless and colored asymptotic states in flat space, while it is possible that the N bc approaches smoothly the flat space limit. Truncating the scaling dimension of $\mathrm{tr}[JJ]$ to the leading order correction (5.63) gives the estimate (5.2) for the transition in the Marginality scenario.

5.3.2 Boundary RG flow from bulk dynamics

In this section, we show how an RG flow can be induced in the boundary CFT when an irrelevant boundary operator becomes marginal. The analysis will be given for a general bulk and boundary theory, with the assumption that in the UV the bulk theory is conformal and the boundary theory has no relevant deformations. The latter assumption is not essential, but it simplifies the analysis that follows. We denote by $\hat{O}$ the lowest dimensional irrelevant scalar singlet operator of the boundary CFT and by O the leading bulk operator, whose coupling $\widetilde{\lambda}$ govern the CFT data of the boundary theory. We take $\lambda = \widetilde{\lambda}\, L^{d+1-\Delta_O}$, where Δ_O is the scaling dimension of O in the bulk CFT at $\widetilde{\lambda} = 0$, in such a way that λ is dimensionless.

Suppose then that there exists a value $\lambda_{\rm crit}$ (or alternatively a critical AdS length $L_{\rm crit}$), where $\Delta_{\hat{O}}(\lambda_{\rm crit}) = d$. Let us denote by $\eta \ll 1$ the coupling associated to $\hat{O}$ when this is close to marginal, and by $\delta\lambda = \lambda - \lambda_{\rm crit}$ the deviation of the coupling from its critical value. We take

$$\delta\lambda \ll \eta \ll 1\,, \qquad\qquad \delta\lambda \sim \eta^2\,, \tag{5.66}$$

and use η as expansion parameter. We determine the beta function β_η of the coupling η up to order η^2 by using techniques similar to those employed in conformal perturbation theory, i.e. we expand a correlation function of bulk operators around the bulk critical theory in absence of boundary deformations. A simple choice is to consider the one-point function of the bulk operator O itself, the one associated with the deformation $\delta\lambda$.

We have

$$\langle O(x_1)\rangle_{\delta\lambda,\eta} = \langle O(x_1)\rangle_0 - \eta\langle O(x_1)\int d\hat{x}\,\hat{O}(x)\rangle_0 + \frac{\eta^2}{2}\langle O(x_1)\int d\hat{x}\,\hat{O}(x)\int d\hat{y}\,\hat{O}(y)\rangle_0 - \delta\widetilde{\lambda}\langle O(x_1)\int dx\,O(x)\rangle_0 + \dots\,, \tag{5.67}$$

where the subscript 0 means that the correlator is evaluated at $\delta\widetilde{\lambda} = \eta = 0$ and $d\hat{x} \equiv d^d x$ denotes the measure at the boundary. The renormalization of the boundary coupling η is determined by the short-distance behavior of the above correlators, which is fixed using the OPE and the bOPE expansions. The latter still exists despite the bulk theory is generally non-conformal at $\lambda = \lambda_{\text{crit}}$. The contribution to β_η coming from the third term in the first row of (5.67) is computed using standard techniques of conformal perturbation theory (see e.g. chapter 5 of [187]). Short-distance divergences occur when x approaches y. We can then use the OPE to rewrite that term as

$$\int d\hat{x}\,\hat{O}(x)\int d\hat{y}\,\hat{O}(y) \approx \int d\hat{x}\int_{|w|\geq a} d\hat{w}\left(C_{\hat{O}}w^{-2d} + C_{\hat{O}\hat{O}}{}^{\hat{O}}w^{-d}\hat{O}(x) + \dots\right), \tag{5.68}$$

where $w_i = (x-y)_i$, a is a short-distance cut-off, $C_{\hat{O}}$ and $C_{\hat{O}\hat{O}}{}^{\hat{O}}$ are the coefficients entering the two-point function and the OPE coefficient of the three-point function of $\hat{O}$. Universal contributions to β_η arise from the second term in (5.68).[6] We have

$$\int d\hat{x}\,\hat{O}(x)\int d\hat{y}\,\hat{O}(y)\Big|_{\text{div}} \approx -\Omega_{d-1}C_{\hat{O}\hat{O}}{}^{\hat{O}}\log(a)\int d\hat{x}\,\hat{O}(x)\,. \tag{5.69}$$

The first term in the second row of (5.67) is UV divergent when the bulk operator approaches the boundary. In this limit we can expand the bulk field in terms of boundary operators using the bOPE. Noting that AdS is related by a Weyl transformation to half-flat space, we get that an operator O in AdS with dimension Δ_O satisfies $O_{\text{AdS}} = (z/L)^{\Delta_O}O_{\text{half-space}}$. Eq.(2.38) can be then rescaled into

$$L^{\Delta_O}O(x) = \sum_{\hat{O}_k} z^{\hat{\Delta}_k}B_O^{\hat{O}_k}\hat{O}_k(x) = B_O^{\hat{\mathbf{1}}} + B_O^{\hat{O}}z^d\hat{O}(x) + \dots\,, \tag{5.70}$$

the subscript AdS being omitted in all operators. We then have

$$O(x_1)\int dx\,O(x) \approx L^{d+1-\Delta_O}O(x_1)\int d\hat{x}\int_a^\infty \frac{dz}{z^{d+1}}\left(B_O^{\hat{\mathbf{1}}} + B_O^{\hat{O}}z^d\hat{O}(x) + \dots\right). \tag{5.71}$$

As in (5.68), universal logarithmic contributions arise only from the second term in (5.70),

[6] For example, using the regularization (5.137), the first term in eq. (5.68) is UV finite.

which gives

$$O(x_1)\int dx\, O(x)\Big|_{\rm div} \approx -\log(a) L^{d+1-\Delta_O} B_O^{\hat{O}}\, O(x_1)\int d\hat{x}\, \hat{O}(x)\,. \tag{5.72}$$

In general both the 3-point OPE and the bOPE coefficients $C_{\hat{O}\hat{O}\hat{O}}$ and $B_{O\hat{O}}$ depend on λ. From (5.67), (5.69) and (5.72) we immediately get

$$\beta_\eta = -a\frac{d\eta}{da} = c_1\eta^2 + c_2\delta\lambda\,, \tag{5.73}$$

where

$$\begin{aligned} c_1 &= \frac{1}{2}\Omega_{d-1} C_{\hat{O}\hat{O}}{}^{\hat{O}}(\lambda_{\rm crit})\,,\\ c_2 &= -B_O^{\hat{O}}(\lambda_{\rm crit})\,. \end{aligned} \tag{5.74}$$

Application to YM

We have shown that in the vicinity of $g^2 \sim g^2_{\rm crit}$, the beta function for the boundary marginal coupling $\eta\,{\rm tr}[JJ]$ is given by

$$\beta_\eta = c_1\eta^2 + c_2\left(\frac{1}{g^2} - \frac{1}{g^2_{\rm crit}}\right) + \text{subleading}\,, \tag{5.75}$$

where, for $d = 3$,

$$c_1 = 2\pi\frac{C_3}{C_2}\Big|_{g^2=g^2_{\rm crit}}\,, \qquad\qquad c_2 = -\frac{B}{C_2}\Big|_{g^2=g^2_{\rm crit}}\,, \tag{5.76}$$

with C_2 and C_3 the two- and three-point function coefficients of ${\rm tr}[JJ]$, and B the coefficient of the two-point function between the bulk Lagrangian ${\rm tr}[\frac{1}{4}F_{\mu\nu}F^{\mu\nu}]$ and ${\rm tr}[JJ]$:

$$\left\langle {\rm tr}[\tfrac{1}{2}F_{\mu\nu}F^{\mu\nu}](X){\rm tr}[JJ](P)\right\rangle = \frac{B(g^2)}{(-2P\cdot X)^d}\,. \tag{5.77}$$

At leading order for $g^2 \ll 1$, $C_2 > 0$ is given by (5.83) below, $C_3 > 0$, and $B = -g^2 C_{O\mathcal{D}} > 0$, with $C_{O\mathcal{D}}$ given in (5.62). The value of these coefficients at $g^2_{\rm crit}$ is beyond the reach of perturbation theory. Nevertheless, the assumption that the D bc is a viable unitary boundary condition that preserves AdS isometries in the range of coupling $0 \le g^2 \le g^2_{\rm crit}$ guarantees that β_η must have real zeros for $g^2 \lesssim g^2_{\rm crit}$. This implies that c_1 and c_2 must have opposite signs. As a result β_η has two real zeros, at $\eta_\pm = \pm\sqrt{c_2/c_1(g_{\rm crit}^{-2} - g^{-2})}$. So, at least close to $g^2_{\rm crit}$, another boundary condition D^* must exist, which gives rise to another boundary CFT, with the same global symmetry of the D CFT, namely the group G. To the operator $O_+ = {\rm tr}[JJ]$ of the D theory is associated another singlet scalar operator O_- of the D^* theory. Their dimensions are

$$\Delta_\pm = d + 2|c_1|\eta_\pm\,. \tag{5.78}$$

Deforming the D^* CFT with O_- leads to a (short) RG flow ending in the CFT D. When $g^2 = g^2_{\rm crit}$, the two CFTs merge and annihilate, namely they turn to complex CFT for $g^2 > g^2_{\rm crit}$, with purely imaginary anomalous dimensions for $O_\pm$ close to the merging point [111].

Note that this mechanism of loss of conformality has been advocated in [56] as a possible explanation of how conformal windows terminate in $4d$ non-abelian gauge theories with matter. In that context, the role of g^{-2} is played by the number of flavors.[7] Interestingly enough, here we are advocating the possibility that confinement itself in pure Yang-Mills theory can be explained as a mechanism of loss of conformality, but this time the CFT in question is a $3d$ CFT living at the boundary of AdS space.

It is also interesting to observe that a similar instability of the D bc exists in three-dimensional gauge theories in AdS_3. In that case however the singlet scalar operator bilinear in the currents is actually marginal at zero bulk coupling, causing the Dirichlet boundary condition to be unavailable already in perturbation theory, see e.g. [179, 188].

5.3.3 Anomalous dimensions from $J^a J^b$ two-point function

We now restrict to D bc and compute the anomalous dimensions of the lightest scalar primaries with different representations of $SU(n_c)$. To do this, we perform a direct computation of Witten diagrams contributing to the two-point functions of $J^a J^b(x) = J^{ia} J_i{}^b(x)$. Here vector indices are contracted, while color indices are left open. From now on we drop the superscript D in Dirichlet propagators, as N bc will no longer enter our discussion.

The operator $J^a J^b$ is the symmetric product of two fields in the adjoint, which decomposes into irreducible representations according to

$$R_A \otimes R_A|_{\rm sym} = R_+ = \mathbf{1} \oplus R_A \oplus R_3\,, \tag{5.79}$$

where $\mathbf{1}$ is the singlet, R_A is the adjoint, and R_3 is defined in appendix C.[8] Note that the singlet corresponds to the displacement operator $\mathrm{tr}[JJ]$, which we studied in the previous subsection. Matching (5.63) with the result obtained with a direct computation will be a non-trivial check of our computations.

Given a scalar primary operator O of classical dimension $\Delta_O^{(0)}$, its two-point function is given by

$$\langle O(x) O(0)\rangle = \frac{c_O(g^2)}{x^{2\Delta_O}}\,, \tag{5.80}$$

where $\Delta_O = \Delta_O^{(0)} + \gamma_O$. In perturbation theory, the anomalous dimension can be expanded as $\gamma_O(g^2) = \gamma_O^{(0)} g^2 + \mathcal{O}(g^4)$. We can hence determine the leading-order anomalous dimension γ_O

[7] In the Veneziano limit the number of flavors is replaced by a continuous parameter and the merge and annihilation scenario can be analyzed in controlled set-ups, see e.g. [153]. In this limit, the role of η is played by a double trace deformation.

[8] This decomposition is valid only for $n_c > 3$, while for $n_c = 2, 3$ the representation R_3 is absent.

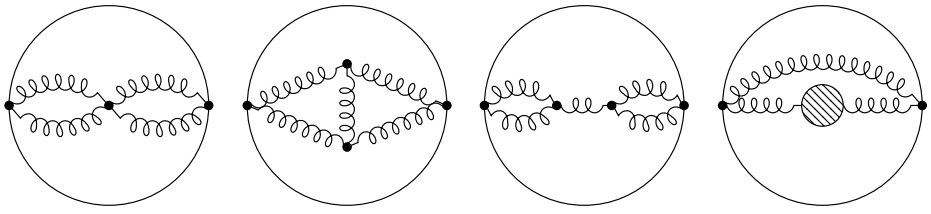

(a) Q_{QU} (b) Q_{TR} (c) Q'_{TR} (d) Q_{RED}

Figure 5.3: Next-to-leading corrections to the two-point function of $J^a J^b$: the quartic (a), the triple (b), and the reducible (d) diagram. The diagram (c) evaluates to zero since it has a vanishing color structure and the diagram (d), being free of logarithmic terms, does not affect the anomalous dimension.

by looking at the logarithmic part of the next-to-leading correction to the two-point function:

$$\gamma_O(g^2) = -\frac{\langle O(x_1)O(x_2)\rangle^1|_{\log x^2}}{\langle O(x_1)O(x_2)\rangle^0} + \mathcal{O}(g^4)\,. \tag{5.81}$$

Here and in the following we use the superscript 0 and 1 to denote the leading order and the next-to-leading order respectively.

We first compute the leading order and the logarithmic terms at the next-to-leading order of the two-point function $\langle J^{a_1}J^{b_1}(x_1)J^{a_2}J^{b_2}(x_2)\rangle$ and then project onto irreducible representations. At the leading order, the two-point function in $d = 3$ reads

$$\langle J^{a_1}J^{b_1}(x_1)J^{a_2}J^{b_2}(x_2)\rangle^0 = \frac{C^0_{JJ}}{g^4}(\delta^{a_1a_2}\delta^{b_1b_2} + \delta^{a_1b_2}\delta^{b_1a_2})\frac{1}{x_{12}^{2\Delta^0_{JJ}}}\,, \tag{5.82}$$

with

$$C^0_{JJ} = 3(C^0_J)^2 = \frac{12}{\pi^4}, \qquad \Delta^0_{JJ} = 2\Delta_J = 4\,, \tag{5.83}$$

where C^0_J is defined in (5.14). Let us now compute the next-to-leading order.

We consider the bulk two-point function of the composite operator $A^{\mu a}A^b_\mu$,

$$g^4 Q(x_1, x_2) = \langle A^{\mu_1 a_1}A^{b_1}_{\mu_1}(x_1)A^{\mu_2 a_2}A^{b_2}_{\mu_2}(x_2)\rangle\,. \tag{5.84}$$

We then uplift it to embedding coordinates and take the external points to the boundary to compute $Q^\partial(P_1, P_2)$. While Q is not gauge invariant, the ξ-dependence cancels when we take the boundary limit, making Q^∂ gauge invariant instead.

At next-to-leading order, $Q(x_1, x_2)$ is given by three contributions, corresponding to the diagrams depicted in figure 5.3,

$$Q^{(1)}(x_1, x_2) = Q_{\mathrm{QU}}(x_1, x_2) + Q_{\mathrm{TR}}(x_1, x_2) + Q_{\mathrm{RED}}(x_1, x_2)\,. \tag{5.85}$$

We call these diagrams the quartic, the triple, and the reducible diagram respectively. By reducible here we refer to the fact that the last diagram is simply the contraction between the vector propagator at tree level and its one-loop correction. This contribution can be

disregarded, as currents are protected by gauge symmetry and do not get an anomalous dimension. Let us instead focus on the first two terms of the sum in (5.85).

Quartic diagram

The quartic diagram is easier to deal with, as it involves integration over only one point,

$$\begin{aligned} Q_{\text{QU}}(x_1,x_2) = -g^2(T+U)\int dx\, \big(&\Pi^{\mu_1\nu}\Pi_{\mu_1\nu}(x_1,x)\Pi^{\lambda\mu_2}\Pi_{\lambda\mu_2}(x,x_2) \\ &- \Pi^{\mu_1\nu}\Pi_{\mu_1\lambda}(x_1,x)\Pi^{\lambda\mu_2}\Pi_{\nu\mu_2}(x,x_2)\big)\,, \end{aligned} \tag{5.86}$$

where we have factored out T and U channel color structures defined as

$$T = f^{a_1a_2c}f^{b_1b_2c}, \qquad U = f^{a_1b_2c}f^{b_1a_2c}\,. \tag{5.87}$$

Uplifting to embedding space and taking the boundary limit as in (5.36), we have

$$\begin{aligned} Q^{\partial}_{\text{QU}}(P_1,P_2) = -\frac{1}{g^2}(T+U)\int dX (&K^{A_1B}K_{A_1B}(P_1,X)K^{CA_2}K_{CA_2}(X,P_2) \\ &- K^{A_1B}K_{A_1C}(P_1,X)K_{BA_2}K^{CA_2}(X,P_2))\,. \end{aligned} \tag{5.88}$$

We then plug in the expression for the bulk-to-boundary propagator in (5.37) to get

$$\begin{aligned} Q^{\partial}_{\text{QU}}(P_1,P_2) = \frac{1}{g^2}(T+U)&\frac{2^{4d}\Gamma(\frac{d+1}{2})^4\pi^{2d+1}}{16(d-2)^4} \\ &\int dX \frac{(P_1\cdot P_2)^2 + 2(P_1\cdot P_2)(P_1\cdot X)(P_2\cdot X) - d(d-1)(P_1\cdot X)^2(P_2\cdot X)^2}{(-2P_1\cdot X)^{2d}\,(-2P_2\cdot X)^{2d}}\,. \end{aligned} \tag{5.89}$$

This is a linear combination of scalar integrals of the form

$$\mathcal{I}_\Delta = \int dX \frac{1}{(-2P_1\cdot X)^\Delta}\frac{1}{(-2P_2\cdot X)^\Delta}\,, \tag{5.90}$$

which evaluates to

$$\mathcal{I}_\Delta = \frac{\pi^{\frac{d}{2}}\Gamma\left(\Delta-\frac{d}{2}\right)}{\Gamma(\Delta)(-2P_1\cdot P_2)^\Delta}\left(\log\left(\frac{-2P_1\cdot P_2}{\delta^2}\right) - \psi(\Delta) + \psi\left(1-\frac{d}{2}+\Delta\right)\right)\,, \tag{5.91}$$

where $\delta \ll 1$ is an IR regulator expressing the distance from the boundary. See appendix E.1 for a derivation of (5.91).

Plugging in (5.89), setting $d=3$, and focusing on the logarithm part we get

$$Q^{\partial}_{\text{QU}}(P_1,P_2)\big|_{\log} = -\frac{1}{g^2}(T+U)\frac{27}{2\pi^6(-2P_1\cdot P_2)^4}\,. \tag{5.92}$$

Triple diagram

The triple diagram reads

$$Q_{\rm TR}(x_1,x_2) = g^2(T+U)\int dx\,dy\;\Pi^{\lambda}_{\ \lambda'}(x,y)W_{\leftarrow\mu_1\mu_2}(x,x_1,x_2)W^{\leftarrow'\mu_1\mu_2}(y,x_1,x_2)\,, \tag{5.93}$$

where we have introduced

$$\begin{aligned} W_{\leftarrow\mu_1\mu_2}(x,x_1,x_2) &= 2\Pi_{\mu_1\lambda}(x_1,x)\overset{\leftrightarrow}{\nabla}{}^{\nu}_{x}\Pi_{\nu\mu_2}(x,x_2) \\ &\quad - \Pi_{\mu_1\nu}(x_1,x)\overset{\leftrightarrow}{\nabla}{}^{x}_{\lambda}\Pi^{\nu}{}_{\mu_2}(x,x_2) - \Pi_{\mu_1\nu}(x_1,x)\overset{\leftrightarrow}{\nabla}{}^{\nu}_{x}\Pi_{\lambda\mu_2}(x,x_2)\,, \end{aligned} \tag{5.94}$$

with $F\overset{\leftrightarrow}{\nabla}_\mu G = F(\nabla_\mu G) - (\nabla_\mu F)G$.[9] Uplifting to embedding space and taking the boundary limit as in (5.36), we get

$$Q^{\partial}_{\rm TR}(P_1,P_2) = \frac{1}{g^2}(T+U)\int dX\,dY\;\Pi^{C}_{\ C'}(X,Y)W_{CA_1A_2}(X,P_1,P_2)W^{C'A_1A_2}(Y,P_1,P_2)\,, \tag{5.95}$$

with

$$\begin{aligned} W_{CA_1A_2}(X,P_1,P_2) &= 2K_{A_1C}(P_1,X)\overset{\leftrightarrow}{\nabla}{}^{B}_{X}K_{BA_2}(X,P_2) \\ &\quad - K_{A_1B}(P_1,X)\overset{\leftrightarrow}{\nabla}{}^{X}_{C}K^{B}{}_{A_2}(X,P_2) - K_{A_1B}(P_1,X)\overset{\leftrightarrow}{\nabla}{}^{B}_{X}K_{CA_2}(X,P_2)\,. \end{aligned} \tag{5.96}$$

We plug the expression for the bulk-to-boundary in (5.37) and the bulk-to-bulk gauge propagator in FY gauge in (5.32), getting in this way a linear combination of integrals in the form

$$\mathcal{I}_{4\Delta} = \int dX\,dY(-2P_1\cdot X)^{\Delta_1}(-2P_1\cdot Y)^{\Delta_3}(-2P_2\cdot X)^{\Delta_2}(-2P_2\cdot Y)^{\Delta_4}f(u(X,Y))\,. \tag{5.97}$$

To solve this integral, we express $f(u(X,Y))$ as a function of the variable

$$\zeta = \frac{1}{1+u} = \frac{2zw}{w^2+z^2+(x-y)^2}\,, \tag{5.98}$$

and then expand it in powers of ζ,

$$f(\zeta) = \sum_{k=0}^{\infty} a_k\zeta^{\Delta_k}\,, \tag{5.99}$$

with $\Delta_k = \Delta_0 + k$.

[9] To obtain this expression for W we have performed an integration by parts to get rid of the term in the triple vertex with a derivative acting on the external propagator. As we discuss in appendix E.2, this does not give rise to additional boundary terms.

The result can be written as

$$\mathcal{I}_{4\Delta} = \sum_{k=0}^{\infty} a_k \, \mathcal{I}_{4\Delta}^{(k)} \,, \tag{5.100}$$

with

$$\mathcal{I}_{4\Delta}^{(k)} = \sum_{m=0}^{\infty} \frac{\pi^{\frac{d}{2}} 2^{\Delta_k - 1} \Gamma\left(\frac{\Delta_{1234}-d}{2}\right) \Gamma\left(\frac{\Delta_{34k}-d}{2}\right) \Gamma\left(\frac{\Delta_{4k,3}+2m}{2}\right) \Gamma\left(\frac{\Delta_{3k,4}}{2}\right) \Gamma(m+\Delta_3)}{m! \, \Gamma(\Delta_1) \Gamma(\Delta_3) \Gamma(\Delta_k) \Gamma\left(\frac{\Delta_{124k}+\Delta_4+2m-d}{2}\right) (-2P_1 \cdot P_2)^{\frac{\Delta_{12,k}-2m}{2}}} \mathcal{I}_{\tilde{\Delta}^{(k,m)}} \,, \tag{5.101}$$

where we introduced the notation

$$\Delta_{i_1 i_2 \ldots, j_1 j_2 \ldots} = (\Delta_{i_1} + \Delta_{i_2} + \ldots) - (\Delta_{j_1} + \Delta_{j_2} + \ldots) \tag{5.102}$$

and we used that all the integrals that contribute to the triple diagram satisfy $\Delta_{13} = \Delta_{24}$, which gives

$$\tilde{\Delta}^{(k,m)} = \frac{\Delta_{34k} + 2m}{2} \,. \tag{5.103}$$

We refer to appendix E.3 for a derivation of the result (5.101). The sum over m in (5.101) can be performed analytically and gives rise to a linear combination of generalized hypergeometric functions depending on k. We numerically sum over k setting $d = 3$.[10] The sum is convergent, but with a rather slow rate, so we adopt Padé approximants to improve on the final accuracy. The final result with 400 terms is

$$Q^{\partial}_{\mathrm{TR}}(P_1, P_2)\big|_{\log} \approx \frac{1}{g^2}(T+U) \frac{0.01976}{(-2P_1 \cdot P_2)^4} \,. \tag{5.104}$$

Summing all the terms together and downlifting to Poincaré coordinates we get

$$\langle J^{a_1} J^{b_1}(x_1) J^{a_2} J^{b_2}(x_2) \rangle^1 \big|_{\log} = Q^{(1)\partial}(x_1, x_2)\big|_{\log} \approx \frac{1}{g^2}(T+U) \frac{0.005721}{x_{12}^8} \,. \tag{5.105}$$

5.3.4 Projecting onto irreducible representations

As explained at the beginning of this section, to obtain primary operators we need to project $J^a J^b$ onto irreducible representations of $SU(n_c)$. A tensor T^{ab} in the reducible representation given by the products of two adjoints can be easily projected in the singlet representation taking the trace of the tensor. The singlet projector P_S can be then defined as

$$(P_S T)^{ab} = \frac{\delta_{cd} T^{cd}}{n_c^2 - 1} \delta^{ab} \,. \tag{5.106}$$

[10] Actually, we have to set $d = 3 + \epsilon$, with $\epsilon \ll 1$, in order to avoid spurious poles in $1/(d-3)$ which appear in intermediate steps but cancel in the total sum.

The two-point function of the singlet operator $JJ_S^{ab} = (P_S JJ)^{ab}$ is then obtained by acting with this projector on eq.(5.82) and eq.(5.105) as follows

$$\langle JJ_S^{a_1b_1}(x_1) JJ_S^{a_2b_2}(x_2)\rangle = \delta^{a_1b_1}\delta^{a_2b_2}\left(\langle JJ_S(x_1)JJ_S(x_2)\rangle^0 + \langle JJ_S(x_1)JJ_S(x_2)\rangle^1\right) , \tag{5.107}$$

with

$$\langle JJ_S(x_1)JJ_S(x_2)\rangle^0 = \frac{1}{g^4}\frac{24}{\pi^4(n_c^2-1)}\frac{1}{x_{12}^8} , \tag{5.108}$$

$$\langle JJ_S^{a_1b_1}(x_1) JJ_S^{a_2b_2}(x_2)\rangle^1\big|_{\log} \approx \frac{1}{g^2}\frac{2n_c}{n_c^2-1}\frac{0.005721}{x_{12}^8} . \tag{5.109}$$

Plugging in (5.81), we get that the anomalous dimension of the singlet operator is

$$\gamma_{JJ_S} \approx -0.04644\, n_c\, g^2 . \tag{5.110}$$

This result matches with (5.63), providing a non-trivial check of our computation. This correspondence allows to identify the 0.005721 in (5.105) as the analytic result $11/(2\pi^6)$, which we replace from now on.

Consider now the other representations. We will not need to project the result individually to each irreducible representation, as all the non-singlets ones acquire at this order the same anomalous dimension. This is seen by projecting out the singlet by introducing the operator $JJ_{S^\perp}^{ab} = ((1-P_S)JJ)^{ab}$ and computing its two-point function,

$$\begin{aligned}\langle JJ_{S^\perp}^{a_1b_1}(x_1) JJ_{S^\perp}^{a_2b_2}(x_2)\rangle = &\left(\delta^{a_1a_2}\delta^{b_1b_2} + \delta^{a_1b_2}\delta^{a_2b_1} - \frac{2}{n_c^2-1}\delta^{a_1b_1}\delta^{a_2b_2}\right)\\ &\left(\langle JJ_{S^\perp}(x_1)JJ_{S^\perp}(x_2)\rangle^0 + \langle JJ_{S^\perp}(x_1)JJ_{S^\perp}(x_2)\rangle^1\right) ,\end{aligned} \tag{5.111}$$

with

$$\langle JJ_{S^\perp}(x_1)JJ_{S^\perp}(x_2)\rangle^0 = \frac{1}{g^4}\frac{12}{\pi^4(n_c^2-1)}\frac{1}{x_{12}^8} , \tag{5.112}$$

$$\langle JJ_{S^\perp}(x)JJ_{S^\perp}(y)\rangle^1\big|_{\log} = -\frac{1}{g^2}\frac{11n_c}{2\pi^6(n_c^2-2)}g^2\frac{1}{x_{12}^8} . \tag{5.113}$$

Since the group structure factorizes, all the representations that are not the singlet get the same anomalous dimension, which reads

$$\gamma_{JJ_{S^\perp}} = \frac{11}{24\pi^2}\frac{n_c}{n_c^2-2}g^2 . \tag{5.114}$$

5.4 Current two-point function

In this section we compute the current two-point function (5.13) at the next-to-leading order. Since there is no anomalous dimension for a conserved current, the correction amounts to

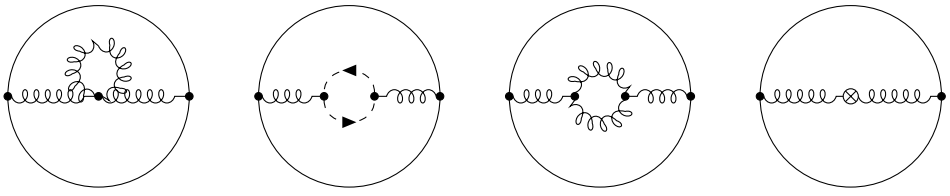

(a) Π_{QU} (b) Π_{GH} (c) Π_{TR} (d) Π_{CT}

Figure 5.4: One-loop corrections to the current J two-point function: the quartic (a), ghost (b), triple (c), and counterterm (d) diagram.

rescaling of the correlator. In embedding space, this reads

$$K(P_1, P_2) = \langle J_{A_1}(P_1) J_{A_2}(P_2) \rangle = \frac{C_J}{g^2} \frac{\mathcal{P}_{A_1 A_2}(P_1, P_2)}{(-2P_1 \cdot P_2)^{d-1}}\,, \tag{5.115}$$

where $\mathcal{P}_{A_1 A_2}(P_1, P_2)$ is the boundary limit of (5.42), and we have introduced

$$C_J = C_J^0 \Big(1 + C_J^1 g^2 + \mathcal{O}(g^4)\Big)\,. \tag{5.116}$$

We determine C_J^1 by computing the one-loop corrections to the D bulk-to-bulk gauge propagator in ambient configuration space. After that, we uplift the result in embedding space and take the boundary limit. We then evaluate the necessary integrals and finally extract the value of C_J^1. We work in the FY gauge.

5.4.1 Computation of the diagrams: external points in the bulk

The leading perturbative corrections of the vector two-point function is given by the one-loop diagrams depicted in figure 5.4. They read schematically

$$g^2 \Pi^{(1)}_{\mathrm{tot}}(x_1, x_2) = \langle A(x_1) A(x_2) \rangle = g^2 \Pi^{(1)}(x_1, x_2) + g^2 \Pi_{\mathrm{CT}}(x_1, x_2)\,, \tag{5.117}$$

where x_1 and x_2 are points in the bulk that we send to the boundary at the end of the calculation. The one-loop contribution $\Pi^{(1)}$ is the sum of three diagrams:

$$\Pi^{(1)} = \Pi_{\mathrm{QU}} + \Pi_{\mathrm{GH}} + \Pi_{\mathrm{TR}}\,, \tag{5.118}$$

which we call quartic, ghost, and triple diagram. Π_{CT} denotes the one-loop counterterm contribution. Since the color structure of each contribution is diagonal in the color indices, $(\Pi_\bullet)^{a_1 a_2}_{\mu_1 \mu_2}(x_1, x_2) = \delta^{a_1 a_2} (\Pi_\bullet)_{\mu_1 \mu_2}(x_1, x_2)$, we omit the color indices in what follows.

Quartic diagram

The quartic diagram Π_{QU} is the simplest as it involves integrating only over a bulk point.

It reads

$$(\Pi_{\rm QU})_{\mu_1\mu_2}(x_1,x_2) = -n_c\, g^2 \int dx\, \Pi_{\mu_1\lambda}(x_1,x)\Pi_{\mu_2\nu}(x_2,x)\Pi_{\rho\sigma}(x,x)(g^{\lambda\nu}g^{\rho\sigma} - g^{\lambda\rho}g^{\nu\sigma})\,. \quad (5.119)$$

We can evaluate the tadpole $\Pi_{\rho\sigma}(x,x)$ by expanding the gauge propagator for small values of the chordal distance. In dimensional regularization, the only surviving term in the expansion is the constant one, but remarkably this vanishes when we select the FY gauge. This is not in contrast with the results of flat space, where the diagram is zero regardless of the value of ξ, because if we reintroduce the dependence on the AdS radius L, we see that the diagram is of order $\mathcal{O}(1/L^2)$, and therefore its contribution vanishes in the flat space limit.

Ghost diagram

The ghost contribution $\Pi_{\rm GH}$ reads

$$(\Pi_{\rm GH})_{i_1 i_2}(x_1,x_2) = n_c g^2 \int dx\, dy\; \Pi^{\lambda}_{i_1}(x_1,x)\Pi^{\lambda'}_{i_2}(x_2,y)(\nabla_\lambda G_{\rm GH}\nabla_{\lambda'}G_{\rm GH})\,. \quad (5.120)$$

Replacing the expression of the ghost propagator (5.120) and using the basis of eq. (D.3), we obtain

$$\nabla_\lambda G_{\rm GH}\nabla_{\lambda'}G_{\rm GH} = f_{\rm GH1}(u)g_{\lambda\lambda'} + f_{\rm GH2}(u)n_\lambda n_{\lambda'}\,, \quad (5.121)$$

where

$$f_{\rm GH1}(u) = 0\,, \quad f_{\rm GH2}(u) = \frac{\Gamma\left(\frac{d+1}{2}\right)^2}{4\pi^{d+1}(u(2+u))^{d+1}}\,. \quad (5.122)$$

Note that despite the ghost propagator involves hypergeometric functions, the combination (5.121) gives rise to meromorphic functions of the same kind as those appearing in the gauge propagator (5.32) in the FY gauge.

Triple diagram

We now turn to the computation of the triple gauge diagram $\Pi_{\rm TR}$, which is the most involved. Considering all Wick contractions among the two triple couplings, integration by parts, and after some algebra, we get

$$\begin{aligned}(\Pi_{\rm TR})_{i_1 i_2}(x_1,x_2) = n_c g^2 \int dx\, dy\; \Pi_{i_1\lambda}(x_1,x)\; \Pi_{i_2\lambda'}(x_2,y)\Big(&4\left(\Pi^{\nu\nu'}\nabla_\nu\nabla_{\nu'}\Pi^{\lambda\lambda'} - \nabla_\nu\Pi^{\lambda\nu'}\nabla_{\nu'}\Pi^{\nu\lambda'}\right)\\
&- 2\left(\Pi_{\nu\nu'}\nabla^\nu\nabla^{\lambda'}\Pi^{\lambda\nu'} - \nabla^\nu\Pi^{\lambda\nu'}\nabla^{\lambda'}\Pi_{\nu\nu'}\right) - 2\left(\Pi_{\nu\nu'}\nabla^\lambda\nabla^{\nu'}\Pi^{\nu\lambda'} - \nabla^\lambda\Pi_{\nu\nu'}\nabla^{\nu'}\Pi^{\nu\lambda'}\right)\\
&+ \left(\Pi_{\nu\nu'}\nabla^\lambda\nabla^{\lambda'}\Pi^{\nu\nu'} - \nabla^\lambda\Pi_{\nu\nu'}\nabla^{\lambda'}\Pi^{\nu\nu'}\right) + \left(\Pi^{\lambda\lambda'}\nabla_\nu\nabla_{\nu'}\Pi^{\nu\nu'} - \nabla_\nu\Pi^{\nu\lambda'}\nabla_{\nu'}\Pi^{\lambda\nu'}\right) \quad (5.123)\\
&- 2\left(\nabla_{\nu'}\nabla_\nu\Pi^{\nu\lambda'}\Pi^{\lambda\nu'} - \nabla_{\nu'}\Pi^{\lambda\lambda'}\nabla_\nu\Pi^{\nu\nu'}\right) - 2\left(\Pi^{\nu\lambda'}\nabla_\nu\nabla_{\nu'}\Pi^{\lambda\nu'} - \nabla^\lambda\Pi^{\nu\lambda'}\nabla^{\nu'}\Pi_{\nu\nu'}\right)\\
&+ \left(\nabla^{\lambda'}\nabla^\nu\Pi_{\nu\nu'}\Pi^{\lambda\nu'} - \nabla^{\lambda'}\Pi^{\lambda\nu'}\nabla^\nu\Pi_{\nu\nu'}\right) + \left(\Pi^{\nu\lambda'}\nabla^\lambda\nabla^{\nu'}\Pi_{\nu\nu'} - \nabla^\lambda\Pi^{\nu\lambda'}\nabla^{\nu'}\Pi_{\nu\nu'}\right)\Big)\,.\end{aligned}$$

Plugging the expression (5.28) for the gauge propagator in the basis of [5] and using eq. (D.4), we can rewrite this term in the form

$$(\Pi_{\rm TR})_{i_1 i_2}(x_1,x_2) = n_c g^2 \int dx\, dy\; \Pi_{i_1\lambda}(x_1,x)\Pi_{i_2\lambda'}(x_2,y) f_{\rm TR}^{\lambda\lambda'}(x,y)\,, \tag{5.124}$$

with

$$\begin{aligned} f_{\rm TR}^{\lambda\lambda'}(x,y) &= f_{\rm TR1}(u) g^{\lambda\lambda'} + f_{\rm TR2}(u) n^\lambda n^{\lambda'}, \\ f_{\rm TR1}(u) &= \frac{(d-4)(d-1)\Gamma\left(\frac{d+1}{2}\right)^2 (1+u)}{4(d-2)^2\pi^{d+1}(u(2+u))^d}\,, \\ f_{\rm TR2}(u) &= \frac{\Gamma\left(\frac{d+1}{2}\right)^2 \Big(4(1+u)+d\big(d-6+u(d-5)\big)\Big)}{4(d-2)^2\pi^{d+1}(u(2+u))^d}\,. \end{aligned} \tag{5.125}$$

In deriving (5.124) from (5.123) one has to pay attention to possible contact terms, which can arise since eq. (5.123) contains propagators inside the loop that are derived twice. A way to take care of this is by replacing the equation of motion for the gauge propagator (5.25) in (5.124). However, since contact terms produce tadpoles of the gauge propagator, these contributions vanish in the FY gauge, as it happens in the quartic diagram.

Total contribution

The sum of the ghost and triple diagram contributions $\Pi^{(1)} = \Pi_{\rm GH} + \Pi_{\rm TR}$ can be rewritten, interestingly enough, in terms of gauge propagators only in the following form,

$$(\Pi^{(1)})_{i_1 i_2}(x_1,x_2) = \Big(\frac{4}{d}-1\Big) n_c\; g^2 \int dx\, dy\; \nabla_\nu \Pi_{i_1\lambda}(x_1,x)\nabla_{\nu'}\Pi_{i_2\lambda'}(x_2,y)(\Pi^{\nu\nu'}\Pi^{\lambda\lambda'} - \Pi^{\lambda\nu'}\Pi^{\nu\lambda'})\,. \tag{5.126}$$

The expression (5.126) has been conveniently written in a way in which the derivatives act on each of the two external legs. In this way, we avoid double derivatives acting on external propagators, which may be generated after integration over one of the internal points. The resulting contact terms, contrary to those discussed below eq. (5.125), in general would not vanish.

5.4.2 Counterterm

The counterterm contribution reads

$$\begin{aligned} (\Pi_{\rm CT})_{\mu_1\mu_2}(x_1,x_2) = -g^2\Bigg(&(\delta_T - \delta_{g^2}) \int dx\, \Big(\nabla^\nu \Pi_{\mu_1\lambda}(x_1,x)\nabla^\lambda \Pi_{\mu_2\nu}(x_2,x)\Big) \\ &+ \delta_L \int dx\, \Big(\frac{1}{\xi}\nabla^\nu \Pi_{\mu_1\nu}(x_1,x)\nabla^\lambda \Pi_{\mu_2\lambda}(x_2,x)\Big)\Bigg)\,, \end{aligned} \tag{5.127}$$

where the coefficients δ_T, δ_{g^2} and δ_L are a flat space result (see eq.(4.69) for a definition). In ($\overline{\text{MS}}$) scheme and $d = 3 + 2\epsilon$ we have (see e.g. [145])

$$\delta_T - \delta_{g^2} = \frac{C_A}{32\pi^2}\left(\frac{10}{3} + (1-\xi)\right)\left(-\frac{1}{\epsilon} - \gamma_E + \log(4\pi)\right) + \mathcal{O}(g^4)\,, \qquad \delta_L = 0\,, \tag{5.128}$$

with $C_A = n_c$ for the $SU(n_c)$ group.

5.4.3 Final result

We uplift in embedding space (5.126) and (5.127) and take the boundary limit of the points $X_{1,2}$. This gives

$$\begin{aligned}(K^{(1)})_{A_1A_2}(P_1,P_2) &= \Big(\frac{4}{d}-1\Big)n_c \int dX\, dY\ \nabla_B K_{A_1A}(P_1,X)\nabla_{B'}K_{A_2A'}(P_2,Y) \\ &\qquad \times (\Pi^{BB'}\Pi^{AA'} - \Pi^{AB'}\Pi^{BA'})\,, \end{aligned} \tag{5.129}$$

$$(K_{\text{CT}})_{A_1A_2}(P_1,P_2) = -(\delta_T - \delta_{g^2})\int dX\, \nabla^C K_{A_1B}(P_1,X)\nabla^B K_{A_2C}(P_2,X)\,. \tag{5.130}$$

The loop and counterterm contributions can be written in terms of scalar contributions $K^{(1)}$ and K_{CT} as follows,

$$\begin{aligned}(K^{(1)})_{A_1A_2}(P_1,P_2) &\equiv \mathcal{P}_{A_1A_2}(P_1,P_2)K^{(1)}\,, \\ (K_{\text{CT}})_{A_1A_2}(P_1,P_2) &\equiv \mathcal{P}_{A_1A_2}(P_1,P_2)K_{\text{CT}}\,. \end{aligned} \tag{5.131}$$

We evaluate the integrals appearing in (5.129) and (5.130), starting from the simpler counterterm contribution. We insert the expression for the D bulk-to-boundary propagator (5.37) and use Lorentz invariance to reduce (5.130) to scalar integrals only. The resulting expression can be written in the form (5.131) with

$$\begin{aligned} K_{\text{CT}} &= -(\delta_T - \delta_{g^2})\frac{\Gamma(d)^2}{\Gamma(\frac{d}{2})^2\pi^d d}\int dX \frac{(d-1)(P_1\cdot P_2) + (d-2)(P_1\cdot X)(P_2\cdot X)}{(-2P_1\cdot X)^d\,(-2P_2\cdot X)^d} \\ &= (\delta_T - \delta_{g^2})\frac{\Gamma\left(\frac{d+1}{2}\right)(d-2)}{2\pi^{\frac{d+1}{2}}d^2(-P_1\cdot P_2)^{d-1}}\,, \end{aligned} \tag{5.132}$$

where we used (5.91) in the last step. Note that the log terms appearing in (5.91) cancel in (5.132), as expected, since the currents J_i^a are conserved and cannot acquire an anomalous dimension.

We consider now $\Pi^{(1)}$ in (5.129). First, we use the expression of the bulk-to-boundary and bulk-to-bulk gauge propagators and act with an inversion transformation (see the beginning of section E.3 in the appendix for the detailed form of the transformation). After some

algebra, the integral can be written as in (5.131), namely

$$K^{(1)} = \int dX \frac{(d-1)(P_1\cdot P_2)+(d-2)(P_1\cdot X)(P_2\cdot X)}{(-2P_1\cdot X)^d(-2P_2\cdot X)} I_Y(z), \tag{5.133}$$

with

$$I_Y(z) = \kappa_d \int_0^\infty dw \int_0^\infty dy \, \frac{w^{2d-3}y^{d+1}z^{2d-1}}{(y^2+(w+z)^2)^d(y^2+(w-z)^2)^d}\,, \tag{5.134}$$

and

$$\kappa_d = \Big(\frac{4}{d}-1\Big) n_c \frac{2^{4d-5}(d-1)\Gamma(\frac{d+1}{2})^4\Omega_{d-1}}{d^2(d-2)^2\pi^{2d+2}}, \tag{5.135}$$

where $\Omega_{d-1} = 2\pi^{\frac{d}{2}}/\Gamma(\frac{d}{2})$ is the volume of the $(d-1)-$dimensional sphere with unit radius. It is useful to introduce two Schwinger parameters t_1 and t_2 and rewrite $I_Y(z)$ as

$$\begin{aligned} I_Y(z) = \frac{\kappa_d}{\Gamma(d)^2}\int_0^\infty dt_1 \int_0^\infty dt_2 \int_0^\infty dw \int_0^\infty dy \; w^{2d-3}y^{d+1}z^{2d-1}t_1^{d-1}t_2^{d-1} \\ \times\, e^{-(y^2+(w+z)^2)t_1} e^{-(y^2+(w-z)^2)t_2}\,. \end{aligned} \tag{5.136}$$

The integral over y and w can be computed analytically and we are left with an integral over t_1 and t_2. Following [189], we perform a change of variables $t_1 = us,\ t_2 = (1-u)s$. The integral over s can be computed analytically and we are left with the integral over u, which is UV divergent. This last integral is computed using the same trick used on the sphere in eq.(4.94-4.97): we isolate the divergences by expanding around coincident points ($u=0$) up to a sufficient order so that the remaining part is finite and can be safely computed. The divergent terms are regulated by using

$$\int_0^1 du\; u^{a-1} = \frac{1}{a}\,, \tag{5.137}$$

which is valid for $a>0$, but is extendable to any d-dependent a by analytic continuation in d. We then sum both contributions to obtain

$$I_Y(z) = z^{d-1} n_c 2^{d+1}\Big(\frac{4}{d}-1\Big)\left(-\frac{1}{24\pi^6\epsilon}+\frac{-1+9\gamma_E+9\log\pi}{72\pi^6}\right). \tag{5.138}$$

The z^{d-1} term appearing in (5.138) is such that $(-2P_2\cdot X)$ in (5.133) turns into $(-2P_2\cdot X)^d$ thanks to (E.19). The dX integral in (5.133) can then be evaluated using again (5.90) and (5.91). We get

$$K^{(1)} = \frac{\pi^{\frac{d}{2}}(d-4)(d-2)\Gamma\left(\frac{d}{2}\right)}{d^2\Gamma(d)(-P_1\cdot P_2)^{d-1}}\left(-\frac{1}{12\pi^6\epsilon}+\frac{-1+9\gamma_E+9\log\pi}{36\pi^6}\right). \tag{5.139}$$

Again, the log terms in (5.91) cancel in (5.139), as expected. We sum loop and counterterm

contribution, and set $\xi = d/(d-2)$ in $(\delta_T - \delta_{g^2})$ in (5.128). In this way we get

$$K^{(1)}_{\text{tot}} = K_{\text{CT}} + K^{(1)} = -n_c \frac{10 + 3\gamma_E}{162\pi^4} \frac{1}{(-2P_1 \cdot P_2)^2} \,. \tag{5.140}$$

The cancellation of the UV divergences, as of course expected from the renormalization of the theory, provides a sanity check of the computation. Matching with eq. (5.115), finally allows us to determine the correction to C_J,

$$\boxed{C^1_J = -\frac{10 + 3\gamma_E}{324\pi^2} \, n_c \,.} \tag{5.141}$$

From this result we extract the estimate (5.5) for the Decoupling scenario. Note that the value of C^1_J is renormalization scheme-dependent. The value (5.141) is in the $\overline{\text{MS}}$ scheme.[11]

Outlook In this chapter, we studied Yang-Mills theory in four-dimensional AdS space, focusing on the deconfinement/confinement transition occurring with Dirichlet boundary conditions as the radius increased. We used perturbation theory to get insights into the nature of this transition. We computed the anomalous dimensions for the lightest scalar operators at the boundary, both in the singlet and in non-trivial representations, finding a negative and positive value respectively, see eq.s (5.63) and (5.114). We also determined the correction to the coefficient C_J, finding a negative value as in eq.(5.141). We conclude that the Higgsing scenario for the transition is disfavored, while both the Marginality and the Decoupling scenarios are compatible with our results. We found that the singlet operator's scaling dimension approaches marginality before C_J vanishes, suggesting the Marginality to be the more compelling scenario. For Neumann boundary conditions, the lightest scalar operator exhibited a positive anomalous dimension, consistently with a smooth extrapolation to flat space.

[11] Beyond the leading order computed in this chapter, also the g^2 expansion of boundary scaling dimensions is scheme-dependent. One way to get rid of scheme-dependence is to eliminate g^2 and express the scaling dimensions, that are physical, as an expansion in the physical quantity $1/C_J$. Doing so, all the coefficients in the expansion are themselves physical. Given the function $\Delta_{\text{tr}[JJ]}(1/C_J)$, the question of Marginality vs Decoupling becomes the question of whether $\Delta_{\text{tr}[JJ]}(1/C_J) = 3$ for any positive C_J.

Chapter 6

Conclusions

In this thesis, we have investigated several key aspects of gauge theories, employing perturbation theory to gain deeper insights into the behavior and properties of their phases.

In the first part, we applied the ϵ-expansion to examine gauge theories in $d = 3$ and $d = 5$. In Chapter 3, we found evidence for the existence of UV fixed points of non-abelian gauge-theories in $d = 5$ and we computed the dimension of the leading relevant operator at those fixed points. In Chapter 4, we calculated the S^d partition function of the WF fixed point for non-abelian gauge theories, to test possible RG trajectories via the generalized $\widetilde{F}$-theorem, both in $d = 3$ and $d = 5$.

While successful in many contexts, the ϵ-expansion is not a rigorous method. Going forward, it would be interesting to assess its reliability in the context of gauge theories. A possible verification could come from the comparison with non-perturbative results obtained with the lattice or the conformal bootstrap. To that end, the anomalous dimensions obtained in Chapter 3 can provide a useful benchmark, even if the estimated relative error is typically rather large. Looking ahead, it would be useful to improve the precision of the predictions by performing computations at higher loop order and to extend the investigation to other observables. Obvious observables to consider are the scaling dimensions of heavier operators. One-loop anomalous dimensions of some higher-dimensional operators in $4d$ Yang-Mills have been computed in [135]. In addition to local operators, one can also consider observables associated to the line operators of Yang-Mills theory, such as the coefficient h in the one-point function of the stress-tensor in the presence of the line [136], or the Bremsstrahlung function [137].

Another possibility to examine the robustness of the ϵ-expansion in the context of gauge theories is to consider cases in which the existence of a fixed point, and the associated data, are known from other methods such as supersymmetry or holography. For instance, one could apply it to the $4d$ theory with the same matter content as $5d$ $\mathcal{N} = 1$ $SU(2)$ SYM with n_f fundamental flavors, and check if the ϵ-expansion finds a UV fixed point that extrapolates to the E_{n_f+1} SCFT in $5d$. Note that when continuing the fields to $4d$ one does not land on a supersymmetric theory: the $5d$ vector multiplet contains a real scalar, a $5d$ vector, and

a symplectic Majorana fermion, all in the adjoint representation, and their continuation to $4d$ gives rise to a real scalar, a $4d$ vector, and a Dirac fermion, which is not the content of a supersymmetric theory in $4d$. As a result, supersymmetry is expected to emerge only in the limit $d \to 5$. To check the existence of fixed points in $d = 4 + 2\epsilon$ one then needs the coupled system of beta functions for the gauge coupling in the presence of both fermionic and bosonic adjoint matter, and of the Yukawa coupling, see e.g. the Lagrangian (15) in [158]. Note that these beta functions are known at lower loop order compared to the case with only fermionic matter that was used in Chapter 3, see [159, 160]. We leave this as direction for future studies.

In this thesis, we considered the case of $SU(n_c)$ gauge group, but our results can be easily generalized to other gauge groups. In particular, the perturbative expansion of the free energy found in Chapter 4 is insensitive to the global structure of the gauge group, except the log term where the volume of the gauge group appears. It would be interesting to compare our results for F with non-pertubative computations which are instead sensitive to topological properties of the gauge group, like the lattice or localization (for SCFT).

In the second part of the thesis, inspired by [17], we have explored confinement in non-abelian gauge theories in AdS_4, from the perspective of the boundary CFT_3. Among the three possibilities reviewed in Chapter 2, our results disfavor the Higgsing scenario, are compatible with the Decoupling scenario, and favor the Marginality one.

There are several open questions that would be important to address in future studies. The merging scenario implies the existence of a new theory D^* which has the same global symmetry of the D CFT. Finding possible candidates for D^* is an important point that we did not address. In particular, it would be useful to see if there exist candidates for D^* in the vicinity of $g^2 = 0$, i.e. at weak coupling. Moreover, even if the most likely possibility is that D and D^* annihilate while the N bc exists for all values of $L\Lambda_{\mathrm{YM}}$, more work is needed to firmly exclude more exotic possibilities. For instance it is in principle possible that the symmetry G appears as an emergent symmetry in the N bc, allowing D and N to annihilate, leaving some other boundary condition at strong coupling. Even in the most likely scenario, an important question is whether the theory settles to the N boundary condition after the merger, and if this is the case, whether this happens continuously or discontinuously. As pointed out in [94], anomalies in generalized symmetries can sometimes rigorously rule out the continuity between N and D.

Having reformulated confinement purely in terms of properties of a non-local boundary CFT, it would be extremely interesting to see if the conformal bootstrap [34, 35] might be used to rigorously assess the merging scenario as the only consistent one. Recent progress in the study of four-point functions of non-abelian conserved currents in $3d$ [190] makes this direction feasible in the near future.

From a more theoretical point of view, it would be important to properly define what confinement means in AdS space. As is well known, in flat space confinement is detected by the area law of large Wilson loops. Recently, the area law and confinement have been

reformulated more sharply as the phase in which (e.g. for $SU(n_c)$ gauge theories) the electric $\mathbb{Z}_{n_c}^{(1)}$ one-form symmetry is unbroken [191]. In AdS at finite L, there is no intrinsic distinction between perimeter and area law, and hence it is not clear if one-form symmetries still characterize the possible phases. The space has however a boundary and perhaps a sharp characterization is provided by the boundary conditions. In fact, the one conjectured in our thesis is one of these: confinement in AdS is characterized by the absence of the D bc. It would be important to understand how this definition is related to the usual one in terms of one-form symmetries and to verify if other definitions are in principle possible.

Moving forward, it would be intriguing to explore how our results are influenced by the introduction of fermionic matter. Specifically, we expect that the deconfinement/confinement transition still occurs if the number of fermions remains sufficiently small, though conclusions regarding the various scenarios for the transition may change depending on the value of n_f. More speculatively, one could consider values of n_f for which the theory is instead IR free and search for signals of the end of the conformal window in the boundary CFT data.

Moreover, it would be interesting to explore possible applications of the general result we found for the scaling dimension of the displacement operator. Recently correlation functions involving the bulk stress tensor and boundary operators along bulk RG flows were studied in [98, 161]. These papers derived sum rules for the scaling dimension of the boundary operator, which can be applied in particular to the displacement operator. It would be interesting to compare the sum rules to the result for the scaling dimension of $\mathcal{D}$ presented here. Matching the two results, it should be possible to obtain a sum rule for the bulk beta function, e.g. to express the one-loop beta function in terms of a sum involving boundary CFT data. In the context of amplitudes in flat space, ref.s [192–195] studied how various RG coefficients, including beta function coefficients, can be extracted from scattering data. It would be interesting to explore further how boundary correlation functions in AdS encode bulk RG coefficients and the relation to the flat space results via the flat space limit.

Finally, one could join the approaches presented in this thesis by applying the ϵ-expansion to gauge theories in AdS space. Starting from the AdS propagators and the Witten diagrams techniques introduced in Chapter 5, one may study the boundary critical behavior of the gauge WF fixed point and extract some of the BCFT data in $d = 4 + 2\epsilon$. The results thus obtained could be validated by applying bulk equations to the bulk two-point functions, as was done in [109, 110] to extract anomalous dimensions of boundary operators in the critical $O(N)$ and Gross-Neveu models.

Appendix A

Sphere gauge propagator

In this appendix we follow ref. [5] for the computation of the vector propagator. We report the main steps, generalizing the computation to an arbitrary choice of the gauge.

We have seen in the main text that the vector propagator $Q^{ab}_{\nu\lambda}(x,x') = \delta^{ab} g_0^2 Q_{\nu\lambda}(x,x')$ satisfies eq. (4.52) and can be written as in eq. (4.53) where α and β are generic functions of the geodesic distance. Using the relations in eq. (4.45) we can decompose eq. (4.53) in two parts, respectively proportional to $g_{\nu\lambda'}$ and $n_\nu n_{\lambda'}$:

$$\begin{aligned}
\alpha'' + & \ (d-1)A\alpha' + \big((A+C)^2 + (d-1)\big)\,\alpha + 2AC\beta \\
& - \left(1 - \frac{1}{\xi}\right) C\,(\beta' - \alpha' - (d-1)(A+C)\alpha + (d-1)A\beta) = -\delta(x,x')\,, \\
\beta'' + & \ (d-1)A\beta' + \big((A+C)^2 - d(A^2+C^2) - (d-1)\big)\,\beta + (d-2)(A+C)^2\alpha \\
& + \left(1 - \frac{1}{\xi}\right)\Big(\beta'' - \alpha'' + ((d-1)A + C)\beta' - (d(A+C) - A)\alpha' \\
& + \big((d-1)AC + (d-1)A'\big)\beta + A'\big(-(d-1)C(A+C) + (1-d)A' + (1-d)C'\big)\alpha\Big) = 0\,.
\end{aligned} \tag{A.1}$$

This is a system of two coupled second order differential equations, which is in general hard to solve. To make the computation easier it is convenient to introduce a new maximally symmetric gauge invariant bitensor defined as

$$\langle F^a_{\mu\nu} F_b^{\mu'\nu'} \rangle = 4\delta^a{}_b\ \nabla_{[\mu}\nabla^{[\mu'} Q_{\nu]}^{\ \nu']} = \delta^a{}_b\ \left(\sigma(\mu) h^{[\mu'}_{[\mu}\, h^{\nu']}_{\nu]} + \tau(\mu) n_{[\mu} h^{[\nu'}_{\nu]}\, n^{\mu']}\right), \tag{A.2}$$

with square brackets meaning antisymmetrized indices and τ and σ being generic functions of the geodesic distance. From the definition of $Q_{\nu\lambda'}$ in terms of α and β and eq. (4.45), we get

$$\sigma = 4C\,[\alpha' + (A+C)\alpha - C\beta]\,, \tag{A.3}$$

$$\tau = C^{-1}\,[\sigma' + 2(A+C)\sigma]\,. \tag{A.4}$$

Now, taking the covariant derivative of eq. (A.2) and using eq. (4.52) properly antisym-

metrized, one can find the equation of motion for σ and τ:

$$\nabla^{\mu}\nabla_{[\mu}\nabla^{[\mu'}Q_{\nu]}^{\nu']} = \frac{1}{\xi}\nabla_{\nu}\left(\nabla^{\mu}\nabla^{[\mu'}Q_{\mu}^{\nu']}\right) = 0\,. \tag{A.5}$$

The last equality in (A.5) derives from the fact that the bitensor in parenthesis has two primed antisymmetrized indices, while the only (0,2) bitensor structures are symmetric. In terms of σ and τ defined in eq. (A.2), eq. (A.5) reads

$$\sigma' - \frac{1}{2}\tau' + (d-2)(A+C)\sigma - \frac{1}{2}(d-2)A\tau = 0. \tag{A.6}$$

Plugging the expression for τ in eq. (A.4), we get a second order differential equation for σ, which will be useful in the following to solve the system for α and β:

$$\sigma'' + (d+1)A\sigma' - 2(d-1)\sigma = 0\ . \tag{A.7}$$

This equation can be rewritten as a function of the variable z defined in eq. (4.47):

$$z(1-z)\frac{d^2\sigma}{dz^2} + \frac{1}{2}(d+2)(1-2z)\frac{d\sigma}{dz} - 2(d-1)\sigma = 0\ , \tag{A.8}$$

which is solved by two linearly independent hypergeometric functions. The correct solution is chosen by imposing regularity at antipodals point ($z = 0$) and the correct limit of coincident points ($z = 1$). The last condition can be computed by starting from the expression in coordinate space of the gauge propagator in flat space

$$\langle A_a^{\mu}(x)A_{\nu'}^{b}(x')\rangle_{\text{flat}} = \delta^{b}{}_{a}\left(\frac{\Gamma\left(\frac{d}{2}-1\right)(1+\xi)}{2(4\pi)^{\frac{d}{2}}|x-x'|^{d-2}}\delta^{\mu}{}_{\nu'} + \frac{\Gamma\left(\frac{d}{2}\right)(1-\xi)}{(4\pi)^{\frac{d}{2}}|x-x'|^{d}}x^{\mu}x_{\nu'}\right) \tag{A.9}$$

and the flat space expression for σ:

$$\sigma(z)_{\text{flat}} = \frac{2\Gamma\left(\frac{d}{2}\right)}{(4\pi)^{\frac{d}{2}}(1-z)^{\frac{d}{2}}}\,. \tag{A.10}$$

We find then

$$\sigma(z) = p\ {}_2F_1\Big(d-1, 2, \frac{d}{2}+1, z\Big)\ , \tag{A.11}$$

with

$$p = \frac{\Gamma(d-1)}{\Gamma(\frac{d}{2}+1)2^{d-1}\pi^{\frac{d}{2}}}\ . \tag{A.12}$$

We can use this result to compute α, proceeding as follows: we compute β as a function of α and σ from eq. (A.3) and we replace the result in eq. (A.1). This leads to the following

inhomogenous equation for α:

$$\begin{aligned}\alpha''+(d+1)A\alpha' - d\alpha - \frac{A}{2C}\sigma - \left(1-\frac{1}{\xi}\right)\left(\alpha'' + \left(\frac{C'}{C} - Ad\right)\alpha'\right.\\ \left. - \left(d-1-A'+\frac{AC}{C'}\right)\alpha - \frac{1}{4C}\sigma + \left(\frac{C'}{2C} - \frac{A}{4C}(d-1)\right)\sigma\right) = -\delta(x,x').\end{aligned} \tag{A.13}$$

The solution is given by the sum of the solution of the corresponding homogenous equation (again we should impose the flat space limit and regularity at $z=0$) and a particular solution to reproduce the correct source term. We have

$$\alpha(z) = q\ {}_2F_1\Big(d,1,\frac{d}{2}+1,1-z\Big) + \tilde{\alpha}(z), \tag{A.14}$$

where the first term is the solution of the homogeneous equation, with a normalization q to be fixed, and $\tilde{\alpha}$ is a particular solution of the full equation, that plugging the expression for σ, C and A takes the form

$$\begin{aligned}&z(1-z)\frac{d^2\tilde{\alpha}}{dz^2} + \Big(\frac{d}{2}+1-(d+2)z\Big)\frac{d\tilde{\alpha}}{dz} - d\tilde{\alpha} = \frac{\pi^{-\frac{d}{2}}\Gamma(d-1)}{2^{d+1}}\\ &\left((d+2-\xi)(1-2z){}_2F_1\Big(2,d-1;\frac{d}{2}+1;z\Big) - 4(d-\xi)(z-1)z\,{}_2F_1\Big(3,d;\frac{d}{2}+2;z\Big)\right).\end{aligned} \tag{A.15}$$

A solution for $\tilde{\alpha}$ can be found as follows [5]. We introduce the hypergeometric operator

$$H(a,b,c) = z(1-z)\frac{d^2}{dz^2} + \left(\big(c-(a+b+1)z\frac{d}{dz}\big) - ab\right), \tag{A.16}$$

in order to rewrite the left-hand side of eq. (A.15) as

$$H\left(a_1+1,b_1-1,c_1\right)\tilde{\alpha}\,, \tag{A.17}$$

with $a_1 = d-1$, $b_1 = 2$, $c_1 = \frac{d}{2}+1$. Then, we rewrite the right-hand-side of eq. (A.15) as $H(a_1+1,b_1-1,c_1)f$, with f a function to be determined, using identities among hypergeometric functions (see e.g. chapter 15 of ref. [196]). A particular solution would then be $\tilde{\alpha} = f$. The right-hand-side of eq. (A.15) is first rewritten as a function of ${}_2F_1\left(a_1,b_1,c_1,z\right)$, ${}_2F_1\left(a_1-1,b_1,c_1,z\right)$ and ${}_2F_1\left(a_1+1,b_1-1,c_1,z\right)$ only. Then, the following identities are used:

$$\begin{aligned}{}_2F_1\left(a_1,b_1,c_1,z\right) &= \frac{1}{d-2}H\left(a_1+1,b_1-1,c_1\right){}_2F_1\left(a_1,b_1,c_1,z\right), \qquad (A.18)\\ {}_2F_1\left(a_1-1,b_1,c_1,z\right) &= \frac{1}{2(d-3)}H\left(a_1+1,b_1-1,c_1\right)\left({}_2F_1\left(a_1-1,b_1,c_1,z\right)+{}_2F_1(a_1,b_1,c_1,z)\right),\\ {}_2F_1\left(a_1+1,b_1-1,c_1,z\right) &= \frac{1}{b_1-a_1-2}\,H\left(a_1+1,b_1-1,c_1\right)\left(\frac{\partial}{\partial a}-\frac{\partial}{\partial b}\right){}_2F_1(a,b,c_1,z)\Big|_{\substack{a=a_1+1\\b=b_1-1}}.\end{aligned}$$

Matching with the left hand side of eq. (A.15) gives the particular solution $\tilde{\alpha} = f$:

$$\begin{aligned}\tilde{\alpha} = \frac{p}{4(d-3)^2}\Big(&-2\ {}_2F_1\left(a_1-1, b_1+1, c_1, z\right) + (d-4)\ {}_2F_1\left(a_1-1, b_1, c_1, z\right) \\ &+\big(2+(d-3)(1-\xi)\big)(3-d)\left(\frac{\partial}{\partial a}-\frac{\partial}{\partial b}\right)\ {}_2F_1(a,b,c_1,z)\Big|_{\substack{a=a_1+1\\ b=b_1-1}}\Big)\,.\end{aligned} \tag{A.19}$$

The value of the coefficient q appearing in eq. (A.14) is determined by imposing the correct flat space limit of α. which is the term proportional to $\delta^{\mu}_{\nu'}$ in eq. (A.9). We get

$$q = p\frac{(d-1)(d-2)-(2+(d-3)(1-\xi))(d-3)(\psi(d)-\psi(1))}{4(d-3)^2}\,. \tag{A.20}$$

Finally, we obtain the expression for β by replacing α and σ in eq. (A.3):

$$\begin{aligned}\beta = &-\frac{(z-1)\Gamma(d-1)}{2^d\pi^{\frac{d}{2}}(d-3)\Gamma\left(\frac{d}{2}+1\right)} \\ &\Big(\frac{d}{dz}\Big(-z(2+(d-3)(1-\xi))(3-d)\left(\frac{\partial}{\partial a}-\frac{\partial}{\partial b}\right)\ {}_2F_1(a,b,c_1,z)|_{\substack{a=a_1+1\\ b=b_1-1}}\Big) \\ &+\Gamma\left(\frac{d}{2}+1\right)\Big({}_2F_1\Big(2,d;\frac{d}{2}+1;z\Big)\Big(-\big((d-3)(1-\xi)+2\big)(\psi^{(0)}(d)+\gamma)-2dz+d+2z-4\Big) \\ &-4(z-1)\,{}_2F_1\Big(3,d;\frac{d}{2}+1;z\Big)\Big)\Big)\,.\end{aligned} \tag{A.21}$$

Summarizing, the gauge propagator on S^d is obtained by replacing in eq. (4.53) the expression for α in eqs.(A.14,A.19), the one for β just reported, together with the expressions for the coefficients p and q in eqs.(A.12,A.20).

Let us now explain how to expand α and β around coincident points ($z = 1$). First, note that the hypergeometrics have branch points in $z = 1$. In order to expand in powers of $(z-1)$ it is then convenient to use an identity to obtain only hypergeometric functions with argument $1-z$. In this way the non-analytic dependence on $z-1$ will be captured completely by the power-law prefactors. The identity that we will use for this purpose is

$$\begin{aligned}{}_2F_1(a,b,c,z) =&\frac{\Gamma(c)\Gamma(c-a-b)}{\Gamma(c-a)\Gamma(c-b)}{}_2F_1(a,b,a+b+1-c,1-z) \\ &+\frac{\Gamma(c)\Gamma(a+b-c)}{\Gamma(a)\Gamma(b)}(1-z)^{c-a-b}{}_2F_1(c-a,c-b,1+c-a-b,1-z)\,.\end{aligned} \tag{A.22}$$

Derivatives of the hypergeometrics with respect to the parameter a and b appear in both α and β. In order to obtain the expansion in $(1-z)$ for these derivatives, we first apply the identity in eq. (A.22) and then we expand the hypergeometric as

$${}_2F_1\left(a,b,c,1-z\right) = \sum_{n=0}^{\infty}\frac{(a)_n\,(b)_n}{(c)_n}\frac{(1-z)^n}{n!}\,, \tag{A.23}$$

where $(x)_n$ are the Pochammer symbols. We truncate the series at a sufficiently high order and then we apply the derivatives with respect to a and b to this truuncated series. In order to improve the efficiency of the numerical integration of hypergeometrics needed to get the finite terms (4.108)-(4.110), it is useful to split the interval of integration $0 \leq z \leq 1$ in two parts (i.e. [0,1/2] and [1/2,1]) and expand respectively around 0 and around 1 the hypergeometrics.

Appendix B

Subtleties on the computation of the free energy on the sphere

B.1 Contact terms and integration by parts on the sphere

In this appendix we show the subtleties that can arise when integrating propagators derived multiple times on S^d. This analysis is relevant for our purposes in presence of two derivatives acting on the same propagator. For simplicity we will consider a scalar propagator satisfying the equation

$$(-\nabla^2 + m^2)G(x, x') = \delta(x, x')\,, \tag{B.1}$$

but the same remarks hold for the vector propagator and can be applied to eq. (4.82). Let us consider the integral

$$\int_{S^d} d^d x\sqrt{h}\ f(\mu)\nabla^2 G(x, 0)\,, \tag{B.2}$$

where f is a function of the geodesic distance $\mu = \mu(x, 0)$, which is taken to be smooth and bounded on S^d. If one tries to compute this integral by specifying some coordinate system and writing explicitly the action of the laplacian on the resulting function in the chosen coordinates, one gets a wrong answer. This is because the resulting expression for $\nabla^2 G(x, 0)$ misses the contact term, and the answer one gets would correspond to substituting simply $\nabla^2 G(x, 0) = m^2 G(x, 0)$ inside the integral.

A strategy to obtain the correct answer is to integrate by parts

$$\int_{S^d} d^d x\sqrt{h}\ f(\mu(x, 0))\nabla^2 G(x, 0) = -\int_{S^d} d^d x\sqrt{h}\ \nabla^\nu f(\mu(x, 0))\nabla_\nu G(x, 0)\ . \tag{B.3}$$

To check that this works, let us start by separating two regions in the integral

$$\int_{S^d\setminus B_\delta} d^d x\sqrt{h}\ f(\mu)\nabla^2 G(x, 0) + \int_{B_\delta} d^d x\sqrt{h}\ f(\mu)\nabla^2 G(x, 0)\ , \tag{B.4}$$

where B_δ is defined as a small d-dimensional ball of radius δ centered at the origin. In the second integral, for $\delta \to 0$, we get the contact term $-f(0)$. In the first term, we integrate by parts

$$\int_{S^d\setminus B_\delta} d^dx\sqrt{h}f(\mu)\nabla^2 G(x,0) = -\int_{S^d\setminus B_\delta} d^dx\sqrt{h}\nabla^\nu f(\mu)\nabla_\nu G(x,0) + \int_{S^d\setminus B_\delta} d^dx\sqrt{h}\nabla^\nu\big(f(\mu)\nabla_\nu G(x,0)\big)\,. \tag{B.5}$$

In the first integral the limit $\delta \to 0$ is straightforward, while the second integral requires more care. It is a boundary term that we can rewrite using the first relations in eqs. (4.45), (4.46) and the chain rule as

$$\begin{aligned}&\int_{S^d\setminus B_\delta} d^dx\sqrt{h}\ \nabla^\nu(f(\mu)\nabla_\nu G(x,0)) = \int_{S^d\setminus B_\delta} d^dx\sqrt{h}\ \nabla^\nu\Big(f(\mu(z))G'(z)\frac{\partial z}{\partial\mu}n_\nu\Big)\\ &= \int_{S^d\setminus B_\delta} d^dx\sqrt{h}\left(A(d-1)f(\mu(z))G'(z)\frac{\partial z}{\partial\mu} + \frac{\partial}{\partial z}\Big(f(\mu(z))G'(z)\frac{\partial z}{\partial\mu}\Big)\frac{\partial z}{\partial\mu}\right)\,.\end{aligned} \tag{B.6}$$

Here we used the variable z defined in (4.49). By changing the integration variable to z we get

$$\lim_{\delta'\to 0}\frac{2^d\pi^{\frac{d}{2}}}{\Gamma\left(\frac{d}{2}\right)}\int_0^{1-\delta'} dz\frac{\partial}{\partial z}\left((z(1-z))^{\frac{d-1}{2}}f(\mu(z))G'(z)\frac{\partial z}{\partial\mu}\right)\,. \tag{B.7}$$

The above integral would vanish for well-defined functions on S^d, as expected from Stokes theorem, but the propagator is actually a distribution which is singular at coincident points $z \to 1$, so care is required. In the limit $z \to 1$ the scalar propagator can be approximated to

$$G(z) \simeq \frac{\pi^{1-\frac{d}{2}}}{2^d\Gamma\left(2-\frac{d}{2}\right)\sin\left(\frac{d\pi}{2}\right)}(1-z)^{1-\frac{d}{2}} + \dots \tag{B.8}$$

Replacing eq. (B.8) in eq. (B.7) gives a non-vanishing result:

$$\lim_{\delta'\to 0} f(\mu(z))z^{\frac{d}{2}}\Big|_{z=1-\delta'} = f(\mu=0)\,. \tag{B.9}$$

This boundary term exactly cancels the contribution coming from the second term in eq. (B.4), proving eq. (B.3). Summarizing, the evaluation of eq. (B.2) without integrating by parts would require to pay attention to contact terms by introducing a regulator, while upon integrating by parts the contact term contribution is compensated by another contact term arising from a total derivative contribution.

B.2 Alternative gauge-fixing procedure

In section 4.2.2 we have seen that the quantization of non-abelian gauge theories on S^d using an ordinary Faddeev-Popov formalism leads to ghost zero modes. In this appendix we would like to show that our heuristic treatment of the zero modes is confirmed by a more rigorous

treatment using a Batalin-Vilkovisky formalism and ghosts for ghosts, see e.g. ref. [197] for a nice introduction or ref. [198] for a more detailed treatment. We start by briefly recalling the method in Yang-Mills theories on flat space and then apply it on S^d, where we reproduce the action presented in ref. [143]. We then compute the ghost contribution in eq. (4.66) using the new action and show that it matches with eq. (4.83) obtained with the more heuristic treatment discussed in the main text.

B.2.1 Gauge theories on S^d

Yang-Mills theories on flat space do not require ghosts for ghosts and can be treated with the Faddeev-Popov method. Let us briefly review how the same gauge-fixing can be obtained with the Batalin-Vilkovisky formalism. Recall that in this formalism for each field ϕ_A we introduce an antifield ϕ^*_A and we require the master equation

$$(S, S) = 0\,, \tag{B.10}$$

where

$$(F, G) \equiv \frac{\delta_R F}{\delta \phi^A}\frac{\delta_L G}{\delta \phi^*_A} - \frac{\delta_R F}{\delta \phi^*_A}\frac{\delta_L G}{\delta \phi^A}\,. \tag{B.11}$$

In the Yang-Mills theory case, $\phi^A = \{A, c\}$, where c are the ghost fields needed to take into account of the gauge redundancy of the classical action. The action satisfying the master equation (B.10) reads

$$S_{\text{flat}} = S_{\text{YM}}[A] + \int d^d x \left(A^* Dc - ic^* c^2 + \bar{c}^* B\right), \tag{B.12}$$

where $D = \partial - i[A, \cdot\,]$, $[\phi_1, \phi_2] = i f_{abc} t^a_f \phi^b_1 \phi^c_2$, with t^a_f and f_{abc} the generators in the fundamental representation and the structure constants of the Lie algebra, respectively. In eq. (B.12) trace over group indices and Lorentz indices are implicit and we have added an auxiliary pair of fields $\bar{c}/B$ and their corresponding antifields, which do not affect the master equation. Note that only $\bar{c}^*$ and B enter the action but also $\bar{c}$ and B^* are integrated over in the path integral. A gauge-fixing is introduced through a fermionic functional $\Psi[\phi]$ which fixes the value of the antifields:

$$\phi^*_A = \frac{\delta \Psi[\phi]}{\delta \phi^A}\,, \tag{B.13}$$

where now $\phi^A = \{A, c, \bar{c}, B\}$. An appropriate choice for the gauge-fixing functional is

$$\Psi = \int d^d x\ \bar{c}\left(-\frac{\xi}{2}B - \partial A\right), \tag{B.14}$$

which leads to

$$S^{\text{g.f.}}_{\text{flat}} = S_{\text{YM}}[A] + \int d^d x \left(\bar{c}\ \partial D c - B\Big(\frac{\xi}{2}B + \partial A\Big)\right), \tag{B.15}$$

which is the usual R_ξ gauge fixing of the Yang-Mills action.

On S^d an important difference arises. Covariantly constant modes leave the gauge field invariant, so the transformation $c \to c + \theta \tilde{a}_0$, with θ a Grassmann constant parameter, leaves the gauge field invariant, provided that

$$D\tilde{a}_0 = 0\,. \tag{B.16}$$

The mode $\tilde{a}_0$ is a (bosonic) ghost for ghost. We should then add $\tilde{a}_0$ to the set of fields in the action, together with its antifield. $\tilde{a}_0$ is actually not a field, but a single mode of a field, the covariantly constant one. For simplicity we keep this implicit. The solution to the master equation reads now

$$S = S_{\rm YM}[A] + \int d^dx\,\sqrt{h}\Big(A^*Dc + c^*a_0 - ic^*c^2 + ia_0{}^*[c,a_0] + \bar{c}^*B\, + \bar{a}_0^*\bar{c}_0 + b_0{}^*c_0\Big)\,, \tag{B.17}$$

where we have added two pairs $\bar{a}_0/\bar{c}_0$ and b_0/c_0 of fields (and their antifields), composed only of a covariantly constant mode, like $\tilde{a}_0$. In a perturbative treatment, where we expand in modes the quadratic action, the covariantly constant mode $\tilde{a}_0$ should be replaced by a constant mode a_0 satisfying

$$\nabla a_0 = 0\,, \tag{B.18}$$

which corresponds to the ghost zero modes found in the ordinary Faddeev-Popov procedure followed in section 4.2.2. The action (B.17) no longer solves the classical master equation if $\tilde{a}_0 \to a_0$. We now have

$$(S,S) = 2A^*Da_0 = 2iA^*[a_0,A] \neq 0\,, \tag{B.19}$$

However, adding appropriate terms to the action we can introduce a new action $\tilde{S} = S + \delta S$ such that

$$(\tilde{S},\tilde{S}) = 2i\phi_A^*[a_0,\phi^A]\,. \tag{B.20}$$

In this way, after gauge-fixing we have

$$(\tilde{S},\tilde{S}) = 2i\frac{\delta\Psi}{\delta\phi^A}[a_0,\phi^A]\, = 2i[a_0,\Psi[\phi]]\,. \tag{B.21}$$

For appropriate choices of the fermionic functional Ψ (gauge-fixing), the last term in eq. (B.21) vanishes and the master equations are satisfied, together with gauge-fixing independence of correlations function of gauge-invariant operators. In order to satisfy eq. (B.20), we add to S in eq. (B.17) a term

$$\delta S = i\int d^dx\sqrt{h}\Big(B^*[a_0,\bar{c}] + \bar{c}_0^*[a_0,\bar{a}_0] + c_0^*[a_0,b_0] + a_0{}^*[a_0,c]\Big)\,. \tag{B.22}$$

The BRST transformation of fields is given by $\delta_\theta\phi^A = \theta(-1)^{\epsilon_A}(S,\phi^A)$, $\delta_\theta\phi^*_A = -\theta(-1)^{\epsilon_A}(S,\phi^*_A)$,

with $\epsilon_A = 0, 1$ depending on the statistics of ϕ_A . Explicitly we get

$$\begin{aligned} &\delta_\theta A = \theta D c\,, \qquad \delta_\theta c = \theta\big(-a_0 + ic^2\big), \quad \delta_\theta \bar{c} = -\theta B, \quad \delta_\theta B = i\theta[a_0, \bar{c}]\,, \\ &\delta_\theta a_0 = 0\,, \quad \delta_\theta \bar{c}_0 = -i\theta[a_0, \bar{a}_0]\,, \quad \delta_\theta c_0 = -i\theta[a_0, b_0], \qquad \delta_\theta \bar{a}_0 = \theta \bar{c}_0\,, \quad \delta_\theta b_0 = \theta c_0\,, \end{aligned}$$

so that $\delta_{\theta_1}\delta_{\theta_2}\phi = -i\theta_1\theta_2[a_0, \phi]$ for any field ϕ. The gauge-fixing fermionic functional is taken as

$$\Psi = \int d^d x\, \sqrt{h}\left(\bar{c}\Big(-\frac{\xi}{2}B - \nabla A - b_0\Big) + \bar{a}_0 c\right), \tag{B.23}$$

providing

$$\begin{aligned} &A^* = -\nabla\bar{c}\,, \quad c^* = \bar{a}_0\,, \quad \bar{c}^* = -\frac{\xi}{2}B - \nabla A - b_0\,, \\ &B^* = -\frac{\xi}{2}\bar{c}, \quad b_0^* = \bar{c}\,, \quad \bar{a}_0^* = c\,. \end{aligned} \tag{B.24}$$

We then get

$$S^{\text{g.f.}} = S_{\text{YM}}[A] + \int d^d x\, \sqrt{h}\Big(\bar{c}\nabla D c + B\Big(-\frac{\xi}{2}B + \nabla A + b_0\Big) + \bar{a}_0 a_0 + c\bar{c}_0 + \bar{c}c_0 + i\xi\ \bar{c}^2 a_0 - ic^2\bar{a}_0\Big)\,, \tag{B.25}$$

which is the same action of eq.(4.2) in ref. [143].[1] We have then the following path integral:

$$\begin{aligned} Z_{\text{YM}} &= \frac{1}{\text{vol}(\mathcal{G}, g)}\int \mathcal{D}A \exp(-S_{\text{YM}}) \\ &= \frac{1}{\text{vol}(G)\sqrt{\text{vol}(S^d)^{\dim(G)}}}\int \mathcal{D}A\ \mathcal{D}c\ \mathcal{D}\bar{c}\ \mathcal{D}B\ \mathcal{D}a_0\ \mathcal{D}\bar{a}_0\ \mathcal{D}b_0\ \mathcal{D}\bar{c}_0\ \mathcal{D}c_0 \exp(-S^{\text{g.f.}})\,. \end{aligned} \tag{B.26}$$

The volume factor obtained after gauge fixing is the same found with the procedure used in the rest of this chapter: we can indeed verify that integrating out all fields and proceeding in reverse order to what we did in sec. 4.2.2, we reproduce the path integral in the first line of eq. (B.26). The integration of $\bar{c}_0, c_0$ and b_0 removes the zero modes respectively of $c, \bar{c}$ and B. Integrating out a_0 (along an imaginary contour to have a convergent path integral) sets also $\bar{a}_0$ to zero, while the gaussian integration in B reproduces the usual gauge fixing term $(\nabla A)^2/(2\xi)$.

[1] The precise matching, in the notation of ref. [143], is $\bar{c} \to i\tilde{c}$, $B \to -ib$, $\bar{a}_0 \to \tilde{a}_0 - \xi_2 a_0/2$, where ξ_2 is another gauge fixing parameter which does not affect the total path integral. Note that ref. [143] takes the fields to be antihermitian and not hermitian as in our case.

B.2.2 Computation of the ghost propagator

In the previous section we explained how to perform the gauge-fixing of Yang-Mills theories on S^d with the field-antifield formalism. The action that we obtained contains many fields that were not present in our main computation. As mentioned, one possibility is to integrate them out: in such a way we recover our original action and we can proceed as we already did. The other possibility is to keep the action (B.25) as it is and compute Feynman rules directly from it. We will focus in particular on the ghost action, which is

$$S_{\text{ghost}} = \int d^dx\, \sqrt{h}\; \bar{c}\nabla Dc + c\bar{c}_0 + \bar{c}c_0 + i\xi\; \bar{c}^2 a_0 - ic^2\bar{a}_0\,. \tag{B.27}$$

In order to compute the propagator, we should rewrite the quadratic part of this action as

$$S_{\text{ghost}} = \int d^d\sqrt{h}\; \frac{1}{2}\begin{pmatrix}\bar{c} & c\end{pmatrix} M \begin{pmatrix}c\\ \bar{c}\end{pmatrix} + c\bar{c}_0 + \bar{c}c_0\,, \tag{B.28}$$

with

$$M^{ab} = \begin{pmatrix}\delta^{ab}\nabla^2 & -\xi f^{abc}a_{0c}\\ f^{abc}\bar{a}_{0c} & -\delta^{ab}\nabla^2\end{pmatrix}. \tag{B.29}$$

As explained before, the terms linear in $\bar{c}_0$ and c_0 set to zero the constant modes. As opposed to the standard ghost action, we do not have only the ghost-antighost term, but also terms quadratic in ghosts and antighosts. The propagator will then be a matrix

$$G_{ab} = \begin{pmatrix}\text{--}\blacktriangleright\text{---}\blacktriangleright\text{--} & \text{--}\blacktriangleleft\text{---}\blacktriangleright\text{--}\\ \text{--}\blacktriangleright\text{---}\blacktriangleleft\text{--} & \text{--}\blacktriangleleft\text{---}\blacktriangleleft\text{--}\end{pmatrix} = \begin{pmatrix}\langle\bar{c}'_a c'_b\rangle & \langle c'_a c'_b\rangle\\ \langle\bar{c}'_a\bar{c}'_b\rangle & \langle c'_a\bar{c}'_b\rangle\end{pmatrix} \tag{B.30}$$

with all entries different from zero, satisfying

$$M^{ij}_{ab}G^{bc}_{jk} = -\delta^i_k\;\delta^c_a\;\delta(x-x')\,. \tag{B.31}$$

Let us consider the following ansatz and verify if there exists such a solution:

$$G_{ab} = \begin{pmatrix}\delta_{ab}f_1(z) + a_{0b}\bar{a}_{0a}f_2(z) & f_{abc}a_0{}^c g_1(z)\\ f_{abc}\bar{a}_0^c h_1(z) & -\delta_{ab}f_1(z) - a_{0a}\bar{a}_{0b}f_2(z)\end{pmatrix}, \tag{B.32}$$

with $f_1(z), f_2(z), g(z), h(z)$ generic functions of the stereographic coordinates. By replacing in eq. (B.31) and contracting color indices,[2] we get

$$\begin{aligned}\nabla^2 f_1 &= -\xi\frac{n_c}{n_c^2-2}(a_0\bar{a}_0)h_1(z) + \delta(x-x')\,, \quad & \nabla^2 h_1 &= -f_1\,,\\ \nabla^2 f_2 &= \xi\frac{n_c}{n_c^2-2}h_1(z)\,, & g_1 &= \xi h_1\,.\end{aligned} \tag{B.33}$$

[2]We recall that for $SU(n_c)$ gauge group the following identity holds: $f_{abc}f_{a'b'c} = \frac{n_c}{n_c^2-2}\left(\delta_{aa'}\delta_{bb'} - \delta_{ab'}\delta_{ba'}\right)$.

This is a system of coupled ordinary differential equations. The solution is easily found by decomposing in spherical harmonics each function of z:

$$f(z) = \sum_{\ell>0} f_\ell \; Y_\ell(x) Y_\ell(x') \,, \tag{B.34}$$

where we exclude the constant mode $\ell = 0$ because of the linear terms in eq. (B.28). We get

$$\begin{aligned}
f_{1\ell} &= \frac{1}{2}\left(\frac{1}{-\ell(\ell+d-1)+m^2} + \frac{1}{-\ell(\ell+d-1)-m^2}\right) , \\
h_{1\ell} &= \frac{1}{2m^2}\left(\frac{1}{-\ell(\ell+d-1)+m^2} - \frac{1}{-\ell(\ell+d-1)-m^2}\right) , \\
f_{2\ell} &= \frac{\xi}{2m^4}\left(\frac{1}{-\ell(\ell+d-1)+m^2} + \frac{1}{-\ell(\ell+d-1)-m^2} - \frac{2}{-\ell(\ell+d-1)}\right) , \\
g_{1\ell} &= \xi f_{1\ell} \,,
\end{aligned} \tag{B.35}$$

where

$$m^2 \equiv \sqrt{\frac{\xi n_c}{n_c^2-2}} (a_0 \bar{a}_0)^{\frac{1}{2}} \,. \tag{B.36}$$

Following the notation of sec.4.3.2, we denote by $G_{\rm reg}(x, m^2)$ the solution of the scalar propagator equation on S^d with zero modes removed:

$$G_{\rm reg}(z, m^2) = \sum_{\ell>0} \frac{1}{-\ell(\ell+d-1)+m^2} Y_\ell(x) Y_\ell(x'). \tag{B.37}$$

Summing over the non-constant modes we then find

$$\begin{aligned}
f_1 &= \frac{1}{2}\left(G_{\rm reg}(z,m^2) + G_{\rm reg}(z,-m^2)\right) , \\
f_2 &= \frac{\xi}{2m^4}\left(G_{\rm reg}(z,m^2) + G_{\rm reg}(z,-m^2) - 2G_{\rm reg}(z,0)\right) , \\
h_1 &= \frac{1}{2m^2}\left(G_{\rm reg}(z,m^2) - G_{\rm reg}(z,-m^2)\right) , \\
g_1 &= \xi h_1 \,.
\end{aligned} \tag{B.38}$$

B.2.3 Match with eq. (4.83)

Let us now consider how the ghost contribution $G_2^{\rm ghost}$ is modified when the propagator in eq. (B.30) is used. As in this case also Wick contractions of two ghosts or two antighosts are allowed, the number of ghost diagrams increases. We have

$$\widetilde{G}_2^{\rm ghost} = \quad + \quad = \widetilde{G}_2^{\rm ghost1} + \widetilde{G}_2^{\rm ghost2}, \tag{B.39}$$

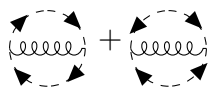

with

$$\widetilde{G}_2^{\text{ghost1}} = g_0^2 \int d^d x \; d^d x' \sqrt{h}\sqrt{h'} \Big(n_c \left(n_c^2 - 1\right) \nabla_\mu f_1 \nabla_{\mu'} f_1 + \frac{n_c}{n_c^2 - 2} ({a_0}^2 \bar{a}_0^2 - (a_0 \bar{a}_0)^2) \nabla_\mu f_2 \nabla_{\mu'} f_2 \Big) Q^{\mu\mu'},$$

$$\widetilde{G}_2^{\text{ghost2}} = g_0^2 \frac{n_c^2}{n_c^2 - 2} \xi (a_0 \bar{a}_0) \int d^d x \; d^d x' \sqrt{h}\sqrt{h'} \; (\nabla_{\mu'} \nabla_\mu h_1) \, h_1 Q^{\mu\mu'} \, . \tag{B.40}$$

The evaluation of eq. (B.40) for generic ξ, which includes integrating over a_0 and $\bar{a}_0$, is a non-trivial task. The computation remarkably simplifies in the Landau gauge $\xi \to 0$. In this limit $m^2 \to 0$, the functions f_1 and h_1 are of order 1, while f_2 and g_1 are subleading in ξ. The only contribution left in the limit is given by the first term in G_2^{ghost1}, the one involving the product of two f_1. For $\xi \to 0$, $f_1 \to G_{\text{reg}}(z, 0)$, which coincides with the ghost propagator in eq. (4.58), and we reproduce exactly the result in eq. (4.83):

$$\lim_{\xi \to 0} \widetilde{G}_2^{\text{ghost}} = G_2^{\text{ghost}} \, . \tag{B.41}$$

This is a sanity check of the validity of the heuristic Faddeev-Popov approach followed in the main text.

Appendix C

Mean field theory of $SU(n_c)$ adjoint currents

The spectrum of CFT operators on $\mathbb{R}^d$, or equivalently of states on $S^{d-1} \times \mathbb{R}$, can be encoded in a grand-canonical partition function on $S^{d-1} \times S^1$, with S^1 being a compact Euclidean thermal cycle. In particular, we are interested in the spectrum of the mean-field theory of $SU(n_c)$ adjoint currents in $d = 3$ dimensions. Following the approach of [167, 168], this can be determined from the single-particle partition function

$$z_{J,R_A}(q, x, y, r) = z_J(q, x) X_{R_A}(y, r) \,. \tag{C.1}$$

Here,

$$z_J(q, x) = \mathrm{tr}_J \left(q^\Delta x^j \right) = \chi_{(2,1)}(q, x) - \chi_{(3,0)}(q, x) \equiv \chi^{short}_{(2,1)}(q, x) \,, \tag{C.2}$$

is the single-particle partition function of a $U(1)$ conserved current J in $d = 3$, with

$$\chi_{(\Delta,\ell)}(q, x) = \frac{q^\Delta}{(1-q)(1-qx)(1-q/x)} \sum_{j=-\ell}^{\ell} x^j \,, \qquad q = e^{-\beta} \,,\ x = e^{\mu} \,, \tag{C.3}$$

being the conformal characters associated with primary operators with scaling dimension Δ and $SO(3) \sim SU(2)$ spin ℓ, for which we have turned on fugacities q and x, respectively. Similarly,

$$X_{R_A}(y, r) = y^{-r} \left(\sum_{p=0}^{r} y^p \right)^2 - 1 \,, \tag{C.4}$$

is the character for the $SU(r+1)$ adjoint representation R_A, with a common fugacity y for the diagonal Cartan generators. The spectrum of the mean-field theory of $SU(r+1)$ adjoint currents is encoded in the multi-particle partition function

$$Z(q, x, y, \eta, r) = \exp \left(\sum_{k=1}^{\infty} \eta^k \frac{z_{J,R_A}(q^k, x^k, y^k, r)}{k} \right) \,, \tag{C.5}$$

where we have also introduced a fugacity η that keeps track of the number of currents entering each primary operator. The partition function Z can be systematically expanded in powers of q, x, η in order to obtain the spectrum to arbitrary order. Up to scaling dimension $\Delta = 7$, omitting to write the common (q, x)-dependence on all characters, one finds

$$\begin{aligned}
Z(q,x,y,\eta,r) &= 1 + \eta\chi^{short}_{(2,1)} X_{R_A}(y,r) + \eta^2\chi_{(4,0)}X_+ + \eta^2\chi_{(4,1)}X_- + \eta^2\chi_{(4,2)}X_+ \\
&+ \eta^2\chi_{(5,0)}X_+ + \eta^2\chi_{(5,1)}X_- + \eta^2\chi_{(5,2)}(X_+ + X_-) + \eta^2\chi_{(5,3)}X_- + \eta^2\chi_{(6,0)}X_+ \\
&+ \eta^3\chi_{(6,0)}Y_- + \eta^2\chi_{(6,1)}X_- + \eta^3\chi_{(6,1)}(Y_+ + Z) + 2\eta^2\chi_{(6,2)}X_+ + \eta^3\chi_{(6,2)}Z \\
&+ \eta^2\chi_{(6,3)}(X_+ + X_-) + \eta^3\chi_{(6,3)}Y_+ + \eta^2\chi_{(6,4)}X_+ + \eta^2\chi_{(7,0)}X_+ \\
&+ \eta^3\chi_{(7,0)}(Y_- + Z) + \eta^2\chi_{(7,1)}X_- + \eta^3\chi_{(7,1)}(3Z + 2Y_+ + Y_-) + \eta^2\chi_{(7,2)}(X_+ + X_-) \\
&+ \eta^3\chi_{(7,2)}(3Z + Y_+ + 2Y_-) + 2\eta^2\chi_{(7,3)}(q,x)X_- + \eta^3\chi_{(7,3)}(2Z + Y_+ + Y_-) \\
&+ \eta^2\chi_{(7,4)}(X_+ + X_-) + \eta^3\chi_{(7,4)}Z + \eta^2\chi_{(7,5)}X_- + O(q^8)\,,
\end{aligned} \tag{C.6}$$

where we have defined the group character combinations

$$\begin{aligned}
X_\pm &\equiv \frac{X^2_{R_A}(y,r) \pm X_{R_A}(y^2,r)}{2}\,, \\
Y_\pm &\equiv \frac{X^3_{R_A}(y,r) \pm 3X_{R_A}(y,r)X_{R_A}(y^2,r) + 2X_{R_A}(y^3,r)}{6}\,, \qquad Z \equiv \frac{X^3_{R_A}(y,r) - X_{R_A}(y^3,r)}{3}\,.
\end{aligned} \tag{C.7}$$

The $SU(r+1)$ representations under which the operators in (C.6) transform are encoded in the combinations (C.7). For simplicity, we work out here the character decomposition for the primaries with $\Delta \leq 5$, which involve only the combinations $X_\pm$. We first consider the general $SU(r+1)$ case with $r > 3$. The cases $r = 1, 2, 3$ are special and will be treated after. The decomposition of two adjoint representations reads

$$R_A \otimes R_A = R_+ \oplus R_-\,, \quad R_+ = \mathbf{1} \oplus R_3 \oplus R_A\,, \quad R_- = R_1 \oplus R_2 \oplus \overline{R}_2 \oplus R_A\,, \tag{C.8}$$

where $\mathbf{1}$ is the singlet and R_i are representations with Dynkin labels

$$\begin{aligned}
R_1 &= (2,0,\ldots,0,2)\,, & \dim R_1 &= \frac{(n_c+3)n_c^2(n_c-1)}{4}\,, \\
R_2 &= (0,1,0,\ldots,0,2)\,, & \dim R_2 &= \frac{(n_c^2-4)(n_c^2-1)}{4}\,, \\
\overline{R}_2 &= (2,0,\ldots,0,1,0)\,, & \dim \overline{R}_2 &= \dim R_2 \\
R_3 &= (0,1,0,\ldots,0,1,0)\,, & \dim R_3 &= \frac{n_c^2(n_c-3)(n_c+1)}{4} \\
R_A &= (1,0,\ldots,0,1)\,, & \dim R_A &= n_c^2 - 1\,,
\end{aligned} \tag{C.9}$$

with $n_c = r + 1$. One can check that the following character decomposition holds,

$$\begin{aligned} X_+ &= 1 + X_{R_1}(y,r) + X_{R_3}(y,r) + X_{R_A}(y,r)\,, \\ X_- &= X_{R_2}(y,r) + X_{\overline{R}_2}(y,r) + X_{R_A}(y,r)\,. \end{aligned} \tag{C.10}$$

For $r = 3$ the decomposition (C.8) and (C.10) applies, but the Dynkin labels of R_3 are modified:

$$R_3 = (0,2,0)\,, \qquad \dim R_3 = 20\,, \qquad (r=3)\,. \tag{C.11}$$

For $r = 2$ the representation R_3 does not exist, and we have

$$\begin{aligned} R_1 = (2,2)\,, \qquad & \dim R_1 = 27\,, \qquad (r=2)\,, \\ R_2 = (3,0)\,, \quad \overline{R}_2 = (0,3)\,, \qquad & \dim R_2 = \dim \overline{R}_2 = 10\,, \qquad (r=2)\,. \end{aligned} \tag{C.12}$$

For $r = 1$ the decomposition trivializes,

$$X_+ = 1 + X_2(y,r)\,, \qquad X_- = X_1(y,r)\,, \qquad (r=1)\,, \tag{C.13}$$

where the subscripts refer to the spin j of the representation ($j = 1$ is the adjoint).

Appendix D

Bulk-to-bulk gauge propagator

D.1 Map to the notation of [5]

It is convenient to express propagators and their derivatives with the notation presented in [5] for maximally symmetric spaces. Let us denote by $\mu(x,y)$ the geodesic distance, which can be expressed in terms of the chordal distance as

$$\mu(x,y) = \cosh^{-1}\Big(1+u(x,y)\Big)\,. \tag{D.1}$$

In this notation, the building blocks are the parallel propagator $g^{\nu}{}_{\nu'}(x,y)$ transporting vectors along geodesics from x to y, and the unit vectors $n_\nu(x,y)$ and $n_{\nu'}(x,y)$, tangent to the geodesic at x and y respectively,

$$n_\nu\,(x,y) = \nabla_\nu \mu(x,y) \quad \text{ and } \quad n_{\nu'}\,(x,y) = \nabla_{\nu'}\mu\,(x,y)\ . \tag{D.2}$$

Any bitensor in a maximally symmetric space can be expressed as sums and products of these building blocks, with coefficients that are only functions of μ, or equivalently of u. For example, a bitensor with an index in x and an index in y, such as the gauge propagator Π, can be decomposed as

$$\Pi_{\mu\mu'}(x,y) = \pi_0(u) g_{\mu\mu'} + \pi_1(u) n_\mu n_{\mu'}\,. \tag{D.3}$$

In AdS space we also have [5]

$$\begin{aligned}
\nabla_\nu n_\mu &= \frac{(1+u)}{\sqrt{u(u+2)}}\,(g_{\nu\mu} - n_\nu n_\mu)\ , \\
\nabla_\nu n_{\mu'} &= -\frac{1}{\sqrt{u(u+2)}}\,(g_{\nu\mu'} + n_\nu n_{\mu'})\ , \\
\nabla_\nu g_{\mu\mu'} &= -\frac{u}{\sqrt{u(u+2)}}\,(g_{\nu\mu} n_{\mu'} + g_{\nu\mu'} n_\mu)\,,
\end{aligned} \tag{D.4}$$

which are useful relations to compute derivatives of propagators. We can map between the parametrization (5.28) and the one given in (D.3) by the relations

$$\nabla_\mu u = \sqrt{u(u+2)} n_\mu \,, \qquad \nabla_{\mu'} \nabla_\mu u = -g_{\mu\mu'} + u\; n_\mu n_{\mu'} \,. \tag{D.5}$$

We get

$$\pi_0(u) = g_0(u) \,, \qquad \pi_1(u) = u(u+2) g_1(u) - u g_0(u) \,. \tag{D.6}$$

D.2 Spectral representation

We briefly review here the minimal properties of spin ℓ harmonic functions on AdS $\Omega_\nu^{(\ell)}$ needed for the derivation of the bulk gauge propagator, referring to [173] for further details. We focus on $\ell = 0, 1$, which are the only cases of interest for us. Harmonic functions on AdS can be conveniently defined in embedding space as suitable integrals over the boundary of two bulk-to-boundary propagators. They satisfy the relations

$$\begin{aligned} -\nabla_X^2 \Omega^{(1)}_{\nu AB}(X,Y) &= \left(\nu^2 + \frac{d^2}{4} + 1\right) \Omega^{(1)}_{\nu AB}(X,Y), \\ -\nabla_X^A \Omega^{(1)}_{\nu AB}(X,Y) &= 0 \,, \\ -\nabla_X^2 \Omega^{(0)}_{\nu}(X,Y) &= \left(\nu^2 + \frac{d^2}{4}\right) \Omega^{(0)}_{\nu}(X,Y), \end{aligned} \tag{D.7}$$

as well as nice orthogonality properties. The harmonic functions can be written as

$$\Omega_\nu^{(\ell)}(X_1, X_2; W_1, W_2) = \frac{i\nu}{2\pi} \left(G_{\frac{d}{2}+i\nu,\ell}(X_1, X_2; W_1, W_2) - G_{\frac{d}{2}-i\nu,\ell}(X_1, X_2; W_1, W_2) \right), \tag{D.8}$$

where $G_{\Delta,\ell}$ is the analytic continuation for complex Δ of the bulk propagators for a massive spin ℓ field [173].

Let us review how to get the N and D bulk propagators for a scalar field with mass $m^2 = \Delta(\Delta - d)$ using the spectral representation. We take $\Delta > d/2$. In embedding space the equation of motion reads

$$(-\nabla^2 + m^2)\Pi(X_1, X_2) = \delta(X_1, X_2) \,. \tag{D.9}$$

We look for a particular solution of (D.9) by writing

$$\Pi(X_1, X_2) = \int_{-\infty}^{\infty} d\nu \, a_0(\nu) \Omega_\nu^{(0)}(X_1, X_2) \,, \tag{D.10}$$

and the spectral representation of the delta function

$$\delta(X_1, X_2) = \int_{-\infty}^{\infty} d\nu \, \Omega_\nu^{(0)}(X_1, X_2) \,. \tag{D.11}$$

Using the third relation in (D.7) it is immediate to determine a_0:

$$a_0(\nu) = \frac{1}{\nu^2 + \left(\Delta - \frac{d}{2}\right)^2}\,. \tag{D.12}$$

The integral in ν in (D.10) can be performed using (D.8) and residue theorem. Given the boundary behavior $G_{\Delta,0} \sim u^{-\Delta}$ as $u \to \infty$, we have to close the contour at infinity in the lower and upper half-plane for $G_{d/2+i\nu,0}$ and $G_{d/2-i\nu,0}$ respectively. The only poles are the ones given by $a_0(\nu)$, at $\nu_0 = i(\Delta - d/2)$ and ν_0^*, the two residues giving the same contribution. We get

$$\Pi^{(D)}(X_1, X_2) = 2\int_{C_{\nu_0^*}} d\nu\, a_0(\nu)\frac{i\nu}{2\pi} G_{\frac{d}{2}+i\nu,0}(X_1, X_2) = G_{\frac{d}{2}+i\nu_0^*,0}(X_1, X_2) = G_{\Delta,0}(X_1, X_2)\,, \tag{D.13}$$

where $C_{\nu_0^*}$ is a small circle around ν_0^*. The function $\Pi^{(D)}$ is identified as the bulk propagator with D bc. The N bulk propagator $\Pi^{(N)}$ is determined by noticing that $\Omega^{(0)}_{\nu_0}$ is a solution of the homogeneous equation of motion, so $\Pi(X_1, X_2) + c\,\Omega^{(0)}_{\nu_0}$ is a solution of (D.10) for any constant c. Demanding that $\phi \sim u^{\Delta-d}$ as $u \to \infty$ fixes the constant to be $c = 2\pi/(i\nu_0)$. This can also be written as

$$\begin{aligned}\Pi^{(N)}(X_1, X_2) &= \Pi^{(D)}(X_1, X_2) - 2\int_{C_{\nu_0}} d\nu\, a_0(\nu)\frac{i\nu}{2\pi}(G_{\frac{d}{2}+i\nu,0}(X_1, X_2) - G_{\frac{d}{2}-i\nu,0}(X_1, X_2)) \\ &= 2\int_{C_{\nu_0}} d\nu\, a_0(\nu)\frac{i\nu}{2\pi} G_{\frac{d}{2}+i\nu,0}(X_1, X_2) = G_{\frac{d}{2}+i\nu_0,0}(X_1, X_2) = G_{d-\Delta,0}(X_1, X_2)\,.\end{aligned} \tag{D.14}$$

We see that the N bulk propagator can be expressed, in the spectral representation, by the same integrand of the D bulk propagator, but evaluated at the "opposite" residues. In this way, the correct boundary behavior is obtained. The same mechanism works for massive spin 1 and massless gauge propagators. In particular, the massive spin 1 propagator can be decomposed as follows in terms of harmonic functions [173],

$$\begin{aligned}\Pi_{\Delta,1}(X_1, X_2; W_1, W_2) = &\int d\nu\, \frac{1}{\nu^2 + (\Delta - d/2)^2}\Omega^{(1)}_\nu(X_1, X_2; W_1, W_2) \\ &+ (W_1\cdot\nabla_1)(W_2\cdot\nabla_2)\int d\nu\, \frac{1}{(\Delta-1)(\Delta-d+1)}\frac{1}{\nu^2 + d^2/4}\Omega^{(0)}_\nu(X_1, X_2)\,.\end{aligned} \tag{D.15}$$

As for the scalar case above, N and D propagators are obtained by appropriately choosing the contour of the ν integration in the two cases.

D.3 General expression in any ξ-gauge

We report below the expression for the functions $g_0^{(D,N)}(u)$ and $g_1^{(D,N)}(u)$ entering the bulk-to-bulk gauge propagators (5.27) and (5.28) for any ξ-gauge. For clarity, we split them in their transverse (ξ-independent) and longitudinal (proportional to ξ) components,

$$g_i(u) = g_{i,\perp}(u) + \xi\, g_{i,L}(u)\,, \qquad i = 0, 1. \tag{D.16}$$

The Dirichlet bulk-to-bulk propagator is given by

$$\begin{aligned}
g_{0,\perp}^{(D)} &= \frac{\Gamma\left(\frac{d+1}{2}\right)\left(-\frac{1}{d} - \psi\left(\frac{d}{2}\right) + \psi(d) + u(u+2) - \frac{1}{2}\log(4u(u+2))\right)}{2\pi^{\frac{d+1}{2}}(d-2)(u(u+2))^{\frac{d+1}{2}}} \\
&\quad + \frac{\Gamma\left(\frac{d+1}{2}\right)\left(\frac{\partial}{\partial b} + 2\frac{\partial}{\partial c}\right){}_2F_1\left(\frac{d+1}{2}, \frac{d+2}{2}+b, \frac{d+2}{2}+c, \frac{1}{(u+1)^2}\right)\Big|_{b=c=0}}{4\pi^{\frac{d+1}{2}}(d-2)(u+1)^{d+1}}\,, \\
g_{0,L}^{(D)} &= \frac{\Gamma\left(\frac{d+1}{2}\right)\left(H_{\frac{d}{2}} - \frac{1}{d} - \psi(d) + \log(2(u+2)) - \gamma_E\right)}{2\pi^{\frac{d+1}{2}} d(u(u+2))^{\frac{d+1}{2}}} \\
&\quad - \frac{\Gamma\left(\frac{d+1}{2}\right)\left(\frac{\partial}{\partial a} + 2\frac{\partial}{\partial c}\right){}_2F_1\left(d+1+a, \frac{d+1}{2}, d+1+c, -\frac{2}{u}\right)\big|_{a=c=0}}{2\pi^{\frac{d+1}{2}} du^{d+1}}\,, \\
g_{1,\perp}^{(D)} &= \frac{(u+1)\Gamma\left(\frac{d+1}{2}\right)\left(u(u+2) - \frac{1}{2}\log\left(\frac{u(u+2)}{(u+1)^2}\right) - (d+1)\left(\psi\left(\frac{d}{2}\right) - \psi(d) + \log(2(u+1))\right) - \frac{1}{d}\right)}{2\pi^{\frac{d+1}{2}}(d-2)(u(u+2))^{\frac{d+3}{2}}} \\
&\quad + \frac{\Gamma\left(\frac{d+1}{2}\right)\left(\frac{\partial}{\partial b} + 2\frac{\partial}{\partial c}\right){}_2F_1\left(\frac{d+1}{2}, \frac{d+2}{2}+b, \frac{d+2}{2}+c, \frac{1}{(u+1)^2}\right)\Big|_{b=c=0}}{4\pi^{\frac{d+1}{2}}(d-2)u(u+2)(u+1)^d} \\
&\quad + \frac{d\Gamma\left(\frac{d+1}{2}\right)\left(\frac{\partial}{\partial a} + \frac{\partial}{\partial b} + 2\frac{\partial}{\partial c}\right){}_2F_1\left(\frac{d+1}{2}+a, \frac{d}{2}+b, \frac{d}{2}+c, \frac{1}{(u+1)^2}\right)\Big|_{a=b=c=0}}{4\pi^{\frac{d+1}{2}}(d-2)u(u+2)(u+1)^d}\,, \\
g_{1,L}^{(D)} &= -\frac{\partial}{\partial u} g_{0,L}^{(D)}\,.
\end{aligned} \tag{D.17}$$

We have checked that the bulk propagator in the Feynman gauge $\xi = 1$ agrees with what is found in [5]. It is remarkable that in the FY gauge $\xi = d/(d-2)$, the D propagator in (D.17) boils down to the simple expression (5.32).

The Neumann bulk-to-bulk propagator is given by

$$
\begin{aligned}
g_{0,\perp}^{(N)} &= \frac{{}_2F_1\left(\frac{1}{2},1;1-\frac{d}{2};\frac{1}{(u+1)^2}\right)\left(-H_{1-\frac{d}{2}}-\frac{2}{d-1}+\frac{1}{d}-\log(2(u+1))+1\right)}{4\pi^{d/2}\Gamma\left(2-\frac{d}{2}\right)(u+1)} \\
&\quad - \frac{(d-2)u(u+2)\,{}_2\widetilde{F}_1\left(\frac{3}{2},2;2-\frac{d}{2};\frac{1}{(u+1)^2}\right)}{2\pi^{d/2}(d-1)d(u+1)^3} \\
&\quad + \frac{(d-1)\pi^{-d/2}\left(\frac{\partial}{\partial a}+\frac{\partial}{\partial b}+2\frac{\partial}{\partial c}\right){}_2F_1\left(\frac{1}{2}+a,1+b,2-\frac{d}{2}+c,\frac{1}{(u+1)^2}\right)\Big|_{a=b=c=0}}{8(d-2)\Gamma\left(2-\frac{d}{2}\right)(u+1)} \\
&\quad + \frac{\left(\frac{\partial}{\partial a}+\frac{\partial}{\partial b}+2\frac{\partial}{\partial c}\right){}_2F_1\left(\frac{3}{2}+a,1+b,2-\frac{d}{2}+c,\frac{1}{(u+1)^2}\right)\Big|_{a=b=c=0}}{4\pi^{d/2}(d-2)^2(u+1)\Gamma\left(1-\frac{d}{2}\right)}\,, \\
g_{0,L}^{(N)} &= \frac{\Gamma\left(\frac{d+1}{2}\right)\left(H_{-\frac{d}{2}-\frac{1}{2}}+H_{\frac{d}{2}}-\frac{2}{d}+\pi\tan\left(\frac{\pi d}{2}\right)-2(\psi(d)+\gamma_E)+\log\left(\frac{4(u+2)}{u}\right)\right)}{2\pi^{\frac{d+1}{2}}d(u(u+2))^{\frac{d+1}{2}}} \\
&\quad + \frac{{}_2F_1\left(1,\frac{1-d}{2};1-d;-\frac{2}{u}\right)\left(\pi\cot\left(\frac{\pi d}{2}\right)+2\psi(d)-\psi\left(\frac{d+1}{2}\right)+\log\left(\frac{u}{2}\right)+\gamma_E\right)}{\pi^{d/2}d^2u\Gamma\left(-\frac{d}{2}\right)} \\
&\quad - \frac{\left(\frac{\partial}{\partial a}+\frac{\partial}{\partial b}+2\frac{\partial}{\partial c}\right){}_2F_1\left(1+a,\frac{1-d}{2}+b,1-d+c,-\frac{2}{u}\right)\Big|_{a=b=c=0}}{\pi^{d/2}d^2u\Gamma\left(-\frac{d}{2}\right)} \\
&\quad + \frac{\Gamma\left(\frac{d+1}{2}\right)\frac{\partial}{\partial b}\,{}_2F_1\left(d+1,\frac{d+1}{2}+b,d+1,-\frac{2}{u}\right)\Big|_{b=0}}{2\pi^{\frac{d+1}{2}}du^{d+1}}\,, \\
g_{1,\perp}^{(N)} &= \frac{(d^2-1)\,{}_2F_1\left(\frac{1}{2},1;2-\frac{d}{2};\frac{1}{(u+1)^2}\right)\left(-\frac{u(u+2)}{d^2-1}+H_{1-\frac{d}{2}}+\log(2(u+1))-1\right)}{4\pi^{d/2}(d-2)u^2(u+2)^2\Gamma\left(2-\frac{d}{2}\right)} \\
&\quad - \frac{(d+(u+1)^2)\left(H_{1-\frac{d}{2}}+\log(2(u+1))-1\right)}{4\pi^{d/2}u^2(u+2)^2\Gamma\left(2-\frac{d}{2}\right)} \\
&\quad + \frac{(d-1)\left(\frac{\partial}{\partial a}+\frac{\partial}{\partial b}+2\frac{\partial}{\partial c}\right){}_2F_1\left(\frac{1}{2}+a,1+b,2-\frac{d}{2}+c,\frac{1}{(u+1)^2}\right)\Big|_{a=b=c=0}}{8\pi^{d/2}(d-2)u(u+2)\Gamma\left(2-\frac{d}{2}\right)} \\
&\quad - \frac{(d+(u+1)^2)\left(\frac{\partial}{\partial a}+\frac{\partial}{\partial b}+2\frac{\partial}{\partial c}\right){}_2F_1\left(\frac{3}{2}+a,1+b,2-\frac{d}{2}+c,\frac{1}{(u+1)^2}\right)\Big|_{a=b=c=0}}{8\pi^{d/2}(d-2)u(u+1)^2(u+2)\Gamma\left(2-\frac{d}{2}\right)}\,, \\
g_{1,L}^{(N)} &= -\frac{\partial}{\partial u}g_{0,L}^{(N)}\,.
\end{aligned}
\tag{D.18}
$$

Appendix E

Tools for the computation of Witten diagrams

Developing tools for the computation of Witten diagrams at loop level is an active field of research in itself, see e.g. [82, 189, 199–214]. In this appendix, we provide details on several technical points required to compute the Witten diagrams presented in sections 5.3 and 5.4.

E.1 Mass shift diagram

We want to compute the integral corresponding, modulo some prefactors that we will make explicit later, to the mass shift of a scalar field of dimension Δ, which is

$$\mathcal{I}_\Delta = \int dX \frac{1}{(-2P_1 \cdot X)^\Delta} \frac{1}{(-2P_2 \cdot X)^\Delta} , \tag{E.1}$$

where X is a point in the bulk and P_1, P_2 are points at the boundary. The integral (E.1) is divergent, but it can be regulated for $\Delta \neq d/2$ by putting P_1 and P_2 at distance $z_{1,2} = \delta \ll 1$ from the boundary. Consider then the analog bulk integral

$$\widetilde{\mathcal{I}}_\Delta = \int dX \, G_{\Delta,0}(X_1, X) G_{\Delta,0}(X, X_2) , \tag{E.2}$$

with X_1 and X_2 points in the bulk and $G_{\Delta,0}$ the bulk-to-bulk propagator of a scalar field with dimension Δ. We assume from now that $\Delta \neq d/2$. In spectral representation, the scalar propagator with D bc can be written as

$$G_{\Delta,0}(X_1, X_2) = \int_{-\infty}^{+\infty} d\nu \, \frac{1}{\nu^2 + \left(\Delta - \frac{d}{2}\right)^2} \Omega_\nu^{(0)}(X_1, X_2) . \tag{E.3}$$

Using (E.3) and the orthogonality relation for harmonic functions

$$\int dX \, \Omega_\nu^{(0)}(X_1, X) \Omega_{\nu'}^{(0)}(X, X_2) = \frac{\delta(\nu - \nu') + \delta(\nu + \nu')}{2} \Omega_\nu^{(0)}(X_1, X_2) , \tag{E.4}$$

we can rewrite the integral (E.2) as

$$\widetilde{\mathcal{I}}_\Delta = \int_{-\infty}^{+\infty} d\nu \frac{1}{\left(\nu^2 + \left(\Delta - \frac{d}{2}\right)^2\right)^2} \Omega_\nu^{(0)}(X_1, X_2) = -\frac{1}{2\Delta - d} \frac{d}{d\Delta} G_{\Delta,0}(X_1, X_2) \,. \tag{E.5}$$

Taking the external points to the boundary we get

$$\mathcal{I}_\Delta = \lim_{z_{1,2}\to\delta} \left[(z_1 z_2)^{-\Delta} \widetilde{\mathcal{I}}_\Delta\right] = -\frac{1}{2\Delta - d} \frac{1}{(C_0(\Delta))^2} \lim_{z_{1,2}\to\delta} \left[(z_1 z_2)^{-\Delta} \frac{d}{d\Delta} G_{\Delta,0}(X_1, X_2)\right] . \tag{E.6}$$

We now use the relation between the bulk-to-bulk and the bulk-to-boundary propagator

$$G_{\Delta,0}(X_i, X) \underset{z_i\to\delta}{\sim} z_i^\Delta \frac{C_0(\Delta)}{(-2P_i \cdot X)^\Delta} \,, \tag{E.7}$$

where

$$C_0(\Delta) = \frac{\Gamma(\Delta)}{2\pi^{\frac{d}{2}} \Gamma\left(1 - \frac{d}{2} + \Delta\right)} \,. \tag{E.8}$$

We compute the limit by using (E.7), taking now both points to the boundary:

$$G_{\Delta,0}(X_1, X_2) \underset{z_{1,2}\to 0}{\sim} z_1^\Delta z_2^\Delta \frac{C_0(\Delta)}{(-2P_1 \cdot P_2)^\Delta} \,. \tag{E.9}$$

This gives the final result

$$\mathcal{I}_\Delta = \frac{1}{d - 2\Delta} \frac{1}{(C_0(\Delta))^2} \left[-C_0(\Delta) \log\left(\frac{-2P_1 \cdot P_2}{\delta^2}\right) + \frac{d}{d\Delta} C_0(\Delta)\right] \frac{1}{(-2P_1 \cdot P_2)^\Delta} \,, \tag{E.10}$$

which equals (5.91) in the main text.

E.2 Integration by parts in AdS space

We show that integration by parts in AdS gives vanishing boundary terms if the derivatives that we are moving act on bulk-to-bulk propagators. This is not the case when bulk-to-boundary propagators are involved in the diagrams. Let us consider the following integral,

$$\int dx \, \langle A_i^{a_1}(x_1) \nabla_\nu A_\lambda^a(x) \rangle A^{\nu b} A^{\lambda c}(x) \,. \tag{E.11}$$

Let us integrate by parts and focus only on the boundary term, which is

$$\lim_{\delta\to 0} \int_{z=\delta} d\hat{x} \frac{1}{\delta^{d+1}} \delta^2 \left(-\langle A_{i_1}^{a_1}(x_1) A_\lambda^a(\hat{x}; \delta)\rangle A_z^b A_\lambda^c(\hat{x}, \delta)\right) \,, \tag{E.12}$$

$d\hat{x} \equiv d^d x$ denotes the measure at the boundary. Now, we have

$$A_i^a(x,\delta) \underset{\delta\to 0}{\sim} \delta^{d-2} J_i^a(x)\,, \qquad A_z^a(x,\delta) \underset{\delta\to 0}{\sim} \delta^{d-1} b^a(x)\,, \tag{E.13}$$

where J_i^a are the boundary currents and b^a is some function which does not depend on δ. This implies that the boundary contribution vanishes for sufficiently large d. We can repeat the same argument for the ghost vertex,

$$\int dx\ \langle A_{i_1}^{a_1}(x_1) A_\nu^b(x)\rangle \nabla^\nu \bar{c}^a c^c\,. \tag{E.14}$$

Let us integrate by parts and focus only on the boundary term, which is

$$\lim_{\delta\to 0}\int_{z=\delta} d\hat{x}\frac{1}{\delta^{d+1}}\delta^2\left(-\langle A_{i_1}^{a_1}(x_1) A_z^b(x,\delta)\rangle \bar{c}^a c^c(x,\delta)\right)\,. \tag{E.15}$$

Now we have eq.(E.13) and

$$\bar{c}(x,\delta) \underset{\delta\to 0}{\sim} \delta^d \hat{\bar{c}}_d(x)\,, \quad c(x,\delta) \underset{\delta\to 0}{\sim} \delta^d \hat{c}_d(x)\,, \tag{E.16}$$

with c_0 and $\bar{c}_0$ generic Grassmann-odd functions independent of δ, which again makes the boundary term vanish.

E.3 A useful integral

Let us compute the following integral, which enters in the triple diagram contribution to the $J^a J^b$ two-point function,

$$\mathcal{I}_{4\Delta}^{(k)} = \int dX\ dY\ (-2P_1\cdot X)^{-\Delta_1}(-2P_1\cdot Y)^{-\Delta_3}(-2P_2\cdot X)^{-\Delta_2}(-2P_2\cdot Y)^{-\Delta_4}\zeta^{\Delta_k}\,, \tag{E.17}$$

with ζ as defined in (5.98). We exploit AdS symmetries to simplify the expression of this integral. We begin by using translation symmetry to set $P_2 = (1,0,0)$. We then use inversion, which acts in embedding coordinates by exchanging X^+ and X^- coordinates. This corresponds to taking $P_2 = (0,1,0)$ and implies that, given

$$X = \frac{1}{z}\left(1, z^2+x^2, x^i\right)\,, \qquad Y = \frac{1}{w}\left(1, w^2+y^2, y^i\right)\,, \tag{E.18}$$

we have

$$(-2P_2\cdot X) = \frac{1}{z}\,, \qquad (-2P_2\cdot Y) = \frac{1}{w}\,. \tag{E.19}$$

The other scalar products are instead given by

$$(-2P_1\cdot X) = \frac{(x-y_1)^2+z^2}{z y_1^2}\,, \qquad (-2P_1\cdot Y) = \frac{(y-y_1)^2+w^2}{w y_1^2}\,. \tag{E.20}$$

Note that the chordal distance and the metric determinant are not affected by this transformation. The integral thus obtained is invariant under the change of variable $y^i \to x^i + y^i$, which instead simplifies the expression of the chordal distance

$$u = \frac{(z-w)^2 + y^2}{2zw} \quad \longrightarrow \quad \zeta = \frac{2zw}{w^2 + z^2 + y^2}\,. \tag{E.21}$$

Using the notation of eq.(5.102) in the main text, we can rewrite $\mathcal{I}^{(k)}_{4\Delta}$ as follows,

$$\mathcal{I}^{(k)}_{4\Delta} = \int \frac{dz d^d x}{z^{d+1}} \int \frac{dw d^d y}{w^{d+1}} \frac{2^{\Delta_k} y_1^{2\Delta_{13}} w^{\Delta_{34k}} z^{\Delta_{12k}}}{(z^2 + (x-y_1)^2)^{\Delta_1} (w^2 + (y-y_1)^2)^{\Delta_3} (w^2+z^2+y^2)^{\Delta_k}}\,. \tag{E.22}$$

We introduce Feynman parameters to rewrite the relevant terms in the denominator as

$$\frac{\Gamma(\Delta_{3k})}{\Gamma(\Delta_3)\Gamma(\Delta_k)} \int_0^1 d\alpha (1-\alpha)^{\Delta_3 - 1} \alpha^{\Delta_k - 1} (w^2 + y^2 + \alpha(z^2 + (1-\alpha)(x - y_1^2))\,. \tag{E.23}$$

The integral over y and w is now straightforward. The result, after rescaling $z \to \sqrt{1-\alpha}\, z$, is

$$\mathcal{I}^{(k)}_{4\Delta} = \int \frac{dz d^d x}{z^{d+1}} \int_0^1 d\alpha \frac{\Gamma\left(\frac{\Delta_{3k,4}}{2}\right) \Gamma\left(\frac{\Delta_{34k}-d}{2}\right)}{\Gamma(\Delta_3)\Gamma(\Delta_k)} \frac{2^{\Delta_k - 1} \pi^{\frac{d}{2}} y_1^{2\Delta_{13}} z^{\Delta_{12k}} \alpha^{\frac{\Delta_{4k,3}-2}{2}} (1-\alpha)^{\frac{\Delta_{1234}-d-2}{2}}}{((1-\alpha)z^2 + (x-y_1)^2)^{\Delta_1} (z^2 + (x-y_1)^2)^{\frac{\Delta_{3k,4}}{2}}}\,.$$

Performing the integral over α gives

$$\begin{aligned} \mathcal{I}^{(k)}_{4\Delta} = & \frac{\Gamma\left(\frac{\Delta_{1234}-d}{2}\right) \Gamma\left(\frac{\Delta_{3k,4}}{2}\right) \Gamma\left(\frac{\Delta_{4k,3}}{2}\right) \Gamma\left(\frac{\Delta_{34k}-d}{2}\right)}{\Gamma(\Delta_3)\Gamma(\Delta_k)\Gamma\left(\frac{\Delta_{124k}+\Delta_4-d}{2}\right)} \\ & \int \frac{dz d^d x}{z^{d+1}} \frac{2^{\Delta_k - 1} \pi^{\frac{d}{2}} y_1^{2\Delta_{13}} z^{\Delta_{12k}}\ {}_2F_1\left(\Delta_1, \frac{\Delta_{4k,3}}{2}, \frac{\Delta_{124k}+\Delta_4-d}{2}, \frac{z^2}{(x-y_1)^2+z^2}\right)}{((x-y_1)^2 + z^2)^{\frac{\Delta_{13k,4}+\Delta_1}{2}}}\,. \end{aligned} \tag{E.24}$$

Now we can replace ${}_2F_1$ by its series expansion,

$${}_2F_1(a,b,c,z) = \sum_{m=0}^{\infty} \frac{(a)_m (b)_m}{m!(c)_m} z^m \tag{E.25}$$

and go back to embedding coordinates using eq.(E.20). Imposing the condition $\Delta_{13} = \Delta_{24}$, which is satisfied by each of the integrals of interest, we finally get (5.101) reported in the main text.

Bibliography

[1] F. De Cesare, L. Di Pietro, and M. Serone, *Five-dimensional CFTs from the ε-expansion*, *Phys. Rev. D* **104** (2021), no. 10 105015, [arXiv:2107.00342].

[2] F. De Cesare, L. Di Pietro, and M. Serone, *Free Energy on the Sphere for Non-Abelian Gauge Theories*, arXiv:2212.11848.

[3] R. Ciccone, F. De Cesare, L. Di Pietro, and M. Serone, *Exploring Confinement in Anti-de Sitter Space*, arXiv:2407.06268.

[4] I. Jack, *Two Loop Background Field Calculations for Gauge Theories With Scalar Fields*, *J. Phys. A* **16** (1983) 1083.

[5] B. Allen and T. Jacobson, *Vector two-point functions in maximally symmetric spaces*, *Comm. Math. Phys.* **103** (1986), no. 4 669–692.

[6] D. Poland and L. Rastelli, *Snowmass Topical Summary: Formal QFT*, in *Snowmass 2021*, 10, 2022. arXiv:2210.03128.

[7] P. Boyle et al., *Lattice QCD and the Computational Frontier*, in *2022 Snowmass Summer Study*, 3, 2022. arXiv:2204.00039.

[8] Z. Davoudi et al., *Report of the Snowmass 2021 Topical Group on Lattice Gauge Theory*, in *2022 Snowmass Summer Study*, 9, 2022. arXiv:2209.10758.

[9] S. Catterall and J. Giedt, *Supersymmetric Lattice Theories: Contribution to Snowmass 2022*, in *2022 Snowmass Summer Study*, 2, 2022. arXiv:2202.08154.

[10] D. Poland and D. Simmons-Duffin, *Snowmass White Paper: The Numerical Conformal Bootstrap*, in *2022 Snowmass Summer Study*, 3, 2022. arXiv:2203.08117.

[11] T. Hartman, D. Mazac, D. Simmons-Duffin, and A. Zhiboedov, *Snowmass White Paper: The Analytic Conformal Bootstrap*, in *2022 Snowmass Summer Study*, 2, 2022. arXiv:2202.11012.

[12] M. Kruczenski, J. Penedones, and B. C. van Rees, *Snowmass White Paper: S-matrix Bootstrap*, arXiv:2203.02421.

[13] C. de Rham, S. Kundu, M. Reece, A. J. Tolley, and S.-Y. Zhou, *Snowmass White Paper: UV Constraints on IR Physics*, in *2022 Snowmass Summer Study*, 3, 2022. arXiv:2203.06805.

[14] C. Cordova, T. T. Dumitrescu, K. Intriligator, and S.-H. Shao, *Snowmass White Paper: Generalized Symmetries in Quantum Field Theory and Beyond*, in *2022 Snowmass Summer Study*, 5, 2022. arXiv:2205.09545.

[15] J. Ecalle, *Les fonctions résurgentes*. Publications mathématiques d'Orsay. Dépt. de mathématique, Univ. de Paris-Sud, 1985.

[16] L. Fei, S. Giombi, I. R. Klebanov, and G. Tarnopolsky, *Generalized F-theorem and the ϵ expansion*, *Journal of High Energy Physics* **2015** (Dec, 2015) 1–37.

[17] O. Aharony, M. Berkooz, D. Tong, and S. Yankielowicz, *Confinement in Anti-de Sitter Space*, *JHEP* **02** (2013) 076, [arXiv:1210.5195].

[18] P. C. Argyres, J. J. Heckman, K. Intriligator, and M. Martone, *Snowmass White Paper on SCFTs*, arXiv:2202.07683.

[19] P. Benetti Genolini, M. Honda, H.-C. Kim, D. Tong, and C. Vafa, *Evidence for a Non-Supersymmetric 5d CFT from Deformations of 5d $SU(2)$ SYM*, *JHEP* **05** (2020) 058, [arXiv:2001.00023].

[20] S. Rychkov, *EPFL Lectures on Conformal Field Theory in D>= 3 Dimensions*. SpringerBriefs in Physics. 1, 2016.

[21] J. Penedones and M. Meineri, *Conformal Field Theory and Gravity EPFL doctoral course*. 2019. https://www.epfl.ch/labs/fsl/wp-content/uploads/2022/05/CFTandGravity.pdf.

[22] D. Tong, *Gauge theory*. 2018. https://www.damtp.cam.ac.uk/user/tong/gaugetheory/gt.pdf.

[23] M. Serone, *Notes on Quantum Field Theory 1*. https://www.sissa.it/tpp/phdsection/OnlineResources/4018/QFT_Review_Aug17_2022.pdf.

[24] M. Bertolini, *Lectures on Supersymmetry*. 2024. https://people.sissa.it/~bertmat/susycourse.pdf.

[25] K. G. Wilson and J. B. Kogut, *The Renormalization group and the epsilon expansion*, *Phys. Rept.* **12** (1974) 75–199.

[26] J. M. Maldacena, *The Large N limit of superconformal field theories and supergravity*, *Adv. Theor. Math. Phys.* **2** (1998) 231–252, [hep-th/9711200].

[27] E. Witten, *Anti-de Sitter space and holography*, *Adv. Theor. Math. Phys.* **2** (1998) 253–291, [hep-th/9802150].

[28] S. S. Gubser, I. R. Klebanov, and A. M. Polyakov, *Gauge theory correlators from noncritical string theory*, *Phys. Lett. B* **428** (1998) 105–114, [hep-th/9802109].

[29] D. Kutasov, A. Schwimmer, and N. Seiberg, *Chiral rings, singularity theory and electric - magnetic duality*, *Nucl. Phys. B* **459** (1996) 455–496, [hep-th/9510222].

[30] W. Caswell, *Asymptotic behavior of non-abelian gauge theories to two-loop order*, *Physical Review Letters* **33** (1974), no. 4 244.

[31] T. Banks and A. Zaks, *On the phase structure of vector-like gauge theories with massless fermions*, *Nuclear Physics B* **196** (1982), no. 2 189–204.

[32] D. Simmons-Duffin, *The Conformal Bootstrap*, in *Proceedings, Theoretical Advanced Study Institute in Elementary Particle Physics: New Frontiers in Fields and Strings (TASI 2015): Boulder, CO, USA, June 1-26, 2015*, pp. 1–74, 2017. arXiv:1602.07982.

[33] P. Francesco, P. Mathieu, and D. Sénéchal, *Conformal field theory*. Springer Science & Business Media, 2012.

[34] D. Poland, S. Rychkov, and A. Vichi, *The Conformal Bootstrap: Theory, Numerical Techniques, and Applications*, *Rev. Mod. Phys.* **91** (2019) 015002, [arXiv:1805.04405].

[35] S. Rychkov and N. Su, *New Developments in the Numerical Conformal Bootstrap*, arXiv:2311.15844.

[36] R. F. Streater and A. S. Wightman, *PCT, spin and statistics, and all that*. 1989.

[37] G. 't Hooft, *A Planar Diagram Theory for Strong Interactions*, *Nucl. Phys. B* **72** (1974) 461.

[38] M. Moshe and J. Zinn-Justin, *Quantum field theory in the large N limit: A Review*, *Phys. Rept.* **385** (2003) 69–228, [hep-th/0306133].

[39] K. G. Wilson and M. E. Fisher, *Critical exponents in 3.99 dimensions*, *Phys. Rev. Lett.* **28** (1972) 240–243.

[40] S. El-Showk, M. F. Paulos, D. Poland, S. Rychkov, D. Simmons-Duffin, and A. Vichi, *Solving the 3d Ising Model with the Conformal Bootstrap II. c-Minimization and Precise Critical Exponents*, *J. Stat. Phys.* **157** (2014) 869, [arXiv:1403.4545].

[41] A. B. Zamolodchikov, *Irreversibility of the Flux of the Renormalization Group in a 2D Field Theory*, *JETP Lett.* **43** (1986) 730–732.

[42] J. L. Cardy, *Is There a c Theorem in Four-Dimensions?*, *Phys. Lett. B* **215** (1988) 749–752.

[43] Z. Komargodski and A. Schwimmer, *On Renormalization Group Flows in Four Dimensions*, *JHEP* **12** (2011) 099, [arXiv:1107.3987].

[44] Z. Komargodski, *The Constraints of Conformal Symmetry on RG Flows*, *JHEP* **07** (2012) 069, [arXiv:1112.4538].

[45] H. Casini, M. Huerta, and R. C. Myers, *Towards a derivation of holographic entanglement entropy*, *JHEP* **05** (2011) 036, [arXiv:1102.0440].

[46] H. Casini and M. Huerta, *On the RG running of the entanglement entropy of a circle*, *Phys. Rev. D* **85** (2012) 125016, [arXiv:1202.5650].

[47] S. Giombi and I. R. Klebanov, *Interpolating between a and F*, *JHEP* **03** (2015) 117, [arXiv:1409.1937].

[48] L. Fei, S. Giombi, I. R. Klebanov, and G. Tarnopolsky, *Generalized F-Theorem and the ϵ Expansion*, *JHEP* **12** (2015) 155, [arXiv:1507.01960].

[49] E. Witten, *Multitrace operators, boundary conditions, and AdS / CFT correspondence*, hep-th/0112258.

[50] S. S. Gubser and I. R. Klebanov, *A Universal result on central charges in the presence of double trace deformations*, *Nucl. Phys.* **B656** (2003) 23–36, [hep-th/0212138].

[51] D. E. Diaz and H. Dorn, *Partition functions and double-trace deformations in AdS/CFT*, *JHEP* **05** (2007) 046, [hep-th/0702163].

[52] L. D. Faddeev and V. N. Popov, *Feynman Diagrams for the Yang-Mills Field*, *Phys. Lett. B* **25** (1967) 29–30.

[53] A. M. Jaffe and E. Witten, *Quantum Yang-Mills theory*, .

[54] Y. Choi, H. T. Lam, and S.-H. Shao, *Noninvertible Global Symmetries in the Standard Model*, *Phys. Rev. Lett.* **129** (2022), no. 16 161601, [arXiv:2205.05086].

[55] C. Cordova and K. Ohmori, *Noninvertible Chiral Symmetry and Exponential Hierarchies*, *Phys. Rev. X* **13** (2023), no. 1 011034, [arXiv:2205.06243].

[56] D. B. Kaplan, J.-W. Lee, D. T. Son, and M. A. Stephanov, *Conformality Lost*, *Phys. Rev.* **D80** (2009) 125005, [arXiv:0905.4752].

[57] T. Appelquist, J. Terning, and L. C. R. Wijewardhana, *The Zero temperature chiral phase transition in SU(N) gauge theories*, *Phys. Rev. Lett.* **77** (1996) 1214–1217, [hep-ph/9602385].

[58] H. Gies and J. Jaeckel, *Chiral phase structure of QCD with many flavors*, *Eur. Phys. J.* **C46** (2006) 433–438, [hep-ph/0507171].

[59] F. Kuipers, U. Gursoy, and Y. Kuznetsov, *Bifurcations in the RG-flow of QCD*, *JHEP* **07** (2019) 075, [arXiv:1812.05179].

[60] T. A. Ryttov and R. Shrock, *Infrared Zero of β and Value of γ_m for an SU(3) Gauge Theory at the Five-Loop Level*, *Phys. Rev.* **D94** (2016), no. 10 105015, [arXiv:1607.06866].

[61] O. Antipin, A. Maiezza, and J. C. Vasquez, *Resummation in QFT with Meijer G-functions*, *Nucl. Phys.* **B941** (2019) 72–90, [arXiv:1807.05060].

[62] B. S. Kim, D. K. Hong, and J.-W. Lee, *Into the conformal window: multi-representation gauge theories*, arXiv:2001.02690.

[63] T. A. Ryttov and R. Shrock, *Physics of the non-Abelian Coulomb phase: Insights from Padé approximants*, *Phys. Rev.* **D97** (2018), no. 2 025004, [arXiv:1710.06944].

[64] L. Di Pietro and M. Serone, *Looking through the QCD Conformal Window with Perturbation Theory*, *JHEP* **07** (2020) 049, [arXiv:2003.01742].

[65] J. Goldstone, A. Salam, and S. Weinberg, *Broken Symmetries*, *Phys. Rev.* **127** (1962) 965–970.

[66] S. Weinberg, *Approximate symmetries and pseudoGoldstone bosons*, *Phys. Rev. Lett.* **29** (1972) 1698–1701.

[67] C. Wang, A. Nahum, M. A. Metlitski, C. Xu, and T. Senthil, *Deconfined quantum critical points: symmetries and dualities*, *Phys. Rev. X* **7** (2017), no. 3 031051, [arXiv:1703.02426].

[68] D. Gaiotto, Z. Komargodski, and N. Seiberg, *Time-reversal breaking in QCD_4, walls, and dualities in 2 + 1 dimensions*, *JHEP* **01** (2018) 110, [arXiv:1708.06806].

[69] T. Appelquist, D. Nash, and L. C. R. Wijewardhana, *Critical Behavior in (2+1)-Dimensional QED*, *Phys. Rev. Lett.* **60** (1988) 2575.

[70] T. Appelquist and D. Nash, *Critical Behavior in (2+1)-dimensional QCD*, *Phys. Rev. Lett.* **64** (1990) 721.

[71] C. Vafa and E. Witten, *Restrictions on Symmetry Breaking in Vector-Like Gauge Theories*, *Nucl. Phys. B* **234** (1984) 173–188.

[72] C. Vafa and E. Witten, *Eigenvalue Inequalities for Fermions in Gauge Theories*, *Commun. Math. Phys.* **95** (1984) 257.

[73] S. Giombi, I. R. Klebanov, and G. Tarnopolsky, *Conformal QEDd, F-theorem and the ϵ expansion*, *Journal of Physics A: Mathematical and Theoretical* **49** (Feb, 2016) 135403.

[74] M. Peskin, *Critical point behavior of the Wilson loop*, *Physics Letters B* **94** (1980), no. 2 161 – 165.

[75] L. Fei, S. Giombi, and I. R. Klebanov, *Critical $O(N)$ models in $6-\epsilon$ dimensions*, *Phys. Rev. D* **90** (2014), no. 2 025018, [arXiv:1404.1094].

[76] S. Giombi, R. Huang, I. R. Klebanov, S. S. Pufu, and G. Tarnopolsky, *The $O(N)$ Model in $4<d<6$: Instantons and complex CFTs*, *Phys. Rev. D* **101** (2020), no. 4 045013, [arXiv:1910.02462].

[77] T. Morris, *Renormalizable extra-dimensional models*, *Journal of High Energy Physics* **2005** (Jan, 2005) 002–002.

[78] C. G. Callan, Jr. and F. Wilczek, *INFRARED BEHAVIOR AT NEGATIVE CURVATURE*, *Nucl. Phys. B* **340** (1990) 366–386.

[79] J. Polchinski, *S matrices from AdS space-time*, hep-th/9901076.

[80] S. B. Giddings, *The Boundary S matrix and the AdS to CFT dictionary*, *Phys. Rev. Lett.* **83** (1999) 2707–2710, [hep-th/9903048].

[81] A. L. Fitzpatrick, E. Katz, D. Poland, and D. Simmons-Duffin, *Effective Conformal Theory and the Flat-Space Limit of AdS*, *JHEP* **07** (2011) 023, [arXiv:1007.2412].

[82] J. Penedones, *Writing CFT correlation functions as AdS scattering amplitudes*, *JHEP* **03** (2011) 025, [arXiv:1011.1485].

[83] M. F. Paulos, J. Penedones, J. Toledo, B. C. van Rees, and P. Vieira, *The S-matrix bootstrap. Part I: QFT in AdS*, *JHEP* **11** (2017) 133, [arXiv:1607.06109].

[84] D. Mazac, *Analytic bounds and emergence of AdS_2 physics from the conformal bootstrap*, *JHEP* **04** (2017) 146, [arXiv:1611.10060].

[85] D. Mazac and M. F. Paulos, *The analytic functional bootstrap. Part I: 1D CFTs and 2D S-matrices*, *JHEP* **02** (2019) 162, [arXiv:1803.10233].

[86] S. Komatsu, M. F. Paulos, B. C. Van Rees, and X. Zhao, *Landau diagrams in AdS and S-matrices from conformal correlators*, *JHEP* **11** (2020) 046, [arXiv:2007.13745].

[87] Y.-Z. Li, *Notes on flat-space limit of AdS/CFT*, *JHEP* **09** (2021) 027, [arXiv:2106.04606].

[88] W. Knop and D. Mazac, *Dispersive sum rules in AdS_2*, *JHEP* **10** (2022) 038, [arXiv:2203.11170].

[89] L. Córdova, Y. He, and M. F. Paulos, *From conformal correlators to analytic S-matrices: CFT_1/QFT_2*, *JHEP* **08** (2022) 186, [arXiv:2203.10840].

[90] A. Gadde and T. Sharma, *A scattering amplitude for massive particles in AdS*, *JHEP* **09** (2022) 157, [arXiv:2204.06462].

[91] B. C. van Rees and X. Zhao, *Quantum Field Theory in AdS Space instead of Lehmann-Symanzik-Zimmerman Axioms*, *Phys. Rev. Lett.* **130** (2023), no. 19 191601, [arXiv:2210.15683].

[92] B. C. van Rees and X. Zhao, *Flat-space Partial Waves From Conformal OPE Densities*, arXiv:2312.02273.

[93] D. Carmi, L. Di Pietro, and S. Komatsu, *A Study of Quantum Field Theories in AdS at Finite Coupling*, *JHEP* **01** (2019) 200, [arXiv:1810.04185].

[94] C. Copetti, L. Di Pietro, Z. Ji, and S. Komatsu, *Taming Mass Gap with Anti-de-Sitter Space*, arXiv:2312.09277.

[95] M. Hogervorst, M. Meineri, J. Penedones, and K. S. Vaziri, *Hamiltonian truncation in Anti-de Sitter spacetime*, *JHEP* **08** (2021) 063, [arXiv:2104.10689].

[96] A. Antunes, M. S. Costa, J. a. Penedones, A. Salgarkar, and B. C. van Rees, *Towards bootstrapping RG flows: sine-Gordon in AdS*, *JHEP* **12** (2021) 094, [arXiv:2109.13261].

[97] N. Levine and M. F. Paulos, *Bootstrapping bulk locality. Part I: Sum rules for AdS form factors*, *JHEP* **01** (2024) 049, [arXiv:2305.07078].

[98] M. Meineri, J. Penedones, and T. Spirig, *Renormalization group flows in AdS and the bootstrap program*, arXiv:2305.11209.

[99] A. Antunes, E. Lauria, and B. C. van Rees, *A bootstrap study of minimal model deformations*, *JHEP* **05** (2024) 027, [arXiv:2401.06818].

[100] A. Kakkar and S. Sarkar, *On partition functions and phases of scalars in AdS*, *JHEP* **07** (2022) 089, [arXiv:2201.09043].

[101] A. Kakkar and S. Sarkar, *Phases of theories with fermions in AdS*, *JHEP* **06** (2023) 009, [arXiv:2303.02711].

[102] M. Beccaria, S. Giombi, and A. A. Tseytlin, *Correlators on non-supersymmetric Wilson line in $\mathcal{N} = 4$ SYM and AdS_2/CFT_1*, *JHEP* **05** (2019) 122, [arXiv:1903.04365].

[103] M. Beccaria and A. A. Tseytlin, *On boundary correlators in Liouville theory on AdS_2*, *JHEP* **07** (2019) 008, [arXiv:1904.12753].

[104] M. Beccaria, H. Jiang, and A. A. Tseytlin, *Non-abelian Toda theory on AdS_2 and $AdS_2/CFT_2^{1/2}$ duality*, *JHEP* **09** (2019) 036, [arXiv:1907.01357].

[105] M. Beccaria, H. Jiang, and A. A. Tseytlin, *Supersymmetric Liouville theory in AdS_2 and AdS/CFT*, *JHEP* **11** (2019) 051, [arXiv:1909.10255].

[106] M. Beccaria, H. Jiang, and A. A. Tseytlin, *Boundary correlators in WZW model on AdS_2*, *JHEP* **05** (2020) 099, [arXiv:2001.11269].

[107] S. Giombi, E. Helfenberger, Z. Ji, and H. Khanchandani, *Monodromy defects from hyperbolic space*, *JHEP* **02** (2022) 041, [arXiv:2102.11815].

[108] C. P. Herzog and I. Shamir, *On Marginal Operators in Boundary Conformal Field Theory*, *JHEP* **10** (2019) 088, [arXiv:1906.11281].

[109] S. Giombi and H. Khanchandani, *CFT in AdS and boundary RG flows*, *JHEP* **11** (2020) 118, [arXiv:2007.04955].

[110] S. Giombi, E. Helfenberger, and H. Khanchandani, *Fermions in AdS and Gross-Neveu BCFT*, *JHEP* **07** (2022) 018, [arXiv:2110.04268].

[111] V. Gorbenko, S. Rychkov, and B. Zan, *Walking, Weak first-order transitions, and Complex CFTs*, *JHEP* **10** (2018) 108, [arXiv:1807.11512].

[112] W. E. Caswell, *Asymptotic Behavior of Nonabelian Gauge Theories to Two Loop Order*, *Phys. Rev. Lett.* **33** (1974) 244.

[113] T. Banks and A. Zaks, *On the Phase Structure of Vector-Like Gauge Theories with Massless Fermions*, *Nucl. Phys.* **B196** (1982) 189–204.

[114] P. A. Baikov, K. G. Chetyrkin, and J. H. Kuhn, *Five-Loop Running of the QCD coupling constant*, *Phys. Rev. Lett.* **118** (2017), no. 8 082002, [arXiv:1606.08659].

[115] F. Herzog, B. Ruijl, T. Ueda, J. A. M. Vermaseren, and A. Vogt, *The five-loop beta function of Yang-Mills theory with fermions*, *JHEP* **02** (2017) 090, [arXiv:1701.01404].

[116] T. Luthe, A. Maier, P. Marquard, and Y. Schroder, *The five-loop Beta function for a general gauge group and anomalous dimensions beyond Feynman gauge*, *JHEP* **10** (2017) 166, [arXiv:1709.07718].

[117] K. G. Chetyrkin, G. Falcioni, F. Herzog, and J. A. M. Vermaseren, *Five-loop renormalisation of QCD in covariant gauges*, *JHEP* **10** (2017) 179, [arXiv:1709.08541]. [Addendum: JHEP12,006(2017)].

[118] F. J. Dyson, *Divergence of perturbation theory in quantum electrodynamics*, *Phys. Rev.* **85** (1952) 631–632.

[119] P. A. Baikov, K. G. Chetyrkin, and J. H. Kuhn, *Quark Mass and Field Anomalous Dimensions to $\mathcal{O}(\alpha_s^5)$*, *JHEP* **10** (2014) 076, [arXiv:1402.6611].

[120] T. Luthe, A. Maier, P. Marquard, and Y. Schroder, *Five-loop quark mass and field anomalous dimensions for a general gauge group*, *JHEP* **01** (2017) 081, [arXiv:1612.05512].

[121] P. A. Baikov, K. G. Chetyrkin, and J. H. Kuhn, *Five-loop fermion anomalous dimension for a general gauge group from four-loop massless propagators*, *JHEP* **04** (2017) 119, [arXiv:1702.01458].

[122] J. A. Gracey, *The QCD Beta function at $O(1/N_f)$*, *Phys. Lett.* **B373** (1996) 178–184, [hep-ph/9602214].

[123] B. Holdom, *Large N flavor beta-functions: a recap*, *Phys. Lett.* **B694** (2011) 74–79, [arXiv:1006.2119].

[124] D. Espriu, A. Palanques-Mestre, P. Pascual, and R. Tarrach, *The γ Function in the $1/N_f$ Expansion*, *Z. Phys.* **C13** (1982) 153.

[125] A. Palanques-Mestre and P. Pascual, *The $1/N_f$ Expansion of the γ and Beta Functions in QED*, *Commun. Math. Phys.* **95** (1984) 277.

[126] H. Gies, *Renormalizability of gauge theories in extra dimensions*, *Physical Review D* **68** (Oct, 2003).

[127] M. Creutz, *Confinement and the Critical Dimensionality of Space-Time*, *Phys. Rev. Lett.* **43** (Sep, 1979) 890–890.

[128] H. Kawai, M. Nio, and Y. Okamoto, *On Existence of Non-Renormalizable Field Theory: Pure SU(2) Lattice Gauge Theory in Five Dimensions*, *Progress of Theoretical Physics* **88** (08, 1992) 341–350, [https://academic.oup.com/ptp/article-pdf/88/2/341/5162271/88-2-341.pdf].

[129] A. Florio, J. a. M. V. P. Lopes, J. Matos, and J. a. Penedones, *Searching for continuous phase transitions in 5D SU(2) lattice gauge theory*, *JHEP* **12** (2021) 076, [arXiv:2103.15242].

[130] D. Karateev, P. Kravchuk, M. Serone, and A. Vichi, *Fermion Conformal Bootstrap in 4d*, *JHEP* **06** (2019) 088, [arXiv:1902.05969].

[131] Z. Li and D. Poland, *Searching for gauge theories with the conformal bootstrap*, *JHEP* **03** (2021) 172, [arXiv:2005.01721].

[132] M. Bertolini and F. Mignosa, *Supersymmetry breaking deformations and phase transitions in five dimensions*, *JHEP* **10** (2021) 244, [arXiv:2109.02662].

[133] N. Seiberg, *Five-dimensional SUSY field theories, nontrivial fixed points and string dynamics*, *Phys. Lett. B* **388** (1996) 753–760, [hep-th/9608111].

[134] J. A. Gracey, *Six dimensional QCD at two loops*, *Phys. Rev. D* **93** (2016), no. 2 025025, [arXiv:1512.04443].

[135] J. A. Gracey, *Classification and one loop renormalization of dimension-six and dimension-eight operators in quantum gluodynamics*, *Nucl. Phys. B* **634** (2002) 192–208, [hep-ph/0204266]. [Erratum: Nucl.Phys.B 696, 295–297 (2004)].

[136] A. Kapustin, *Wilson-'t Hooft operators in four-dimensional gauge theories and S-duality*, *Phys. Rev. D* **74** (2006) 025005, [hep-th/0501015].

[137] D. Correa, J. Henn, J. Maldacena, and A. Sever, *An exact formula for the radiation of a moving quark in N=4 super Yang Mills*, *JHEP* **06** (2012) 048, [arXiv:1202.4455].

[138] S. Giombi, I. R. Klebanov, and G. Tarnopolsky, *Conformal QED_d, F-Theorem and the ϵ Expansion*, *J. Phys. A* **49** (2016), no. 13 135403, [arXiv:1508.06354].

[139] Z. Komargodski and N. Seiberg, *A symmetry breaking scenario for QCD_3*, *JHEP* **01** (2018) 109, [arXiv:1706.08755].

[140] A. Sharon, *QCD_3 dualities and the F-theorem*, *JHEP* **08** (2018) 078, [arXiv:1803.06983].

[141] N. Karthik and R. Narayanan, *Scale-invariance and scale-breaking in parity-invariant three-dimensional QCD*, *Phys. Rev. D* **97** (2018), no. 5 054510, [arXiv:1801.02637].

[142] C.-M. Chang, M. Fluder, Y.-H. Lin, and Y. Wang, *Spheres, Charges, Instantons, and Bootstrap: A Five-Dimensional Odyssey*, *JHEP* **03** (2018) 123, [arXiv:1710.08418].

[143] V. Pestun, *Localization of gauge theory on a four-sphere and supersymmetric Wilson loops*, *Commun. Math. Phys.* **313** (2012) 71–129, [arXiv:0712.2824].

[144] M. A. Rubin and C. R. Ordonez, *Symmetric Tensor Eigen Spectrum of the Laplacian on n Spheres*, *J. Math. Phys.* **26** (1985) 65.

[145] M. D. Schwartz, *Quantum Field Theory and the Standard Model*. Cambridge University Press, 3, 2014.

[146] D. H. Bailey, *A fortran 90-based multiprecision system*, *ACM Trans. Math. Softw.* **21** (dec, 1995) 379–387.

[147] I. Jack and H. Osborn, *Background Field Calculations in Curved Space-time. 1. General Formalism and Application to Scalar Fields*, *Nucl. Phys. B* **234** (1984) 331–364.

[148] I. Jack and H. Osborn, *Analogs for the c-Theorem for Four-dimensional Renormalizable Field Theories*, *Nucl. Phys. B* **343** (1990) 647–688.

[149] M. Marino, *Lectures on localization and matrix models in supersymmetric Chern-Simons-matter theories*, *J. Phys. A* **44** (2011) 463001, [arXiv:1104.0783].

[150] I. Affleck, *On the Realization of Chiral Symmetry in (1+1)-dimensions*, *Nucl. Phys. B* **265** (1986) 448–468.

[151] D. Gepner, *Nonabelian Bosonization and Multiflavor QED and QCD in Two-dimensions*, *Nucl. Phys. B* **252** (1985) 481–507.

[152] L. Casarin and A. A. Tseytlin, *One-loop β-functions in 4-derivative gauge theory in 6 dimensions*, *JHEP* **08** (2019) 159, [arXiv:1907.02501].

[153] F. Benini, C. Iossa, and M. Serone, *Conformality Loss, Walking, and 4D Complex Conformal Field Theories at Weak Coupling*, *Phys. Rev. Lett.* **124** (2020), no. 5 051602, [arXiv:1908.04325].

[154] B. i. Halperin, T. C. Lubensky, and S.-k. Ma, *First order phase transitions in superconductors and smectic A liquid crystals*, *Phys. Rev. Lett.* **32** (1974) 292–295.

[155] B. Ihrig, N. Zerf, P. Marquard, I. F. Herbut, and M. M. Scherer, *Abelian Higgs model at four loops, fixed-point collision and deconfined criticality*, *Phys. Rev. B* **100** (2019), no. 13 134507, [arXiv:1907.08140].

[156] M. Bertolini, F. Mignosa, and J. van Muiden, *On non-supersymmetric fixed points in five dimensions*, *JHEP* **10** (2022) 064, [arXiv:2207.11162].

[157] W. Siegel, *Supersymmetric Dimensional Regularization via Dimensional Reduction*, *Phys. Lett. B* **84** (1979) 193–196.

[158] E. A. Mirabelli and M. E. Peskin, *Transmission of supersymmetry breaking from a four-dimensional boundary*, *Phys. Rev. D* **58** (1998) 065002, [hep-th/9712214].

[159] J. Davies, F. Herren, and A. E. Thomsen, *General gauge-Yukawa-quartic β-functions at 4-3-2-loop order*, *JHEP* **01** (2022) 051, [arXiv:2110.05496].

[160] A. Bednyakov and A. Pikelner, *Four-Loop Gauge and Three-Loop Yukawa Beta Functions in a General Renormalizable Theory*, *Phys. Rev. Lett.* **127** (2021), no. 4 041801, [arXiv:2105.09918].

[161] E. Lauria, M. N. Milam, and B. C. van Rees, *Perturbative RG flows in AdS. An étude*, *JHEP* **03** (2024) 005, [arXiv:2309.10031].

[162] H. M. Fried and D. R. Yennie, *New Techniques in the Lamb Shift Calculation*, *Phys. Rev.* **112** (1958) 1391–1404.

[163] D. R. Yennie, S. C. Frautschi, and H. Suura, *The infrared divergence phenomena and high-energy processes*, *Annals Phys.* **13** (1961) 379–452.

[164] E. Witten, *SL(2,Z) action on three-dimensional conformal field theories with Abelian symmetry*, in *From Fields to Strings: Circumnavigating Theoretical Physics: A Conference in Tribute to Ian Kogan*, pp. 1173–1200, 7, 2003. hep-th/0307041.

[165] D. Marolf and S. F. Ross, *Boundary Conditions and New Dualities: Vector Fields in AdS/CFT*, *JHEP* **11** (2006) 085, [hep-th/0606113].

[166] I. Heemskerk, J. Penedones, J. Polchinski, and J. Sully, *Holography from Conformal Field Theory*, *JHEP* **10** (2009) 079, [arXiv:0907.0151].

[167] B. Sundborg, *The Hagedorn transition, deconfinement and N=4 SYM theory*, *Nucl. Phys. B* **573** (2000) 349–363, [hep-th/9908001].

[168] O. Aharony, J. Marsano, S. Minwalla, K. Papadodimas, and M. Van Raamsdonk, *The Hagedorn - deconfinement phase transition in weakly coupled large N gauge theories*, *Adv. Theor. Math. Phys.* **8** (2004) 603–696, [hep-th/0310285].

[169] D. Karateev, P. Kravchuk, and D. Simmons-Duffin, *Harmonic Analysis and Mean Field Theory*, *JHEP* **10** (2019) 217, [arXiv:1809.05111].

[170] D. Z. Freedman, S. D. Mathur, A. Matusis, and L. Rastelli, *Correlation functions in the CFT(d) / AdS(d+1) correspondence*, *Nucl. Phys. B* **546** (1999) 96–118, [hep-th/9804058].

[171] A. Naqvi, *Propagators for massive symmetric tensor and p forms in AdS(d+1)*, *JHEP* **12** (1999) 025, [hep-th/9911182].

[172] T. Leonhardt, W. Ruhl, and R. Manvelyan, *The Group approach to AdS space propagators: A Fast algorithm*, *J. Phys. A* **37** (2004) 7051, [hep-th/0310063].

[173] M. S. Costa, V. Gonçalves, and J. a. Penedones, *Spinning AdS Propagators*, *JHEP* **09** (2014) 064, [arXiv:1404.5625].

[174] E. D'Hoker and D. Z. Freedman, *Gauge boson exchange in AdS(d+1)*, *Nucl. Phys. B* **544** (1999) 612–632, [hep-th/9809179].

[175] E. D'Hoker, D. Z. Freedman, S. D. Mathur, A. Matusis, and L. Rastelli, *Graviton and gauge boson propagators in AdS(d+1)*, *Nucl. Phys. B* **562** (1999) 330–352, [hep-th/9902042].

[176] R. Marotta, K. Skenderis, and M. Verma, *Flat space spinning massive amplitudes from momentum space CFT*, arXiv:2406.06447.

[177] M. S. Costa, J. Penedones, D. Poland, and S. Rychkov, *Spinning Conformal Correlators*, *JHEP* **11** (2011) 071, [arXiv:1107.3554].

[178] P. A. M. Dirac, *Wave equations in conformal space*, *Annals Math.* **37** (1936) 429–442.

[179] Ankur, D. Carmi, and L. Di Pietro, *Scalar QED in AdS*, *JHEP* **10** (2023) 089, [arXiv:2306.05551].

[180] P. Liendo, L. Rastelli, and B. C. van Rees, *The Bootstrap Program for Boundary CFT_d*, *JHEP* **07** (2013) 113, [arXiv:1210.4258].

[181] L. S. Brown and J. C. Collins, *Dimensional Renormalization of Scalar Field Theory in Curved Space-time*, *Annals Phys.* **130** (1980) 215.

[182] S. J. Hathrell, *Trace Anomalies and $\lambda\phi^4$ Theory in Curved Space*, *Annals Phys.* **139** (1982) 136.

[183] S. J. Hathrell, *Trace Anomalies and QED in Curved Space*, *Annals Phys.* **142** (1982) 34.

[184] M. D. Freeman, *The Renormalization of Nonabelian Gauge Theories in Curved Space-time*, *Annals Phys.* **153** (1984) 339.

[185] H. Osborn, *Weyl consistency conditions and a local renormalization group equation for general renormalizable field theories*, *Nucl. Phys. B* **363** (1991) 486–526.

[186] A. Antinucci, G. Galati, and G. Rizi, *On continuous 2-category symmetries and Yang-Mills theory*, *JHEP* **12** (2022) 061, [arXiv:2206.05646].

[187] J. L. Cardy, *Scaling and renormalization in statistical physics*. Cambridge lecture notes in physics. Cambridge Univ. Press, Cambridge, 1996.

[188] T. Faulkner and N. Iqbal, *Friedel oscillations and horizon charge in 1D holographic liquids*, *JHEP* **07** (2013) 060, [arXiv:1207.4208].

[189] I. Bertan, I. Sachs, and E. D. Skvortsov, *Quantum ϕ^4 Theory in AdS_4 and its CFT Dual*, *JHEP* **02** (2019) 099, [arXiv:1810.00907].

[190] Y.-C. He, J. Rong, N. Su, and A. Vichi, *Non-Abelian currents bootstrap*, *JHEP* **03** (2024) 175, [arXiv:2302.11585].

[191] D. Gaiotto, A. Kapustin, N. Seiberg, and B. Willett, *Generalized Global Symmetries*, *JHEP* **02** (2015) 172, [arXiv:1412.5148].

[192] S. Caron-Huot and M. Wilhelm, *Renormalization group coefficients and the S-matrix*, *JHEP* **12** (2016) 010, [arXiv:1607.06448].

[193] J. Elias Miró, J. Ingoldby, and M. Riembau, *EFT anomalous dimensions from the S-matrix*, *JHEP* **09** (2020) 163, [arXiv:2005.06983].

[194] P. Baratella, C. Fernandez, and A. Pomarol, *Renormalization of Higher-Dimensional Operators from On-shell Amplitudes*, *Nucl. Phys. B* **959** (2020) 115155, [arXiv:2005.07129].

[195] P. Baratella, C. Fernandez, B. von Harling, and A. Pomarol, *Anomalous Dimensions of Effective Theories from Partial Waves*, *JHEP* **03** (2021) 287, [arXiv:2010.13809].

[196] M. Abramowitz and I. A. Stegun, *Handbook of Mathematical Functions with Formulas, Graphs, and Mathematical Tables*. Dover, New York, ninth dover printing, tenth gpo printing ed., 1964.

[197] S. Weinberg, *The Quantum Theory of Fields*, vol. 2. Cambridge University Press, 1996.

[198] J. Gomis, J. Paris, and S. Samuel, *Antibracket, antifields and gauge theory quantization*, *Phys. Rept.* **259** (1995) 1–145, [hep-th/9412228].

[199] O. Aharony, L. F. Alday, A. Bissi, and E. Perlmutter, *Loops in AdS from Conformal Field Theory*, *JHEP* **07** (2017) 036, [arXiv:1612.03891].

[200] E. Y. Yuan, *Loops in the Bulk*, arXiv:1710.01361.

[201] E. Y. Yuan, *Simplicity in AdS Perturbative Dynamics*, arXiv:1801.07283.

[202] S. Giombi, C. Sleight, and M. Taronna, *Spinning AdS Loop Diagrams: Two Point Functions*, *JHEP* **06** (2018) 030, [arXiv:1708.08404].

[203] C. Cardona, *Mellin-(Schwinger) representation of One-loop Witten diagrams in AdS*, arXiv:1708.06339.

[204] J. Liu, E. Perlmutter, V. Rosenhaus, and D. Simmons-Duffin, *d-dimensional SYK, AdS Loops, and* $6j$ *Symbols*, *JHEP* **03** (2019) 052, [arXiv:1808.00612].

[205] I. Bertan and I. Sachs, *Loops in Anti–de Sitter Space*, *Phys. Rev. Lett.* **121** (2018), no. 10 101601, [arXiv:1804.01880].

[206] K. Ghosh, *Polyakov-Mellin Bootstrap for AdS loops*, *JHEP* **02** (2020) 006, [arXiv:1811.00504].

[207] D. Ponomarev, *From bulk loops to boundary large-N expansion*, *JHEP* **01** (2020) 154, [arXiv:1908.03974].

[208] D. Carmi, *Loops in AdS: From the Spectral Representation to Position Space*, *JHEP* **06** (2020) 049, [arXiv:1910.14340].

[209] S. Albayrak and S. Kharel, *Spinning loop amplitudes in anti–de Sitter space*, *Phys. Rev. D* **103** (2021), no. 2 026004, [arXiv:2006.12540].

[210] A. Herderschee, *A new framework for higher loop Witten diagrams*, *JHEP* **06** (2024) 008, [arXiv:2112.08226].

[211] D. Carmi, *Loops in AdS: from the spectral representation to position space. Part II*, *JHEP* **07** (2021) 186, [arXiv:2104.10500].

[212] T. Heckelbacher, I. Sachs, E. Skvortsov, and P. Vanhove, *Analytical evaluation of AdS_4 Witten diagrams as flat space multi-loop Feynman integrals*, *JHEP* **08** (2022) 052, [arXiv:2201.09626].

[213] D. Carmi, *Loops in AdS: From the Spectral Representation to Position Space III*, arXiv:2402.02481.

[214] S. L. Cacciatori, H. Epstein, and U. Moschella, *Loops in Anti de Sitter space*, arXiv:2403.13142.